AD-A139 989 THE EFFECT OF STRAKES ON VORTICAL FLOWS APPLIED TO AIRCRAFT..(U) VON KARMAN INST FOR FLUID DYNAMICS RHODE-SAINT-GENESE (BELGIU.. G G ORDONEZ 31 MAR 84 1/2

UNCLASSIFIED VKI-PR-1983-22 EOARD-TR-84-14 AFOSR-83-0126 F/G 20/4 NL

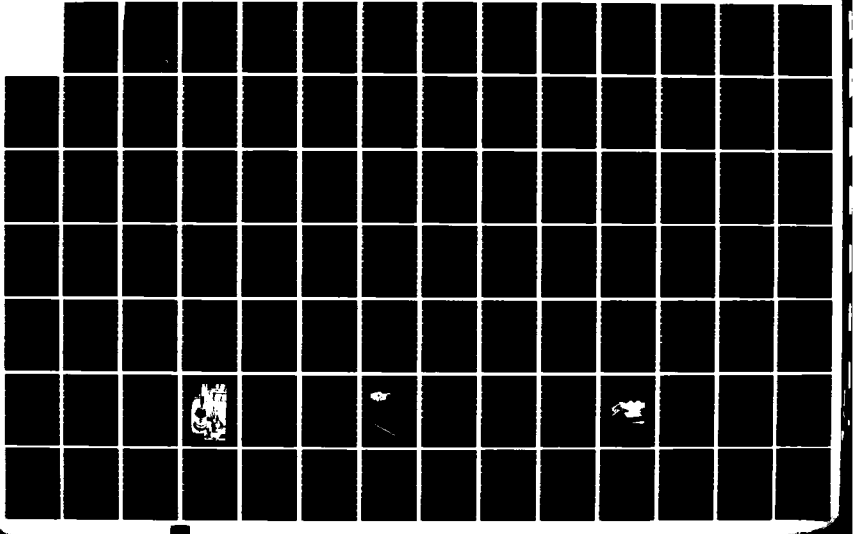

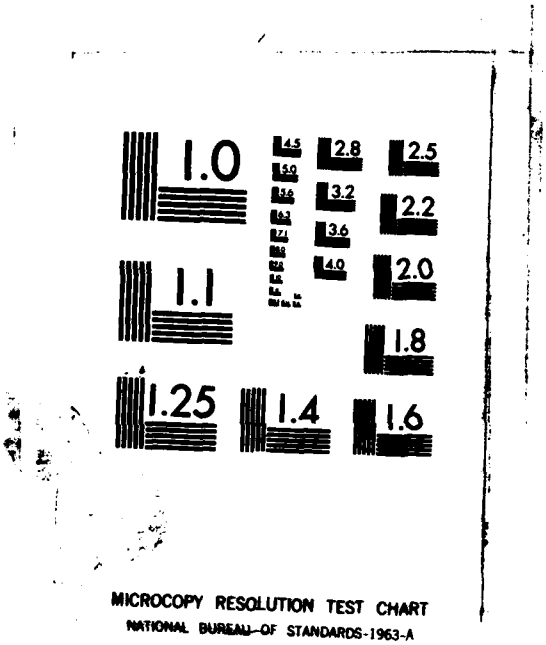

EOARD-TR-84-14

(2)

GRANT AFOSR 83-0126

THE EFFECT OF STRAKES ON VORTICAL FLOWS APPLIED TO AIRCRAFT

GUSTAVO G. ORDONEZ
VON KARMAN INSTITUTE FOR FLUID DYNAMICS
CHAUSSÉE DE WATERLOO, 72
B - 1640 RHODE SAINT GENÈSE, BELGIUM

MARCH 31, 1984

FINAL SCIENTIFIC REPORT, 30 APRIL 1983 - 31 JANUARY 1984

APPROVED FOR PUBLIC RELEASE; DISTRIBUTION UNLIMITED

PREPARED FOR

EUROPEAN OFFICE OF AEROSPACE RESEARCH
AND DEVELOPMENT/CA
FPO NEW YORK, 09510

SECURITY CLASSIFICATION OF THIS PAGE (When Data Entered)

REPORT DOCUMENTATION PAGE

READ INSTRUCTIONS BEFORE COMPLETING FORM

1. REPORT NUMBER	2. GOVT ACCESSION NO.	3. RECIPIENT'S CATALOG NUMBER
EOARD-TR-84-14	AD-A139 989	

4. TITLE (and Subtitle)

THE EFFECT OF STRAKES ON VORTICAL FLOWS APPLIED TO AIRCRAFT

5. TYPE OF REPORT & PERIOD COVERED
Final Scient. Rep., 30 April 83 - 31 Jan. 84

6. PERFORMING ORG. REPORT NUMBER
VKI PR 1983-22

7. AUTHOR(s)
Gustavo G. ORDONEZ

8. CONTRACT OR GRANT NUMBER(s)
AFOSR 83-0126

9. PERFORMING ORGANIZATION NAME AND ADDRESS
von Karman Institute for Fluid Dynamics,
Chaussée de Waterloo, 72,
B-1640 Rhode-Saint-Genèse, Belgium

10. PROGRAM ELEMENT, PROJECT, TASK AREA & WORK UNIT NUMBERS
P.E. 61102F
Proj/task: 2301/D1
Work Unit No. 164

11. CONTROLLING OFFICE NAME AND ADDRESS
European Office of Aerospace Research and Development/CA, Box 14,
FPO New York 09510

12. REPORT DATE
March 31, 1984

13. NUMBER OF PAGES
179

14. MONITORING AGENCY NAME & ADDRESS (if different from Controlling Office)

15. SECURITY CLASS. (of this report)

15a. DECLASSIFICATION/DOWNGRADING SCHEDULE

16. DISTRIBUTION STATEMENT (of this Report)

Approved for public release; distribution unlimited

17. DISTRIBUTION STATEMENT (of the abstract entered in Block 20, if different from Report)

18. SUPPLEMENTARY NOTES

19. KEY WORDS (Continue on reverse side if necessary and identify by block number)

Afterbodies
Vortical wakes
Strakes
Wake surveys
Drag reduction

20. ABSTRACT (Continue on reverse side if necessary and identify by block number)

The influence of strakes placed along vortical flows has been determined in order to define ways of drag reduction on wake-like flow fields present on aircraft afterbodies.

Strakes of different aspect ratio and thickness were tested at different angles of incidence with respect to a vortex path in order to evaluate the best configuration which can reduce, or minimise, the cross flow kinetic energy, thus the vortex drag of a vortical flow.

The flow field in the vicinity of the boattail of a scale cargo aircraft was studied. The aircraft was tested with and without strakes placed on its afterbody, the results confirm that when strakes are properly placed on the boattail, a reduction in drag is achievable.

EOARD-TR-84-14

This report has been reviewed by the EOARD Information Office and is releasable to the National Technical Information Service (NTIS). At NTIS it will be releasable to the general public, including foreign nations.

This technical report has been reviewed and is approved for publication.

ALBERT J. ROSA
Lt Colonel, USAF
Chief Scientist

JERRY R. BETTIS
Lt Colonel, USAF
Deputy Commander

VON KARMAN INSTITUTE FOR FLUID DYNAMICS
CHAUSSÉE DE WATERLOO, 72
B - 1640 RHODE SAINT GENÈSE, BELGIUM

PROJECT REPORT 1983-22 JUNE 1983

THE EFFECT OF STRAKES ON VORTICAL FLOWS APPLIED TO AIRCRAFT

GUSTAVO G. ORDONEZ

SUPERVISOR : M. CARBONARO

TABLE OF CONTENTS

ACKNOWLEDGEMENTS AND DEDICATION

I have the pleasure of presenting this work to my supervisor Professor Mario Carbonaro and share the credit of completing it with him. I am indebted to him for his advice, guidance, patience and willingness to help throughout the research work involved.

My thanks to Roger Conniasselle, Robert Voets and Fernand Van de Broeck for their technical support and the help they kindly offered me; their work proved to be professional par excellence at all times.
To Albin Otte, Félix Thiry and Gérard Degrez for their advice on the data acquisition and reduction programs. To Jean-Claude Lobet and Marcel Blockx whose photographic work deserves praise. Similarly to Viswanath Tata and Jean-Pierre Jeusette who contributed to the realization of this project.
To Stella Sauvan for her kind liaison help throughout the year, and to Nadine Toubeau and Louise Klinkenbergh for their helpful bibliographical services and typing done.

I gratefully acknowledge the help and support provided by the entire staff of the VKI Faculty and Personnel.

This report is dedicated to my father who, among many things, taught me about love, hard work and the pursuit of self-satisfaction in life.

ABSTRACT

The influence of strakes placed along vortical flows has been determined in order to define ways of drag reduction on wake-like flow fields present on aircraft afterbodies.

Strakes of different aspect ratio and thickness were tested at different angles of incidence with respect to a vortex path in order to evaluate the best configuration which can reduce, or minimise, the cross flow kinetic energy, thus the vortex drag of a vortical flow.

The flow field in the vicinity of the boattail of a scale cargo aircraft was studied. The aircraft was tested with and without strakes placed on its afterbody, the results confirm that when strakes are properly placed on the boattail, a reduction in drag is achievable.

LIST OF SYMBOLS

AR	$\frac{b^2}{S}$, wing aspect ratio
b	wing span
BIR	$\frac{\sqrt{(P2-P4)^2+(P1-P3)^2}}{(P5-\bar{P})}$, misalignment parameter
C_p	$\frac{P-P_\infty}{q}$, pressure coefficient
CP	$\frac{(PT-P5)}{q}$, total pressure parameter
CX	$\left[C_{p_{ang}}\left(\frac{\text{projected axial area}}{S}\right)\right]_{\text{forward facing}} - \left[C_{p_{ang}}\left(\frac{\text{projected axial area}}{S}\right)\right]_{\text{rearward facing}}$
D	wake dimension, largest distance between contour points of 1.1 Pr
DCFKE	$\frac{v^2+w^2}{U_0^2}$, dimensionless cross flow kinetic energy
D_1	component of the drag of a vortex wake
H	$\frac{(H_S-H_{WLC})}{D}$
H_s	height of strake
H_T	total head
H_{WLC}	height of wake lower core (lowest portion of Pr = 1.1 isoline)
$\bar{P}$	$\frac{(P1+P2+P3+P4)}{4}$, , average peripheral pressure
PD	$\frac{(P5-\bar{P})}{q}$, dynamic pressure parameter
P_r	$\frac{P_T}{q_\infty}$

P_s	static pressure
PT	total pressure
P1, P2, P3, P4	circumferential pressure measured by five hole probe
P5	pressure measured by the central tube in the five hole probe
P_∞	free stream pressure
q	$\frac{1}{2}\rho V^2$, dynamic pressure
s	$\frac{b}{2}$, wing semispan
S	wing area
u	flow velocity component in the x-axis
U_0, U_∞	free stream velocity
v	flow velocity component in the y-axis
V	total velocity vector
w	flow velocity component in the z-axis
x	lateral axis of the wind tunnel + left (looking upstream)
y	vertical axis of the wind tunnel + upwards
z	longitudinal axis of wind tunnel + downstream

α	angle of attack
α_r	strake angle of attack with respect to a vortex path
α_S	angle of aircraft strake referenced to boattail wake path
γ	yaw angle
θ	misalignment angle, or pitch angle
ξ	x distance downstream of delta wing trailing edge / S
ρ	density of air
ϕ	roll angle

LIST OF FIGURES

1. INTRODUCTION

1.1 Previous investigation

Wind tunnel and flight test results have shown that when strakes are mounted in the afterbody part of an aircraft (or so called "boattail") a reduction in the overall drag may be obtained.

Previous researchers have investigated the flow on afterbodies of representative fuselages of high upswept angle. Different devices such as strakes and flow deflectors have been fitted to such configurations and qualitative conclusions from visualization experiments were drawn. In some cases the effect of applying suction along the boattail area was investigated and the effects on the afterbody induced wake was as well determined qualitatively.

Although helpful, no previous work done on aircraft afterbodies could define exactly what is the effect, and its reason, when a strake is placed along a wake-like flow, or vortical flow, like the ones induced by aircraft with a large unswept boattail angle.

This prompted the desire to carry out a series of experiments at the von Karman Institute in order to define the mechanisms of action of a strake in the presence of vortical flows and its application on aircrafts as a way of drag reduction. This report describes such results.

1.2 Research steps carried out

In order to carry out our proposed projects, several steps were followed.

First, we investigated the flow field existent in an aircraft where the fuselage-boattail combination induces a vortex field.

Secondly, using a delta wing placed at a high angle of attack, the flow field downstream of its trailing edge was studied. This was done since previous research (Ref. 16) has shown that the vortex field induced by aircraft afterbodies is similar to the downstream vortex induced by separation on lifting slender delta wings at high angles of attack.

By placing strakes of different configurations along the vortex path downstream of the delta wing trailing edge, and scanning the flow behind the strakes we determined the effect of strakes in a vortical flow, and most important, defined ways of drag reduction by defining which strake configuration minimizes the vortex cross flow kinetic energy.

The above information served us to know how strakes should be placed on aircraft afterbodies. This was done and the results were validated by measuring the static pressures along the aircraft afterbody surface.

2. THEORY

2.1 Determination of vortex drag

The analysis proposed by Maskell (Ref. 5) which is an extension of the theory due to Betz to calculate the drag of a wing of finite span from a wake survey in one plane downstream of the model was adopted, in order to define what parameters on the wake-drag equation could be minimized so that its drag could be reduced.

Consider the flow generated by a lifting wing of finite span in a closed wind tunnel, where u,v,w are the x,y,z components of velocity, P_s the static pressure, H_T the total head and D the total drag of the wing. If the flow is assumed steady, incompressible and irrotational outside boundary layers and wakes the conservation of momentum equation within a control surface bounded upstream and downstream of the wake requires that

$$D = \iint \left(P_{s1}+\rho u_1^2\right) dS - \iint \left(P_{s2}+\rho u_2^2\right) dS \qquad (1)$$

This equation does not take into account the effect of pressure gradients between the control surfaces.

The total head formula is, by definition :

$$H = P_s + \frac{1}{2} \rho \, (u^2+v^2+w^2) \qquad \text{(inside wake)} \qquad (2)$$

and outside the boundary layer and wake of the wing

$$H_{T_\infty} = P_\infty + \frac{1}{2} \rho U_\infty^2 \qquad (3)$$

where U_∞, P_∞ are the velocity and static pressure of the undisturbed stream.

Substituting equations (2) and (3) into (1) for the two control planes respectively we obtain :

$$D_1 = \iint_W (H_{T_\infty} - H_{T_2})\, dS + \frac{1}{2} \iint (u_1^2 - u_2^2)\, dS$$

$$+ \frac{1}{2} \rho \iint \left[(v_2^2 + w_2^2) - (v_1^2 + w_1^2) \right] dS \qquad (4)$$

where $\iint_W$ denotes the integral over the wake region.

Equation 4 implies that the drag of a wake is proportional to the sum of the cross flow velocity components squared at the control surface downstream of the wake. Also, as the value of the U_2 velocity component approaches the undisturbed stream velocity, the second term of the RHS equation (4) is kept to a minimum.

Note that D_1 does not contain all the terms found in a detailed vortex drag equation. Reference 14 details it including wall effects and blockage terms.

3. EXPERIMENTS

3.1 Data acquisition system and methodology

All measurements were acquired by means of the data acquisition system which can be seen in figure 1a. It consists of a floppy disk driver linked to a Commodore PET computer which acquires a signal at a predetermined lapse by means of a stepping motor-scanivalve combination. The data is digitized, stored in a digital cassette and reduced by the VKI central computing system. The data is reduced as well by the PET computer and some of the results are prompted during testing in order to check the validity of the data acquired. All pressures were checked against a Betz manometer. Figure 1c shows the data acquisition schematic used for our experiments. Depending on whether it was surface static pressures or velocity field plots that we searched for, pressure taps or a five hole probe were connected into a *multiple portion scanivalve*. A Validyne MP45-1 variable reluctance transducer measured the pressure difference with respect to the tunnel static pressure. The voltage signal reached an amplifier of sufficient gain to optimize the accuracy of measurements : an analog to digital converter was placed before the PET Commodore computer.

Figures 2a and 2b show the five hole probe used for our measurements. It was supported by a traversing mechanism fixed along one of the straight walls of the test section and flow field surveys were made by displacing the probe along surface planes perpendicular to the test section. The stem which encloses the probes was aligned with the longitudinal axes of the wind tunnel. A detailed view of the five hole probe can be seen in figure 3 and the support system is shown in figure 4.

The calibration curve for the pressure transducer is shown in figure 5 showing the linearity of the instrument; its deviation is 0.5%.

Appendix I includes the data acquisition program implemented in the PET computer which was used for our tests.

3.2 Measurements using a five hole probe

Flow field measurements were done by means of a five hole probe (Figs. 2a,3) in order to obtain a quantitative description of the three dimensional flow involved in our case. This is of prime importance since we deal with vortex flows where limiting streamline pattern, smoke injection and pressure plots at the surface are not sufficient to understand the flow behaviour.

The five hole probe method of measurement was used since it can be set in a non-nulling mode of operation (i.e., the probe is inserted into the flow in a fixed attitude), and physical quantities describing the flow can be deduced from the pressures recorded by the probe.

Small measurement errors in vortical flows are expected due to the finite probe size in flow gradients, unsteady effects and probe response time.

Disturbances produced by the probe own geometry are accounted for by calibrating it in a free stream of known speed and direction. The calibration speed was the same as test conditions with pitch angle limits higher than the expected in vortex flows.

3.2.1 Calibration of the five hole probe

This type of probe enables the total local pressure and velocity vector components to be deduced from the pressures sensed by the five tubes open to the flow in a configuration shown in figure 3.

The calibration was done following a combination of the methods described by Wickens (Ref. 10) and Meineke (Ref. 7). The parameters listed below are deduced from the pressures measured by the probe. These are :

$$PD = \frac{P5-\bar{P}}{\frac{1}{2}\rho V^2}$$ dynamic pressure parameter

$$CP = \frac{PT-P5}{\frac{1}{2}\rho V^2}$$ total pressure parameter

$$PHI = \frac{P2-P4}{P1-P3}$$ roll parameter

$$BIR = \frac{\sqrt{(P2-P4)+(P1-P3)^2}}{P5-\bar{P}}$$ misalignment parameter

where P1-P4 are the pressures at the probe defined in figure 6B. These relations are sufficient to obtain a calibrated probe if the flow direction is given by the pitch angle θ, and the roll angle ϕ normal to the probe head. The actual roll flow angle can then be deduced from the relation $\tan^{-1}\frac{P2-P4}{P1-P3}$.

The pitch and roll angles and the flow direction quadrants are defined according to the convention shown in figure 6b. The calibration duct used for our probe is shown in figure 6a. By keeping its velocity constant and varying the pitch and roll angles covered by the different quadrants, the calibration data shown in figures 7-11 was finally obtained. These curves were approximated by a N degree polynomial (its degree was chosen depending on the data scatter) and input in the data reduction program. Each of the plots in figures 7-11 show the experimental data curves and points (dashed line) and the polynomial curve (solid line) which was used to approximate the data. The polynomial formulas used can be read from Table 1.

Figure 10 shows the agreement between the calculated roll angle and the one set in the calibration duct

The dynamic pressure parameter variation with respect to the roll angle can be seen in figure 11. Although not as symmetric as Wickens' results, its cyclic variation with quadrants variations is well defined.

3.2.2 Calculation of total pressure and flow velocity components

During tests, the central and circumferential pressures measured from the five hole probe were recorded. These results were used to calculate ϕ, deduce the quadrant from which the flow is coming, and the value for BIR. Knowing BIR, $|\theta|$ could be found from the calibration curves.

Secondly, the parameter PD could be obtained from the calibration polynomials. This allowed us to deduce the value of the local velocity vector using the following relation :

$$V = \sqrt{\frac{P5-\bar{P}}{\frac{1}{2}\rho\ PD}}$$

The parameter CP was then found from the calibration plots. Finally, the total local pressure could be obtained by using $PT = P5 + \frac{1}{2}\rho V^2 CP$.

The probe axis system and the Cartesian system are shown in figure 6b. The transformation formulas used were :

$$\sin|\alpha| = \sin|\theta| \times \cos|\phi|$$

$$\cos|\gamma| = \frac{\cos|\theta|}{\sqrt{1-\sin^2|\theta| \times \cos^2|\phi|}}$$

and vice versa

$$\tan|\phi| = \frac{\sin|\gamma|}{\tan|\alpha|}$$

$$\cos|\theta| = \cos|\alpha| \cdot \cos|\gamma|$$

Velocity component signs were given by knowing the flow quadrant. The quadrant numbering convention was defined as follows :

Quadrant I:	$\alpha > 0°$	$\gamma > 0°$
	P1 > P3,	P4 > P2
Quadrant II:	$\alpha > 0°$	$\gamma < 0°$
	P1 > P3,	P2 > P4
Quadrant III:	$\alpha < 0°$	$\gamma < 0°$
	P3 > P1,	P2 > P4
Quadrant IV:	$\alpha < 0°$	$\gamma < 0°$
	P3 > P1,	P4 > P2

Finally, the flow velocity components were calculated using the following relations :

$$u = V \times \cos\alpha \times \cos\gamma$$

$$v = V \times \cos\alpha \times \sin\gamma$$

$$w = V \times \sin\alpha$$

3.3 The VKI L-2A wind tunnel

The L-2A is an open return closed test section wind tunnel as shown in figure 12. The speeds at which all our measurements were taken was at 29 m/s (50 mm H_2O)). In order to ensure that the cross flow velocity irregularities present in the clean tunnel would not influence the accuracy of our experiments, two flow surveys were made at different test section stations; measurements of turbulence were carried out as well. Figure 13 shows the cross sectional view of the L-2A. The solid line bounds the area where the flow surveys were made and the dashed line is the boundary of the turbulence level measurements. All flow field and turbulent maps are shown looking upstream of the test section.

3.3.1 Flow quality

Figure 14 shows a flow field map of one of the test section stations surveyed. The magnitude of the cross flow velocities is of the order of 0.50 m/s, which gives an average flow angularity on the tunnel of about 1.0 degree. The rotational motion seen in figure 14 is thought to be inherent of tunnels of such classes. The magnitude of the cross flow velocities is small compared to the results of our experiments, therefore no large margin of error was expected. Isolines of total pressure are also shown across the test section. In case one is to compare the magnitude of the cross flow vectors by looking at the length of the arrow-vector itself, the reader should note that the cross flow vector plot of figure 14 is not plotted in the same proportion as the rest of the cross flow vector plots existing in this report.

3.3.2 Turbulence measurements

Figures 15a and 15b show turbulence levels and isolines found at the same station as the cross flow survey was done. The average percent of turbulence found at the center of the test section was of about 0.50%.

Figure 16 shows isolines of P_r, found in the L-2A test section.

Figures 17a and 17b show a schematic from the models tested during our research as they were positioned in the tunnel with the boundaries of flow quality survey and turbulence.

Geometric blockage calculations indicate that for the models tested their value was of 3%.

3.4 The aircraft model

In order to study the flow field in the vicinity of an aircraft afterbody, a 1/72 scale model of a Lockheed Hercules C-130 E was used. Figures 18a and 18b show the aircraft tested, the upswept angle at the fuselage-boattail junction is of approximately 25° and reaches values as high as 30° at the end of the boattail. Forty eight pressure taps were installed in a circumferential manner along the fuselage boattail on four different fuselage stations (12 orifices along each station) and their values measured by means of tubing installed through the aircraft wing (Fig. 57). All tests on the aircraft were done at zero degrees fuselage angle of attack. The Reynolds number of tests based on fuselage diameter was of 1.8×10^5. Transition strips which consisted of sand of height dimensions varying between .420 and .590 mm were placed along the beginning of the fuselage and on the upper surface of the wing. The first one was placed in order to ensure having turbulent flow at the afterbody; the transition strip over the wing was placed to create the correct downwash angle of the wing along the boattail.

Figure 19 shows the experimental set up as the model was installed in the test section. For measuring the static pressures on the boattail, the 48 port scanivalve placed on the lower left corner was used. The traversing mechanism seen on the right was used to displace the five hole probe.

A three view picture of a C-130 model is seen in figure 20. The side view denotes the different fuselage stations where the flow field was surveyed. Fuselage station No. 1 is located at the fuselage-afterbody junction and No. 5 is at the end of the boattail whereas No. 6 is located one fuselage diameter downstream of No. 5.

Note that fuselage station 3 of the aircraft corresponds to the same wind tunnel longitudinal station at which the flow quality survey and turbulence measurements were made.

Pressure taps were installed along fuselage stations Nos. 1,2,3,4 and their positioning can be seen in figure 57.

3.4.1 Oil smoke visualization

By inserting oil smoke upstream of the aircraft the boattail induced wake could be visualized. Such is the case of figure 21 which was taken at fuselage station No. 3. Even though photographic quality is not the best since the pictures were taken with a camera outside the test section focused on a mirror inside, the wake could clearly be seen which also gave us an estimation of the measurement domain of our flow field surveys. The smoke flow visualization results agree qualitatively with the flow field surveys using the five hole probe.

3.4.2 Flow field surveys

In the case of the C-130 where there is a high surface curvature at the junction of the fuselage side panels and the afterbody lower area, the three dimensional boundary layer flow seems to leave the surface near this junction and roll up into trailing vortices which travel along the boattail as they are swept upwards. Such is the indication of the flow field surveys starting at fuselage stations No. 1 to No. 5. A complete wake can be deduced to exist at the end of the boattail area (No. 5)

and this is validated when the flow field is surveyed downstream of the aircraft (F.S. No. 6). The measurement domain could not go higher since the horizontal tail interfered with the probe stem.

Isolines of P_r indicate two areas of pressure loss at the end of the boattail as indicated by figure 26b. The first is along the side of the boattail and the second of slightly less loss, is a bluff wake which leaves the fuselage right behind it. When isolines of cross flow kinetic energy are plotted non dimensionalized with respect to the free stream velocity squared, the location of the wakes is more easily deduced, as shown in figure 26c.

The flow field survey downstream of the boattail (Fig. 27a) shows the final geometry of the wake as it leaves the aircraft in conjunction with other small wakes like the one near the vertical tail. Isolines of P_r (Fig. 27b) denote two areas of large pressure loss which probably are the boattail induced trailing vortex, and the bluff wake which leaves the aircraft through the corner of the end of the boattail.

Figure 27c agrees with the previous figure by locating the position of the boattail induced vortex with isolines of cross flow kinetic energy.

3.4.3 Limiting streamlines visualization

Limiting streamlines visualizations was done by mixing talc, oleic acid, titanium dioxide, gasoline and oil and placing small dots on the afterbody surface. Figure 28a shows the top view of the aircraft, where limiting streamlines travelling close together tend to separate in different directions. Figure 28b gives an idea of the embracing of the flow over the boattail as well as the downwash angle induced by the wing. Two separation lines can be seen, one at the side-panel-bottom junction and the other which is also seen in figure 28c,

corresponding to the bluff wake that leaves the boattail through the afterbody corner. Note on figure 28c the result of stagnated flow present on the upper end of the boattail; some of the mixture used to visualize the limiting streamlines did not move.

3.5 The delta wing

A delta wing of aspect ratio = 1.0 (Fig. 29) placed at 20° angle of attack was positioned on a flat plate and tested in the wind tunnel.

3.5.1 Flow field surveys downstream of it

Surveys were made in order to determine the position of the vortex path as it travels downstream. Figures 30a,b,c show the flow field, P_r and CFKE isolines of a plane $\xi = 0.625$ downstream of the trailing edge. Figures 31a,b show the cross flow field and CFKE values of a plane $\xi = 1.875$ downstream of the trailing edge.

Results of the flow field survey at $\xi = 2.5$ are shown in figures 32a,b and c. The control plane has been increased compared to the ones shown in figures 30 and 31.

The $\xi = 2.5$ station is the basis for our analysis when we will compare these results against the same control plane but having strakes placed before it.

3.5.2 Vortex core travel path

Figure 33 shows the travel path that the delta wing induced vortex follows as it leaves the trailing edge. Note that the helix makes an angle with respect to the momentum flow direction and that as it travels downstream it tends to curve referenced to the tunnel axis. The height of the vortex core is approximately constant as it moves downstream.

3.6 Strakes placed downstream of the delta wing

3.6.1 Thin strakes

Different strake configurations were placed downstream of the delta wing, and pivoted at $\xi = 1.25$, in order to change the angle of incidence with respect to the incoming vortex.

Figure 34 shows how strakes were placed on the flat plate and their position with respect to the wing. The flow field downstream of the strake was studied (at the $\xi = 2.50$ plane).

Measurements of static pressures on the strake surfaces were also done.

Figure 35 shows the different strake configurations that were tested. Water tunnel flow visualization studies were made by placing a delta wing of AR = 1 at 20° angle of attack and observing the vortex path and the field downstream of the strakes qualitatively. Figure 36 shows the set up used. The vortex formed by the delta wing leading edge separation as it travels downstream was observed and strakes were positioned along the path.

The height of the strake was chosen so that it would reach three different levels of H (as defined in figure 37). If we look upstream on the P_r isolines plot of figure 32b, wake dimension D is the distance from the vortex core to the $P_r = 1.1$ isoline (the largest). Therefore H = 0 when the strake reaches $P_r = 1.1$ on the lower side and 1.0 when it reaches the highest point along the curve, H = 0.5 when the height of the strake reaches the vortex core. The angle of attack sign can be defined in the conventional way. It is positive when the leading edge of the strake is moved right and negative when it moves left. The zero alpha position was when the strake is aligned and in the center of the vortex path.

Figure 38 shows that when the strake H = 0 is placed at a negative angle, as the helix moves along the strake the lower part of the vortex which cannot jump to the other side continues having a vortical type motion, but the flow coming out of the forward facing side is streamlined as a result of not having rotational energy or vorticity contributed by the flow on the opposite side of the strake.

The same sort of effect is present when $\alpha_r = 0$, although the streamlined flow has changed positions and the main vortex core has been displaced.

For positive incidence, the appearance of an opposite direction vortex field from the main appears in the lower right corner with small values for its cross velocities. For negative incidences, the values of the velocities are higher than for angles of zero or above.

The same trend is followed by strakes of ratio H = 0.5 (Figs. 41-43) although the magnitude of their cross flow velocities is smaller than for the H = 0 case, especially when $\alpha_r = 0$, which produces a streamlining effect clearly noticed.

At positive angles of attack, a double vortex is definitely present which reduces the magnitude of opposite direction velocities of the velocity vector integral, thus reducing the vortex energy loss.

Water tunnel visualization for H = 0.5 strake is shown in figure 44 which confirms the result shown by the cross flow velocity components plots : an existing vortex is still present at $\alpha_r = -15$ and is streamlined as $\alpha_r = 0$; at positive angles of attack, part of the vortex flow is redirected due to the influence of the strake presence and still maintains vortex motion, and the other plot "jumps over" (Fig. 44b) the strake with its core finding a new equilibrium position near the lower corner of the control plane.

Similar observations are found for strakes of H = 1.0 (Figs. 45-47) with the difference that the velocity components are higher than H = 0.5 and H = 0 expect for α_r = -15°. Strakes of H = 1.0 have a wider area of pressure loss where a vortex core is present. This can be observed on the P_r isoline plots.

Water tunnel visualization for strakes of different H and constant α is seen in figure 48. For the case of strake placed in the lower edge of the vortex, the wing induced vortex does not get influenced as much as the other two cases do. For the H = 1.0 case the vortex impinges on the forward facing surface and does create a more disorganized flow than the H = 0.5 case.

3.6.2 Thick strakes

In order tc evaluate the effect of thickness on the cross flow kinetic energy, strakes of H = 0.5 ratio were tested at different angles of attack. The resultant flow field agrees in trend and in approximate magnitude with the thin strakes placed at similar incidences. Results show that at α_r = 0 the flow field is much more streamlined than α_r = -15 and that for α_r = 15° a double vortex formation of opposite velocity direction occurs.

3.7 Pressure measurements on strakes

Figure 52 shows the three different thick strake configurations that were tested and where static pressure measurements were made on each surface. The reason for these measurements was to find out which strake configuration bends providing a reduction in CFKE, would at the same time create lift or favourable force along its axis.

Figures 53,54 and 55 show pressure distribution for H = 0, 0.5, 1.0 strakes at three different angles of attack.

The results are similar for the three strake configurations. This implies that the height of the strakes is irrelevant for its pressure sensed. When strakes are placed at angles of attack with respect to the incoming vortex of 0° or less, the net result is an increase in lift, which as a result provides an increase in thrust along the strake axis.

Calculations of lift integrals are not possible since the amount of pressure drop was not considered enough. The results, though, give an indication of how a strake works.

3.8 Aircraft model with strakes mounted on its boattail

3.8.1 Criteria for placing the afterbody strakes

Although it will be discussed in detail in the conclusion section, integrals of DCFKE for all strake configurations tested indicate that CFKE is lowest for strakes of $H = 0.5$ and for $\alpha_r = 15°$.

In order to place strakes along the boattail of the aircraft, the location of the wake and its distance from the fuselage had to be found.

Figure 56a shows the wake path along the boattail area as it moves downstream. With that information at hand, a pair of strakes of the same height/length ratio as the ones tested were built whose height when positioned on the boattail, reached the afterbody wake core (Fig. 56b).

The strakes were placed at an $\alpha = 15$ with respect to the wake core and supported to the nearest pressure tap hole. This allowed us to check the pressure measured by the strake and compare that to the pressures obtained in the delta wing-strake combination set up. Besides, the static pressures along the boattail including strakes were measured as shown by figure 57.

Although the best overall configuration (lowest CFKE, highest lift) would be H = 0.5, α_r = 0 strake, α_s = 15° were used in order to validate the CFKE criteria on which our investigation was based.

The location along the fuselage where strakes were placed was arbitrarily chosen along the region where the primary separation line was found from the limiting streamlines visualization.

Figures 58a,b show how strakes were placed along the boattail and their angle with respect to the afterbody lines.

3.9 Limiting streamlines visualization

Limiting streamlines flow visualization of the aircraft with strakes is shown in figure 59. Figure 59a shows how the strake delays the primary separation line; figure 59b shows that the downwash angle along the boattail is reduced, streamlining the flow, probably due to the pressure field induced by the strake. Figure 59c compared to limiting streamlines without strakes shows that the flow is attached to the boattail as it reaches the end of the afterbody area, eliminating the pressure loss and wake induced by the afterbody alone.

3.9.1 Pressure measurements in the aircraft strake

The pressure measured by the strakes placed on the aircraft (Fig. 54c) agree with the results obtained from the pressure measurements study; that is, the strake feels a negative lift on its surface. Its value agree closely with the ones measured on the flat-plate-delta-wing-strake set up.

4. ANALYSIS OF RESULTS

4.1 On strakes

Besides the observations noted earlier on the flow fields some analysis is considered necessary by looking at figure 60. It shows the values of the cross flow kinetic energy obtained for different strake ratios H and different angles of attack. For all ratios of H, the CFKE is lowest at positive angle of attack.

The values of CFKE obtained with a thick strake of H = 0.5 are close to those obtained with a thin strake. Also the resultant flow field induced by a thick strake is similar in trends, and close in magnitude of velocity vectors to the one obtained by a thin strake. This allows us to conclude that the pressure distribution on strakes and their behaviour along a vortex is similarly independent of its thick ones.

4.2 On the pressure distribution along the boattail

The pressure distribution along the aircraft boattail with and without strakes is shown in figure 61. It shows that by properly placing strakes on it, the pressure on the afterbody increases. In other words an extra "push" or "thrust" is created due to the effect induced by the strakes on the surface. The extra axial force obtained when strakes are placed on the surface was found by multiplying the wedge pressure of each tap by the projected boattail area of each hole, which was chosen by drawing centerlines along mid distance points between taps. It was found to be 23% extra. This force is subtracted from the total drag of the aircraft. An estimated reduction in drag for a typical cargo aircraft would be of approximately 0.004 Cx under the conditions described in this section.

5. UNCERTAINTY ANALYSIS

Measurement errors as a result of instrumentation inaccuracies as well as test conditions fluctuations were deduced from calibration curves, and by monitoring deviations that occurred on certain test parameters.

5.1 Accuracy range of equipment used

All pressure measurements were calibrated against a Betz manometer whose accuracy is within ± 0.1 mm H_2O. The deviation of the pressure transducer used for the probe and surface pressures is of 0.5%.

Variations in the tunnel velocity were kept to ± 0.2 mm H_2O with set test conditions.

Pressure variations in the five hole probe tubes when being calibrated were of about 1.0 mm H_2O.

Angle settings in the calibration duct could be easily set within 0.2°.

5.2 Error margins in test data

From the five hole probe calibration data we can deduce its roll and pitch angle deviation. The accuracy of the roll angle is within 2.5° at low values of θ and of 0.89° at larger settings. The probe misalignment angle is as low as 0.4° and a maximum of 2.5°.

From flow quality measurements, the flow angularity of the wind tunnel was found to be of about 1°.

Static pressure coefficients measured on the aircraft boattail and on the strakes surfaces varied within ± 0.05 of C_p.

6. CONCLUSIONS

The main conclusions which can be drawn from this study are :

Aircraft which have a highly upswept afterbody induce a wake-like flow which leaves the boattail as it moves upward.

Strakes, when placed along the path of a vortex, streamline the flow, thus its cross flow kinetic energy is reduced.

When strakes are placed at positive incidence, the resultant flow field downstream of it includes two vortices of opposite direction. By that, the cross flow velocity components integral is reduced.

Strakes provide lift when placed at angles of attack of zero or lower than zero with respect to the vortex path. Therefore, a thrust is created.

When strakes are placed at angles of attack equal or greater than zero, a reduction in the cross flow kinetic energy occurs. Therefore, the vortex drag is also reduced.

Strakes placed properly on an airplane boattail reduce its overall drag by increasing the static pressure in the afterbody surface.

REFERENCES

1. TAYLOR, J.W.R.: Jane's all the world's aircraft.
   New York, McGraw-Hill Book Co., 1981.

2. PEAKE, D.J. & TOBAK, M.: Three dimensional interactions and vortical flows with emphasis in high speeds.
   AGARDograph 252, July 1980.

3. BATCHELOR, G.K.: An introduction to fluid dynamics.
   Cambridge, Cambridge University Press, 1967.

4. SCHLICHTING, H.: Boundary layer theory.
   New York, McGraw-Hill Book Co., 1972.

5. MASKELL, E.C.: Progress towards a method for the measurement of the components of the drag of wings of finite span.
   RAE TR 72232, January 1973.

6. MacWILKINSON, D.G.; BLACKERBY, W.T.; PATERSON, J.H.: Correlations of full-scale drag prediction with flight measurements on the C-141A aircraft - Phase II - Wind tunnel test, analysis, and prediction techniques.
   Vol. I - NASA CR 2333, Feburary 1974
   Vol. II - NASA CR 2334, February 1974.

7. MEINEKE, E.: Measurements in the wake of a sideslipping wing.
   VKI TN 143, June 1982.

8. BRADSHAW, A.L.; HICKS, R.M.; HARRIS, R.V.: Use of grit-type boundary layer transition trips on wind tunnel models.
   NASA TN-D 3579, September 1966.

9. HACKETT, J.E. & BOLES, R.A.: High lift testing in closed wind tunnels.
   AIAA Paper 74-641, July 1974.

10. WICKENS, R.H.: Observations of the vortex wake of a lifting fuselage similar to those on near-loading transport aircraft.
    NRC LR 395, January 1974.

11. PEAKE, D.J.: The flows about upswept rear fuselages of typical cargo aircraft.
    NRC Report DME/NAE 1968/3, July-September 1968.

12. POPE, A. & HARPER, J.J.: Low speed wind tunnel testing.
    New York, Wiley, 1966.

13. HUMMEL, D.: On the vortex formation over a slender wing at large angles of incidence. In: "High Angle of Attack Aerodynamics", AGARD CP 247, 1978, pp 15-1/15-7.

14. WU, J.C.; HACKETT, J.E.; LILLEY, D.E.: A generalized wake-integral approach for drag determination in three dimensional flows. AIAA Paper 79-0279, January 1979.

15. WICKENS, R.; SOUTH, P.; RANGI, R.S.; HENSHAW, D.: Experimental developments in V/STOL wind tunnel testing at the National Aeronautical Establishment. Canadian Aeronautics and Space Journal, Vol. 19, No. 4, April 1973, pp 145-154.

16. RAINBIRD, W.J.; GRABLE, R.S.; PEAKE, D.J.; MEYER, R.F.: Some examples of separation in three-dimensional flows. Canadian Aeronautics and Space Journal, Vol. 12, No. 10, December 1966, pp 409-423.

Quadrant	Independent variable i.e. y	Dependent variable i.e. x	A_0	A_1	A_2	A_3	A_4	A_5	A_6
I	θ	BIR	-0.8374	12.1226	2.3296	-3.2299	1.2841	-2.2683E-1	1.899E-2
	PD	θ	5.8333E-1	2.8778E-3	-1.6356E-4	-1.4225E-5	6.9290E-7	-8.8531E-9	
	CP	θ	7.5369E-4	- 8.1303E-4	-2.0669E-5	2.8294E-5	-4.9759E-7	2.3290E-9	
II	θ	BIR	-0.7472	21.5309	-13.9469	8.9530	-3.2487	5.9037E-1	-4.1485E-2
	PD	θ	5.9093E-1	8.1935E-4	- 6.7776E-5	-5.9604E-6	-1.5378E-7	1.6539E-8	-2.3476E-10
	CP	θ	9.7776E-4	- 3.2565E-3	1.2137E-3	-1.4361E-4	8.7681E-6	-2.1725E-7	1.9070E-9
III	θ	BIR	0.4942	17.2669	- 8.7556	5.7489	-2.1487	3.9653E-1	-2.8316E-2
	PD	θ	5.952E-1	7.5598E-5	1.5644E-4	-4.3459E-5	2.1625E-6	-4.3810E-8	3.2467E-10
	CP	θ	1.4027E-3	- 2.8369E-3	6.1998E-4	-3.4554E-5	1.6512E-6	-2.5172E-8	7.8316E-11
	θ	BIR	-1.2412	13.7286	- 2.1122E-1	-0.9420	2.9331E-1	2.6975E-2	
	PD	θ	5.8701E-1	4.46614E	- 3.9905E-4	-5.3629E-6	5.5383E-7	-7.4054E-9	
	CP	θ		7.0658E-4	- 3.0324E-4	4.8346E-5	-1.4304E-6	2.6121E-8	-2.3198E-10

i.e. $y = A_0 + A_1X + A_2X^2 + A_3X^3 + A_4X^4 + A_5X^5 + A_6X^6$

TABLE I - FIVE HOLE PROBE CALIBRATION COEFFICIENTS

TABLE II

T1 - Flow field velocity vectors tabulation for figure 32a (ξ = 2.5)

T2 - Flow field velocity vectors tabulation for figure 27a (F.S. 6)

Note in all cases, figures are shown looking upstream.

The y-axis increases to the left, and z-axis increases upwards.

The data columns are tabulated in y,z,v,w order

	T1		a
0.281246E-38	0.000000E+00	0.000000E+00	0.000000E+00
0.000000E+00	0.000000E+00	-0.489421E+01	0.185642E+01
0.500000E+01	0.000000E+00	-0.640392E+01	0.225254E+01
0.100000E+02	0.000000E+00	-0.890712E+01	0.307333E+01
0.150000E+02	0.000000E+00	-0.120001E+02	0.287519E+01
0.200000E+02	0.000000E+00	-0.151678E+02	0.139398E+01
0.250000E+02	0.000000E+00	-0.167753E+02	-0.145386E+01
0.300000E+02	0.000000E+00	-0.163984E+02	-0.391138E+01
0.350000E+02	0.000000E+00	-0.135386E+02	-0.656994E+01
0.400000E+02	0.000000E+00	-0.100448E+02	-0.681741E+01
0.450000E+02	0.000000E+00	-0.654021E+01	-0.608125E+01
0.500000E+02	0.000000E+00	-0.461764E+01	-0.605663E+01
0.550000E+02	0.000000E+00	-0.223438E+01	-0.568555E+01
0.600000E+02	0.000000E+00	-0.223429E-01	-0.567128E+01
0.600000E+02	0.500000E+01	0.846999E-01	-0.693252E+01
0.550000E+02	0.500000E+01	-0.198367E+01	-0.701752E+01
0.500000E+02	0.500000E+01	-0.437374E+01	-0.742911E+01
0.450000E+02	0.500000E+01	-0.676640E+01	-0.843786E+01
0.400000E+02	0.500000E+01	-0.987010E+01	-0.846009E+01
0.350000E+02	0.500000E+01	-0.146982E+02	-0.857110E+01
0.300000E+02	0.500000E+01	-0.174721E+02	-0.521012E+01
0.250000E+02	0.500000E+01	-0.170594E+02	-0.156419E+01
0.200000E+02	0.500000E+01	-0.164821E+02	0.261006E+01
0.150000E+02	0.500000E+01	-0.121142E+02	0.475672E+01
0.100000E+02	0.500000E+01	-0.862345E+01	0.462810E+01
0.500000E+01	0.500000E+01	-0.573374E+01	0.325824E+01
0.000000E+00	0.500000E+01	-0.410435E+01	0.295291E+01
0.000000E+00	0.100000E+02	-0.301761E+01	0.425467E+01
0.500000E+01	0.100000E+02	-0.447548E+01	0.555704E+01
0.100000E+02	0.100000E+02	-0.723234E+01	0.823891E+01
0.150000E+02	0.100000E+02	-0.107572E+02	0.942979E+01
0.200000E+02	0.100000E+02	-0.158725E+02	0.619174E+01
0.250000E+02	0.100000E+02	-0.174857E+02	-0.835138E+00
0.300000E+02	0.100000E+02	-0.160712E-03	0.682364E-04
0.350000E+02	0.100000E+02	0.815281E-01	-0.457475E-01
0.400000E+02	0.100000E+02	-0.898685E+01	-0.137215E+02
0.450000E+02	0.100000E+02	-0.566204E+01	-0.117244E+02
0.500000E+02	0.100000E+02	-0.342753E+01	-0.990621E+01
0.550000E+02	0.100000E+02	-0.155106E+01	-0.879629E+01
0.600000E+02	0.100000E+02	0.180791E-01	-0.888802E+01
0.600000E+02	0.150000E+02	-0.437092E+00	-0.101366E+02
0.550000E+02	0.150000E+02	-0.101356E+01	-0.104284E+02
0.500000E+02	0.150000E+02	-0.200848E+01	-0.116875E+02
0.450000E+02	0.150000E+02	-0.322539E+01	-0.146029E+02
0.400000E+02	0.150000E+02	-0.527455E+01	-0.176268E+02
0.350000E+02	0.150000E+02	0.000000E+00	0.000000E+00
0.300000E+02	0.150000E+02	-0.129704E-12	-0.120900E-12
0.250000E+02	0.150000E+02	-0.176122E+02	-0.194824E+00
0.200000E+02	0.150000E+02	-0.118382E+02	0.121132E+02
0.150000E+02	0.150000E+02	-0.638275E+01	0.138097E+02
0.100000E+02	0.150000E+02	-0.408354E+01	0.110528E+02
0.500000E+01	0.150000E+02	-0.265381E+01	0.700973E+01
0.000000E+00	0.150000E+02	-0.140799E+01	0.504675E+01
0.000000E+00	0.200000E+02	-0.328756E+00	0.536977E+01
0.500000E+01	0.200000E+02	-0.331271E+00	0.780777E+01
0.100000E+02	0.200000E+02	-0.878354E-01	0.111731E+02
0.150000E+02	0.200000E+02	0.545726E+00	0.154941E+02
0.200000E+02	0.200000E+02	0.130574E+01	0.155904E+02
0.250000E+02	0.200000E+02	0.328037E+00	0.137044E+02
0.300000E+02	0.200000E+02	0.000000E+00	0.000000E+00
0.350000E+02	0.200000E+02	0.263810E+00	-0.146234E+02
0.400000E+02	0.200000E+02	0.522187E+00	-0.175374E+02
0.450000E+02	0.200000E+02	0.157355E+00	-0.149822E+02

T1 6

0.500000E+02	0.200000E+02	-0.169765E+00	-0.122206E+02
0.550000E+02	0.200000E+02	0.159557E-01	-0.109306E+02
0.600000E+02	0.200000E+02	-0.974652E-01	-0.105231E+02
0.600000E+02	0.250000E+02	-0.117867E+00	-0.104715E+02
0.550000E+02	0.250000E+02	0.545277E+00	-0.107697E+02
0.500000E+02	0.250000E+02	0.148181E+01	-0.117404E+02
0.450000E+02	0.250000E+02	0.288634E+01	-0.138184E+02
0.400000E+02	0.250000E+02	0.531110E+01	-0.155393E+02
0.350000E+02	0.250000E+02	0.111047E+02	-0.129317E+02
0.300000E+02	0.250000E+02	0.000000E+00	0.000000E+00
0.250000E+02	0.250000E+02	0.133890E+02	0.657068E+01
0.200000E+02	0.250000E+02	0.120322E+02	0.136375E+02
0.150000E+02	0.250000E+02	0.684936E+01	0.116924E+02
0.100000E+02	0.250000E+02	0.325763E+01	0.923636E+01
0.500000E+01	0.250000E+02	0.218704E+01	0.652374E+01
0.000000E+00	0.250000E+02	0.599748E+00	0.498070E+01
0.000000E+00	0.300000E+02	0.138933E+01	0.411382E+01
0.500000E+01	0.300000E+02	0.283967E+01	0.481115E+01
0.100000E+02	0.300000E+02	0.530035E+01	0.566391E+01
0.150000E+02	0.300000E+02	0.959132E+01	0.597233E+01
0.200000E+02	0.300000E+02	0.139584E+02	0.683453E+01
0.250000E+02	0.300000E+02	0.174849E+02	0.380635E+01
0.300000E+02	0.300000E+02	0.167891E+02	-0.238385E+01
0.350000E+02	0.300000E+02	0.115837E+02	-0.767463E+01
0.400000E+02	0.300000E+02	0.710935E+01	-0.105896E+02
0.450000E+02	0.300000E+02	0.424939E+01	-0.108388E+02
0.500000E+02	0.300000E+02	0.237894E+01	-0.102314E+02
0.550000E+02	0.300000E+02	0.920225E+00	-0.984809E+01
0.600000E+02	0.300000E+02	0.786076E-01	-0.941791E+01
0.600000E+02	0.350000E+02	-0.119692E+00	-0.826670E+01
0.550000E+02	0.350000E+02	0.971023E+00	-0.872025E+01
0.500000E+02	0.350000E+02	0.251164E+01	-0.867117E+01
0.450000E+02	0.350000E+02	0.409627E+01	-0.860613E+01
0.400000E+02	0.350000E+02	0.626022E+01	-0.782527E+01
0.350000E+02	0.350000E+02	0.893235E+01	-0.492036E+01
0.300000E+02	0.350000E+02	0.108577E+02	-0.176532E+01
0.250000E+02	0.350000E+02	0.114386E+02	0.198939E+01
0.200000E+02	0.350000E+02	0.104665E+02	0.223992E+01
0.150000E+02	0.350000E+02	0.791230E+01	0.250389E+01
0.100000E+02	0.350000E+02	0.541070E+01	0.349615E+01
0.500000E+01	0.350000E+02	0.294009E+01	0.339104E+01
0.000000E+00	0.350000E+02	0.162448E+01	0.330198E+01
0.000000E+00	0.400000E+02	0.173825E+01	0.244061E+01
0.500000E+01	0.400000E+02	0.337346E+01	0.298856E+01
0.100000E+02	0.400000E+02	0.447207E+01	0.246509E+01
0.150000E+02	0.400000E+02	0.530318E+01	0.140004E+01
0.200000E+02	0.400000E+02	0.576823E+01	0.123306E+01
0.250000E+02	0.400000E+02	0.665331E+01	0.102358E+00
0.300000E+02	0.400000E+02	0.719962E+01	-0.157119E+01
0.350000E+02	0.400000E+02	0.620966E+01	-0.366107E+01
0.400000E+02	0.400000E+02	0.493597E+01	-0.545978E+01
0.450000E+02	0.400000E+02	0.349486E+01	-0.672558E+01
0.500000E+02	0.400000E+02	0.192274E+01	-0.689334E+01
0.550000E+02	0.400000E+02	0.739627E+00	-0.721178E+01
0.600000E+02	0.400000E+02	-0.411372E-01	-0.714743E+01

T2

		a	F/b
0.826541E-30	0.200000E+01	0.000000E+00	0.000000E+00
0.000000E+00	0.000000E+00	0.178925E+00	-0.715443E-01
0.500000E+01	0.000000E+00	0.273659E+00	-0.234614E+00
0.100000E+02	0.000000E+00	0.163090E+00	-0.163530E+00
0.150000E+02	0.000000E+00	0.199394E+00	-0.299370E+00
0.200000E+02	0.000000E+00	0.265782E+00	-0.379780E-01
0.250000E+02	0.000000E+00	0.484370E-01	0.650146E-07
0.300000E+02	0.000000E+00	0.250619E+00	-0.212269E+00
0.350000E+02	0.000000E+00	0.844825E-01	-0.842381E-01
0.400000E+02	0.000000E+00	-0.170995E+00	-0.274320E+00
0.450000E+02	0.000000E+00	-0.170326E+00	-0.272745E+00
0.500000E+02	0.000000E+00	0.000000E+00	0.000000E+00
0.550000E+02	0.000000E+00	0.000000E+00	0.000000E+00
0.600000E+02	0.000000E+00	0.000000E+00	-0.168856E+00
0.650000E+02	0.000000E+00	0.965328E-01	-0.803679E-01
0.650000E+02	0.500000E+01	-0.145915E+00	-0.182999E+00
0.600000E+02	0.500000E+01	0.113649E+00	-0.488356E-01
0.550000E+02	0.500000E+01	0.130455E+00	-0.327479E+00
0.500000E+02	0.500000E+01	0.203679E+00	-0.237738E+00
0.450000E+02	0.500000E+01	0.277649E+00	-0.493607E+00
0.400000E+02	0.500000E+01	0.263693E+00	-0.296661E+00
0.350000E+02	0.500000E+01	0.666144E-01	-0.340994E+00
0.300000E+02	0.500000E+01	-0.186278E+00	-0.528327E+00
0.250000E+02	0.500000E+01	0.273514E+00	-0.608200E+00
0.200000E+02	0.500000E+01	0.338728E+00	-0.796950E-01
0.150000E+02	0.500000E+01	0.160717E+00	-0.451041E+00
0.100000E+02	0.500000E+01	0.653488E-01	-0.426883E+00
0.500000E+01	0.500000E+01	0.386926E-01	0.406493E-01
0.000000E+00	0.500000E+01	0.268075E+00	-0.153316E+00
0.000000E+00	0.100000E+02	0.507260E+00	-0.202913E+00
0.500000E+01	0.100000E+02	0.113340E+00	0.148649E-06
0.100000E+02	0.100000E+02	0.154700E+00	-0.558033E+00
0.150000E+02	0.100000E+02	0.166579E+00	-0.367294E+00
0.200000E+02	0.100000E+02	0.320283E+00	-0.100151E+00
0.250000E+02	0.100000E+02	0.144492E+00	-0.217160E+00
0.300000E+02	0.100000E+02	0.371381E+00	-0.782406E-01
0.350000E+02	0.100000E+02	0.783698E-01	-0.473920E-01
0.400000E+02	0.100000E+02	0.000000E+00	0.000000E+00
0.450000E+02	0.100000E+02	0.279060E+00	-0.259382E+00
0.500000E+02	0.100000E+02	0.000000E+00	0.000000E+00
0.550000E+02	0.100000E+02	0.323259E-01	-0.278130E+00
0.600000E+02	0.100000E+02	0.133259E+00	-0.333197E+00
0.650000E+02	0.100000E+02	0.711294E-01	-0.252185E+00
0.650000E+02	0.150000E+02	-0.489784E-01	-0.505186E-01
0.600000E+02	0.150000E+02	0.224478E+00	-0.353085E+00
0.550000E+02	0.150000E+02	0.624406E-01	-0.506279E+00
0.500000E+02	0.150000E+02	-0.329392E-01	-0.477706E+00
0.450000E+02	0.150000E+02	-0.622689E-01	-0.567687E+00
0.400000E+02	0.150000E+02	0.186045E+00	-0.744313E-01
0.350000E+02	0.150000E+02	0.533755E-01	0.136391E-01
0.300000E+02	0.150000E+02	0.189901E+00	-0.133164E+00
0.250000E+02	0.150000E+02	0.000000E+00	0.000000E+00
0.200000E+02	0.150000E+02	0.000000E+00	-0.370044E-03
0.150000E+02	0.150000E+02	0.532369E-01	0.705946E-07
0.100000E+02	0.150000E+02	0.309865E-01	-0.626314E+00
0.500000E+01	0.150000E+02	0.249571E+00	0.383870E-01
0.000000E+00	0.150000E+02	0.232216E+00	-0.213021E+00
0.000000E+00	0.200000E+02	0.296470E+00	-0.329365E+00
0.500000E+01	0.200000E+02	0.116903E+00	0.167932E-01
0.100000E+02	0.200000E+02	0.103047E+00	-0.309419E+00
0.150000E+02	0.200000E+02	0.530428E-01	0.133912E-01
0.200000E+02	0.200000E+02	0.341360E+00	-0.527669E+00
0.250000E+02	0.200000E+02	0.234317E+00	-0.117278E+00

T2 6

0.300000E+02	0.200000E+02	-0.224996E+00	-0.450269E+00
0.350000E+02	0.200000E+02	0.455706E-01	-0.139265E+00
0.400000E+02	0.200000E+02	0.667254E-01	-0.400295E+00
0.450000E+02	0.200000E+02	-0.214383E+00	-0.644401E+00
0.500000E+02	0.200000E+02	-0.263764E+00	-0.329948E+00
0.550000E+02	0.200000E+02	-0.200042E+00	-0.333443E+00
0.600000E+02	0.200000E+02	-0.505497E-01	-0.516735E-01
0.650000E+02	0.200000E+02	0.901428E-01	0.151977E-01
0.650000E+02	0.250000E+02	-0.645090E-01	-0.421910E+00
0.600000E+02	0.250000E+02	-0.167118E+00	-0.313632E-01
0.550000E+02	0.250000E+02	0.000000E+00	0.000000E+00
0.500000E+02	0.250000E+02	0.235603E+00	-0.176877E+00
0.450000E+02	0.250000E+02	0.000000E+00	0.000000E+00
0.400000E+02	0.250000E+02	0.283724E+00	-0.409880E+00
0.350000E+02	0.250000E+02	0.326484E-01	0.110205E-01
0.300000E+02	0.250000E+02	0.000000E+00	0.373133E-01
0.250000E+02	0.250000E+02	0.000000E+00	-0.166445E-02
0.200000E+02	0.250000E+02	0.127721E+00	-0.127268E+00
0.150000E+02	0.250000E+02	0.000000E+00	0.000000E+00
0.100000E+02	0.250000E+02	0.000000E+00	0.000000E+00
0.500000E+01	0.250000E+02	0.250782E+00	-0.135267E+00
0.000000E+00	0.250000E+02	0.398089E+00	0.398086E-01
0.000000E+00	0.300000E+02	0.198378E+00	0.282090E+00
0.500000E+01	0.300000E+02	0.274497E+00	0.176514E+00
0.100000E+02	0.300000E+02	0.267873E+00	0.382694E-01
0.150000E+02	0.300000E+02	0.389238E+00	0.266418E+00
0.200000E+02	0.300000E+02	0.799297E-01	0.103443E+00
0.250000E+02	0.300000E+02	0.825003E-01	-0.165319E+00
0.300000E+02	0.300000E+02	0.721991E-01	-0.253500E+00
0.350000E+02	0.300000E+02	0.000000E+00	0.000000E+00
0.400000E+02	0.300000E+02	0.704415E-01	-0.284012E+00
0.450000E+02	0.300000E+02	-0.136529E+00	-0.684757E-01
0.500000E+02	0.300000E+02	-0.313472E-01	0.127957E-01
0.550000E+02	0.300000E+02	0.289129E+00	-0.385877E+00
0.600000E+02	0.300000E+02	0.000000E+00	-0.455047E+00
0.650000E+02	0.300000E+02	-0.262020E+00	-0.327769E+00
0.650000E+02	0.350000E+02	-0.908001E-01	-0.731660E+00
0.600000E+02	0.350000E+02	0.129160E+00	-0.485584E+00
0.550000E+02	0.350000E+02	0.155767E+00	-0.623426E+00
0.500000E+02	0.350000E+02	-0.403748E+00	-0.151440E+00
0.450000E+02	0.350000E+02	-0.127464E-01	-0.101192E-01
0.400000E+02	0.350000E+02	-0.294348E+00	0.232650E+00
0.350000E+02	0.350000E+02	0.000000E+00	0.136714E-01
0.300000E+02	0.350000E+02	-0.266765E-01	-0.151335E-01
0.250000E+02	0.350000E+02	-0.939202E-01	0.160806E+00
0.200000E+02	0.350000E+02	0.519784E-01	0.618914E-01
0.150000E+02	0.350000E+02	0.249560E+00	0.428160E+00
0.100000E+02	0.350000E+02	0.000000E+00	0.000000E+00
0.500000E+01	0.350000E+02	0.124507E+00	0.106928E+00
0.000000E+00	0.350000E+02	0.765597E-01	0.141150E+00
0.000000E+00	0.400000E+02	0.485108E-01	0.585320E-01
0.500000E+01	0.400000E+02	0.438788E+00	0.376048E+00
0.100000E+02	0.400000E+02	0.176510E-01	0.433415E+00
0.150000E+02	0.400000E+02	0.463101E-01	0.128322E+00
0.200000E+02	0.400000E+02	-0.598026E-01	0.418239E-01
0.250000E+02	0.400000E+02	-0.753788E-01	0.866844E-01
0.300000E+02	0.400000E+02	0.000000E+00	0.000000E+00
0.350000E+02	0.400000E+02	0.000000E+00	0.000000E+00
0.400000E+02	0.400000E+02	0.326085E-01	0.674491E-01
0.450000E+02	0.400000E+02	0.000000E+00	0.000000E+00
0.500000E+02	0.400000E+02	0.000000E+00	-0.228192E-02
0.550000E+02	0.400000E+02	0.368502E-01	-0.255035E-01
0.600000E+02	0.400000E+02	-0.373289E+00	-0.497668E+00

T2 C

0.650000E+02	0.400000E+02	-0.254133E+00	-0.413060E+00
0.650000E+02	0.450000E+02	0.000000E+00	0.000000E+00
0.600000E+02	0.450000E+02	0.000000E+00	0.000000E+00
0.550000E+02	0.450000E+02	0.000000E+00	0.000000E+00
0.500000E+02	0.450000E+02	0.000000E+00	0.000000E+00
0.450000E+02	0.450000E+02	0.000000E+00	0.000000E+00
0.400000E+02	0.450000E+02	-0.261614E+00	0.366644E+00
0.350000E+02	0.450000E+02	-0.268897E+00	0.209191E+00
0.300000E+02	0.450000E+02	-0.445123E-01	0.235653E+00
0.250000E+02	0.450000E+02	-0.175540E+00	0.239567E+00
0.200000E+02	0.450000E+02	0.848669E-01	0.214091E+00
0.150000E+02	0.450000E+02	0.238303E+00	0.306520E+00
0.100000E+02	0.450000E+02	-0.359145E-01	0.510713E+00
0.500000E+01	0.450000E+02	0.150073E+00	0.350163E+00
0.000000E+00	0.450000E+02	0.156981E+00	0.401541E+00
0.000000E+00	0.500000E+02	0.284512E+00	0.759118E+00
0.500000E+01	0.500000E+02	0.303374E+00	0.701910E+00
0.100000E+02	0.500000E+02	0.181905E+00	0.510203E+00
0.150000E+02	0.500000E+02	0.157735E-01	0.703242E+00
0.200000E+02	0.500000E+02	0.000000E+00	0.491593E+00
0.250000E+02	0.500000E+02	-0.396560E+00	0.414527E+00
0.300000E+02	0.500000E+02	-0.173786E+00	0.417305E+00
0.350000E+02	0.500000E+02	-0.278508E+00	0.278540E+00
0.400000E+02	0.500000E+02	-0.570025E+00	-0.142517E+00
0.450000E+02	0.500000E+02	-0.210694E+00	0.111655E+00
0.500000E+02	0.500000E+02	-0.947572E-01	-0.291542E-01
0.550000E+02	0.500000E+02	-0.259661E+00	-0.260110E+00
0.600000E+02	0.500000E+02	-0.219448E+00	-0.501350E+00
0.650000E+02	0.500000E+02	-0.539967E+00	-0.660062E+00
0.650000E+02	0.550000E+02	-0.367300E+00	-0.581927E+00
0.600000E+02	0.550000E+02	-0.207408E+00	-0.888996E+00
0.550000E+02	0.550000E+02	-0.365710E+00	-0.426770E+00
0.500000E+02	0.550000E+02	-0.438175E+00	-0.129875E+00
0.450000E+02	0.550000E+02	-0.492427E-01	-0.179661E-01
0.400000E+02	0.550000E+02	-0.486725E+00	-0.100699E+00
0.350000E+02	0.550000E+02	-0.296090E+00	0.249623E+00
0.300000E+02	0.550000E+02	-0.177732E+00	0.193148E+00
0.250000E+02	0.550000E+02	-0.237191E+00	0.566569E+00
0.200000E+02	0.550000E+02	-0.324275E+00	0.686895E+00
0.150000E+02	0.550000E+02	-0.248076E+00	0.783373E+00
0.100000E+02	0.550000E+02	0.135431E+00	0.738056E+00
0.500000E+01	0.550000E+02	0.311388E+00	0.759824E+00
0.000000E+00	0.550000E+02	0.285060E+00	0.665868E+00
0.000000E+00	0.600000E+02	0.366059E+00	0.867007E+00
0.500000E+01	0.600000E+02	0.191113E+00	0.937419E+00
0.100000E+02	0.600000E+02	-0.139178E+00	0.109705E+01
0.150000E+02	0.600000E+02	-0.200511E+00	0.104327E+01
0.200000E+02	0.600000E+02	-0.354564E+00	0.965399E+00
0.250000E+02	0.600000E+02	-0.485493E+00	0.699087E+00
0.300000E+02	0.600000E+02	-0.609247E+00	0.258512E+00
0.350000E+02	0.600000E+02	-0.423890E+00	0.220436E+00
0.400000E+02	0.600000E+02	-0.324656E+00	-0.103361E+00
0.450000E+02	0.600000E+02	-0.461290E+00	0.604944E-06
0.500000E+02	0.600000E+02	-0.458212E+00	-0.288540E+00
0.550000E+02	0.600000E+02	-0.329792E+00	-0.204161E+00
0.600000E+02	0.600000E+02	-0.332992E+00	-0.222009E+00
0.650000E+02	0.600000E+02	-0.447239E+00	-0.685977E+00
0.650000E+02	0.650000E+02	-0.717996E+00	-0.804167E+00
0.600000E+02	0.650000E+02	-0.679517E+00	-0.639571E+00
0.550000E+02	0.650000E+02	-0.306796E+00	-0.230295E+00
0.500000E+02	0.650000E+02	-0.497569E+00	-0.223087E+00
0.450000E+02	0.650000E+02	-0.698840E+00	-0.245550E+00
0.400000E+02	0.650000E+02	-0.563978E+00	-0.140993E+00

T2 d

0.350000E+02	0.650000E+02	-0.119769E+01	0.384963E+00
0.300000E+02	0.650000E+02	-0.974227E+00	0.656549E+00
0.250000E+02	0.650000E+02	-0.874505E+00	0.831914E+00
0.200000E+02	0.650000E+02	-0.805697E+00	0.113636E+01
0.150000E+02	0.650000E+02	-0.415964E+00	0.160181E+01
0.100000E+02	0.650000E+02	-0.812093E-01	0.116077E+01
0.500000E+01	0.650000E+02	0.142787E+00	0.141068E+01
0.000000E+00	0.650000E+02	0.389381E+00	0.141417E+01
0.000000E+00	0.700000E+02	0.366288E+00	0.159538E+01
0.500000E+01	0.700000E+02	0.151588E+00	0.171074E+01
0.100000E+02	0.700000E+02	-0.282256E+00	0.173767E+01
0.150000E+02	0.700000E+02	-0.523126E+00	0.161182E+01
0.200000E+02	0.700000E+02	-0.645476E+00	0.124942E+01
0.250000E+02	0.700000E+02	-0.121507E+01	0.131807E+01
0.300000E+02	0.700000E+02	-0.152508E+01	0.871487E+00
0.350000E+02	0.700000E+02	-0.139344E+01	0.522543E+00
0.400000E+02	0.700000E+02	-0.127271E+01	0.151002E+00
0.450000E+02	0.700000E+02	-0.844732E+00	-0.120689E+00
0.500000E+02	0.700000E+02	-0.618479E+00	-0.281161E+00
0.550000E+02	0.700000E+02	-0.432097E+00	-0.293946E+00
0.600000E+02	0.700000E+02	-0.485111E+00	-0.636617E+00
0.650000E+02	0.700000E+02	-0.323676E+00	-0.275144E+00
0.650000E+02	0.750000E+02	0.129813E+00	-0.553453E+00
0.600000E+02	0.750000E+02	-0.998372E-01	-0.464400E+00
0.550000E+02	0.750000E+02	-0.436204E+00	-0.560907E+00
0.500000E+02	0.750000E+02	-0.266645E+00	-0.250092E+00
0.450000E+02	0.750000E+02	-0.581726E+00	-0.498695E+00
0.400000E+02	0.750000E+02	-0.114205E+01	-0.153749E+00
0.350000E+02	0.750000E+02	-0.189939E+01	0.671737E+00
0.300000E+02	0.750000E+02	-0.197621E+01	0.181349E+01
0.250000E+02	0.750000E+02	-0.137185E+01	0.190254E+01
0.200000E+02	0.750000E+02	-0.920478E+00	0.194330E+01
0.150000E+02	0.750000E+02	-0.521295E+00	0.185621E+01
0.100000E+02	0.750000E+02	-0.611384E+00	0.181230E+01
0.500000E+01	0.750000E+02	-0.477704E-01	0.222377E+01
0.000000E+00	0.750000E+02	0.909717E-01	0.222527E+01
0.000000E+00	0.800000E+02	0.706555E-01	0.200790E+01
0.500000E+01	0.800000E+02	0.214508E-01	0.200372E+01
0.100000E+02	0.800000E+02	-0.398069E+00	0.205721E+01
0.150000E+02	0.800000E+02	-0.531843E+00	0.231931E+01
0.200000E+02	0.800000E+02	-0.955284E+00	0.286589E+01
0.250000E+02	0.800000E+02	-0.175114E+01	0.297034E+01
0.300000E+02	0.800000E+02	-0.217205E+01	0.214764E+01
0.350000E+02	0.800000E+02	-0.178515E+01	0.768611E+00
0.400000E+02	0.800000E+02	-0.896444E+00	-0.156877E+01
0.450000E+02	0.800000E+02	0.652573E+00	-0.108819E+01
0.500000E+02	0.800000E+02	0.109557E+01	-0.573200E+00
0.550000E+02	0.800000E+02	0.990445E+00	-0.498993E+00
0.600000E+02	0.800000E+02	0.774157E+00	-0.569230E+00
0.650000E+02	0.800000E+02	0.654998E+00	-0.935828E+00
0.650000E+02	0.850000E+02	0.923706E+00	-0.505842E+00
0.600000E+02	0.850000E+02	0.127862E+01	-0.157027E+00
0.550000E+02	0.850000E+02	0.123107E+01	0.165728E+00
0.500000E+02	0.850000E+02	0.169865E+01	0.511714E+00
0.450000E+02	0.850000E+02	0.372504E+01	-0.188875E+01
0.400000E+02	0.850000E+02	0.339183E+01	-0.522595E+01
0.350000E+02	0.850000E+02	-0.375401E+00	-0.249078E+01
0.300000E+02	0.850000E+02	-0.463005E+00	0.247870E+01
0.250000E+02	0.850000E+02	-0.346737E+00	0.365509E+01
0.200000E+02	0.850000E+02	-0.294410E+00	0.358058E+01
0.150000E+02	0.850000E+02	0.288231E+00	0.317063E+01
0.100000E+02	0.850000E+02	0.208449E-01	0.262212E+01
0.500000E+01	0.850000E+02	-0.954510E-01	0.187076E+01

T2 e

0.000000E+00	0.850000E+02	0.000000E+00	0.146773E+01
0.000000E+00	0.900000E+02	-0.827514E-01	0.138342E+01
0.500000E+01	0.900000E+02	0.185226E+00	0.174878E+01
0.100000E+02	0.900000E+02	0.708449E+00	0.269232E+01
0.150000E+02	0.900000E+02	0.901895E+00	0.315687E+01
0.200000E+02	0.900000E+02	0.116121E+01	0.305096E+01
0.250000E+02	0.900000E+02	0.234067E+01	0.349870E+01
0.300000E+02	0.900000E+02	0.331719E+01	-0.719769E+00
0.350000E+02	0.900000E+02	0.347469E+01	-0.595296E+01
0.400000E+02	0.900000E+02	0.430455E+01	-0.667319E+01
0.450000E+02	0.900000E+02	0.342381E+01	-0.103305E+01
0.500000E+02	0.900000E+02	0.209458E+01	0.172159E+01
0.550000E+02	0.900000E+02	0.142322E+01	0.993570E+00
0.600000E+02	0.900000E+02	0.113036E+01	0.688079E+00
0.650000E+02	0.900000E+02	0.888667E+00	-0.148114E+00
0.650000E+02	0.950000E+02	0.932721E+00	0.102602E+01
0.600000E+02	0.950000E+02	0.174199E+01	0.435495E+00
0.550000E+02	0.950000E+02	0.158439E+01	0.115228E+00
0.500000E+02	0.950000E+02	0.867759E+00	-0.542375E-01
0.450000E+02	0.950000E+02	0.986515E+00	-0.314451E+01
0.400000E+02	0.950000E+02	0.234217E+01	-0.507863E+01
0.350000E+02	0.950000E+02	0.373539E+01	-0.450163E+01
0.300000E+02	0.950000E+02	0.492347E+01	-0.123087E+01
0.250000E+02	0.950000E+02	0.369857E+01	0.211348E+01
0.200000E+02	0.950000E+02	0.217195E+01	0.264413E+01
0.150000E+02	0.950000E+02	0.195313E+01	0.323937E+01
0.100000E+02	0.950000E+02	0.140075E+01	0.315853E+01
0.500000E+01	0.950000E+02	0.148435E+01	-0.539769E+00
0.000000E+00	0.950000E+02	0.637903E+00	-0.179413E+01
0.000000E+00	0.100000E+03	0.143283E+01	-0.169941E+01
0.500000E+01	0.100000E+03	-0.488703E+00	-0.205278E+01
0.100000E+02	0.100000E+03	0.476261E+00	0.616345E+00
0.150000E+02	0.100000E+03	0.184303E+01	0.298138E+01
0.200000E+02	0.100000E+03	0.241574E+01	0.181182E+01
0.250000E+02	0.100000E+03	0.268595E+01	0.105296E+00
0.300000E+02	0.100000E+03	0.269304E+01	-0.110064E+01
0.350000E+02	0.100000E+03	0.228315E+01	-0.172314E+01
0.400000E+02	0.100000E+03	0.130242E+01	-0.237049E+01
0.450000E+02	0.100000E+03	0.230550E-01	-0.252723E+01
0.500000E+02	0.100000E+03	-0.361939E+00	-0.186521E+01
0.550000E+02	0.100000E+03	0.000000E+00	-0.194361E+01
0.600000E+02	0.100000E+03	0.395927E+00	-0.670036E+00
0.650000E+02	0.100000E+03	0.458540E+00	-0.639270E+00
0.650000E+02	0.105000E+03	0.406255E+00	0.580571E-01
0.600000E+02	0.105000E+03	0.691737E-01	-0.355672E+00
0.550000E+02	0.105000E+03	0.157249E+00	-0.408653E+00
0.500000E+02	0.105000E+03	-0.165079E+00	-0.127277E+01
0.450000E+02	0.105000E+03	0.225212E+00	-0.132286E+01
0.400000E+02	0.105000E+03	0.997063E+00	-0.138561E+01
0.350000E+02	0.105000E+03	0.116452E+01	-0.952841E+00
0.300000E+02	0.105000E+03	0.159039E+01	-0.128954E+00
0.250000E+02	0.105000E+03	0.128821E+01	-0.442216E-01
0.200000E+02	0.105000E+03	0.868309E+00	0.247003E+00
0.150000E+02	0.105000E+03	0.629692E-01	0.207643E+00
0.100000E+02	0.105000E+03	-0.867731E+00	-0.535057E+00
0.500000E+01	0.105000E+03	-0.861228E+00	-0.574163E+00
0.000000E+00	0.105000E+03	0.181684E+01	-0.493147E+00

APPENDIX I - COMPUTER PROGRAM LISTINGS

A - Cassette digital data readout and implementation of pressure transducer coefficients

B - Program for operating data blocks

C - Program used to interchange data points

D - Program for altering data

E - Calculation of velocity vectors, preparation of streamlines, data matrix, and creation of pressure isolines block

F - Calculation of velocity vectors and creation of cross flow kinetic energy isolines block

G - PET Commodore program used for calibration of five hole probe

H - PET Commodore program used for data acquisition into d digital cassette (G and H require machine language program to relate scanivalve A at set intervals of time)

A1

```
C-----------------------------------------------------------------------C
C  READ FILE CREATED BY CDX AND REWRITE IT AFTER APPLYING COEFFICIENTS  C
C                                                                       C
C       NAME     :       JEUS                                         C
C       AUTHOR   :       OTTE A.                                      C
C       DATE     :       10-MAY-83                                    C
C       SUBROUTINES CALLED : PARAM1, GETCDX                           C
C-----------------------------------------------------------------------C
        PROGRAM JEUS
C
        DIMENSION COEF(2),FC(5)
        LOGICAL*1 YES
C
        NCAN=5
        CALL PARAM1 (COEF,2,1)
C
10      CALL GETCDX (NCAN,COEF,FC,FACT)
C
        STOP
        END
C-------------------------------------------------------------
        SUBROUTINE GETCDX (NPTS,COEF,FC,FACT)
        DIMENSION IVAL(50),IBUF1(256),IBUF2(256),COEF(2),FC(5)
        LOGICAL*1 FILE1(15),FILE2(15),YES
        IV1=1
        IV2=1
        FACT=1.                                          ! JEUSETTE
C
4       TYPE 1
1       FORMAT(/' RAW DATA FILENAME : '$)
        CALL GETSTR (5,FILE1,14)
        CALL ASSIGN (1,FILE1)
        DEFINE FILE 1 (0,256,U,IV1)
C
        TYPE 500
500     FORMAT(' NEW FILENAME       : '$)
        CALL GETSTR (5,FILE2,14)
        CALL ASSIGN (2,FILE2)
        DEFINE FILE 2 (0,256,U,IV2)
C
        IOUT=0
        TYPE 1111
1111    FORMAT(' OUTPUT VERIFICATION ? [Y/N] : '$)
        IF(YES()) IOUT=1
C
100     READ (1'IV1) IBUF1
        WRITE (2'IV2) IBUF1
C
        NCAN=IBUF1(2)
        IF(NPTS.GT.0) GO TO 5
        GO TO 6
5       IF(NCAN.NE.NPTS) NCAN=NPTS
6       NREC=IBUF1(3)
        IF(NPTS.GT.IBUF1(2)) NREC=NREC/NCAN*IBUF1(5)
        IREC=0
10      J1=1
        J2=NCAN
11      READ (1'IV1) IBUF1
15      I=0
20      DO 25 J=J1,J2
        I=I+1
        IF(IBUF1(J).EQ.0) GO TO 4000                     ! JEUS
```

A2

```
25      CONTINUE
        IREC=IREC+1
        IGO=1
        IF(IREC.NE.NREC) GO TO 1000
60      IF(IREC.EQ.NREC) GO TO 40
30      J1=J2+1
        IF(J1.EQ.257) WRITE (2'IV2) IBUF2
        IF(J1.EQ.257) GO TO 10
        J2=J1+NCAN-1
        IF(J2.LE.256) GO TO 15
        I=0
        DO 35 J=J1,256
        I=I+1
        IVAL(I)=IBUF1(J)
35      CONTINUE
        IGO=2
        GO TO 1000
70      WRITE (2'IV2) IBUF2
        J1=1
        J2=J2-256
        GO TO 11
C
1000    K=0
        JE=J2
        IF(IGO.EQ.2) JE=256
        DO 3000 JJ=J1,JE
        K=K+1
        FC(K)=COEF(1)
        DO 2000 II=2,2
        FC(K)=FC(K)+COEF(II)*FLOAT(IVAL(K))**(II-1)
2000    CONTINUE
        IBUF2(JJ)=FC(K)/FACT
3000    CONTINUE
        IF(IOUT.EQ.1) TYPE 9999,J1,J2,(IVAL(N),N=1,5),(IBUF2(N),N=J1,JE)
9999    FORMAT(2I6,' ! ',5I6,' ! ',5I6)
        GO TO (60,70),IGO
C
4000    DO 5000 JJJ=J,256
5000    IBUF2(JJJ)=0
40      CONTINUE
        WRITE (2'IV2) IBUF2
        CALL CLOSE (1)
        CALL CLOSE (2)
        RETURN
        END
```

BI

```
      PROGRAM APPEND
      LOGICAL *1 NAME1(15),NAME2(15),YES
      DIMENSION IBUF(256),IVAL(5)
C
5     TYPE 10
10    FORMAT(' INPUT FILENAME : '$)
      CALL GETSTR(5,NAME1,14)
      DEFINE FILE 1 (0,256,U,IV1)
      CALL ASSIGN (1,NAME1)
      IV1=1
C
      TYPE 15
15    FORMAT(' OUTPUT FILENAME : '$)
      CALL GETSTR(5,NAME2,14)
      CALL ASSIGN (2,NAME2)
      DEFINE FILE 2 (0,5,U,IV2)
      IV2=1
C
20    CALL GETVAL(5,IVAL,ISTAT,NAME,IV1)      ! LECTURE TRAIN DE CANAUX
      TYPE 1234,IVAL
1234  FORMAT(5I10)
      WRITE(2'IV2)IVAL
      IF(IVAL(1).EQ.0) GO TO 30
      GO TO 20
C
30    CALL CLOSE (1)
C
      TYPE 50
50    FORMAT(' DATA FILENAME TO APPEND [Y/N] : '$)
      IF(.NOT.YES()) GO TO 55
      TYPE 60
60    FORMAT(' INPUT FILENAME : '$)
      CALL GETSTR (5,NAME1,14)
      CALL ASSIGN (1,NAME1)
      DEFINE FILE 1 (0,256,U,IV1)
      IV1=1
      GO TO 20
55    CONTINUE
      DO 56 I=1,5
56    IVAL(I)=0
      WRITE(2'IV2) IVAL
      CALL CLOSE (2)
C
      TYPE 40
40    FORMAT(' DO YOU WANT TO CONTINUE ? [Y/N] : '$)
      IF(YES()) GO TO 5
      END
C-------------------------------------------------------------
      SUBROUTINE GETVAL (NPTS,IVAL,K,FILE,IV1)
      DIMENSION IVAL(1),IBUF(256)
      DATA IDEB/0/
      LOGICAL*1 FILE(15)
      K=0                                     ! STATUS INITIALIZATION
      IF(IDEB.NE.0) GO TO 30
      IV1=1
C
      INFILE=0                                ! FILE NOT DEFINED BEFORE CAL
      DO 2 I=1,15
      IF(FILE(I).NE.' ') GO TO 3              ! NO BLANC STRING, FILE EXIST
2     CONTINUE
      GO TO 4
3     INFILE=1                                ! FILE DEFINED BEFORE CALL
```

B2

```
C
4       TYPE 1
1       FORMAT(/' RAW DATA FILENAME : '$)
        CALL GETSTR (5,FILE,14)
        CALL ASSIGN (1,FILE)
        DEFINE FILE 1 (0,256,U,IV1)
C
100     READ (1'IV1) IBUF
        NCAN=IBUF(2)
        IF(NPTS.GT.0) GO TO 5
        GO TO 6
5       IF(NCAN.NE.NPTS) NCAN=NPTS
6       NREC=IBUF(3)
        IF(NPTS.GT.IBUF(2)) NREC=NREC/NCAN*IBUF(5)
7       IREC=0
10      J1=1
        J2=NCAN
        READ (1'IV1) IBUF
15      I=0
20      DO 25 J=J1,J2
        I=I+1
        IVAL(I)=IBUF(J)
        IF(IVAL(I).EQ.0) GO TO 40
25      CONTINUE
        IREC=IREC+1
        IDEB=1
        IF(IREC.NE.NREC) RETURN
        GO TO 40
30      J1=J2+1
        IF(J1.EQ.257) GO TO 10
        J2=J1+NCAN-1
        IF(J2.LE.256) GO TO 15
        I=0
        DO 35 J=J1,256
        I=I+1
        IVAL(I)=IBUF(J)
35      CONTINUE
        READ (1'IV1) IBUF
        J1=1
        J2=J2-256
        GO TO 20
40      IDEB=0
        CONTINUE
        IF(INFILE.EQ.0) CALL CLOSE (1)
        K=-1
        RETURN
        END
```

```
      PROGRAM UPDATE
      DIMENSION IVAL(5),JVAL(5)
      LOGICAL*1 NAME1(15),NAME2(15),YES
10    TYPE 20
20    FORMAT(' NAME OF FILE TO BE UPDATED : '$)
      CALL GETSTR (5,NAME1,14)
      CALL ASSIGN (1,NAME1)
      DEFINE FILE 1 (0,5,U,IV1)
30    TYPE 40
40    FORMAT(' RECORD NUMBER TO BE REPLACED : '$)
      ACCEPT 50,IR1
50    FORMAT(I5)
      IF(IR1.EQ.0) GO TO 999
60    TYPE 70
70    FORMAT(' NAME OF FILE TO PICK UP RECORD : '$)
      CALL GETSTR (5,NAME2,14)
      CALL ASSIGN (2,NAME2)
      DEFINE FILE 2 (0,5,U,IV2)
75    TYPE 80
80    FORMAT(' RECORD NUMBER TO PICK UP : '$)
      ACCEPT 50,IR2
      IF(IR2.EQ.0) GO TO 888
      READ(1'IR1) IVAL
      TYPE 1000,IVAL
1000  FORMAT(5I10)
      READ(2'IR2) JVAL
      TYPE 1000,JVAL
      TYPE 2000
2000  FORMAT(' RECORD O.K.? [Y/N] : '$)
      IF(.NOT.YES()) GO TO 75
      WRITE(1'IR1) JVAL
      CALL CLOSE (2)
      GO TO 30
888   CONTINUE
      CALL CLOSE (2)
999   CONTINUE
CCC   CALL CLOSE (1)
      TYPE 4000
4000  FORMAT(' DO YOU WANT TO DELETE RECORDS ? [Y/N] : '$)
      IF(.NOT.YES()) GO TO 5000
C
      TYPE 4010
4010  FORMAT(' NUMBER OF RECORDS TO BE DELETED : '$)
      ACCEPT 50,NRDEL
      TYPE 4020
4020  FORMAT(' START DELETING FROM RECORD NUMBER : '$)
      ACCEPT 50,ISTART
C
      JR=ISTART+NRDEL
      JW=ISTART
4030  READ(1'JR,END=5000,ERR=5000) IVAL
      TYPE 6000,JW,JR,IVAL
6000  FORMAT(7I8)
      WRITE(1'JW) IVAL
      JR=JR+1
      JW=JW+1
      IF(IVAL(1).NE.0) GO TO 4030
C
5000  CALL CLOSE (1)
C
      TYPE 3000
3000  FORMAT(' DO YOU WANT TO CONTINUE ? [Y/N] : '$)
      IF(YES()) GO TO 10
      STOP
      END
```

```
C       PROGRAM BIN                    D1
C       AUTHOR:GUS ORDONEZ AR'82-83
C       PGM REPLACES VALUE FOUND IN RAW DATA FROM DIGITAL CASSETE
C       TO VALUE ASSIGNED BY THE USER
        DIMENSION IBUF(256)
        LOGICAL NAME1(15)
 10     TYPE 20
 20     FORMAT(' INPUT FILENAME:'$)
        CALL GETSTR(5,NAME1,14)
        CALL ASSIGN(1,NAME1)
        DEFINE FILE 1(0,256,U,IV1)
        IV1=1
        TYPE 30
 30     FORMAT(' BLOCK NUMBER TO BE MODIFIED:'$)
        ACCEPT 50,N
 50     FORMAT(I5)
        N=N+1
        NR =N
        READ(1'N) IBUF
        TYPE 40
 40     FORMAT(' NUMBER OF VALUE IN BLOCK:'$)
        ACCEPT 50,K
        TYPE 100
100     FORMAT (' ENTER NEW VALUE:'$)
        ACCEPT 50,IVAL
        IBUF(K)=IVAL
        WRITE (1'NR) IBUF
        CALL CLOSE(1)
        STOP
        END
```

E1

```
C       PREPARE A DATA FILE FOR STREAMLINES PLOTTING PROGRAM AND ISOLINES
C       NAME    :       NPVGUS
C       GUS ORDONEZ AR'82-83
C       DATE    :       26-MAY-83
C       PGM CALCULATES CROSS FLOW VELOCITY COMPONENTS AND TOTAL PRESSURE
C       AND PREPARES DATA FOR STREAMLINES PLOTTING AND ISOLINES OF
C       TOTAL PRESSURE
        PROGRAM NPVGUS
        COMMON XP(50),YP(50),WP(50),IVAL(5),P(5),XPLISO(50)
        COMMON XPR(50),YR(50),WR(50),TITLE(20),NX,NY
        LOGICAL*1 NAME1(15),NAME2(15),NAME3(15),YES
C
        G=9.806356
        TYPE 100
100     FORMAT(' NUMBER OF POINTS ON X-AXIS : '$)
        ACCEPT 110,NX
110     FORMAT(I5)
        TYPE 120
120     FORMAT(' NUMBER OF POINTS ON Y-AXIS : '$)
        ACCEPT 110,NY
        TYPE 130
130     FORMAT(' INITIAL VALUE FOR X : '$)
        ACCEPT 140,XI
140     FORMAT(F10.0)
        TYPE 150
150     FORMAT(' INITIAL VALUE FOR Y : '$)
        ACCEPT 140,YI
        TYPE 155
155     FORMAT(' STEP FOR X/Y : '$)
        ACCEPT 140,STEP
C
159     TYPE 160
160     FORMAT(' DATA INPUT FILENAME : '$)
        CALL GETSTR(5,NAME1,14)
        CALL ASSIGN(1,NAME1)
        DEFINE FILE 1(0,5,U,IV1)
        IV1=1
C
        N=NX*NY                         ! TOTAL NUMBER OF POINTS
        NNN=N
        N1=N+1
        CALL ASSIGN(2,'STREAM.OUT')
        DEFINE FILE 2(0,8,U,IV2)
C
        TYPE 500
500     FORMAT(' OUTPUT FILENAME FOR ISOLINES : '$)
        CALL GETSTR(5,NAME3,14)
        CALL ASSIGN(3,NAME3)
        TYPE 510
510     FORMAT(' TITLE FOR ISOLINES PLOT : '$)
        ACCEPT 520,TITLE
520     FORMAT(20A4)
        WRITE(3,525) TITLE              ! RECORD 1 FOR PLIS
525     FORMAT(1X,20A4)
        WRITE(3,*) NX,NY                ! RECORD 2
        XP(1)=0.
        DO 530 I=2,NX
530     XP(I)=XP(I-1)+STEP
        WRITE(3,*) (XP(K),K=1,NX)       ! RECORD 3 - X-COORD.
        XP(1)=0.
        DO 540 J=2,NY
540     XP(J)=XP(J-1)+STEP
```

E2

```
C
      WRITE(2'1) N,0,0                    NUMBER OF (X,Y) DATA POINTS
      IY2=2
      YP=YI-STEP
1000  TYPE 1010
1010  FORMAT(' ATMOSPHERIC PRESSURE      ' $)
      ACCEPT 140,PAT
      TYPE 1020
1020  FORMAT(' TEMPERATURE               ' $)
      ACCEPT 140,TO
      TYPE 1030
1030  FORMAT(' DYNAMIC PRESSURE (PSF)    ' $)
      ACCEPT 140,DPMH
      CTE=DPMH*G
      XP(1)=XI-STEP
C.....
      DO 30 J=1,NY
      JL=J
      YP=YP+STEP
      SIG=1.
      IF(MOD(JL,2).EQ.0) SIG=-1
C
      XMIN=XI
      XMAX=STEP*FLOAT(NX-1)+XI
C
1040  IF(MOD(JL,2).EQ.0) XP(1)=XMAX+STEP
      IF(MOD(JL,2).NE.0) XP(1)=XMIN-STEP
C
      DO 20 I=1,NX
      XP(I)=XP(I)+STEP*SIG
      IF(I.GT.1) XP(I)=XP(I-1)+STEP*SIG
      READ (1'IY1) IVAL
      DO 180 K=1,5
      P(K)=FLOAT(IVAL(K))
180   CONTINUE
C
      CALL CALCUL (P,VARG,WARG,PAT,TO,BT)
C
      V(I)=VARG
      W(I)=WARG
      XPR(I)=BT/CTE
C
20    CONTINUE
C.....
200   DO 210 K=1,NX
      WRITE(2'IY2) XP(K),YP,V(K),W(K)
210   CONTINUE
C
      IF(MOD(JL,2).EQ.0) GO TO 400
      KR=0
      DO 300 K=NX,1,-1
      KR=KR+1
300   XPLISO(KR)=XPR(K)
      WRITE(3,*) (XPLISO(K),K=1,NX)          ! RECORD 5
            TYPE 1111,(XPLISO(K),K=1,NX)
1111        FORMAT(5F12.3)
      GO TO 30
400   WRITE(3,*) (XPR(K),K=1,NX)             ! RECORD 5
            TYPE 1111,(XPR(K),K=1,NX)
C
30    CONTINUE
      CALL CLOSE (1)
      CALL CLOSE (2)
```

E3

```
      CALL CLOSE (3)
      CALL ASSIGN (1,NAME3)
      CALL ASSIGN (2,'ISOLINES OUT ')
      READ(1,525) TITLE
      READ(1,*) NX,NY
      READ(1,*) (XPR(K),K=1,NX)
      READ(1,*) (XPR(K),K=1,NY)
C
      DO 9999 J=1,NY
      READ(1,*) (XPLISO(K),K=1,NX)
      WRITE(2,2222) (XPLISO(K),K=1,NX)
2222  FORMAT(1X,10F12.3)
C
9999  CONTINUE
      CALL CLOSE (1)
      CLOSE(UNIT=2,DISP='PRINT')
C
      CALL REVERS
C
      STOP
      END
C-----------------------------------------------------------------------
C     DATA REDUCTION ROUTINE FOR UPDATED DATA.
C     CROSS FLOW VELOCITY COMPONENTS AND TOTAL PRESSURE ARE CALCULATED
      SUBROUTINE CALCUL (P,V,W,PAT,TO,QT)
      DIMENSION P(1)
CCC   ASIN(X)=ATAN(X/SQRT(1.-X*X))
CCC   ACOS(X)=ATAN(SQRT(1.-X*X)/X)
C
      PMOY = (P(1)+P(2)+P(3)+P(4))*0.25
      P(2)=P(2)+18
      P(1)=P(1)+10
      DD   = P(2)-P(4)
      EE   = P(1)-P(3)
      ADD  = ABS(DD)
      AEE  = ABS(EE)
      FF   = AEE - ADD
      IF (EE.EQ.0.)    GO TO 2
      GG   = ABS(DD/EE)
      FIR  = ATAN(GG)
      FI   = 180.*FIR/3.14159
      GO TO 3
    2 FI   = 90.0
      FIR  = 3.14159/2.0
    3 RA   = DD*DD+EE*EE
      BI   = SQRT(RA)
      BIR  = BI/ABS(P(5)-PMOY)
      IF (FF.LE.0.095)   GO TO 4
      IF (EE.GE.0.01)    GO TO 5
      T1   = 13.72858*BIR+(-2.112228E-1)*BIR**2-(.9420486)*BIR**3+
     1 (2.933134E-1)*BIR**4
      T2   = -(2.697529E-2)*BIR**5
      TH   = T1 + T2 - 1.241217
      D1   = (5.870109E-1)+(4.466144E-3)*TH+(-3.990502E-4)*TH**2
      D2   = (-5.362912E-6)*TH**3+(5.538313E-7)*TH**4
      D3   = (-7.405356E-9)*TH**5
C
      PD   = (D1+D2+D3)*1.0
      C1   = (7.065830E-4)*TH+(-3.032390E-4)*TH**2+(4.834588E-5)
     1 *TH**3
      C2   = (-1.430398E-6)*TH**4+(2.612108E-8)*TH**5-(2.319786E-10)
     1 *TH**6
```

E4

```
   10     RHT   = PHT/(287.0*T0)
          AV    = ABS((P(5)-PMDY)*2./(PD*RHT))
          AV    = SQRT(AV)
          BT    = P(5)+CP*PHT*AV**2*0.5
          IF ((P(1).GE.P(3)).AND.(P(4).GE.P(2)))     QU = 1.
          IF ((P(1).GE.P(3)).AND.(P(2).GE.P(4)))     QU = 2.
          IF ((P(1).LE.P(3)).AND.(P(2).GE.P(4)))     QU = 3.
          IF ((P(1).LE.P(3)).AND.(P(4).GE.P(2)))     QU = 4.
          TH    = TH*3.14159/180.0
          IF (CP.LT.0.)   CP = 0.0
          IF(TH.LT.0.) GO TO 832
               SSTH=SIN(TH)
               SSFIR=COS(FIR)
          SAL   = SIN(TH)*COS(FIR)
          CTE=1.-SAL*SAL
          CGA=COS(TH)/SQRT(CTE)
C
CCC          CGA   = COS(TH)/(SQRT(ABS(1.-SAL*SAL)))
          CAL=SQRT(1.-SAL*SAL)
          SGA=SQRT(1.-CGA*CGA)
CCC       TYPE ,TH,FIR,SSTH,SSFIR,SAL,CGA,CTE
CCCC      FORMAT(' TH,FI,STH,CFI,SAL,CGA,CTE'/7F10.4)
          UU=CAL*CGA*AV
          V=CAL*SGA*AV
          W=SAL*AV
          IF(QU EQ.1..OR.QU.EQ.4.) V=-V
          IF(QU EQ.1..OR.QU.EQ.2.) W=-W
          GO TO 833
  832     V=0.
          W=0.
          UU=AV
  833     RETURN
    4     IF (DD.LE.0.01)   GO TO 6
          T1    = 21.53083*BIR-13.94689*BIR**2
          T2    = +8.953023*BIR**3-3.248728*BIR**4
          T3    = (5.903704E-1)*BIR**5-(4.148470E-2)*BIR**6
          TH    = T1 + T2 + T3 - .7471644
          D1    = (5.9093289E-1)+(8.193470E-4)*TH-(6.777613E-5)*TH**2
          D2    = (-5.960415E-6)*TH**3+(-1.537824E-7)*TH**4
          D3    = (1.653859E-8)*TH**5+(-2.347760E-10)*TH**6
          PD    = (D1+D2+D3)*1.0
          C1    = (-3.258468E-3)*TH+(1.213657E-3)*TH**2-(1.436069E-4)*
     1    TH**3
          C2    = (8.769080E-6)*TH**4+(-2.172509E-7)*TH**5+(1.907005E-9)
     1    *TH**6
          CP    = C1+C2+9.777586E-4
          GO TO 10
    5     T1    = 17.26694*BIR-8.755424*BIR**2
          T2    = 5.748909*BIR**3-(2.148792)*BIR**4
          T3    = (3.965276E-1)*BIR**5-(2.831693E-2)*BIR**6
          TH    = T1+T2+T3+0.4941921
          D1    = (5.95200E-1)+(7.559778E-5)*TH+(1.564457E-4)*TH**2
          D2    = (-4.345895E-5)*TH**3+(2.162540E-6)*TH**4
          D3    = (-4.380951E-8)*TH**5+(3.246741E-10)*TH**6
          PD    = (D1+D2+D3)*1.0
          C1    = (-2.836868E-3)*TH+(6.199820E-4)*TH**2-(3.455378E-5)*TH**3
          C2    = (1.651172E-6)*TH**4-(2.517231E-8)*TH**5+(7.831602E-11)
     1    *TH**6
          CP    = C1+C2+1.402665E-3
          GO TO 10
    6     T1  = 12.12255*BIR+(2.329581)*(BIR**2)-3.229866*BIR**3+
     1    (1.284068)*BIR**4
          T2  = (-2.269259E-1)*BIR**5+(1.488861E-2)*BIR**6
```

E5

```
      TH   = T1+T2-0.8373914
      D1   = (5.833296E-1)+(2.877764E-3)*TH+(-1.635622E-4)*TH**2
      D2   = (-1.422516E-5)*TH**3+(6.928993E-7)*TH**4
      D3   = (-8.953081E-9)*TH**5
      PD   = (D1+D2+D3)*1.00
      C1   = (-8.130340E-4)*TH-(2.066893E-5)*TH**2+(2.829430E-5)*TH**3
      C2   = (-4.975929E-7)*TH**4+(2.329037E-9)*TH**5
      CP   = C1+C2+7.536941E-4
      GO TO 10
      END
C-----------------------------------------------------------------
C     SUBROUTINE USED TO PLOT CROSS FLOW VELOCITIES ON PDP PLOTTER
      SUBROUTINE REVERS
      COMMON XP(50),V(50),W(50),IVAL(5),P(5),XPLISO(50)
      COMMON XPR(50),VR(50),WR(50),TITLE(20),NX,NY
C
      CALL ASSIGN (2,'STREAM.OUT')
      DEFINE FILE 2 (0,8,U,IV2)
      IV2=1
      CALL ASSIGN (3,'STREAMP.OUT')
      DEFINE FILE 3 (0,8,U,IV3)
      IV3=1
C
      READ(2'IV2) N,NZ,RNZ
      WRITE(3'IV3) N,NZ,RNZ
C
      DO 40 J=1,NY
      DO 10 I=1,NX
      READ(2'IV2) XP(I),Y,V(I),W(I)
10    CONTINUE
C
      L=0
      DO 20 K=NX,1,-1
      L=L+1
      VR(L)=-V(K)
      WR(L)=W(K)
20    CONTINUE
C
      DO 30 K=1,NX
      WRITE(3'IV3) XP(K),Y,VR(K),WR(K)
30    CONTINUE
40    CONTINUE
      CALL CLOSE(2)
      CALL CLOSE(3)
      RETURN
      END
```

F1

```
C       PREPARE A DATA FILE FOR  ISOLINES
C       NAME    :       NEW PROBE AND VELOCITIES KINETIC (NPVKINET)
C       MODIFIED FOR CROSS FLOW KINETIC ENERGY INTEGRAL - G.ORDONEZ
C       DATE    :       26-MAY-83
C       PGM PREPARES DATA FOR KINETIC ENERGY ISOLINES AND
C       CALCULATES CROS FLOW KINETIC INTEGRAL NONDIMENSIONALIZED WRT
C       MAINSTREAM VELOCITY
        PROGRAM NPVKINET
        DIMENSION XP(50),V(50),W(50),IVAL(5),P(5),KPLIS0(50),CFKEL(50)
        DIMENSION XPR(50),VR(50),WR(50),TITLE(20),DCFKEL(50)
        LOGICAL*1 NAME1(15),NAME2(15),NAME3(15),YES
C
        RHOAIR=1.225
        RHOWAT=1000.
        G=9.806356
        TYPE 100
100     FORMAT(' NUMBER OF POINTS ON X-AXIS : '$)
        ACCEPT 110,NX
110     FORMAT(I5)
        TYPE 120
120     FORMAT(' NUMBER OF POINTS ON Y-AXIS : '$)
        ACCEPT 110,NY
        TYPE 130
130     FORMAT(' INITIAL VALUE FOR X : '$)
        ACCEPT 140,XI
140     FORMAT(F10.0)
        TYPE 150
150     FORMAT(' INITIAL VALUE FOR Y : '$)
        ACCEPT 140,YI
        TYPE 155
155     FORMAT(' STEP FOR X/Y : '$)
        ACCEPT 140,STEP
C
159     TYPE 160
160     FORMAT(' DATA INPUT FILENAME : '$)
        CALL GETSTR (5,NAME1,14)
        CALL ASSIGN (1,NAME1)
        DEFINE FILE 1 (0,5,U,IV1)
        IV1=1
C
        N=NX*NY                         ! TOTAL NUMBER OF POINTS
        NNN=N
        N1=N+1
C
        TYPE 500
500     FORMAT(' OUTPUT FILENAME FOR ISOLINES : '$)
        CALL GETSTR (5,NAME3,14)
        CALL ASSIGN (3,NAME3)
        CALL ASSIGN(4,'KINER.OUT')
        DEFINE FILE 4 (0,8,U,IV4)
        IV4=2
        TYPE 510
510     FORMAT(' TITLE FOR ISOLINES PLOT : '$)
        ACCEPT 520,TITLE
520     FORMAT(20A4)
        WRITE(3,525) TITLE              ! RECORD 1 FOR PLIS
525     FORMAT(1X,20A4)
        WRITE(3,*) NX,NY                ! RECORD 2
        XP(1)=0.
        DO 530 I=2,NX
530     XP(I)=XP(I-1)+STEP
        WRITE(3,*) (XP(K),K=1,NX)       ! RECORD 3 - X-COORD.
```

F2

```
      DO 540 J=2,NY
540   XP(J)=XP(J-1)+STEP
      WRITE(3,*) (XP(K),K=1,NY)          ! RECORD 4 - Y-COORD.
C
      YP=YI-STEP
1000  TYPE 1010
1010  FORMAT(' ATMOSPHERIC PRESSURE : '$)
      ACCEPT 140,PAT
      TYPE 1020
1020  FORMAT(' TEMPERATURE           : '$)
      ACCEPT 140,TO
      TYPE 1030
1030  FORMAT(' DYNAMIC PRESSURE (MM.H2O) : '$)
      ACCEPT 140,DPMH
      VELSQ=(2.*RHOWAT*DPMH)/(RHOAIR*1000.)
      CTE=DPMH*G
      XP(1)=XI-STEP
C
      DCFKET=0.
C.....
      DO 30 J=1,NY
      JL=J
      YP=YP+STEP
      SIG=1.
      IF(MOD(JL,2).EQ.0) SIG=-1
C
      XMIN=XI
      XMAX=STEP*FLOAT(NX-1)+XI
C
1040  IF(MOD(JL,2).EQ.0) XP(1)=XMAX+STEP
      IF(MOD(JL,2).NE.0) XP(1)=XMIN-STEP
C
      DO 20 I=1,NX
      XP(I)=XP(I)+STEP*SIG
      IF(I.GT.1) XP(I)=XP(I-1)+STEP*SIG
      READ (1'IV1) IVAL
      DO 180 K=1,5
      P(K)=FLOAT(IVAL(K))
180   CONTINUE
C
      CALL CALCUL (P,VARG,WARG,PAT,TO )
C
      V(I)=VARG
      U(I)=WARG
      CFKEL(I)=(V(I)**2+U(I)**2)
      DCFKEL(I)=CFKEL(I)/(VELSQ)
      DCFKET=DCFKET+DCFKEL(I)
      TYPE 1111,DCFKET
      XPR(I)=DCFKEL(I)
C
20    CONTINUE
C
      IF(MOD(JL,2).EQ.0) GO TO 400
      KR=0
      DO 300 K=NX,1,-1
      KR=KR+1
300   XPLISO(KR)=XPR(K)
      WRITE(3,*) (XPLISO(K),K=1,NX)          ! RECORD 5
      DO 250 I=1,NX
      WRITE (4'IV4)  V(I),U(I),DCFKEL(I),DCFKET
250   CONTINUE
            TYPE 1111, (V(I),U(I),DCFKEL(I),VELSQ,DCFKET,I=1,NX)
      FORMAT(5E13.7)
```

```
          [illegible]
[illegible] WRITE(3,*) (PPR(K),K=1,NX)                              REPORT 5
          [illegible] 260 [illegible] NX
          WRITE (4,1004) V(I),W(I),[illegible]
[illegible] [illegible]
                  [illegible]

[illegible] CONTINUE
          CALL CLOSE (1)
          CALL CLOSE (3)
          CALL CLOSE (4)
          CALL ASSIGN (1,[illegible])
          CALL ASSIGN (2,[illegible])
          READ(1,525) TITLE
          READ(1,*) NX,NY
          READ(1,*) (PPR(K),K=1,NX)
          READ(1,*) [illegible]
C
          DO 9999 J=1,NY
          READ(1,*) (CALIB(J,K),K=1,NX)
          WRITE(2,2222) (CALIB(J,K),K=1,NX)
2222      FORMAT([illegible]F12.3)
C
9999      CONTINUE
          CALL CLOSE (1)
          CLOSE(UNIT=2,DISP='PRINT')
          STOP
          END
C-----------------------------------------------------------------------------
C         CALCULATION OF VELOCITY VECTORS [illegible] PROBE CALIBRATION
C         POLYNOMIALS AND MISALIGNMENT PRESSURES [illegible] JUNE/83
          SUBROUTINE CALCUL (P,V,W,[illegible])
          DIMENSION P(1)
CCC       ASIN(X)=ATAN(X/SQRT(1.-X*X))
CCC       ACOS(X)=ATAN(SQRT(1.-X*X)[illegible])
C
          PHOY = (P(1)+P(2)+P(3)+P(4))*0.25
C         P(2) AND P(1) WILL BE CORRECTED VALUES MEASURED BY PROBE
          P(2)=P(2)+18.
          P(1)=P(1)+19.
          DD    = P(2)-P(4)
          EE    = P(1)-P(3)
          ADD   = ABS(DD)
          AEE   = ABS(EE)
          FF    = AEE - ADD
          IF (EE.EQ.0.)      GO TO 2
          GG    = ABS(DD/EE)
          FIR   = ATAN(GG)
          FI    = 180.*FIR/3.14159
          GO TO 3
  2       FI    = 90.0
          FIR   = 3.14159/2.0
  3       RA    = DD*DD+EE*EE
          BI    = SQRT(RA)
          BIR   = BI/ABS(P(5)-PHOY)
          IF (FF.LE.0.005)     GO TO 4
          IF (EE.GE.0.01)      GO TO 5
          T1    = 13.72656*BIR+(-2.111228E-1)*FIR**2-(.9420486)*BIR**3+
     1    (2.933134E-1)*BIR**4
          T2    = -(2.697529E-2)*BIR**5
          TH    = T1 + T2 - 1.241217
          DI    = (5.870109E-1)+(4.466144E-3)*TH+(-3.990502E-4)*TH**2
```

F4

```
     [illegible] 405356E-9)*TH**5
C
      [illegible] (D1+D2+D3)*1.0
      [illegible]
      [illegible]
      [illegible]
      [illegible]
      [illegible]
      [illegible]
      [illegible]
      [illegible]
      IF [illegible]                                  RU = 1
      IF (CP[illegible]                               SU = 2
      IF (CP[illegible]                               RI = 3
      IF [illegible]
      [illegible] = TH[illegible]
      IF (CP.LT.[illegible]
      IF(TH.LT.[illegible]) GO TO 832
              SSTH=SIN(TH)
              SSFIR=COS(FIR)
      SAL  = SIN(TH)*COS(FIR)
      CTE=1.-SAL*SAL
      CGA=COS(TH)/[illegible]
C
831   [illegible] CGA  = COS(TH)/(SQRT(ABS(1.-SAL*SAL)))
      CAL=SQRT(1.-SAL*SAL)
      SGA=SQRT(1.-CGA*CGA)
      TYPE [illegible] TH,FIR,SSTH,SSFIR,SAL,CGA,CTE
[illegible] FORMAT([illegible]TH,FI,STH,CFI,SAL,CGA,CTE[illegible]F10.4)
      [illegible]
      [illegible]
      [illegible]
      [illegible]
      [illegible]
      GO TO [illegible]
832   [illegible]
      [illegible]
      [illegible]
833   RETURN
4     IF [illegible] GO TO [illegible]
      T1   = 2.[illegible]
      T2   = +8.[illegible]
      T3   = (5.[illegible]E-1)*BIR**5[illegible]
      TH   = T1+T2+T3[illegible]
      D1   = (5.[illegible]E-1)+(8.[illegible]
      D2   = (-5.[illegible]E-6)*TH**3[illegible]
      D3   = (1.[illegible]E-8)*TH**5[illegible]
      FD   = (D1+D2+D3)*1.0
      C1   = (-3.256466E-3)*TH+(1.21[illegible]E-3)*TH**2-(1.[illegible]E-4)*
     1TH**3
      C2   = (8.768030E-6)*TH**4+(-2.17[illegible]E-7)*TH**5+(1.[illegible]E-9)
     1*TH**6
      CP   = C1+C2+9.777586E-4
      GO TO 10
5     T1   = 17.26694*BIR-8.755524*BIR**2
      T2   = 5.748909*BIR**3-(2.[illegible])*BIR**4
      T3   = (3.965276E-1)*BIR**5-(2.331693E-2)*BIR**6
      TH   = T1+T2+T3+0.4341921
      D1   = (5.95200E-1)+(7.55[illegible]E-3)*TH+(1.564457E-4)*TH**2
      D2   = (-4.345895E-5)*TH**3+(2.162540E-6)*TH**4
      D3   = (-4.380951E-8)*TH**5+(3.240741E-10)*TH**6
```

F5

```
      C1   =  -2.836968E-3)*TH+(6.199[illegible]E-4)*TH**2-(3.455378E-5)*TH**3
      C2   = (1.351172E-6)*TH**4-(2.517[illegible]E-3)*TH**5+(7.931602E-11)
     1*TH**[illegible]
      CP   = C1+C2+1.402665E-3
      GO TO 10
    6 T1   = (2.12255+BIR+(2.32[illegible]) [illegible] -3.22[illegible]*BIR**3+
     1(1.2840[illegible])*BIR**4
      T2   = (-2.069259E-1)*BIR**5+(1.41398[illegible]E-2)*BIR**6
      TH   = T1+T2-0.9372914
      D1   = (5.83329AE-1)+([illegible] 877[illegible])*TH+(-1.83362[illegible]E-4)*TH**2
      D2   = (-1.422016E-3)*TH**[illegible] [illegible]*TH**4
      D3   = (-8.693[illegible]612-9)*TH**5
      PD   = (D1+D2+D3)*1.00
      C1   = (-8.130340E-4)*TH-(2.06[illegible]E-5)*TH**2+(2.829430E-5)*TH**3
      C2   = (-4.975929E-7)*TH**4-(2.32[illegible]37E-9)*TH**5
      CP   = C1+C2+7.536941E-4
      GO TO 10
      END
```

GI

```
1 OPEN 1,4
2 OPEN 4,4,4
5 POKE 848,5
6 POKE 851,1
7 POKE 853,1
8 POKE 852,4
10 PRINT#4:REM ENABLES ERROR DIAGNOSTICS
20 DIM I(8),X(5),Y(5),P(5)
30 DIM CF(5),YC(5)
55 ST(1)=0
60 READ R
70 DATA 287
80 FOR I=1TO5:READ CF(I):NEXT
90 DATA 133.32,9.806356,9.80665E+04,6894.8,1
100 INPUT"DATE";I(3),I(4),I(5)
110 POKE 852,4
120 INPUT"NUMBER OF TRANSDUCERS TO CALIBRATE,0 TO END";NT
130 IF NT=0 THEN 1000
140 POKE 850,1
180 INPUT"WHEN READY TYPE 1";KK
190 IF KK<>1 THEN 180
200 NP=0
210 INPUT"VALUE OF POINT AND UNIT INDEX";RP,IX
220 IF IX=0 THEN 325
230 NP=NP+1
240 REM CLEAR AND INITIALIZE STORE
250 SYS(32017)
280 Y(NP)=RP*CF(IX)
310 V=PEEK(860)*256+PEEK(861)-2048
320 X(NP)=V:PRINT V:GOTO 210
325 GOSUB 5000:REM LINEAR REGRESSION
330 PRINT#1,"CALIBRATION OF CHANNEL"
340 PRINT#1
350 PRINT#1,"PRESSURE","DIGITS","CALCULATED PRESSURE"
355 ER=0
360 FOR J=1TO NP
363 YC(J)=A0+A1*X(J)
365 ER=ER+ABS(YC(J)-Y(J))*100/Y1
370 PRINT#1,Y(J);"PA",X(J),YC(J);"PA":NEXT
380 PRINT#1
400 IF ER<1.00 THEN 420
410 PRINT#1,"POSSIBLE ERROR IN CALIBRATION OF CHANNEL"
420 PRINT#1,"REGRESSION COEFFICIENTS ";A0,A1
440 PRINT#1,"MEAN ERROR";ER:PRINT#1
450 GO TO 110
1000 POKE 850,0
1012 INPUT"P-ATM,CONV:1 FOR HG,2 FOR H2O";PAT,IC
1013 PAT=PAT*CF(IC)
1014 INPUT"P-DYN IN MM H2O";P1
1015 P1=P1*CF(2)
1017 INPUT"ANGLE OF ATTACK";AL
1020 INPUT "TRAVERSE A";I(2)
1030 POKE 02,123
1031 POKE 01,123 :REM INI USR ADD
1032 INPUT "TEST NUMBER";I(1)
1033 FOR J=1TO5
1034 A=USR(I(J))
1035 NEXT J
1040 A=USR(-1)
1090 INPUT"TOTAL TEMP IN DEG-C";T0
1092 T0=T0+273.15
1095 RHT=PAT/(R*T0)
1096 U1=SQR(2*P1/RHT)
```

```
1200 PRINT#1,"DATE";I(3);I(4);I(5):PRINT#1
1202 PRINT#1,"TESTS CONDITIONS":PRINT#1
1203 PRINT#1,"ATM PRESSURE";PAT;"PA"
1204 PRINT#1,"TEMP TOTALE";T0;"K"
1205 PRINT#1,"TRAVERSE A";I(2);"FS"
1206 PRINT#1,"TUNNEL SPEED";U1;"M/S"
1207 PRINT#1,"PR.DYN";P1;"PA"
1208 MU=1.4962E-06*T0↑1.5/(T0+120)
1209 RE=RHT*U1*.062/MU
1210 PRINT#1,"RE NO.";RE:PRINT#1
1211 PRINT#1,"TEST NUMBER";I(1):PRINT#1:PRINT#1:PRINT#1:PRINT#1:PRINT#1
1290 POI=0
1300 INPUT"EQUILIBRATION DELAY";ED
1310 POKE 849,ED
1320 POKE 59459,252:REM VIA DDR PINS 0,1 INPUT
1330 POKE 59471,12:REM PUTS 1 TO OUTPUT PINS 2&3
1345 POI=POI+1
1350 FOR J=1TO5
1370 SYS(32017)
1380 POKE 59471,4:FOR K=1TO95:NEXT
1390 POKE 59471,12:FOR K=1TO500:NEXT
1400 SYS(31945)
1430 V=PEEK(860)*256+PEEK(861)-2048
1440 P(J)=A0+A1*V
1442 A=USR(V)
1443 NEXT
1446 PRINT#1,"POINT";POI,"XS";XS,"YS";YS:PRINT#1
1455 PMOY=(P(1)+P(2)+P(3)+P(4))/4
1460 PDP=(P(5)-PMOY)/P1
1465 DD=P(2)-P(4) :HH=P(1)-P(3)
1468 ADD=ABS(DD) :AEE=ABS(HH) :FF=AEE-ADD
1469 IF DD=0 THEN 1475
1470 GG=ABS(HH/DD) :FIR=ATN(GG):FI=180*FIR/3.14159 :GO TO 1480
1475 FI=90
1480 RA=DD*DD+HH*HH
1484 BI=SQR(RA)
1485 BIR=BI/ABS(P(5)-PMOY)
1486 CP=1-(P(5)/P1)
1527 IF P(1)>=P(3)ANDP(4)>=P(2) THEN QU=1
1528 IF P(1)>=P(3)ANDP(2)>=P(4)THEN QU=2
1529 IF P(1)<=P(3)ANDP(2)>=P(4) THEN QU=3
1530 IF P(1)<=P(3)ANDP(4)>=P(2) THEN QU=4
1541 PRINT#1,"P1";P(1);"PA","P2";P(2),"P3";P(3);"PA":PRINT#1
1542 PRINT#1,"P4";P(4);"PA","P5";P(5);"PA","[FI]";FI;"CP";CP:PRINT#1
1543 PRINT#1,"BIR";BIR,"PDP";PDP,"PMOY";PMOY:PRINT#1:PRINT#1:PRINT#1
1550 GO TO 1850
1710 GO TO 1525
1850 PRINT"ACQUISITION SUSPENDED.FOR NEXT POINT,TYPE 1"
1860 INPUT KK
1870 IF KK=1 THEN 1310
1900 SYS(31862)
1910 PRINT"ACQUISITION SUSPENDED.TO RESUME,TYPE 1"
1920 INPUT KK
1930 IF KK=1 THEN 110
1960 GO TO 2200
2200 END
5000 X1=0:Y1=0:XY=0:X2=0:Y2=0
5010 FORJ=1TONP
5020 X1=X1+X(J):Y1=Y1+Y(J)
5030 XY=XY+X(J)*Y(J)
5040 X2=X2+X(J)↑2:Y2=Y2+Y(J)↑2:NEXT
5050 DN=X2-X1*X1/NP
5060 A1=(XY-X1*Y1/NP)/DN
5070 A0=(Y1-A1*X1)/NP
5080 R2=A1*A1*(X2-X1*X1/NP)/(Y2-Y1*Y1/NP)
```

G2

```
 5100 RETURN
 8000 INPUT"NUMBER CHANNEL";N
 8020 POKE 40970,0
 8030 POKE 40971,0
 8040 A=PEEK(40972):IF NOTA AND 128 THEN      8040
 8050 A=PEEK(40973):IF NOTA AND 128 THEN      8070
 8060 A=A-248:GO TO 8080
 8070 A=A+8
 8080 A=A*256+PEEK(40974)-2048
 8090 PRINT"ON CHANNEL NUMBER";1,A;"DIGITS"
 8100 GO TO 8000
READY.
```

G3

```
1 OPEN 1,4
2 OPEN 4,4,4
5 POKE 848,5
6 POKE 851,1
7 POKE 853,1
8 POKE 852,4
10 PRINT#4:REM ENABLES ERROR DIAGNOSTICS
20 DIM I(8),X(5),Y(5),P(5)
30 DIM CF(5),YC(5)
55 ST(1)=0
60 READ R
70 DATA 287
80 FOR I=1TO5:READ CF(I):NEXT
90 DATA 133.32,9.806356,9.80665E+04,6894.8,1
100 INPUT"DATE";I(3),I(4),I(5)
110 POKE 852,4
120 INPUT"NUMBER OF TRANSDUCERS TO CALIBRATE,0 TO END";NT
130 IF NT=0 THEN 1000
140 POKE 850,1
180 INPUT"WHEN READY TYPE 1";KK
190 IF KK<>1 THEN 180
200 NP=0
210 INPUT"VALUE OF POINT AND UNIT INDEX";RP,IX
220 IF IX=0 THEN 325
230 NP=NP+1
240 REM CLEAR AND INITIALIZE STORE
250 SYS(32017)
280 Y(NP)=RP*CF(IX)
310 V=PEEK(860)*256+PEEK(861)-2048
320 X(NP)=V:PRINT V:GOTO 210
325 GOSUB 5000:REM LINEAR REGRESSION
330 PRINT#1,"CALIBRATION OF CHANNEL"
340 PRINT#1
350 PRINT#1,"PRESSURE","DIGITS","CALCULATED PRESSURE"
355 ER=0
360 FOR J=1TO NP
363 YC(J)=A0+A1*X(J)
365 ER=ER+ABS(YC(J)-Y(J))*100/Y1
370 PRINT#1,Y(J);"PA",X(J),YC(J);"PA":NEXT
380 PRINT#1
400 IF ER<1.00 THEN 420
410 PRINT#1,"POSSIBLE ERROR IN CALIBRATION OF CHANNEL"
420 PRINT#1,"REGRESSION COEFFICIENTS ";A0,A1
440 PRINT#1,"MEAN ERROR";ER:PRINT#1
450 GO TO 110
1000 POKE 850,0
1012 INPUT"P-ATM,CONV:1 FOR HG,2 FOR H2O";PAT,IC
1013 PAT=PAT*CF(IC)
1014 INPUT"P-DYN IN MM H2O";P1
1015 P1=P1*CF(2)
1017 INPUT"ANGLE OF ATTACK";AL
1020 INPUT "TRAVERSE A";I(2)
1030 POKE 02,123
1031 POKE 01,123 :REM INI USR ADD
1032 INPUT "TEST NUMBER";I(1)
1033 FOR J=1TO5
1034 A=USR(I(J))
1035 NEXT J
1040 A=USR(-1)
1090 INPUT"TOTAL TEMP IN DEG-C";T0
1092 T0=T0+273.15
1095 RHT=PAT/(R*T0)
1096 U1=SQR(2*P1/RHT)
```

H2

```
1200 PRINT#1,"DATE";I(3);I(4);I(5):PRINT#1
1202 PRINT#1,"TESTS CONDITIONS":PRINT#1
1203 PRINT#1,"ATM PRESSURE";PAT;"PA"
1204 PRINT#1,"TEMP TOTALE";T0;"K"
1205 PRINT#1,"TRAVERSE A";I(2);"FS"
1206 PRINT#1,"TUNNEL SPEED";U1;"M/S"
1207 PRINT#1,"PR.DYN";P1;"PA"
1208 MU=1.4962E-06*T0↑1.5/(T0+120)
1209 RE=RHT*U1*.062/MU
1210 PRINT#1,"RE NO.";RE:PRINT#1
1211 PRINT#1,"TEST NUMBER";I(1):PRINT#1:PRINT#1:PRINT#1:PRINT#1:PRINT#1
1290 POI=0
1300 INPUT"EQUILIBRATION DELAY";ED
1310 POKE 849,ED
1320 POKE 59459,252:REM VIA DDR PINS 0,1 INPUT
1330 POKE 59471,12:REM PUTS 1 TO OUTPUT PINS 2&3
1345 POI=POI+1
1350 FOR J=1TO5
1370 SYS(32017)
1380 POKE 59471,4:FOR K=1TO95:NEXT
1390 POKE 59471,12:FOR K=1TO500:NEXT
1400 SYS(31945)
1430 V=PEEK(860)*256+PEEK(861)-2048
1440 P(J)=A0+A1*V
1442 A=USR(V)
1443 NEXT
1446 PRINT#1,"POINT";POI,"XS";XS,"YS";YS:PRINT#1
1455 PMOY=(P(1)+P(2)+P(3)+P(4))/4
1464 P(2)=P(2)+18  :P(1)=P(1)+10
1465 DD=P(2)-P(4) :HH=P(1)-P(3)
1468 ADD=ABS(DD) :AEE=ABS(HH) :FF=AEE-ADD
1469 IF HH=0 THEN 1475
1470 GG=ABS(DD/HH) :FIR=ATN(GG):FI=180*FIR/3.14159 :GO TO 1480
1475 FI=90
1480 RA=DD*DD+HH*HH
1484 BI=SQR(RA)
1485 BIR=BI/ABS(P(5)-PMOY)
1490 IF FF<=0.005 THEN 1650
1495 IF HH>=0.01 THEN 1600
1497 T1=13.72858*BIR-(2.11223E-1)*BIR↑2-(0.942049)*BIR↑3+(2.933134E-1)*BIR↑4
1498 T2=-(2.697529E-2)*BIR↑5
1510 TH=T1+T2-1.2412170
1515 D1=(5.870109E-1)+(4.46614E-3)*TH+(-3.990502E-4)*TH↑2
1516 D2=(-5.36291E-6)*TH↑3+(5.538313E-7)*TH↑4
1517 D3=(-7.405356E-9)*TH↑5
1518 PD=(D1+D2+D3)*1.00000
1520 C1=(7.065830E-4)*TH-(3.03239E-4)*TH↑2+(4.834588E-5)*TH↑3
1521 C2=(-1.43039E-6)*TH↑4+(2.612108E-8)*TH↑5-(2.319786E-10)*TH↑6
1522 CP=C1+C2
1525 MV=ABS((P(5)-PMOY)*2/(RHT*PD)):MV=SQR(MV)
1526 BT=P(5)+CP*RHT*MV*MV/2
1527 IF P(1)>=P(3)ANDP(4)>=P(2) THEN QU=1
1528 IF P(1)>=P(3)ANDP(2)>=P(4) THEN QU=2
1529 IF P(1)<=P(3)ANDP(2)>=P(4) THEN QU=3
1530 IF P(1)<=P(3)ANDP(4)>=P(2) THEN QU=4
1531 PP=BT/P1
1541 PRINT#1,"P1";P(1);"PA","QUADRANT";QU,"[THETA]";TH;"DEGRES":PRINT#1
1542 PRINT#1,"P2";P(2);"PA","[FI]";FI;"DEGRES":PRINT#1
1543 PRINT#1,"P3";P(3);"PA","PD";PD,"VELOCITY";MV;"M/S"  :PRINT#1
1544 PRINT#1,"P4";P(4);"PA","CP";CP,"PR.TOT.LOC";BT;"PA"  :PRINT#1
1545 PRINT#1,"P5";P(5);"PA","PMOY";PMOY;"PA","PP";PP  :PRINT#1:PRINT#1:PRINT#
1550 GO TO 1850
1600 T1=21.53083*BIR-13.94689*BIR↑2
1601 T2=8.953023*BIR↑3-(3.248728)*BIR*BIR*BIR*BIR
1602 T3=(5.903704E-1)*BIR↑5-(4.14847E-2)*BIR↑6
```

H3

```
 1620 D1=(5.909329E-1)+(8.193470E-4)*TH-(6.777613E-5)*TH↑2
 1621 D2=(-5.960415E-6)*TH↑3-(1.537824E-7)*TH↑4
 1622 D3=(1.653859E-8)*TH↑5-(2.34760E-10)*TH↑6
 1623 PD=(D1+D2+D3)*1.0
 1625 C1=(-3.25646E-3)*TH+(1.213657E-3)*TH↑2-(1.436069E-4)*TH↑3
 1626 C2=(8.768080E-6)*TH↑4-(2.172509E-7)*TH↑5+(1.907005E-9)*TH↑6
 1629 CP=C1+C2+9.777586E-4
 1630 GO TO 1525
 1650 IF DD<=0.01 THEN 1685
 1660 T1=17.26694*BIR-8.755624*BIR↑2
 1661 T2=5.748909*BIR↑3-2.148792*BIR↑4
 1662 T3=(3.965276E-1)*BIR↑5-(2.831603E-2)*BIR↑6
 1663 TH=T1+T2+T3+0.4941921
 1670 D1=(5.952E-1)+(7.559778E-5)*TH+(1.564457E-4)*TH↑2
 1671 D2=(-4.345895E-5)*TH↑3+(2.162540E-6)*TH↑4
 1672 D3=(-4.38095E-8)*TH↑5+(3.246741E-10)*TH↑6
 1673 PD=(D1+D2+D3)*1.0
 1675 C1=(-2.83687E-3)*TH+(6.199820E-4)*TH↑2-(3.455378E-5)*TH↑3
 1676 C2=(1.651172E-6)*TH↑4-(2.517231E-8)*TH↑5+(7.831602E-11)*TH↑6
 1677 CP=C1+C2+1.402665E-3
 1680 GO TO 1525
 1685 T1=12.12255*BIR+(2.329581)*(BIR↑2)-3.229866*BIR↑3+(1.284068)*BIR↑4
 1686 T2=(-2.268258E-1)*BIR↑5+(1.48998E-2)*BIR↑6
 1687 TH=T1+T2-0.8373914
 1700 D1=(5.833296E-1,+(2.877764E-3)*TH+(-1.535622E-4)*TH↑2
 1701 D2=(-1.422516E-5)*TH↑3+(6.928993E-7)*TH↑4
 1702 D3=(-8.853089E-9)*TH↑5
 1703 PD=(D1+D2+D3)*1.00
 1705 C1=(-8.130340E-4)*TH-(2.066893E-5)*TH↑2+(2.829430E-5)*TH↑3
 1706 C2=(-4.975929E-7)*TH↑4+(2.329037E-9)*TH↑5
 1707 CP=C1+C2+7.536941E-4
 1710 GO TO 1525
 1850 PRINT"ACQUISITION SUSPENDED.FOR NEXT POINT,TYPE 1"
 1860 INPUT KK
 1870 IF KK=1 THEN 1310
 1900 SYS(31862)
 1910 PRINT"ACQUISITION SUSPENDED.TO RESUME,TYPE 1"
 1920 INPUT KK
 1930 IF KK=1 THEN 110
 1960 GO TO 2200
 2200 END
 5000 X1=0:Y1=0:XY=0:X2=0:Y2=0
 5010 FORJ=1TONP
 5020 X1=X1+X(J):Y1=Y1+Y(J)
 5030 XY=XY+X(J)*Y(J)
 5040 X2=X2+X(J)↑2:Y2=Y2+Y(J)↑2:NEXT
 5050 DN=X2-X1*X1/NP
 5060 A1=(XY-X1*Y1/NP)/DN
 5070 A0=(Y1-A1*X1)/NP
 5080 R2=A1*A1*(X2-X1*X1/NP)/(Y2-Y1*Y1/NP)
 5090 R2=SQR(ABS(R2))
 5100 RETURN
 8000 INPUT"NUMBER CHANNEL";N
 8020 POKE 40970,0
 8030 POKE 40971,0
 8040 A=PEEK(40972):IF NOTA AND 128 THEN      8040
 8050 A=PEEK(40973):IF NOTA AND 128 THEN      8070
 8060 A=A-248:GO TO 8080
 8070 A=A+8
 8080 A=A*256+PEEK(40974)-2048
 8090 PRINT"ON CHANNEL NUMBER";1,A;"DIGITS"
 8100 GO TO 8000
READY.
```

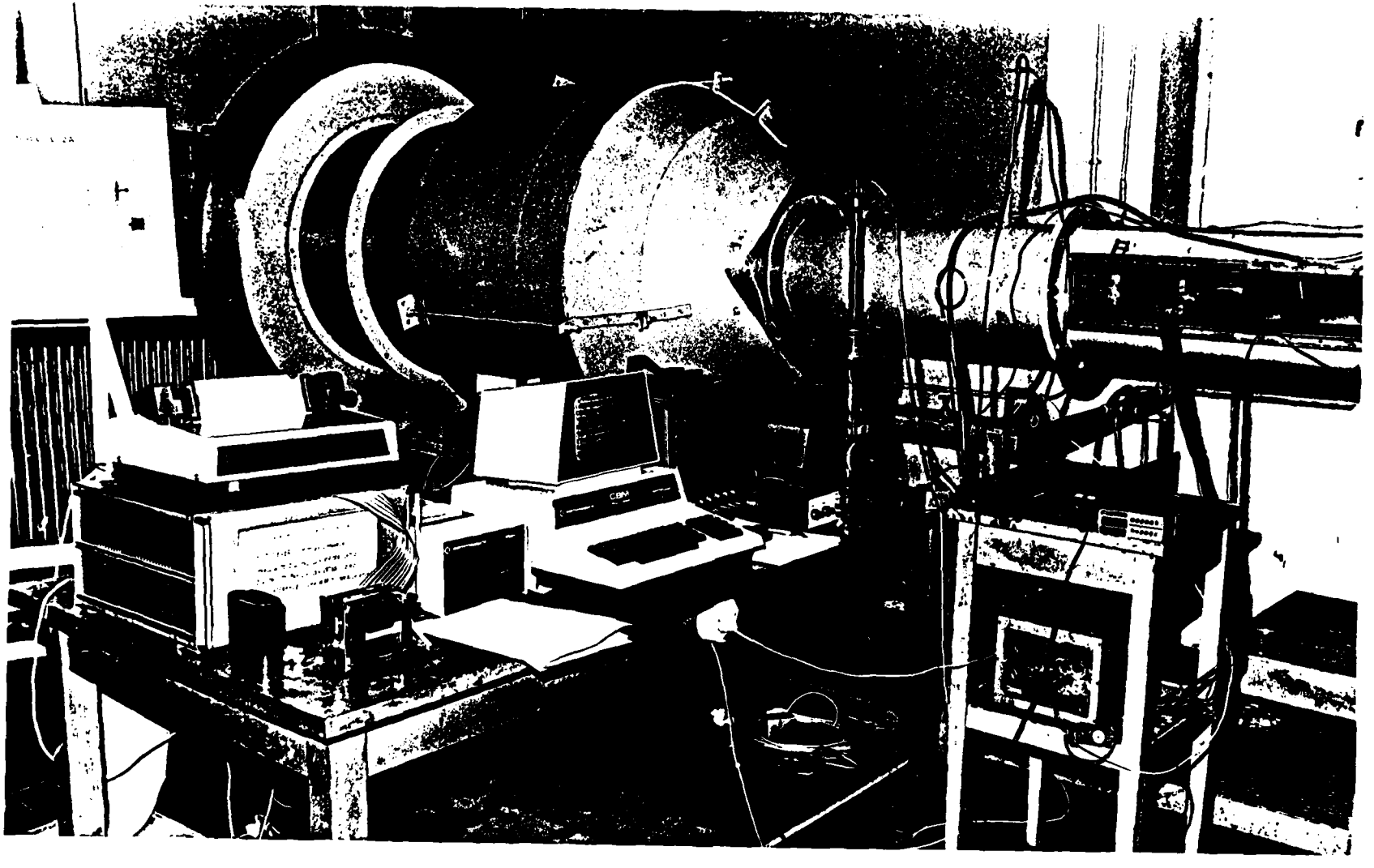

FIG. 1A - DATA ACQUISITION SYSTEM SET UP

1 - PET Commodore computer
2 - Floppy disk driver
3 - Digitizer
4 - Printer
5 - Digital cassette drive
6 - Scanivalve signal sensor and multiple channel box
7 - DC current regulator
8 - Pressure transducer gain box
9 - Betz manometer
10 - Multiple port scanivalve
11 - Scanivalve voltmeter
12 - DC current transformer

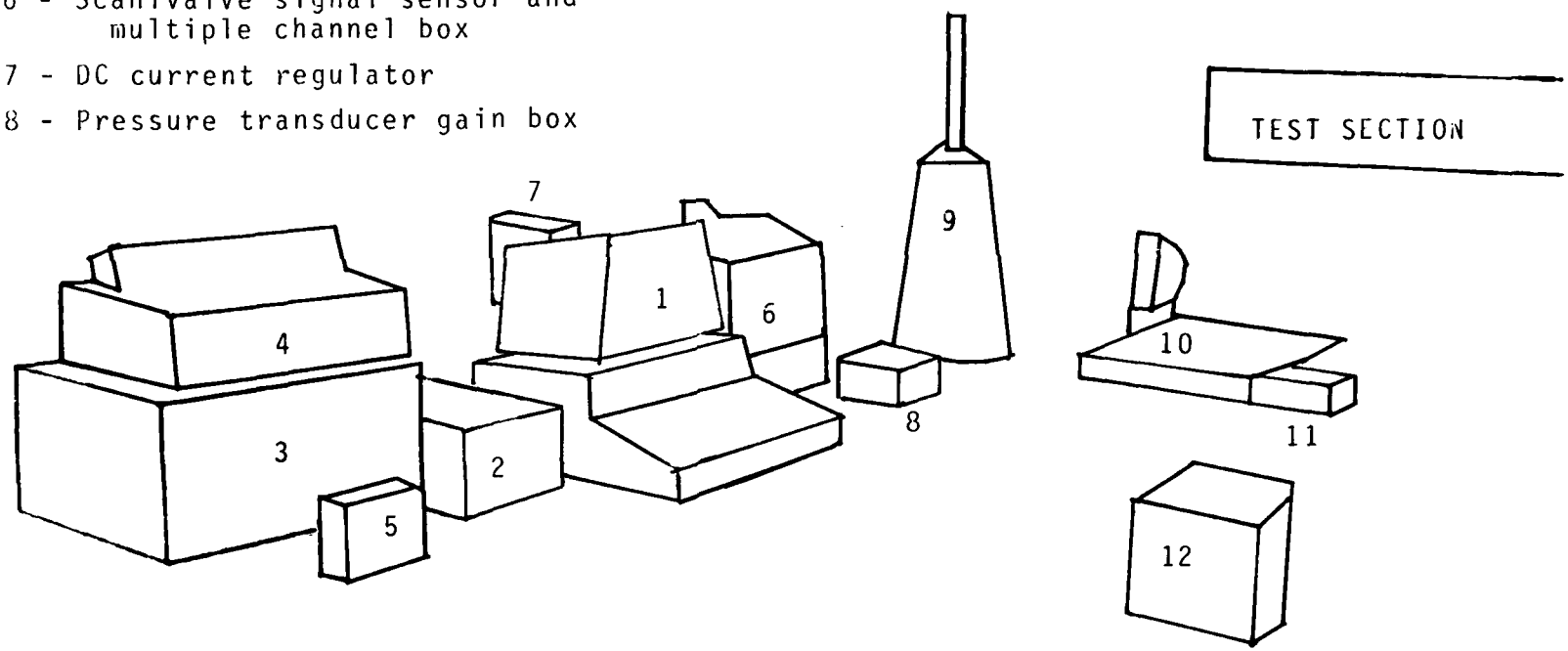

FIG. 1B - TEST INSTRUMENTATION DESCRIPTION

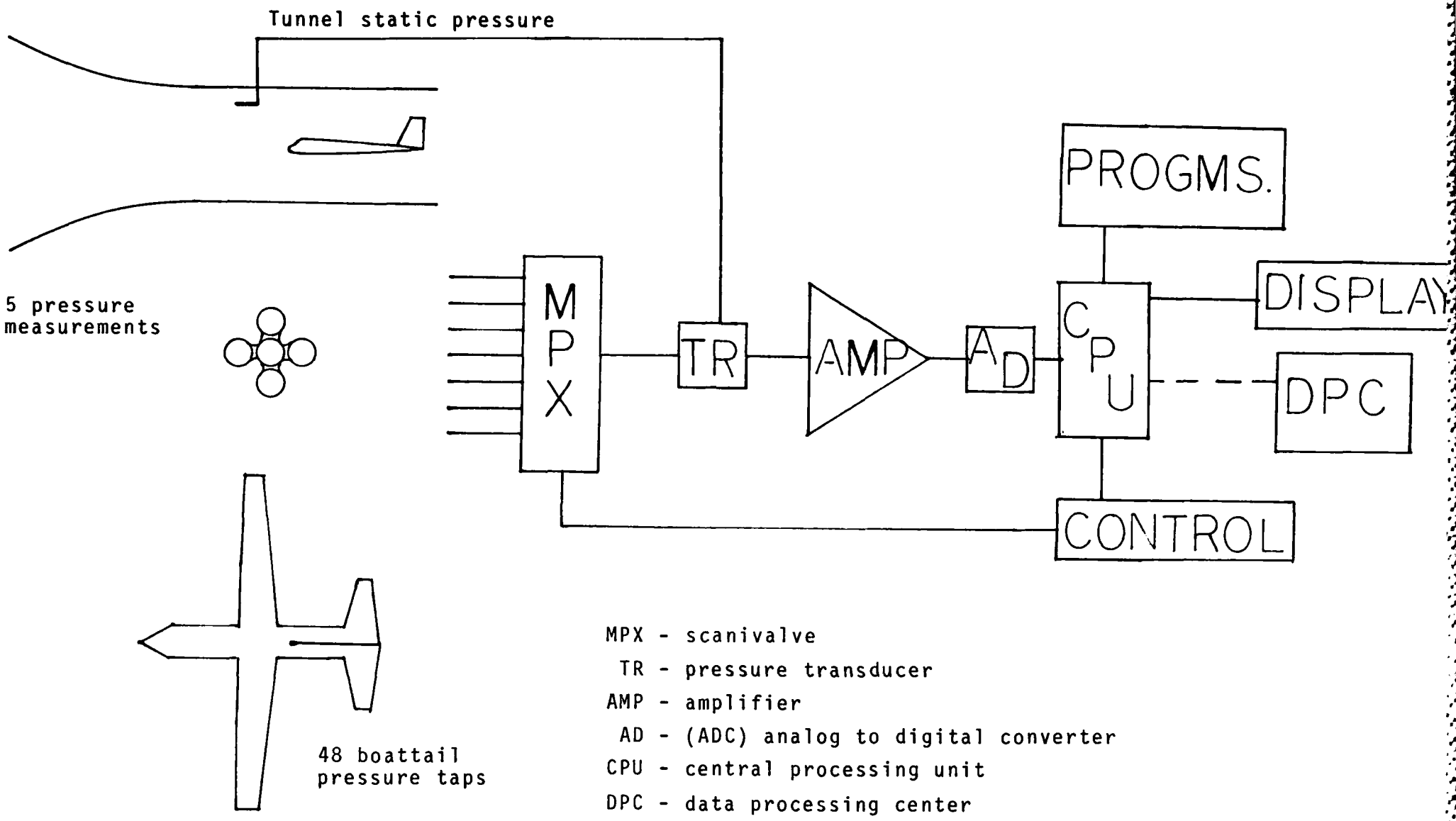

FIG. 1C - DATA ACQUISITION SYSTEM SCHEMATIC

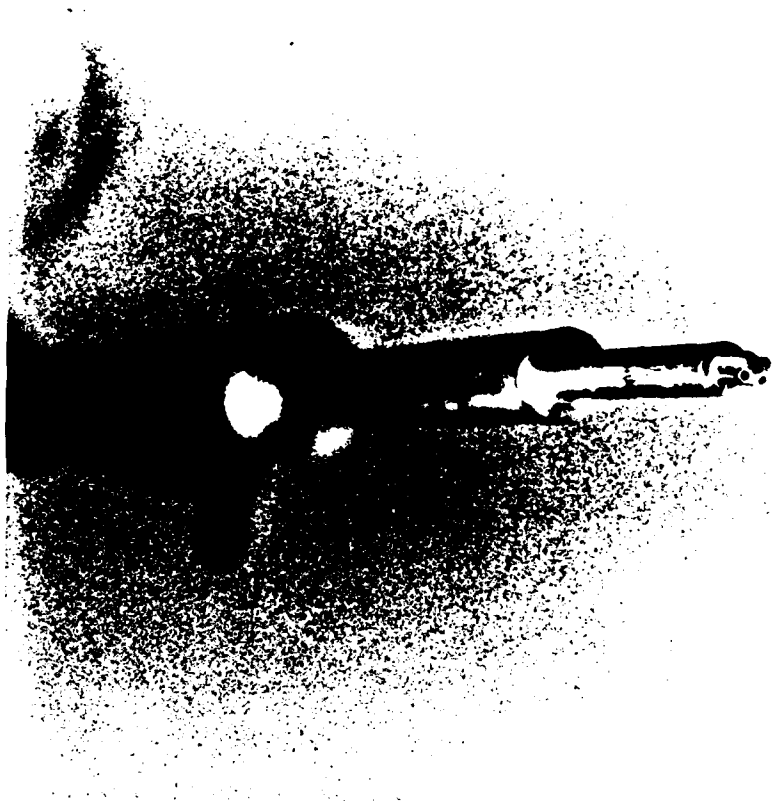

FIG. 2A - FIVE HOLE PROBE VIEW

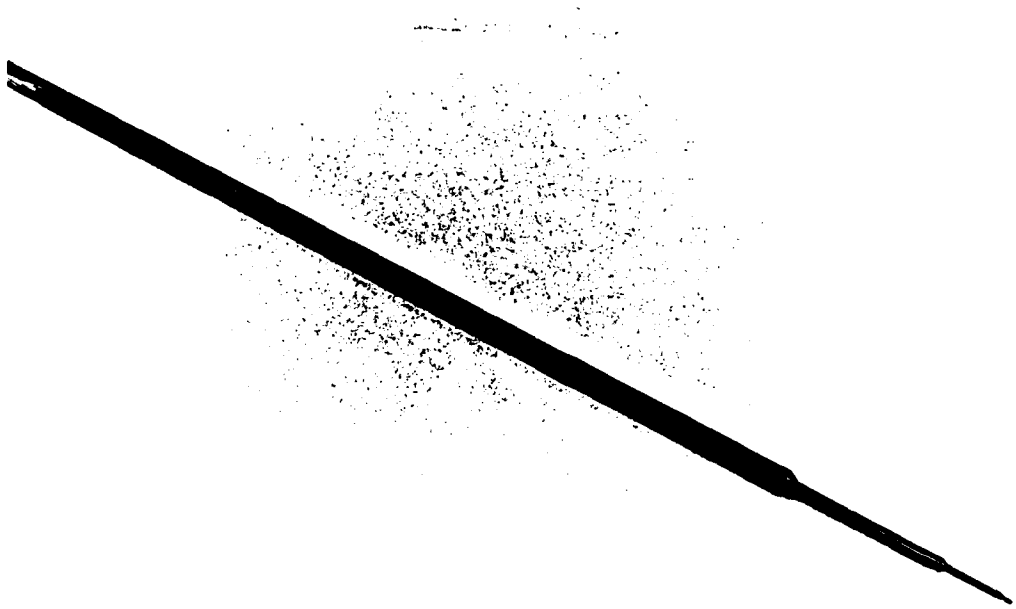

FIG. 2B - SUPPORT STEM FOR FIVE HOLE PROBE

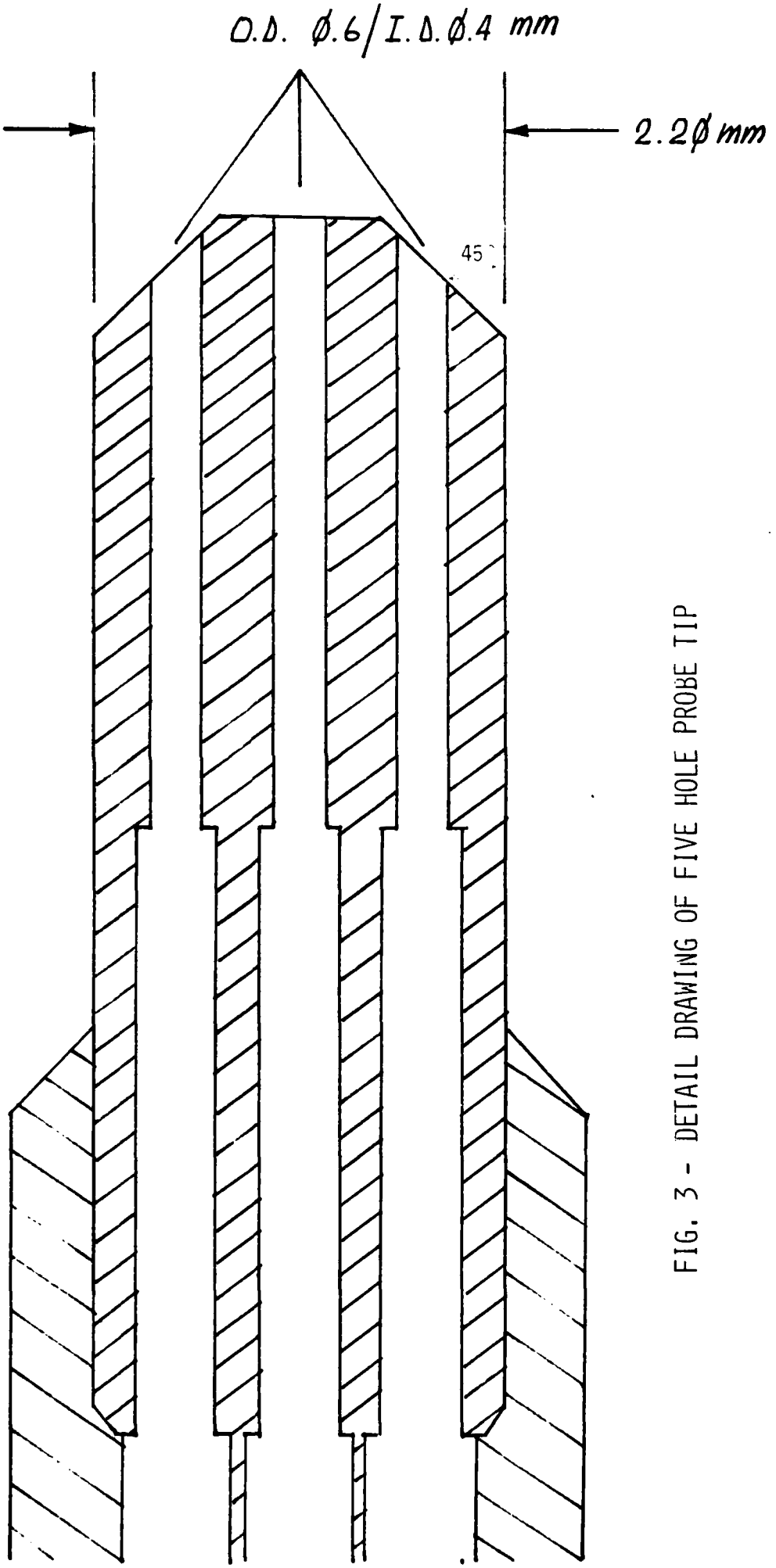

FIG. 3 - DETAIL DRAWING OF FIVE HOLE PROBE TIP

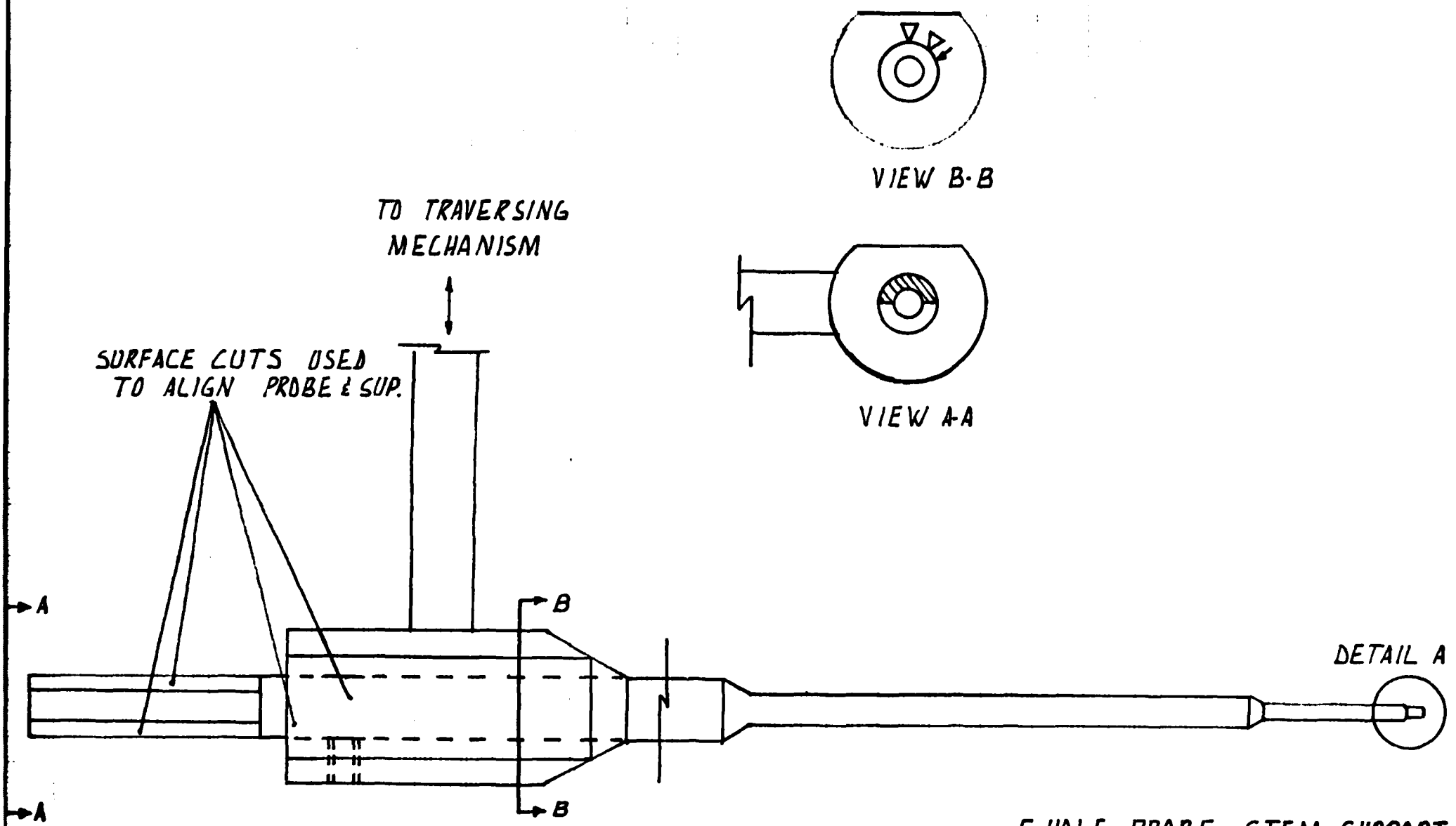

FIG. 4 - FIVE HOLE PROBE - STEM - TRAVERSING MECHANISM LINKAGE DRAWING

PRESSURE VS. SIGNAL OUTPUT OF
VALIDYNE MP 45-1 S-N. 49675 TRANSDUCER
RANGE ± 0.5 PSI DIFFERENTIAL

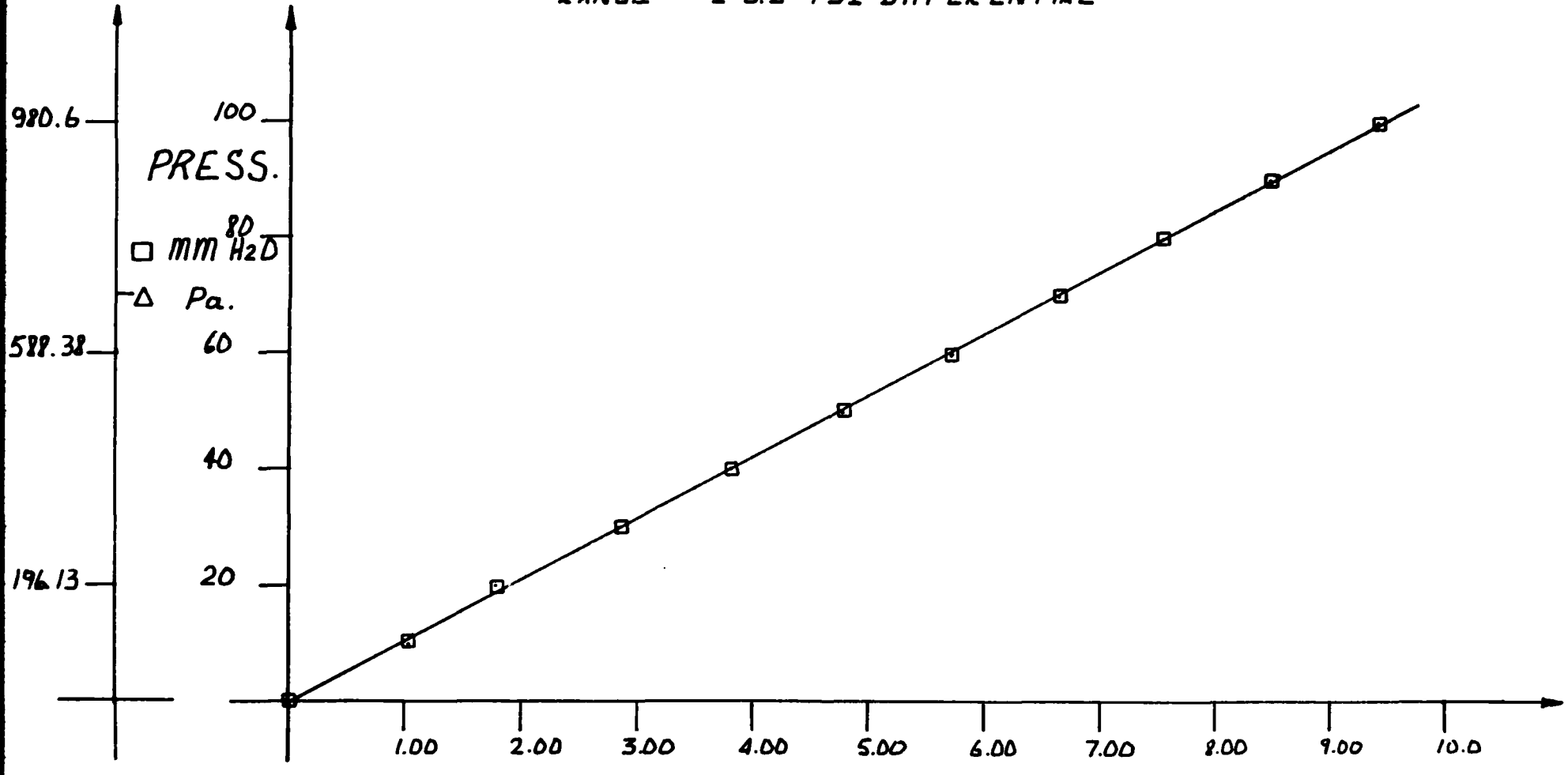

FIG. 5 - CALIBRATION CURVE FOR PRESSURE TRANSDUCER

ORDONEZ 7/83

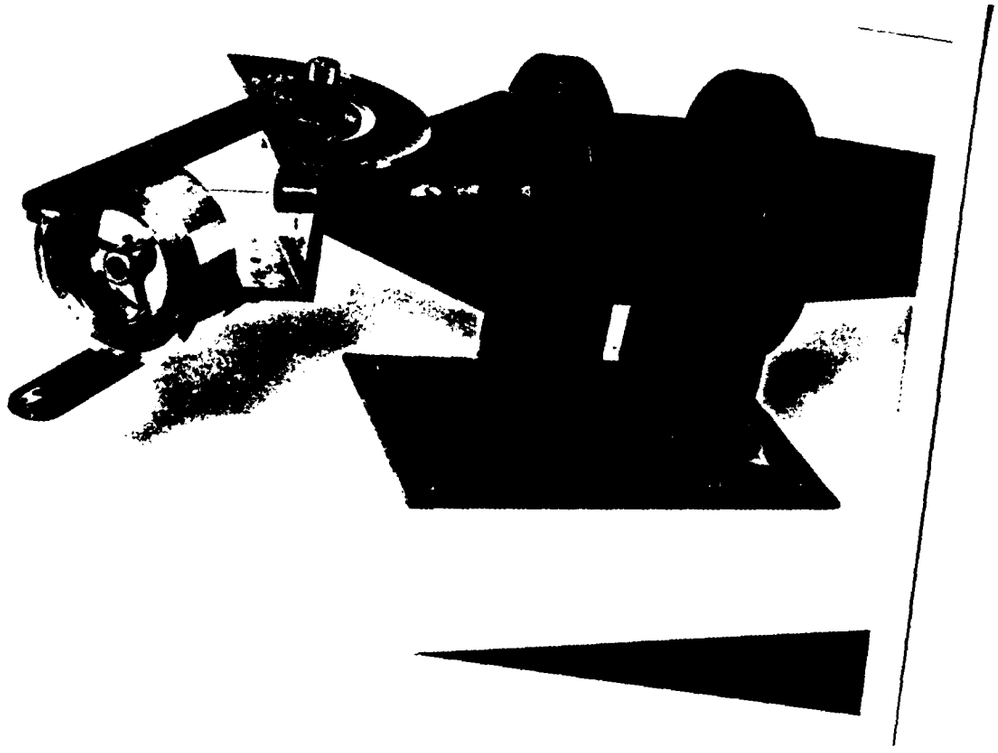

FIG. 6A – FIVE HOLE PROBE CALIBRATION DUCT

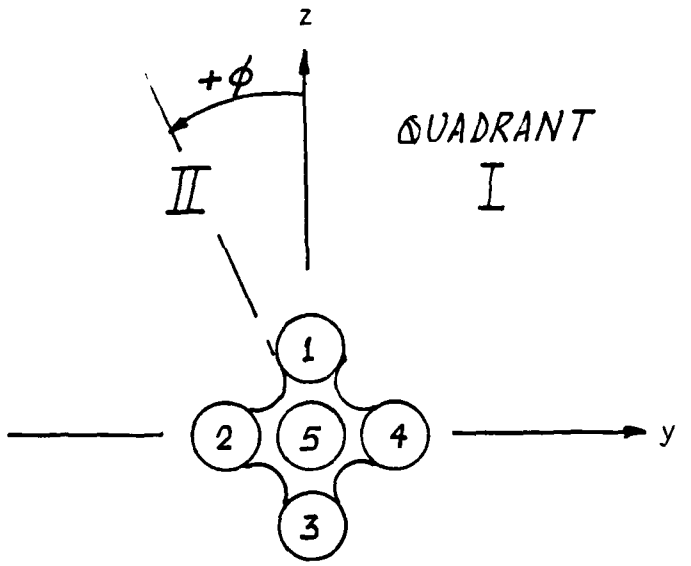

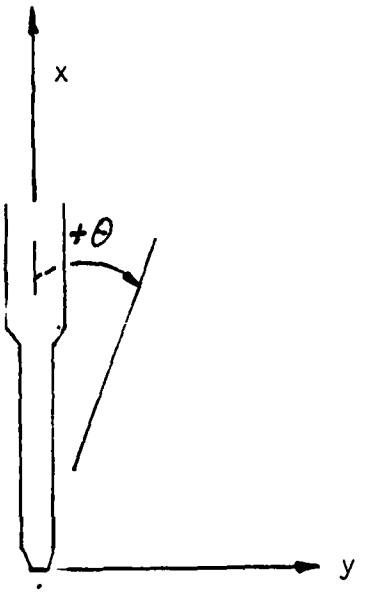

III IV

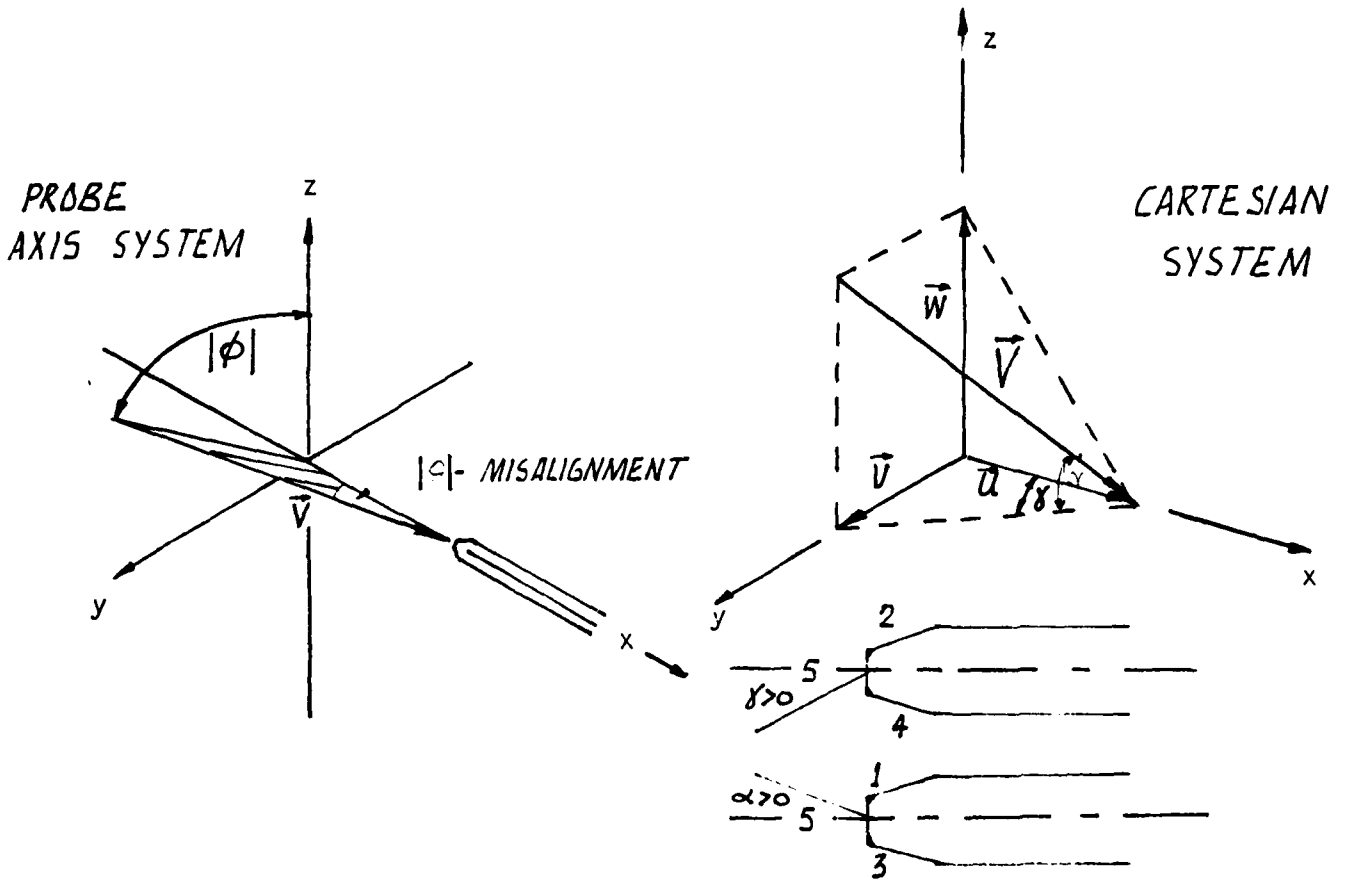

FIG. 6B - AXIS SYSTEM AND QUADRANT DEFINITION

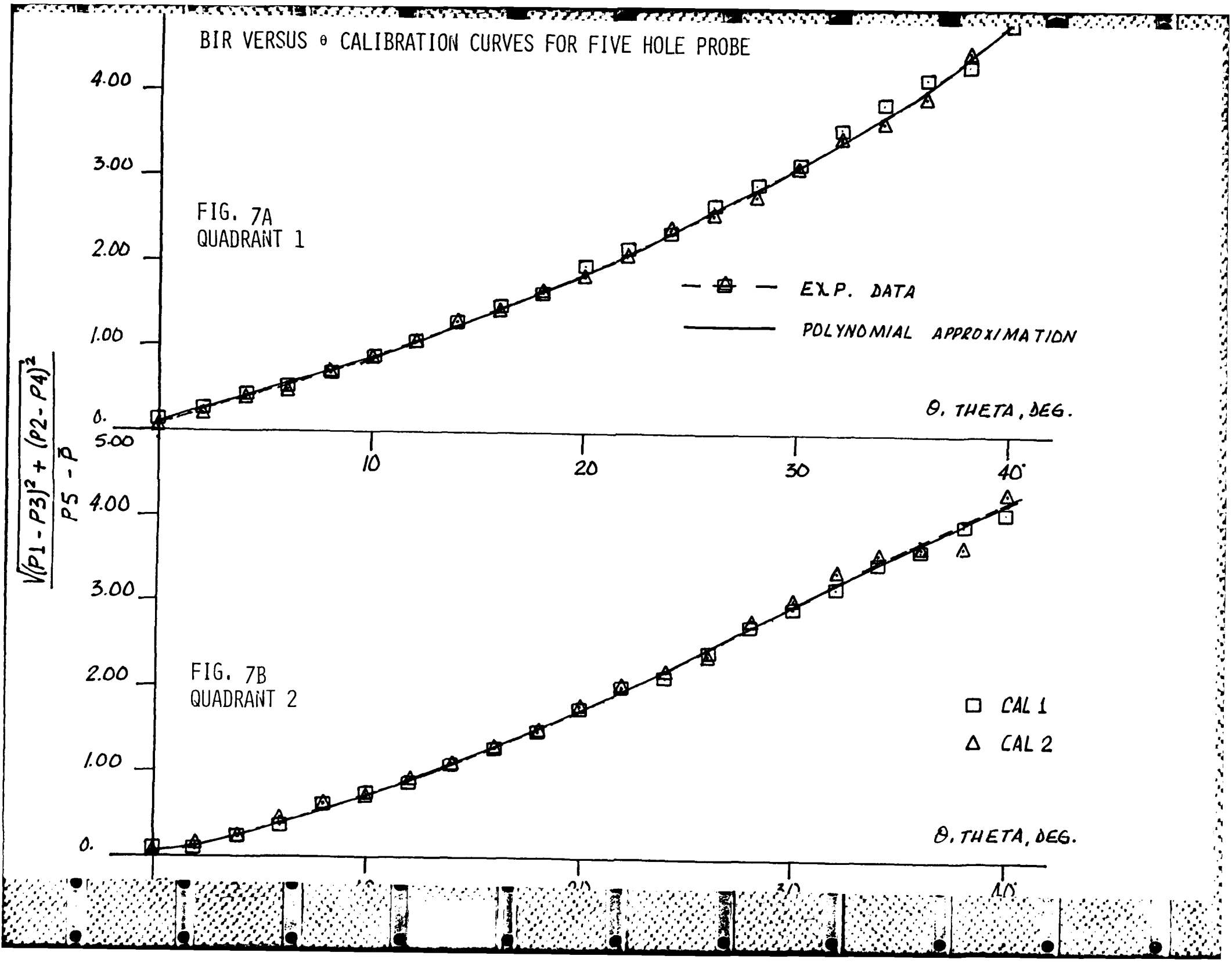
BIR VERSUS θ CALIBRATION CURVES FOR FIVE HOLE PROBE
FIG. 7A
QUADRANT 1
EXP. DATA
POLYNOMIAL APPROXIMATION
θ, THETA, DEG.
$\frac{\sqrt{(P1-P3)^2+(P2-P4)^2}}{P5-\bar{P}}$
4.00
3.00
2.00
1.00
0.
5.00
10
20
30
40°
FIG. 7B
QUADRANT 2
CAL 1
CAL 2
θ, THETA, DEG.

BIR VERSUS θ CALIBRATION CURVES FOR FIVE HOLE PROBE

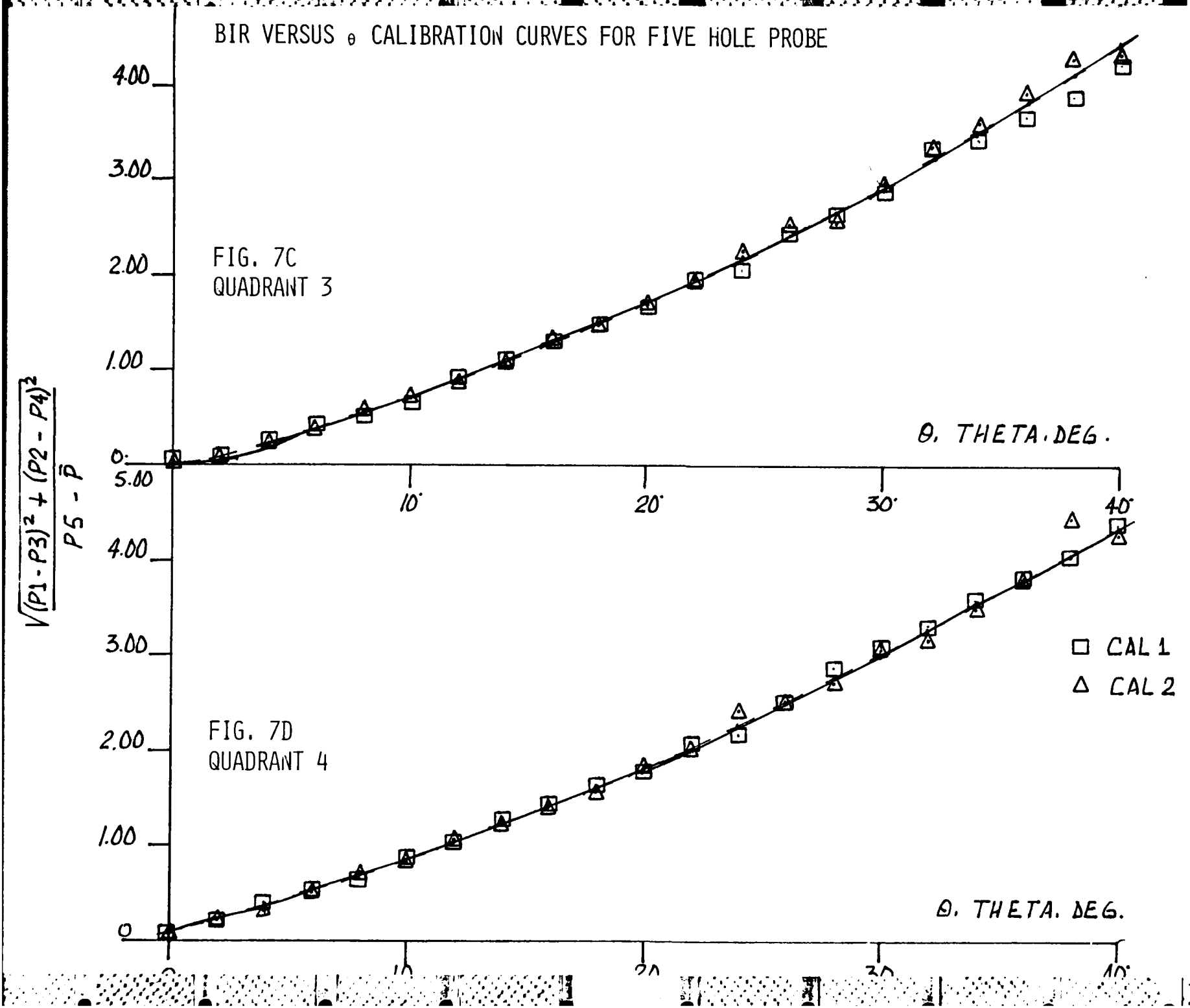

FIG. 7C
QUADRANT 3

FIG. 7D
QUADRANT 4

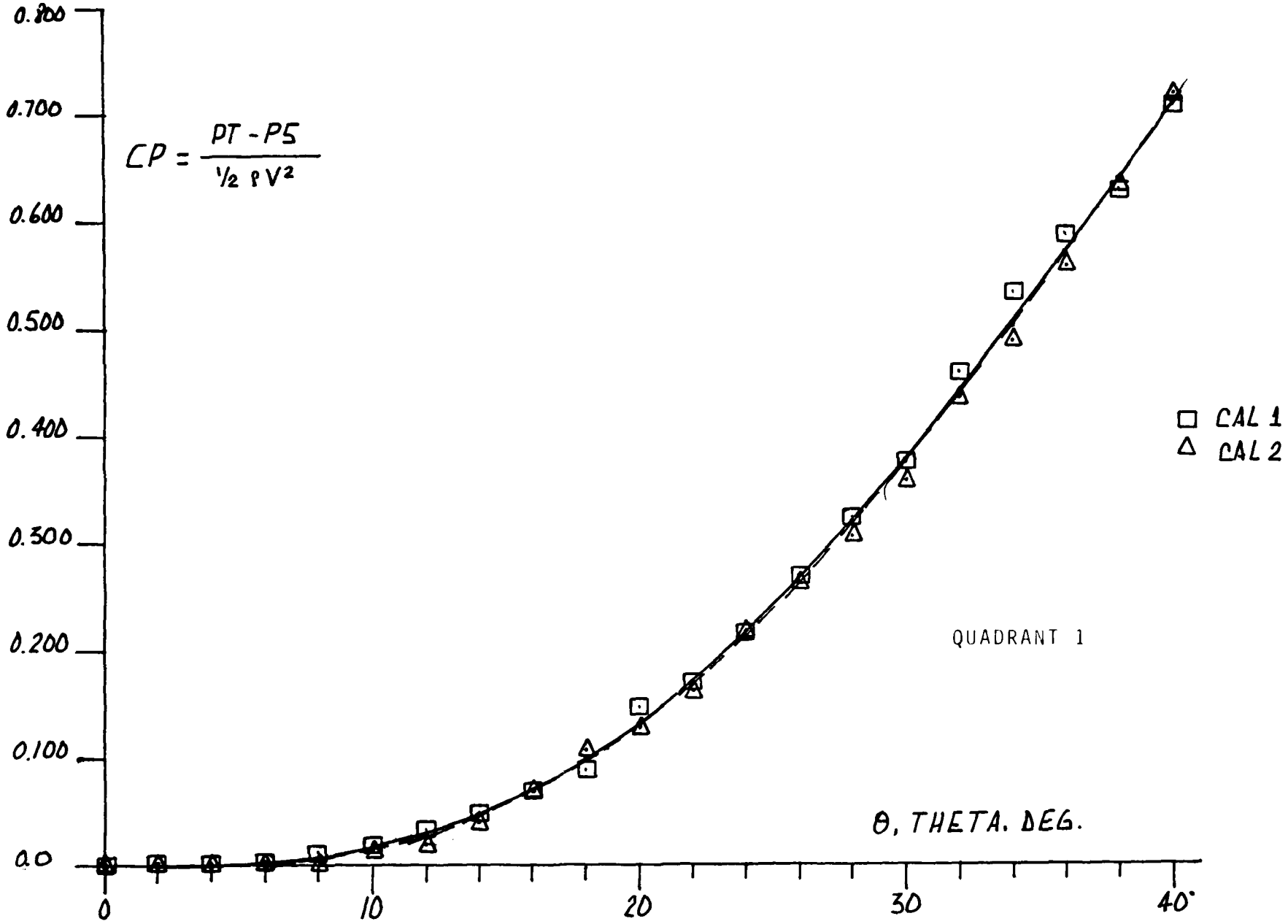

FIG. 3A - CP VERSUS θ CALIBRATION CURVES FOR FIVE HOLE PROBE

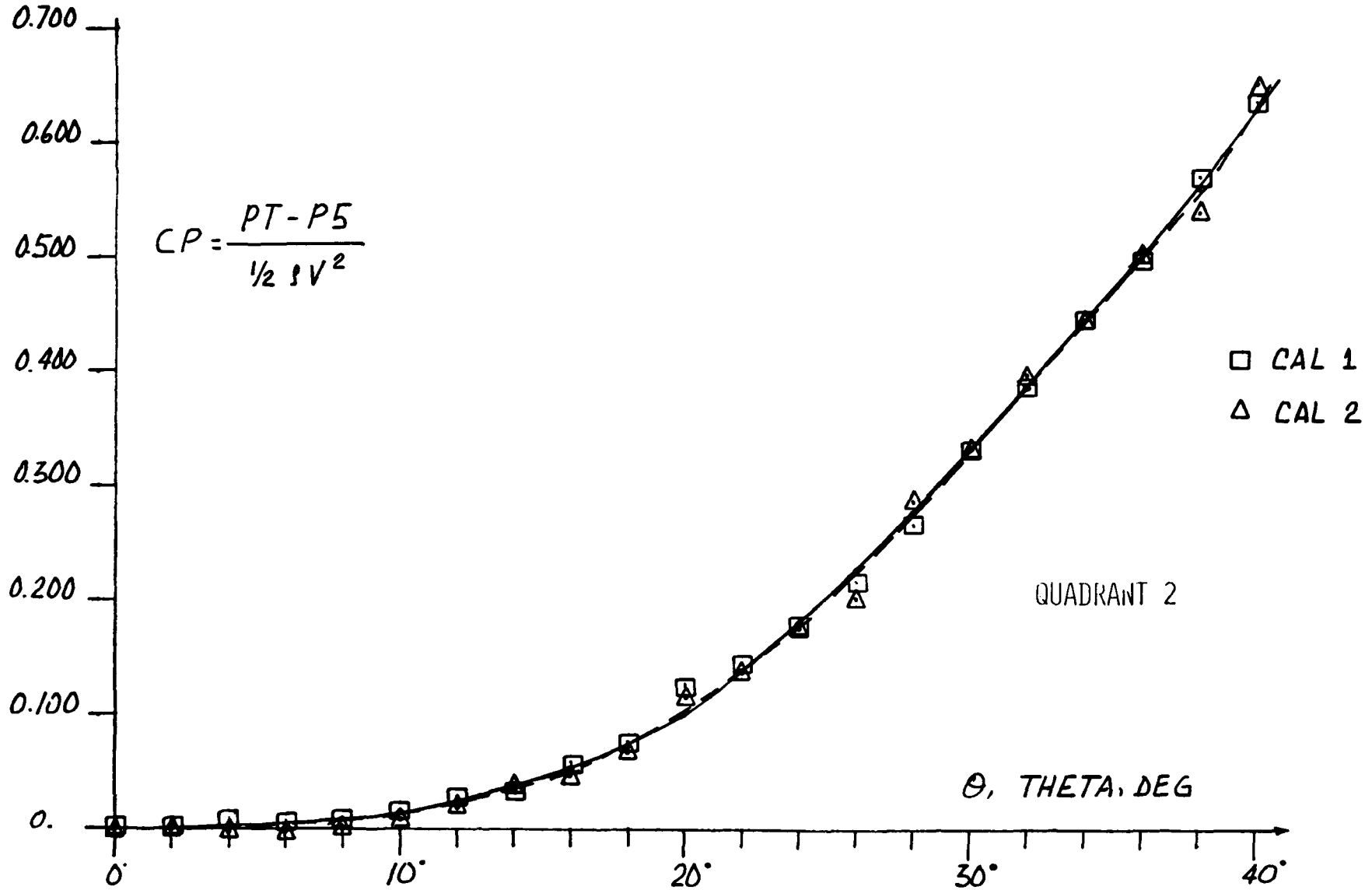

FIG. 8B - CP VERSUS θ CALIBRATION CURVES FOR FIVE HOLE PROBE

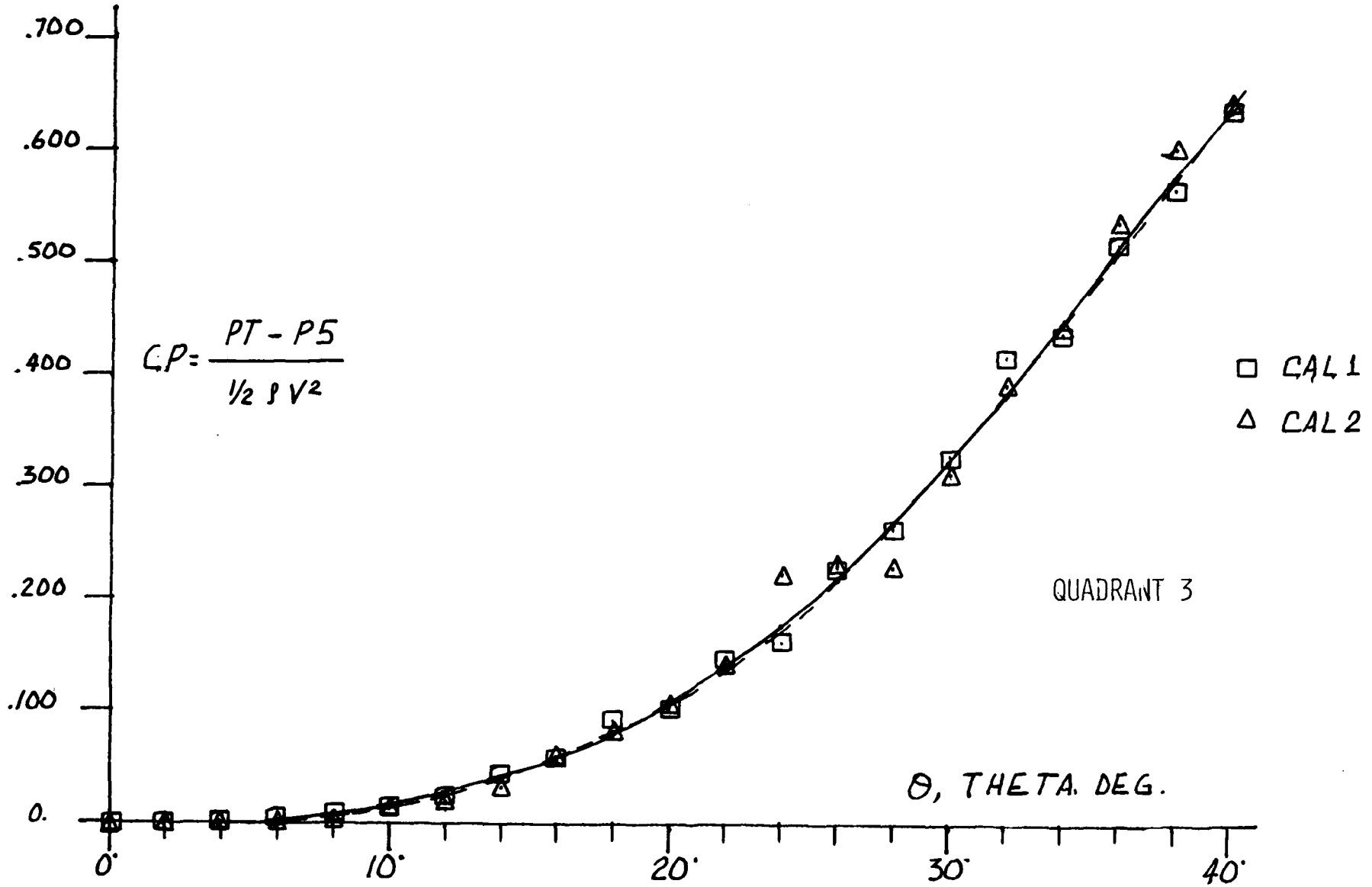

FIG. 8C - CP VERSUS θ CALIBRATION CURVES FOR FIVE HOLE PROBE

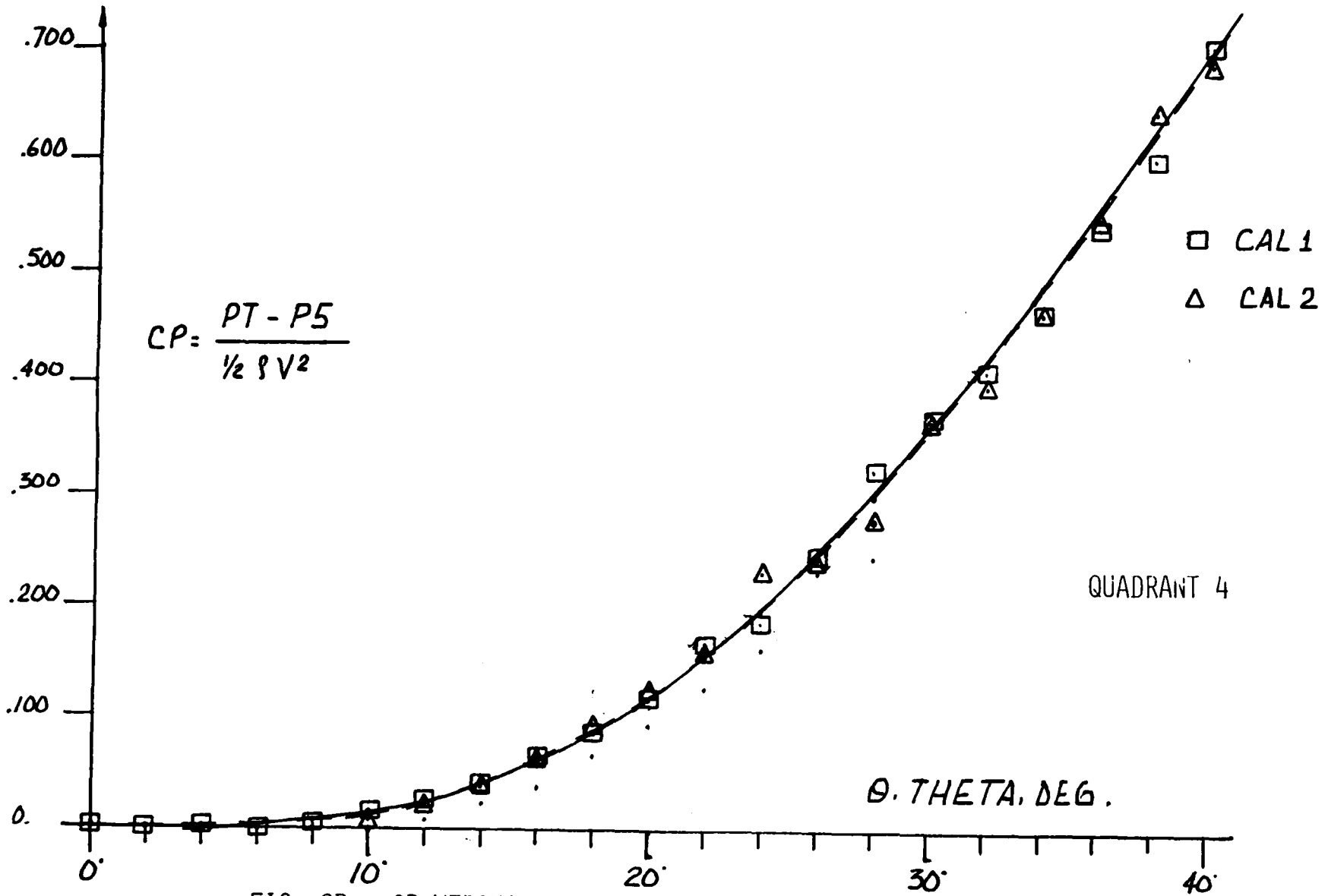

FIG. 8D - CP VERSUS θ CALIBRATION CURVES FOR FIVE HOLE PROBE

FIG. 9A - PD VERSUS θ CALIBRATION CURVES FOR FIVE HOLE PROBE

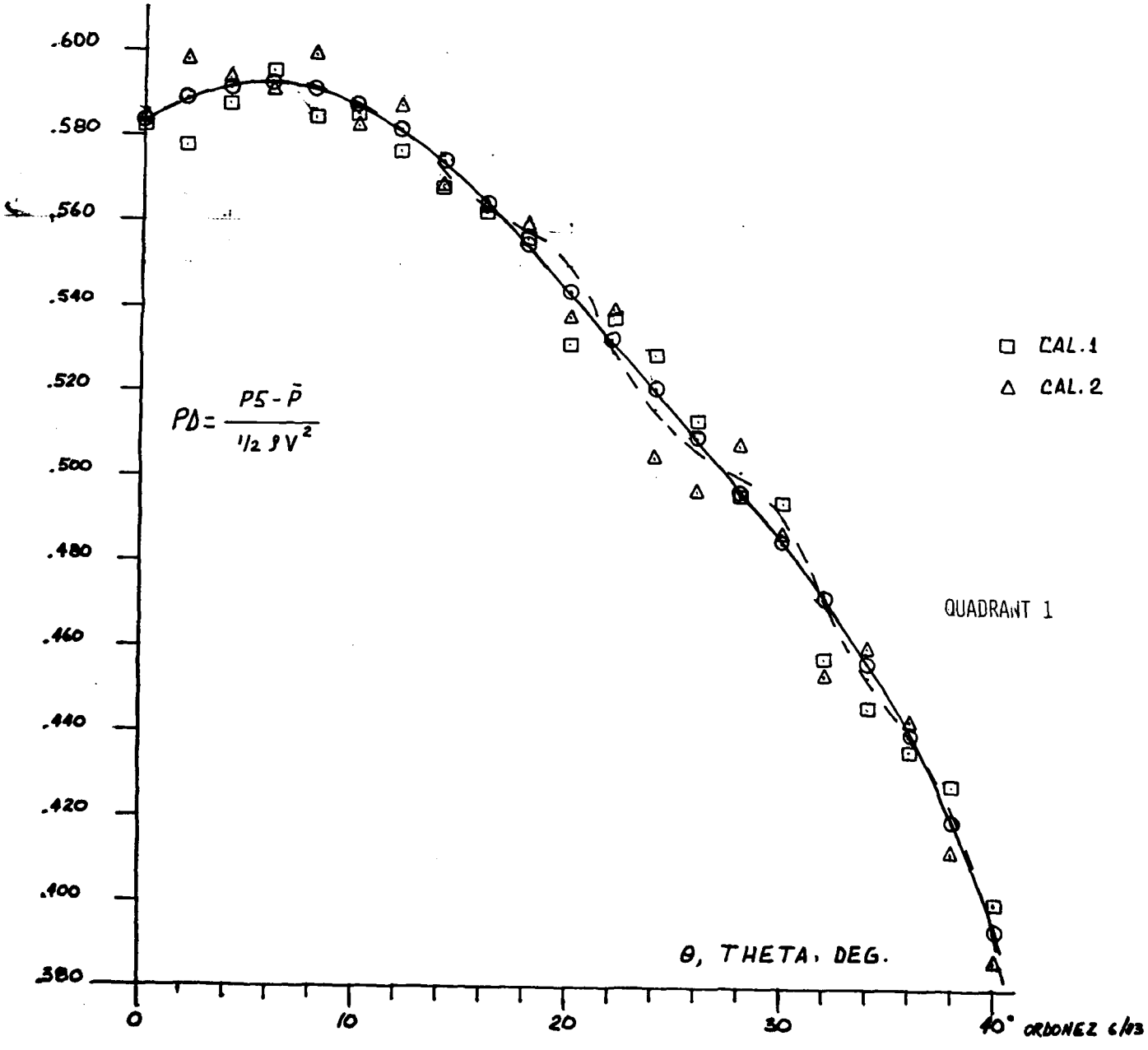

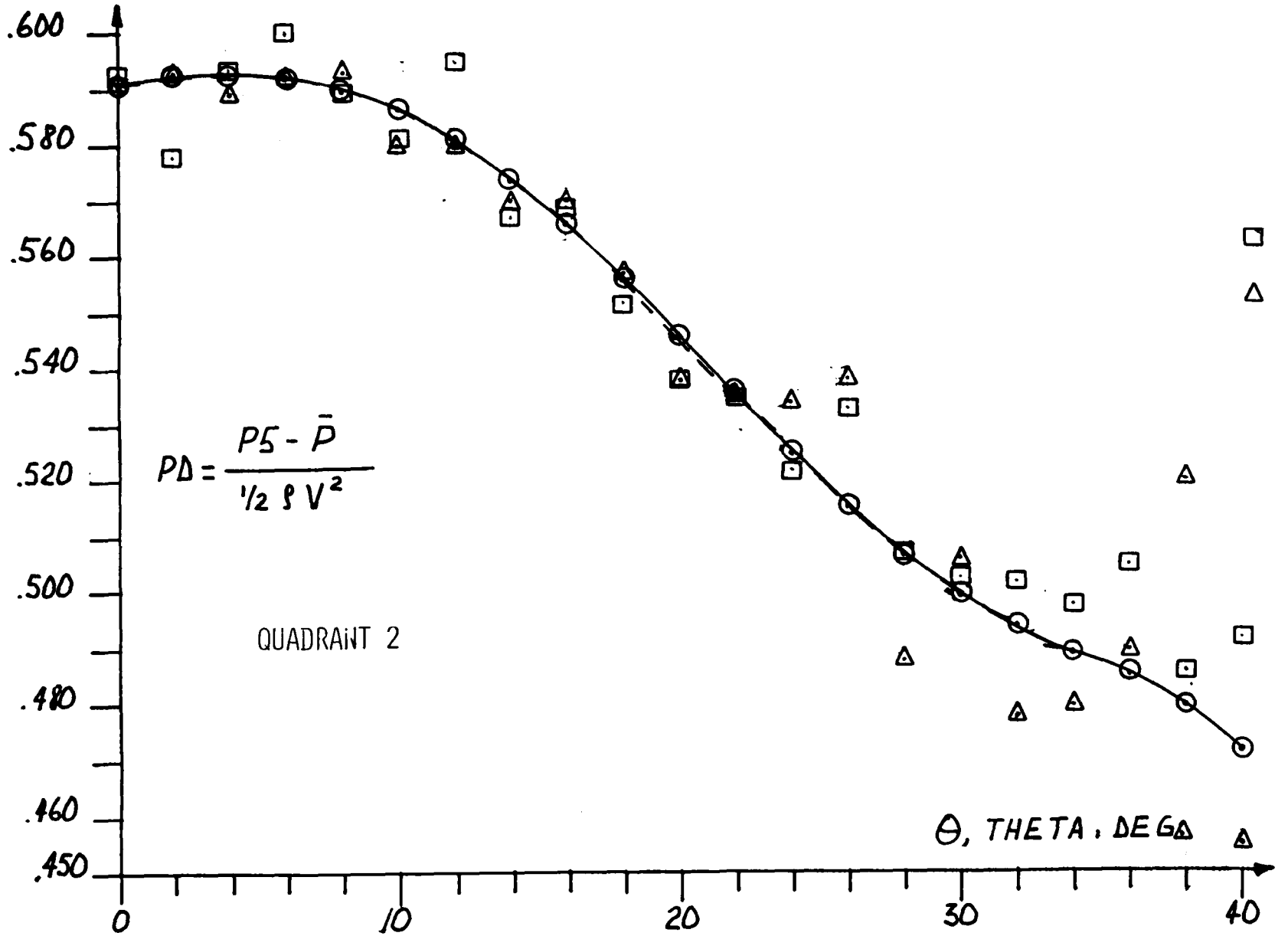

FIG. 9B - PD VERSUS θ CALIBRATION CURVES FOR FIVE HOLE PROBE

ORDONEZ 6/83

FIG. 9C - PD VERSUS θ CALIBRATION CURVE FOR FIVE HOLE PROBE

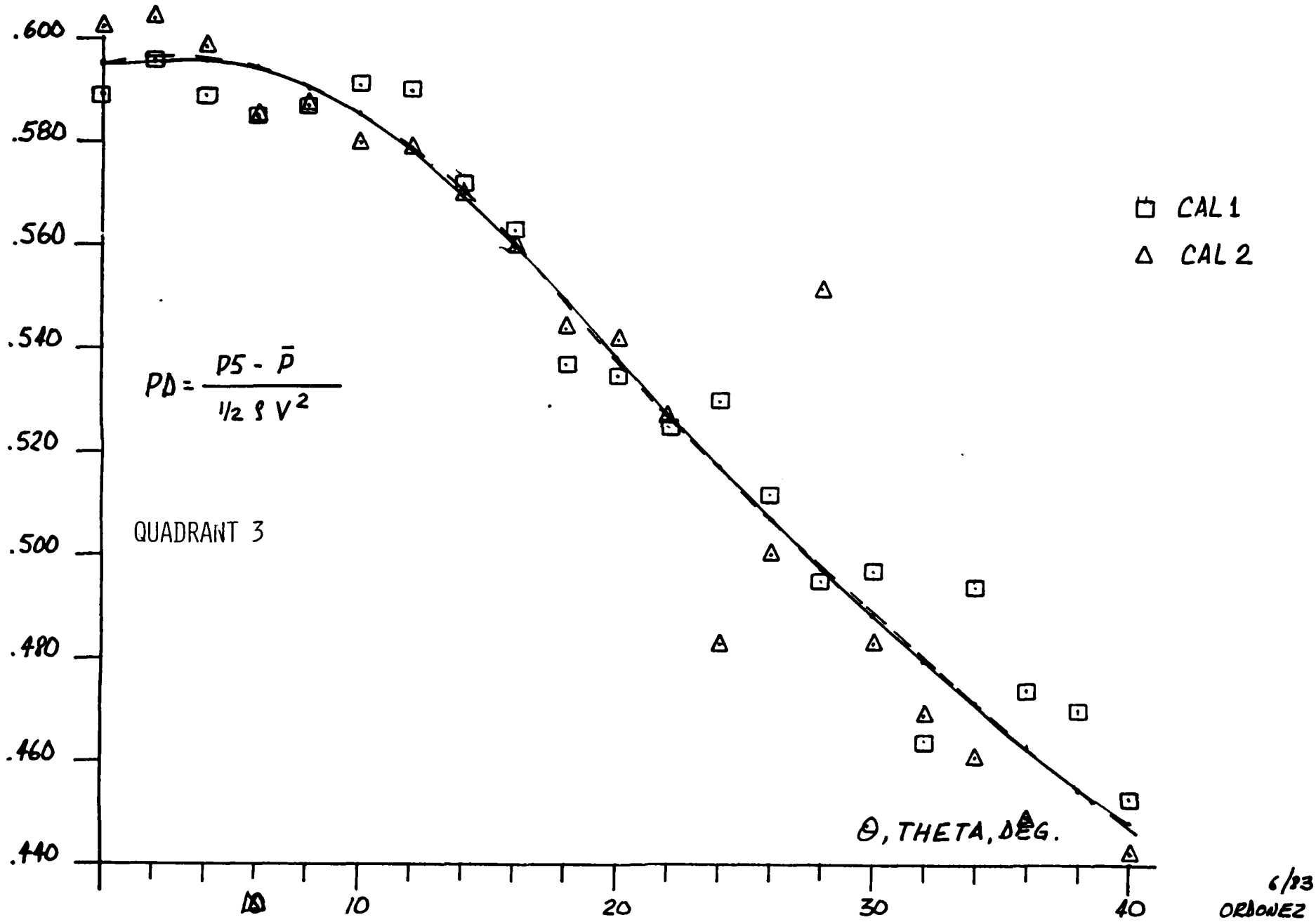

FIG. 9D - PD VERSUS θ CALIBRATION CURVES FOR FIVE HOLE PROBE

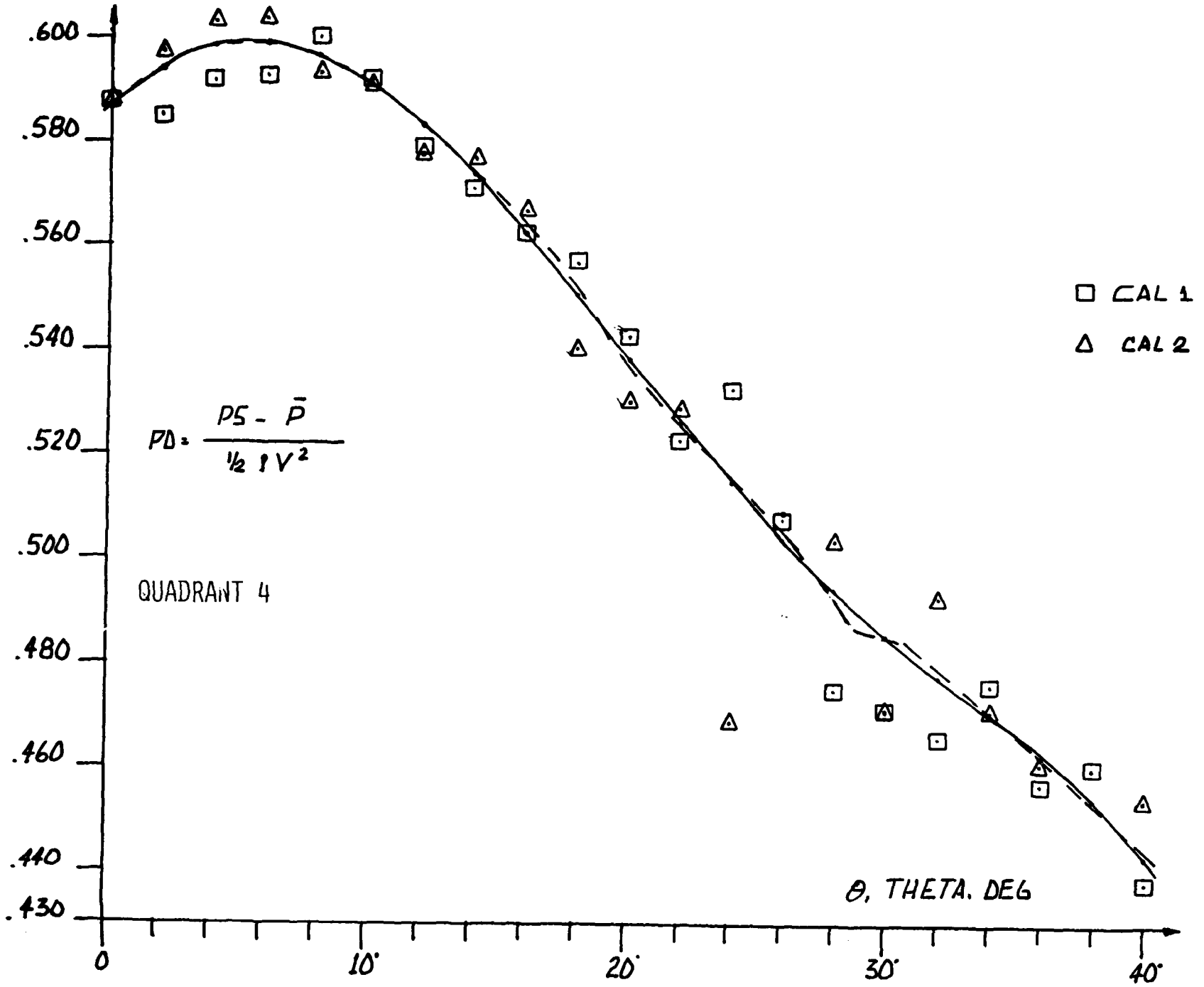

FIG. 10 - CALCULATED ROLL ANGLE VERSUS MEASURED ROLL ANGLE USING FIVE HOLE PROBE

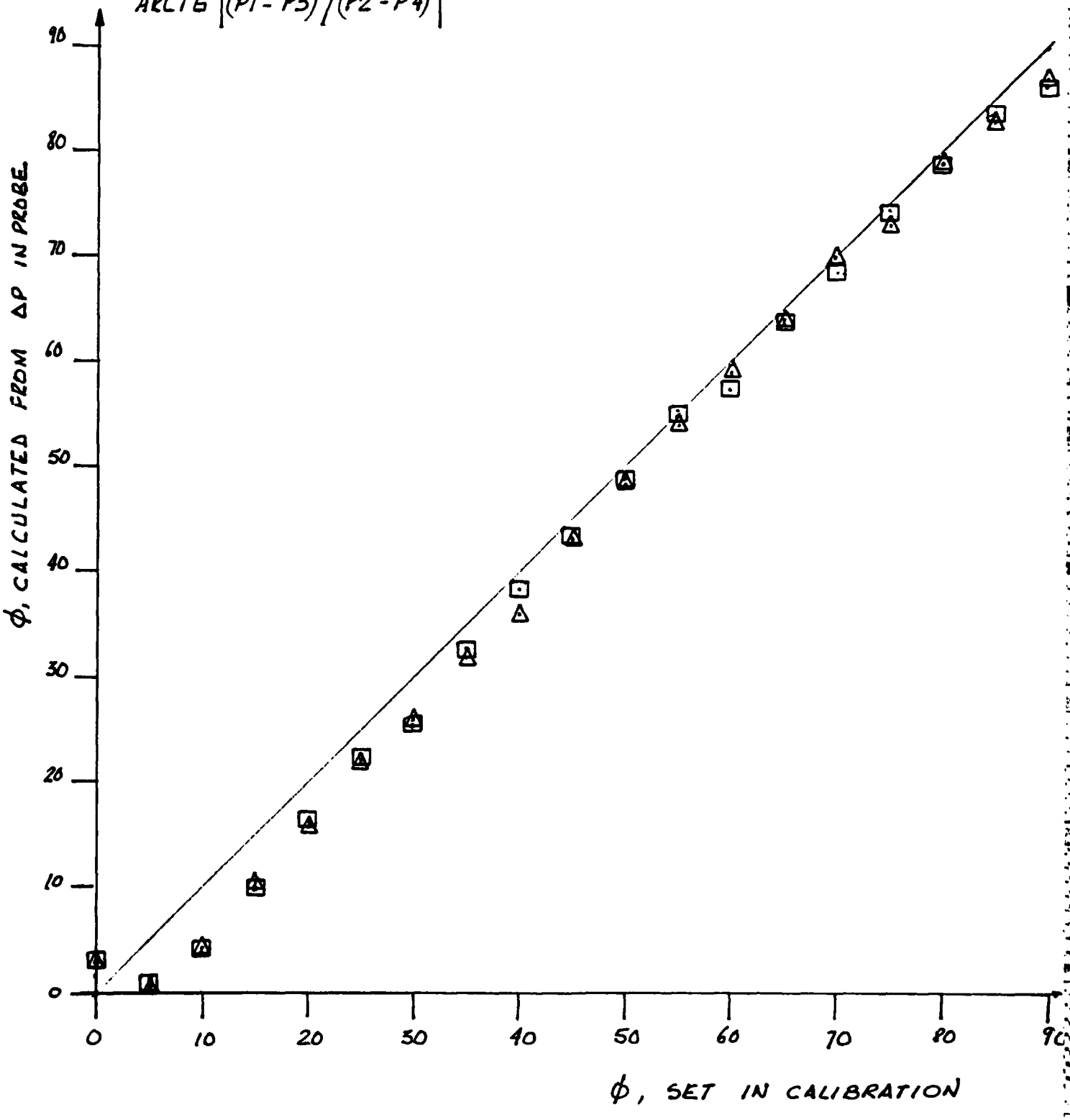

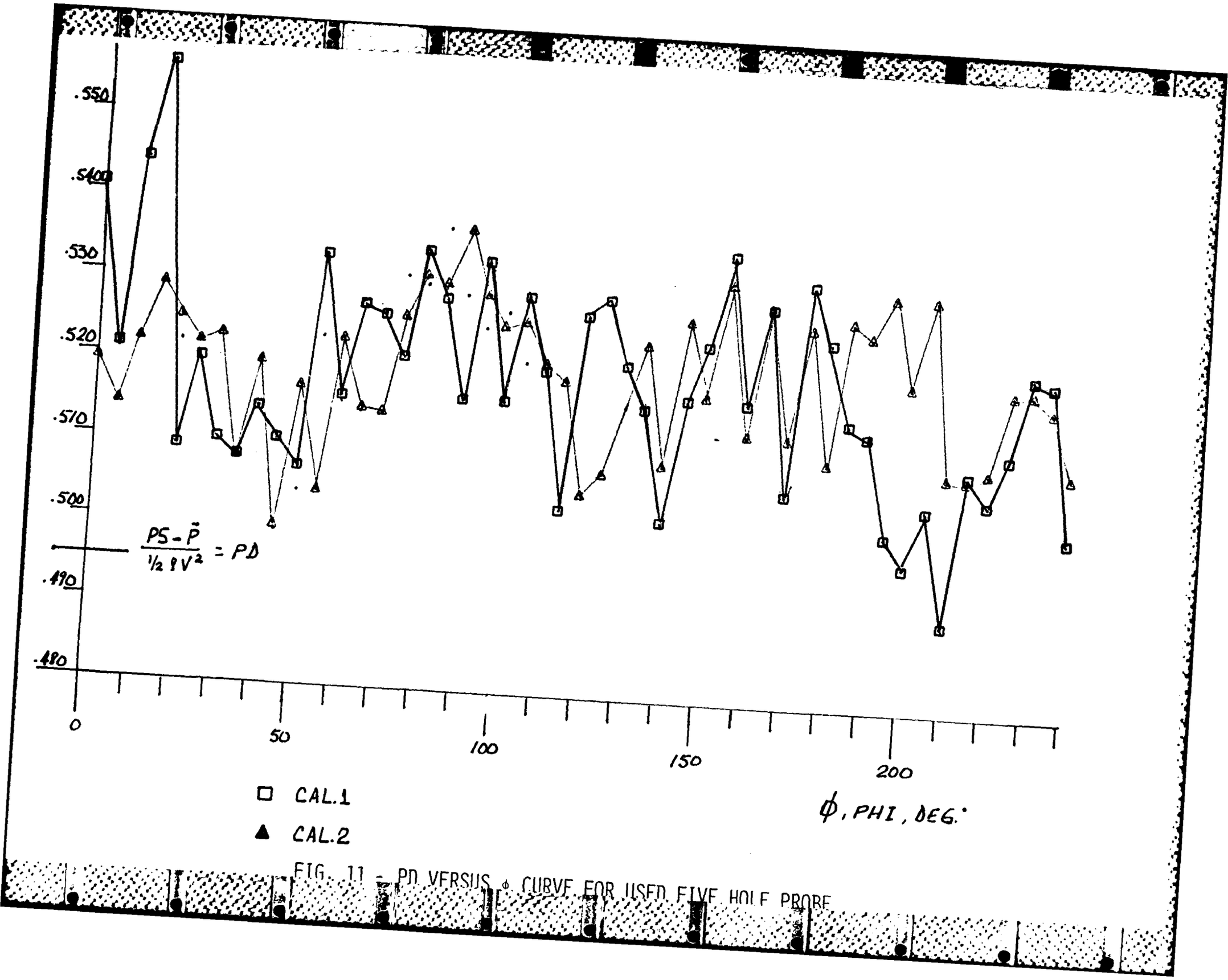

FIG. 11 - PD VERSUS ϕ CURVE FOR USED FIVE HOLE PROBE

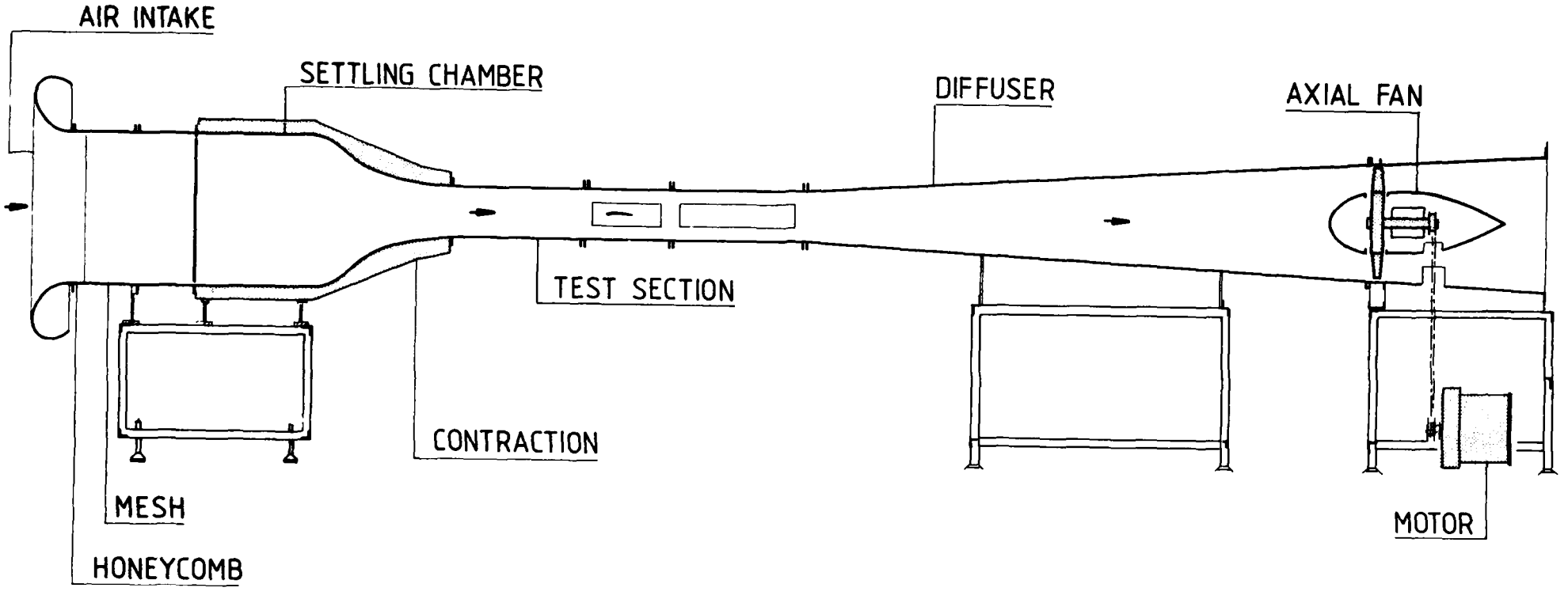

FIG. 12 - LOW SPEED WIND TUNNEL L-2A

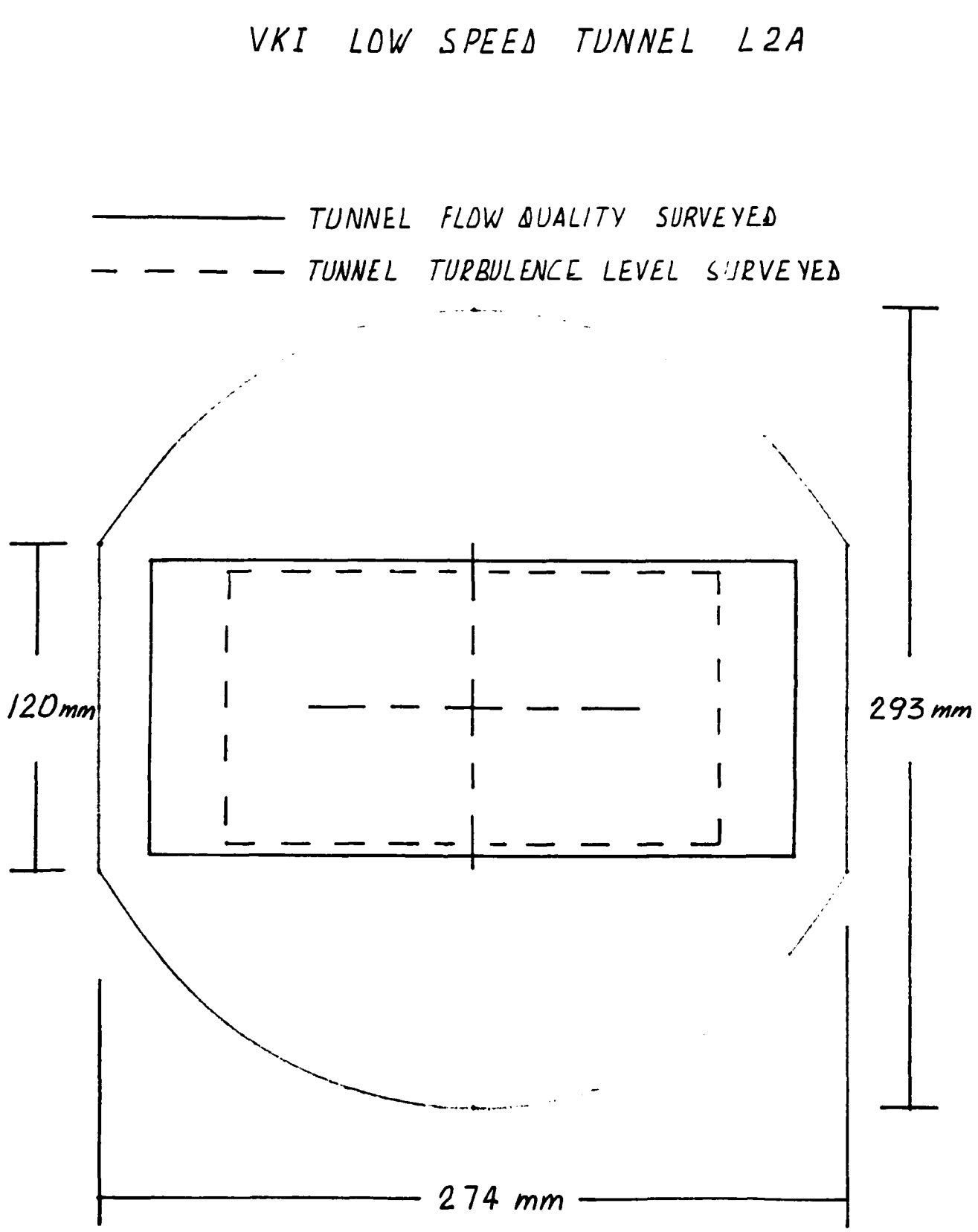

FIG. 13 - CROSS SECTION VIEW OF L-2A TUNNEL WITH MEASUREMENT REGIONS

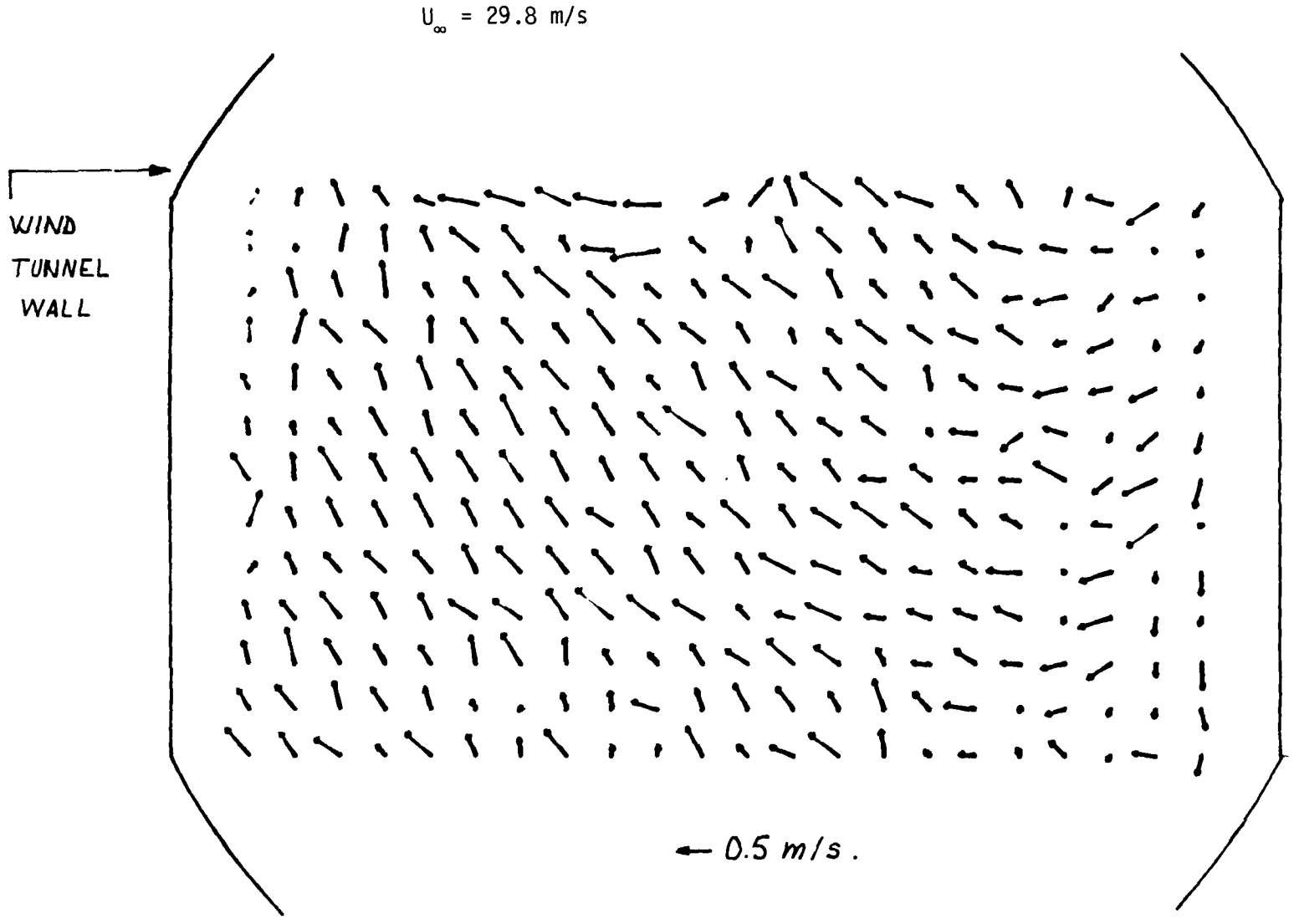

FIG. 14 - FLOW FIELD EXISTING AT A CLEAN TEST SECTION STATION OF THE L-2A

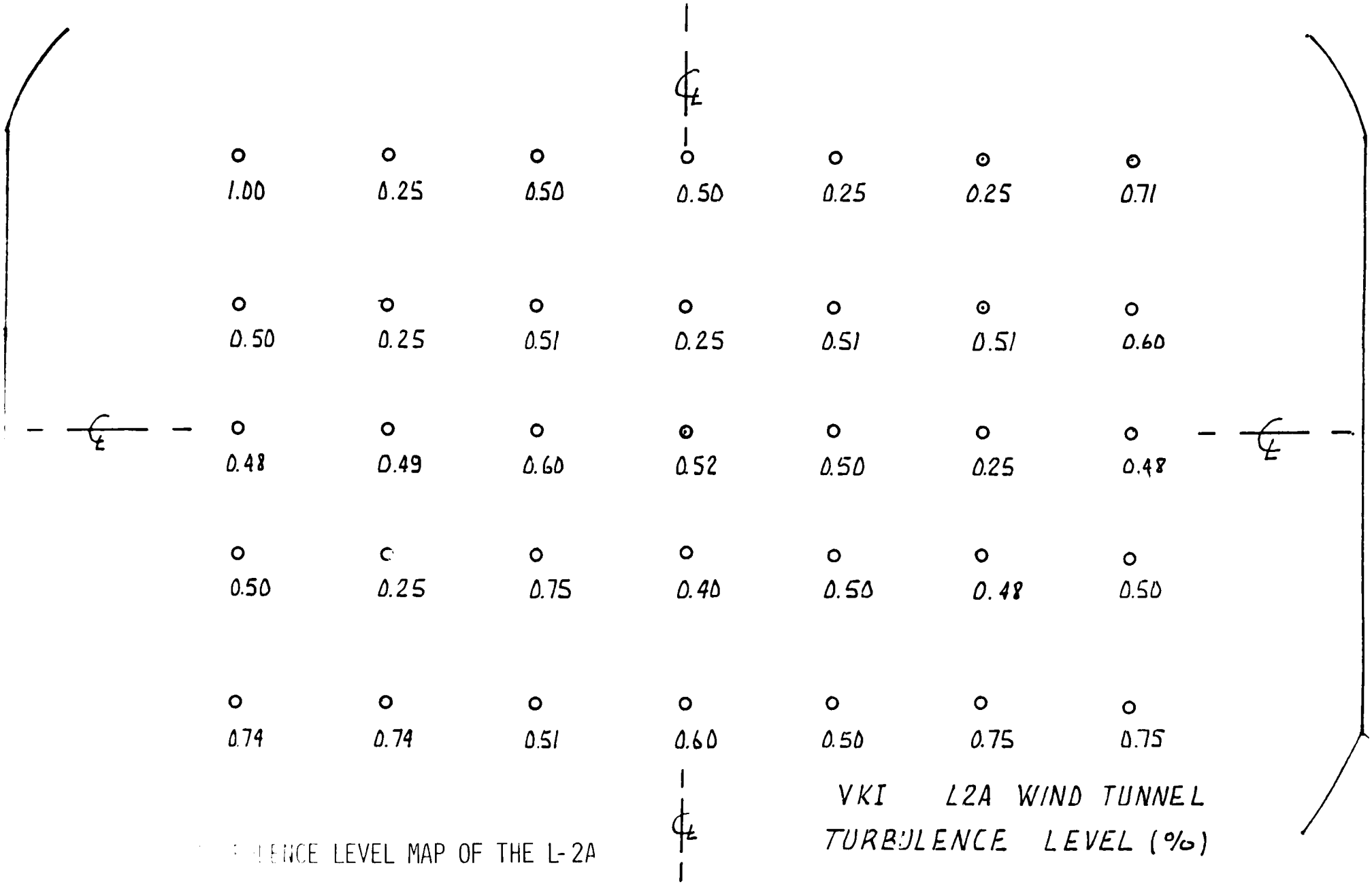

ENCE LEVEL MAP OF THE L-2A

AD-A139 989 THE EFFECT OF STRAKES ON VORTICAL FLOWS APPLIED TO AIRCRAFT..(U) VON KARMAN INST FOR FLUID DYNAMICS RHODE-SAINT-GENESE (BELGIU.. G G ORDONEZ 31 MAR 84 2/2

UNCLASSIFIED VKI-PR-1983-22 EOARD-TR-84-14 AFOSR-83-0126 F/G 20/4 NL

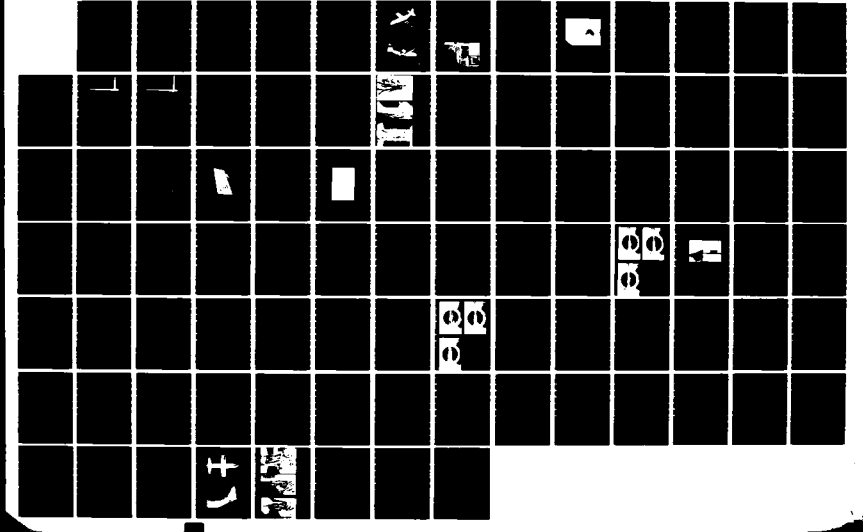

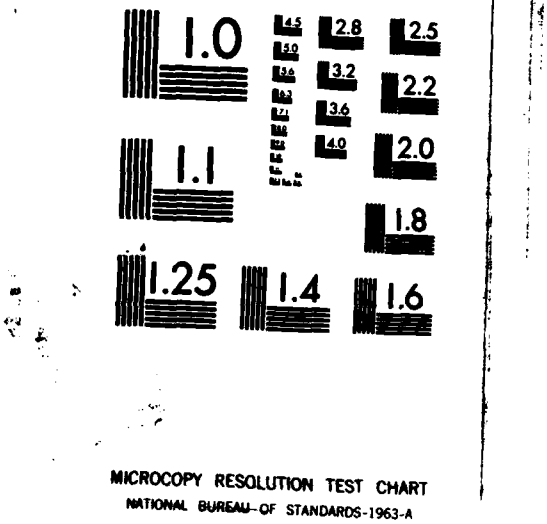

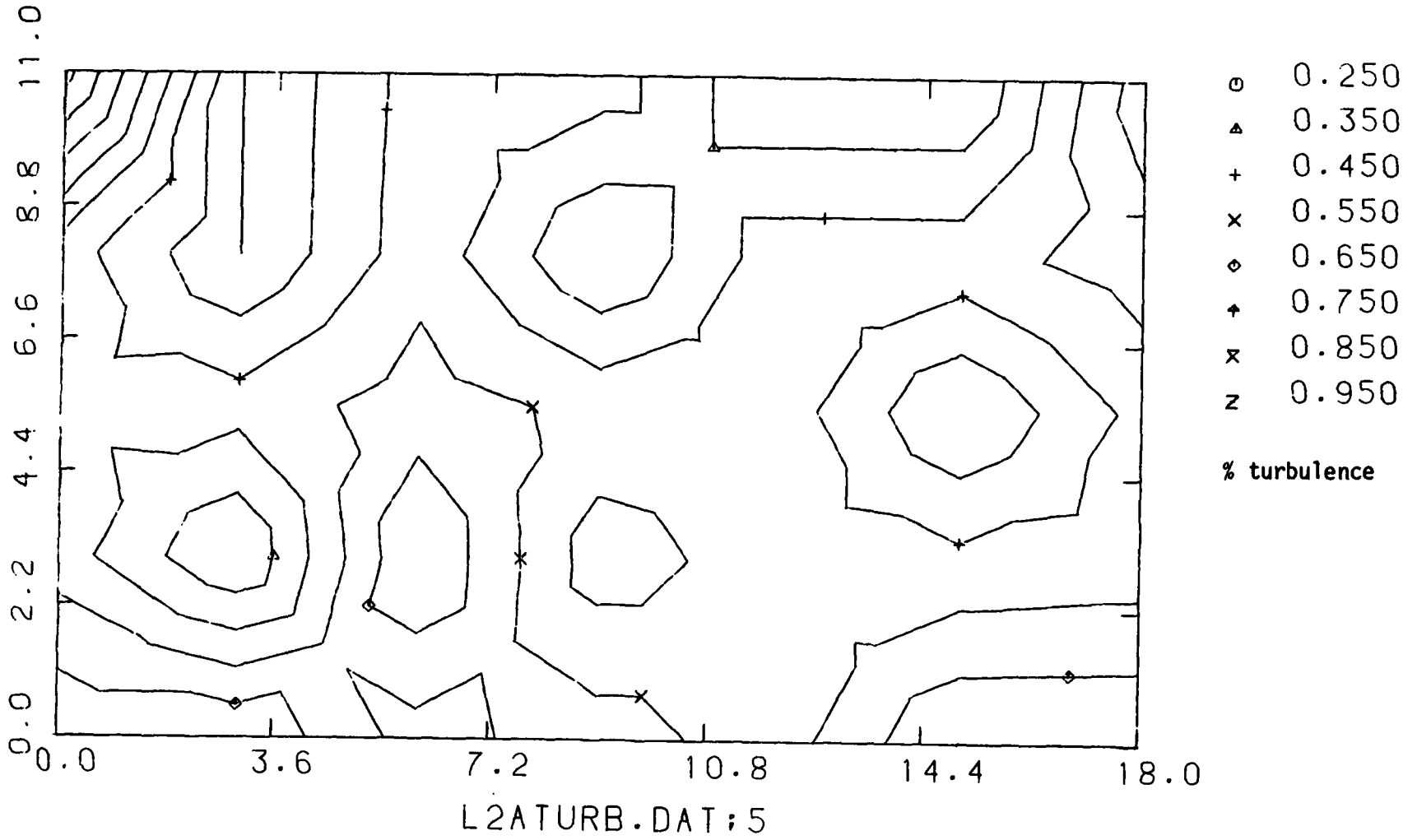

FIG. 15B - TURBULENCE LEVEL ISOLINES ALONG TEST SECTION OF L-2A TUNNEL

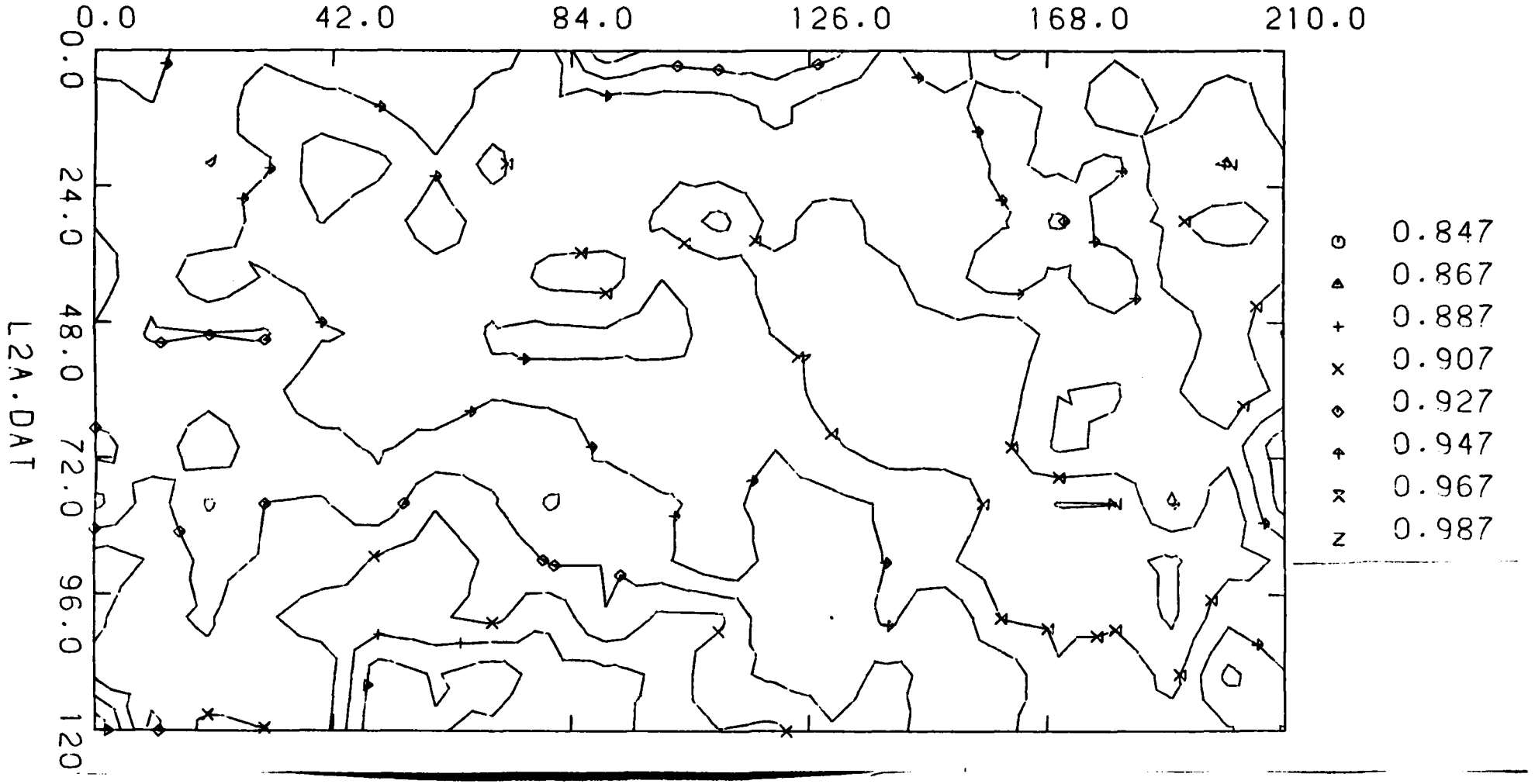

FIG. 16 - TOTAL PRESSURE / DYNAMIC PRESSURE ISOLINES ALONG TEST SECTION OF L-2A TUNNEL

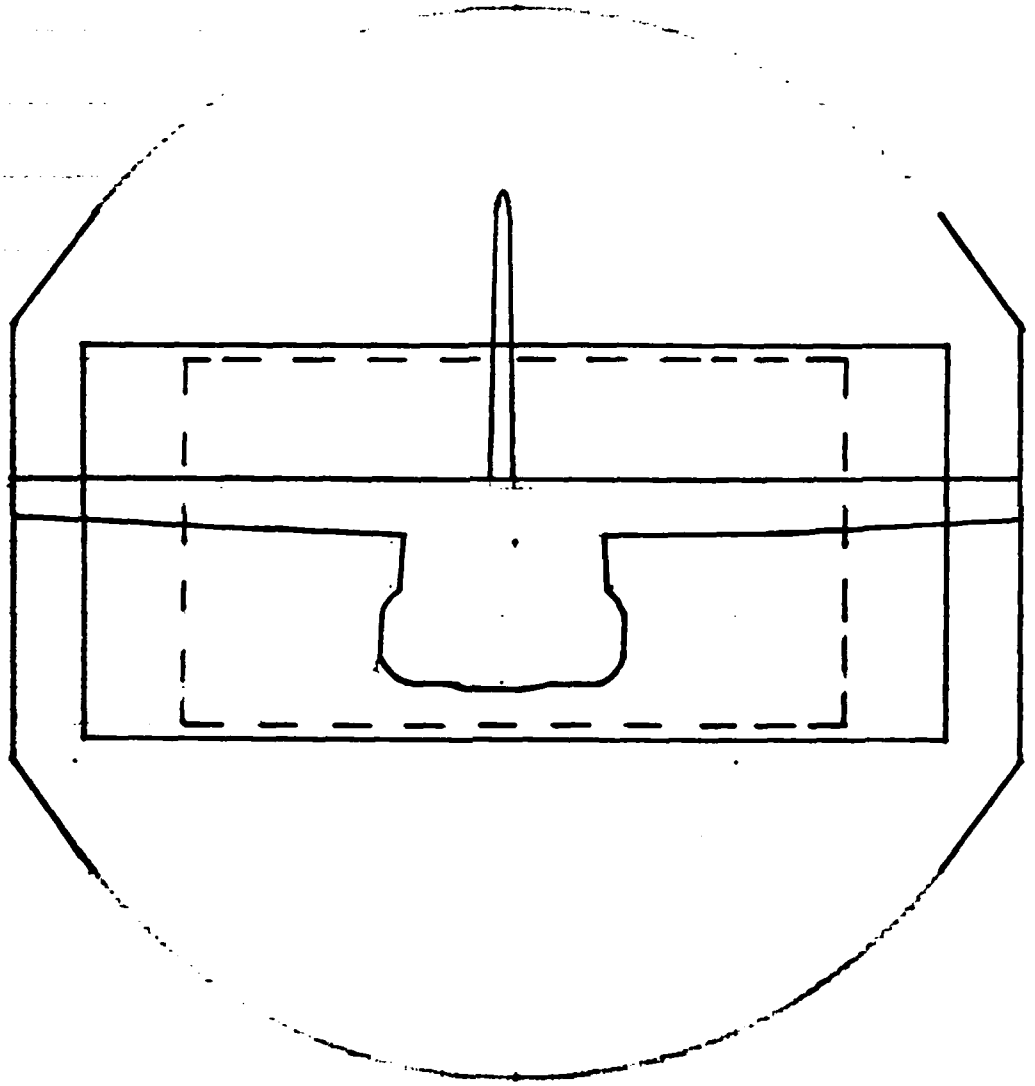

FIG. 17A - L-2A CROSS SECTION WITH C-130 AND MEASUREMENT REGIONS

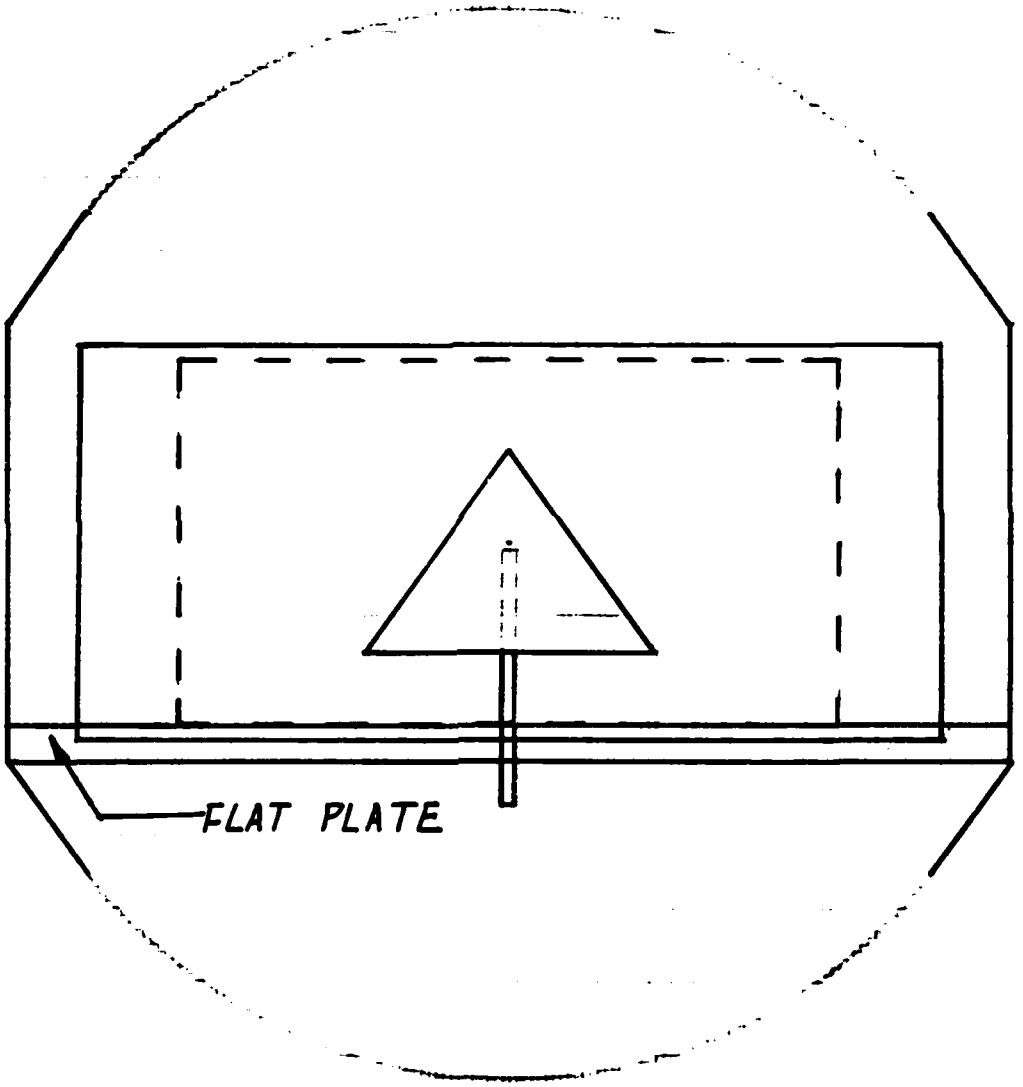

FIG. 17B - L-2A CROSS SECTION WITH DELTA WING AND MEASUREMENT REGIONS

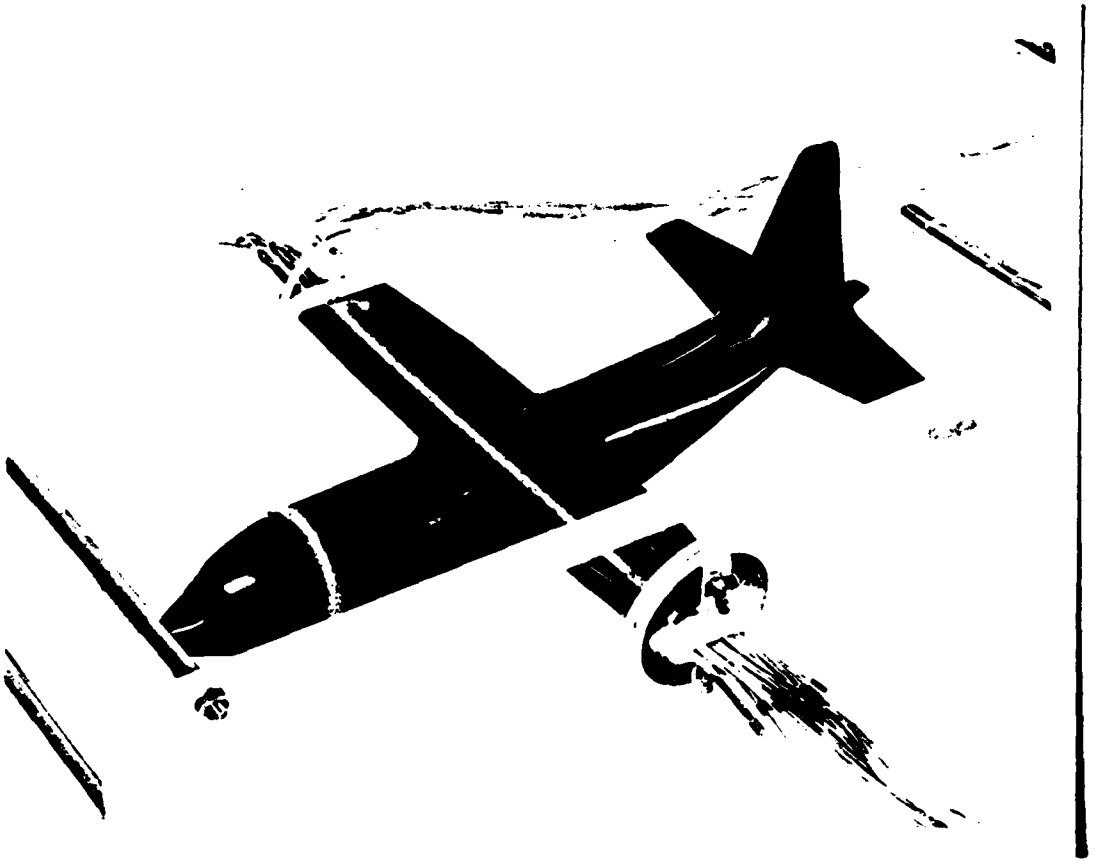

FIG. 18A - GENERAL VIEW OF 1/72 SCALE MODEL OF THE LOCKHEED HERCULES C-130 AIRCRAFT USED

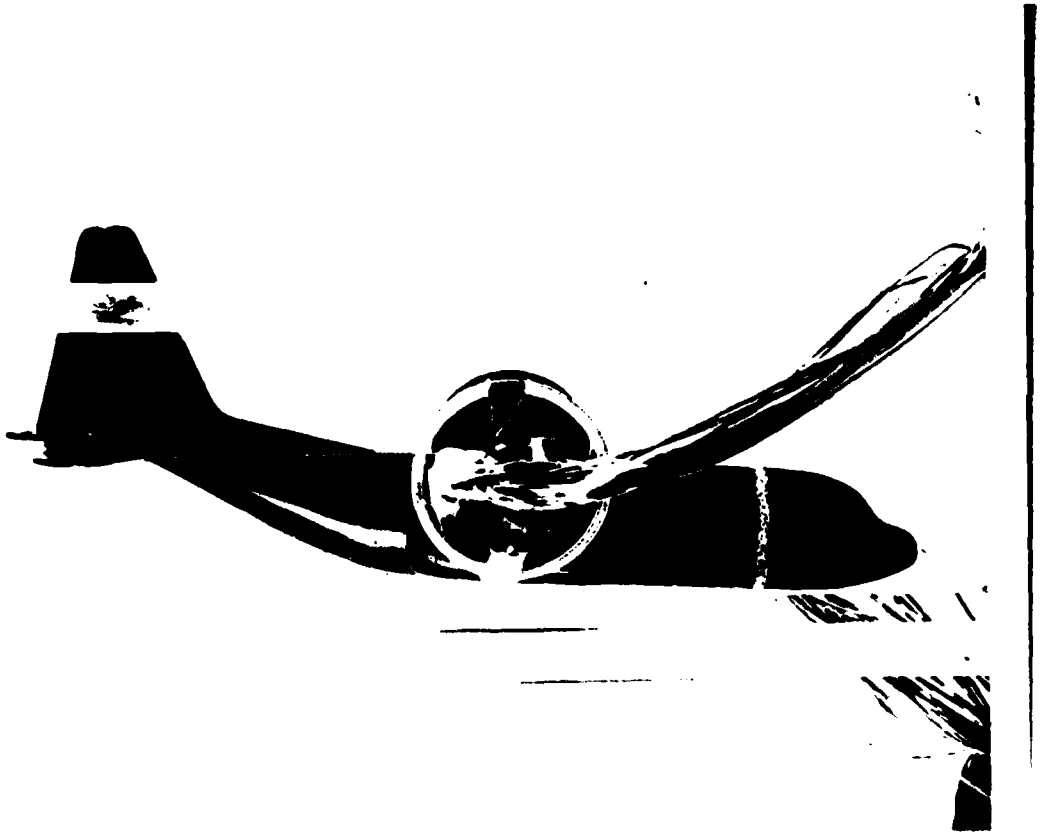

FIG. 18B - SIDE VIEW AND CONNECTING PRESSURE MEASUREMENT TUBES IN THE C-130 AIRCRAFT

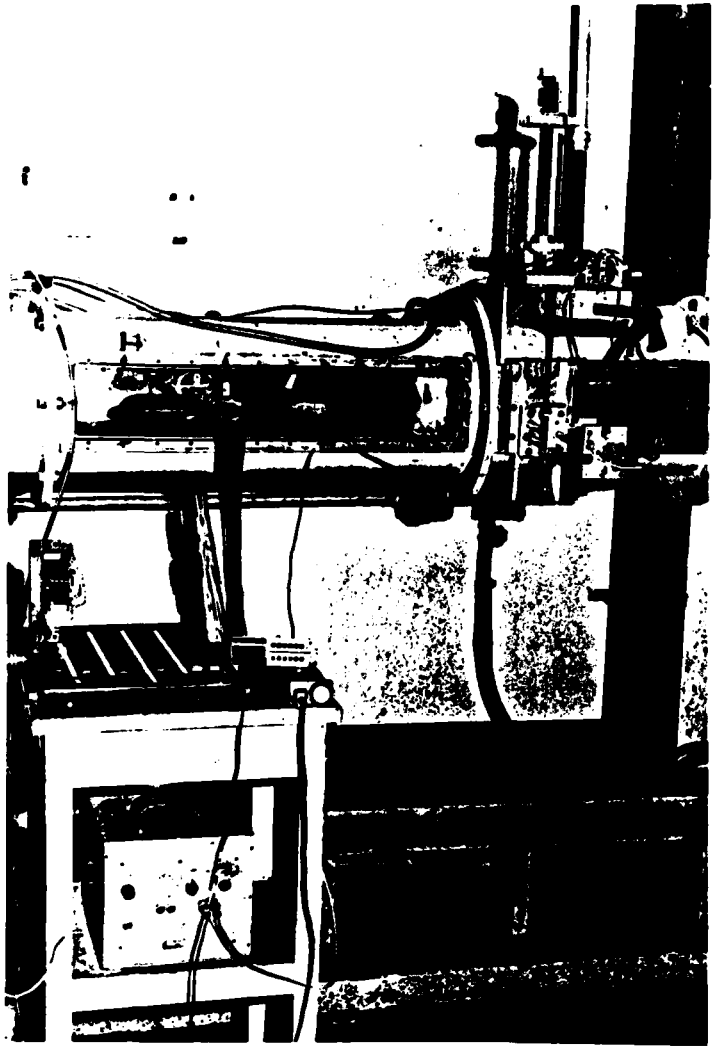

FIG. 19A - WIND TUNNEL TEST SECTION AND MEASUREMENT INSTRUMENTATION

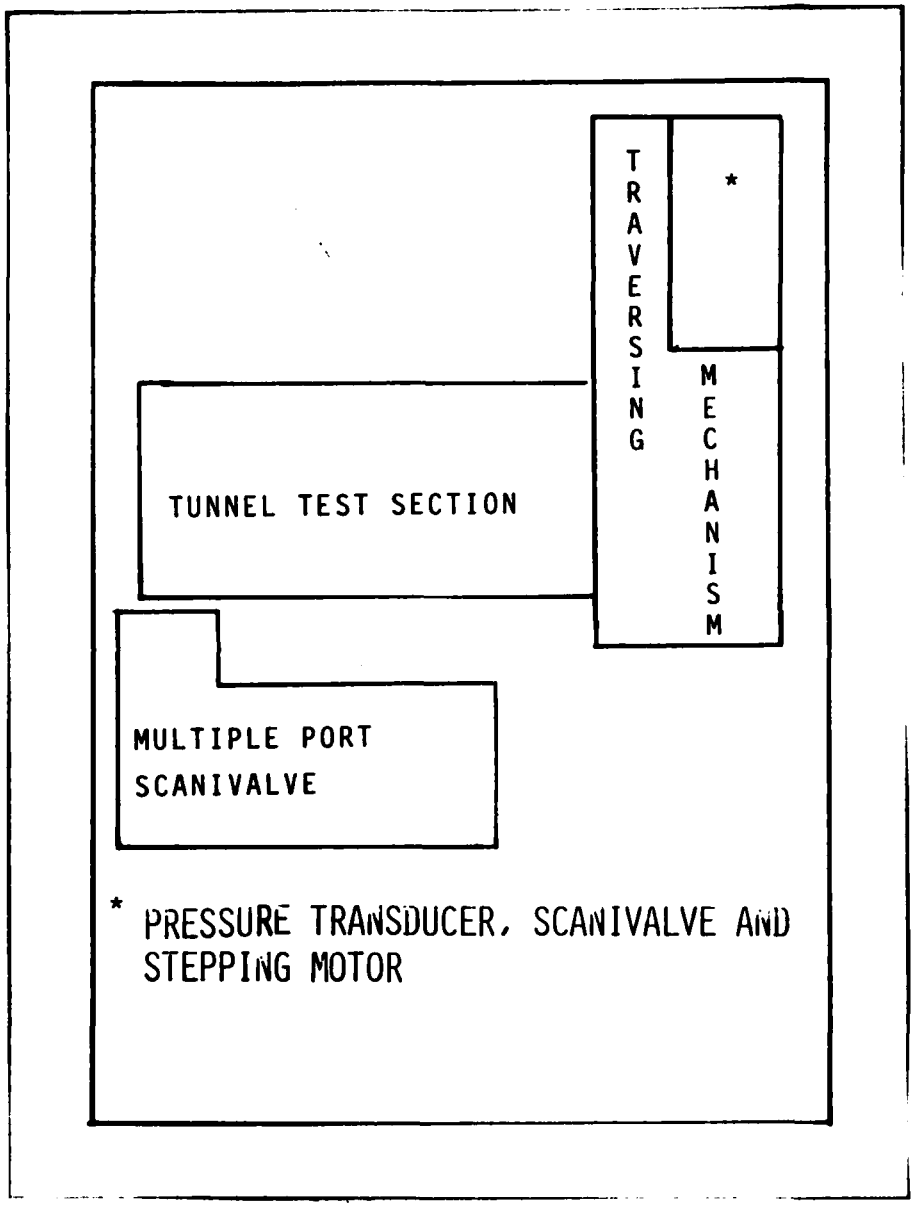

FIG. 19B - DESCRIPTION OF EQUIPMENT

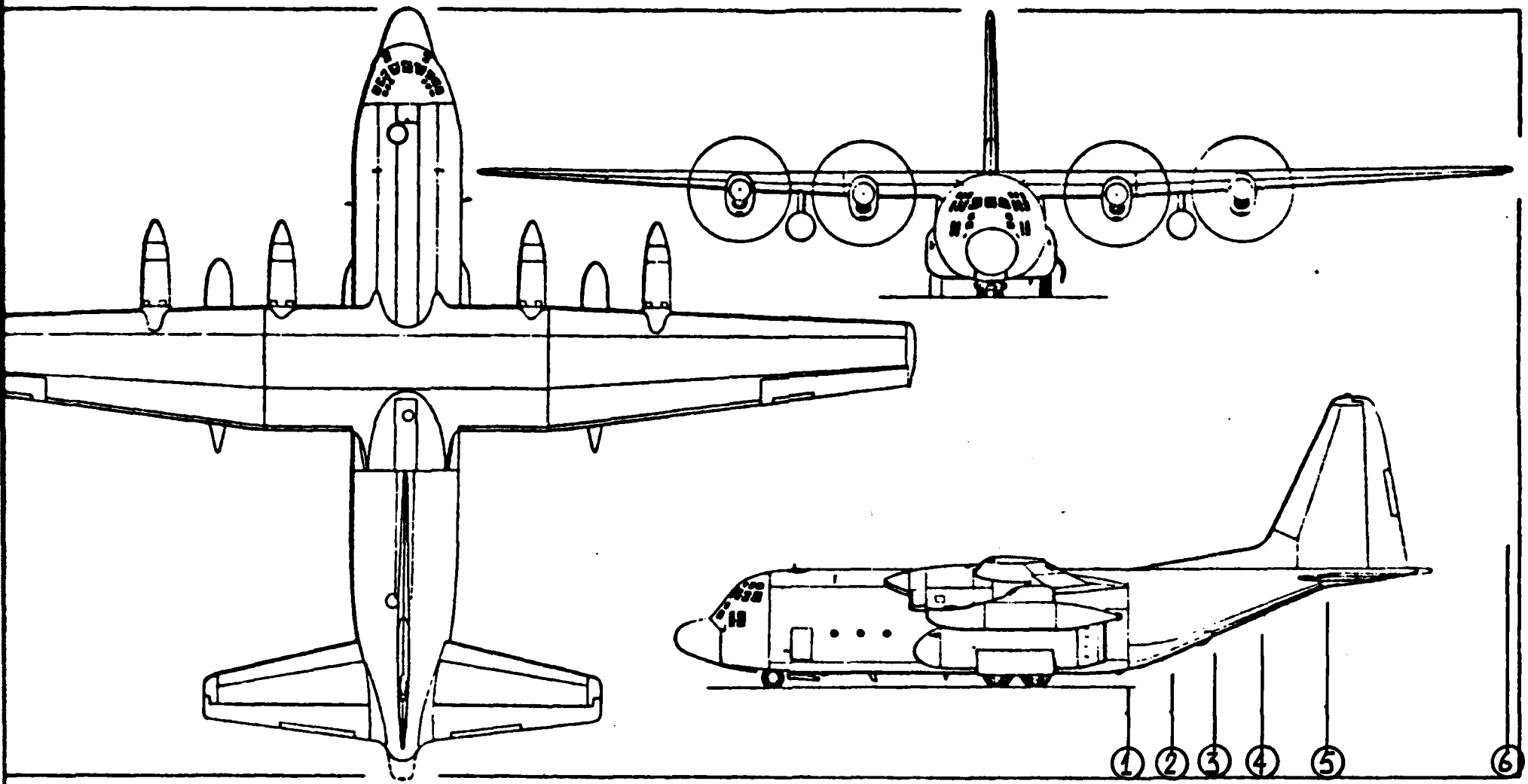

FIG. 20 - THREE VIEW DRAWING OF HERCULES C-130 AIRCRAFT AND FUSELAGE STATIONS WHERE PRESSURES AND FLOW FIELD MEASUREMENTS WERE TAKEN

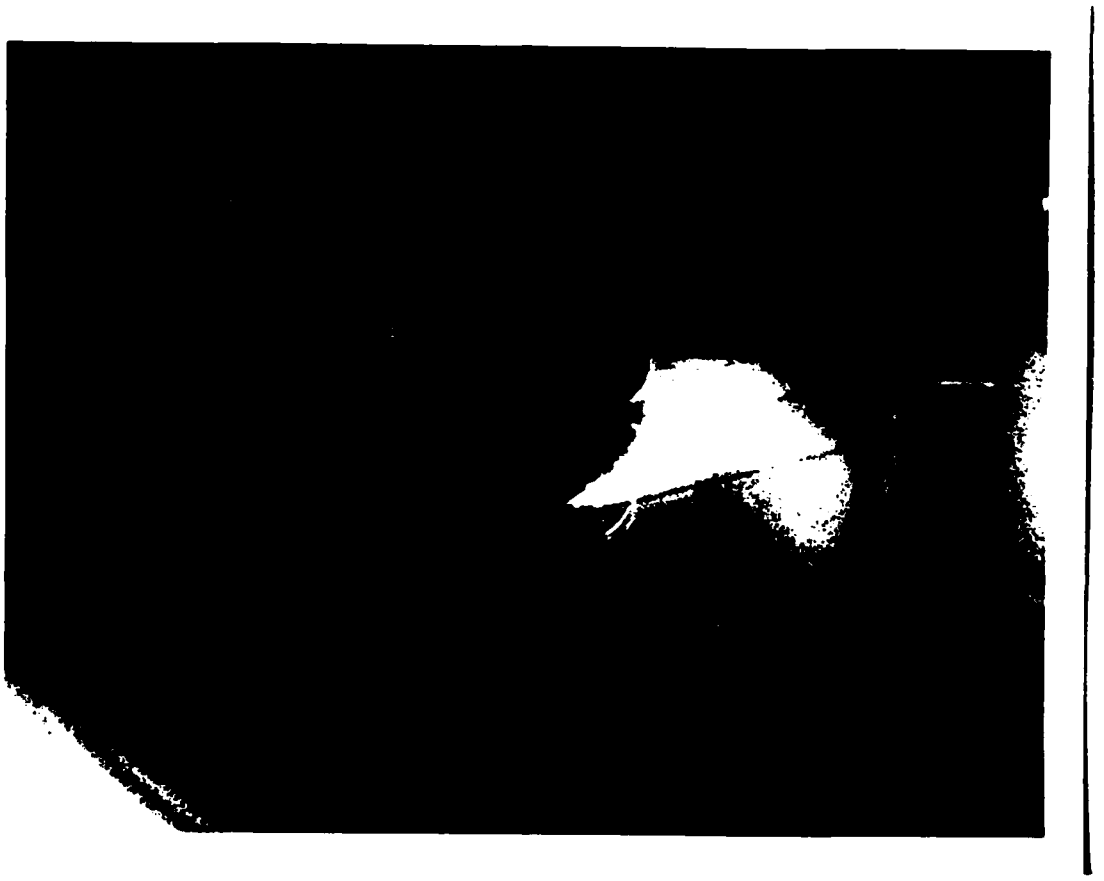

FIG. 21 - SMOKE FLOW VISUALIZATION ALONG FUSELAGE STATION 3 OF THE BOATTAIL OF C-130

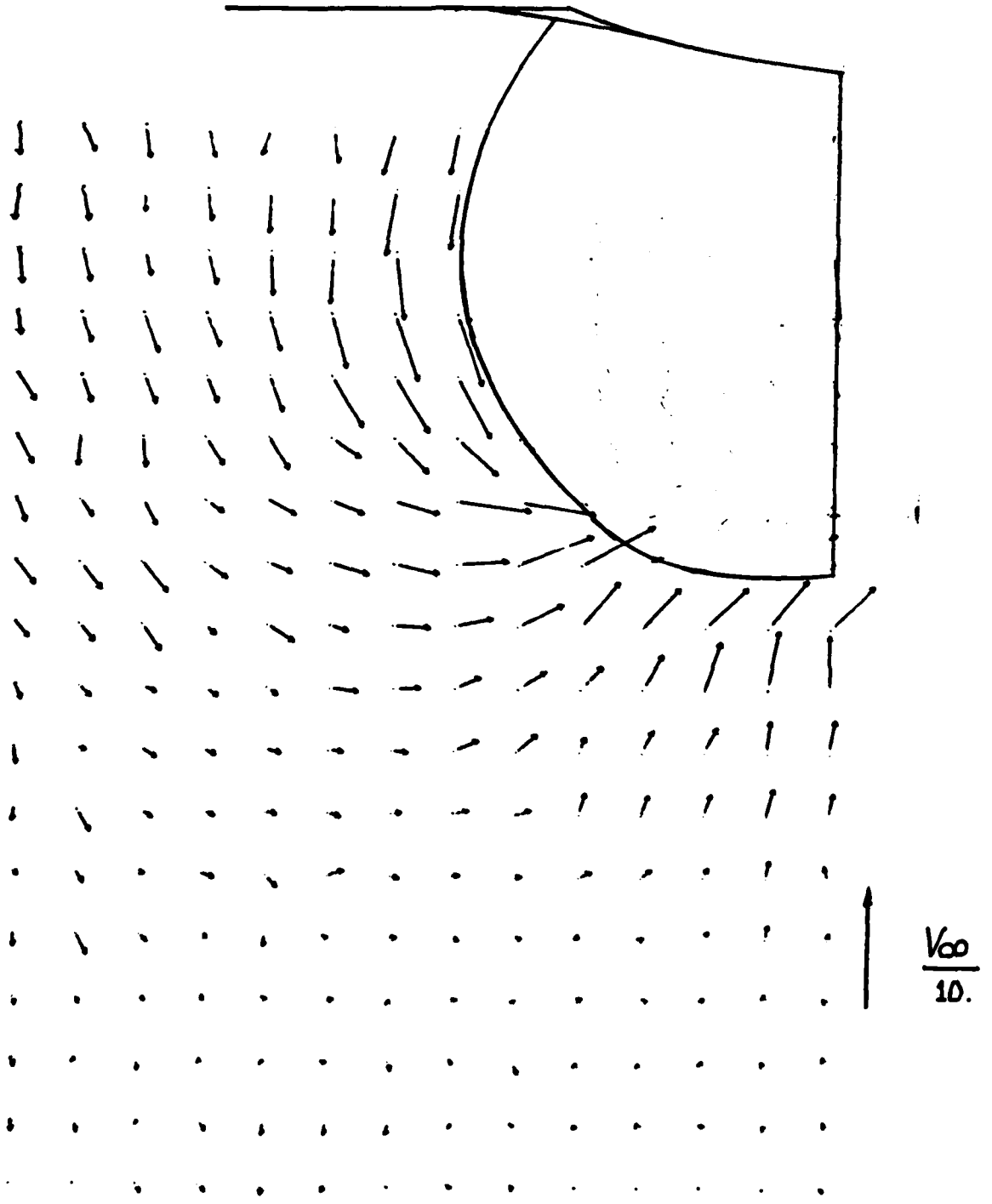

FIG. 22 - FLOW FIELD MAP OF FUSELAGE STATION 1 ALONG BOATTAIL OF C-130

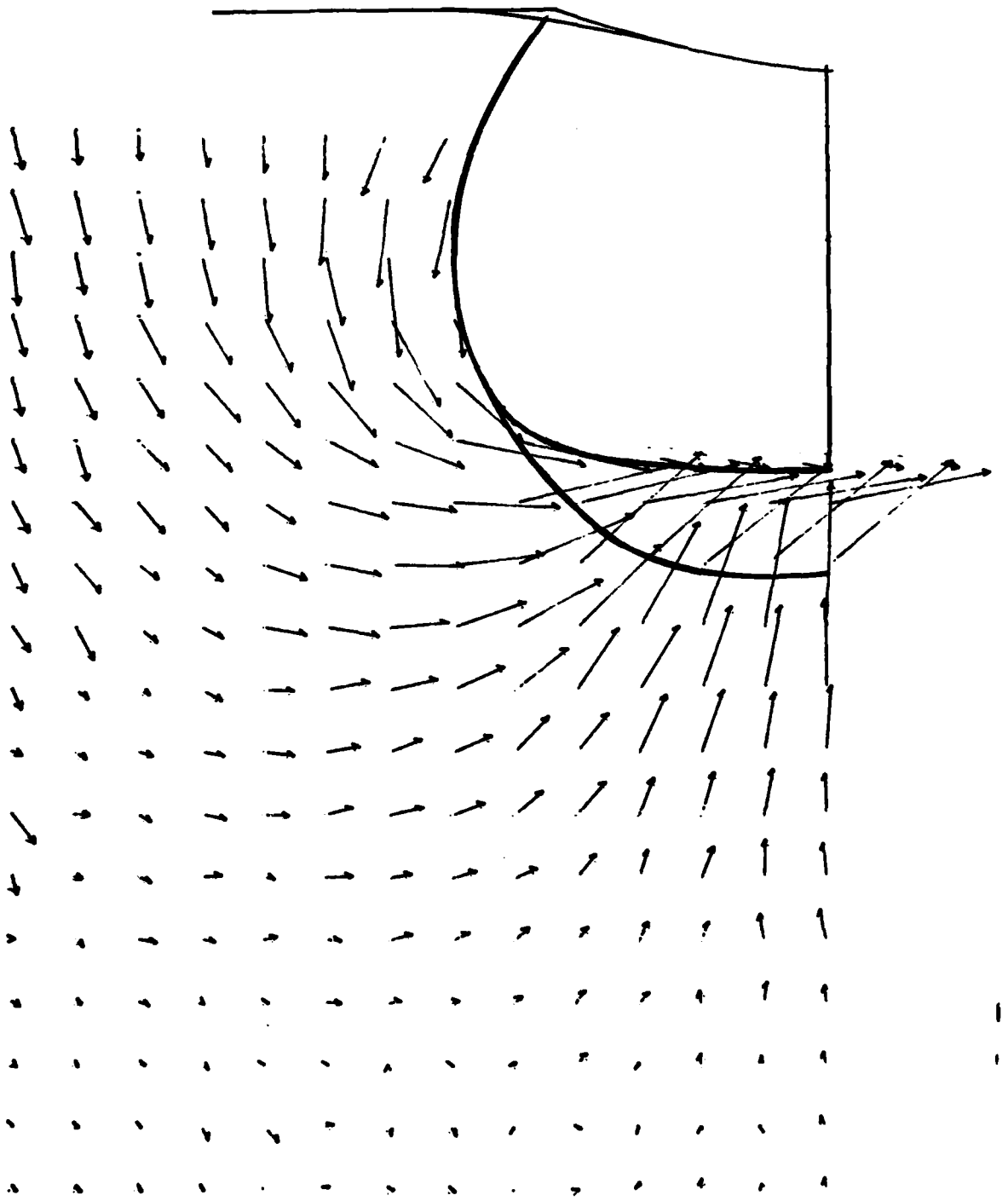

FIG. 23 - FLOW FIELD MAP OF FUSELAGE STATION 2 ALONG BOATTAIL OF C-130

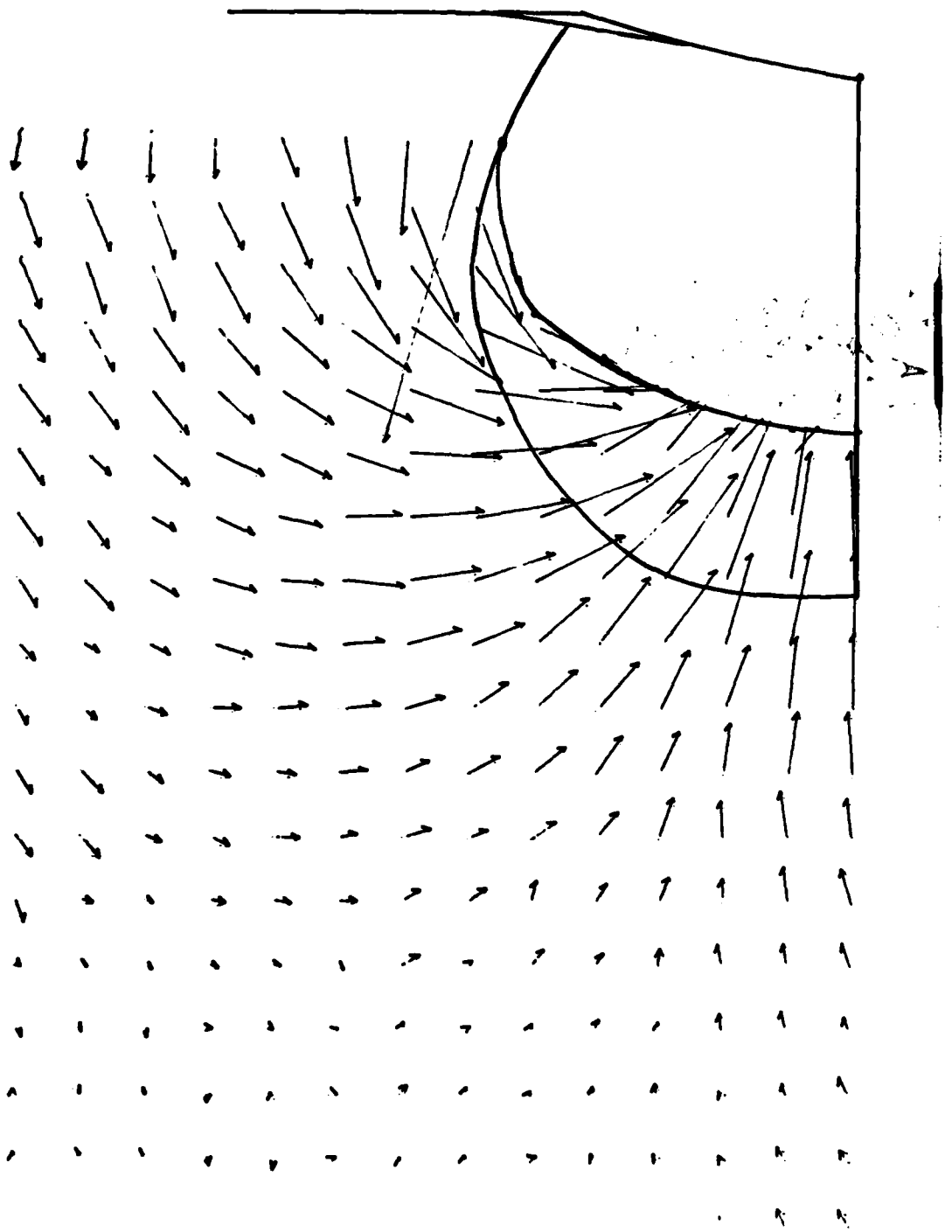

FIG. 24 - FLOW FIELD MAP OF FUSELAGE STATION 3 ALONG BOATTAIL OF C-130

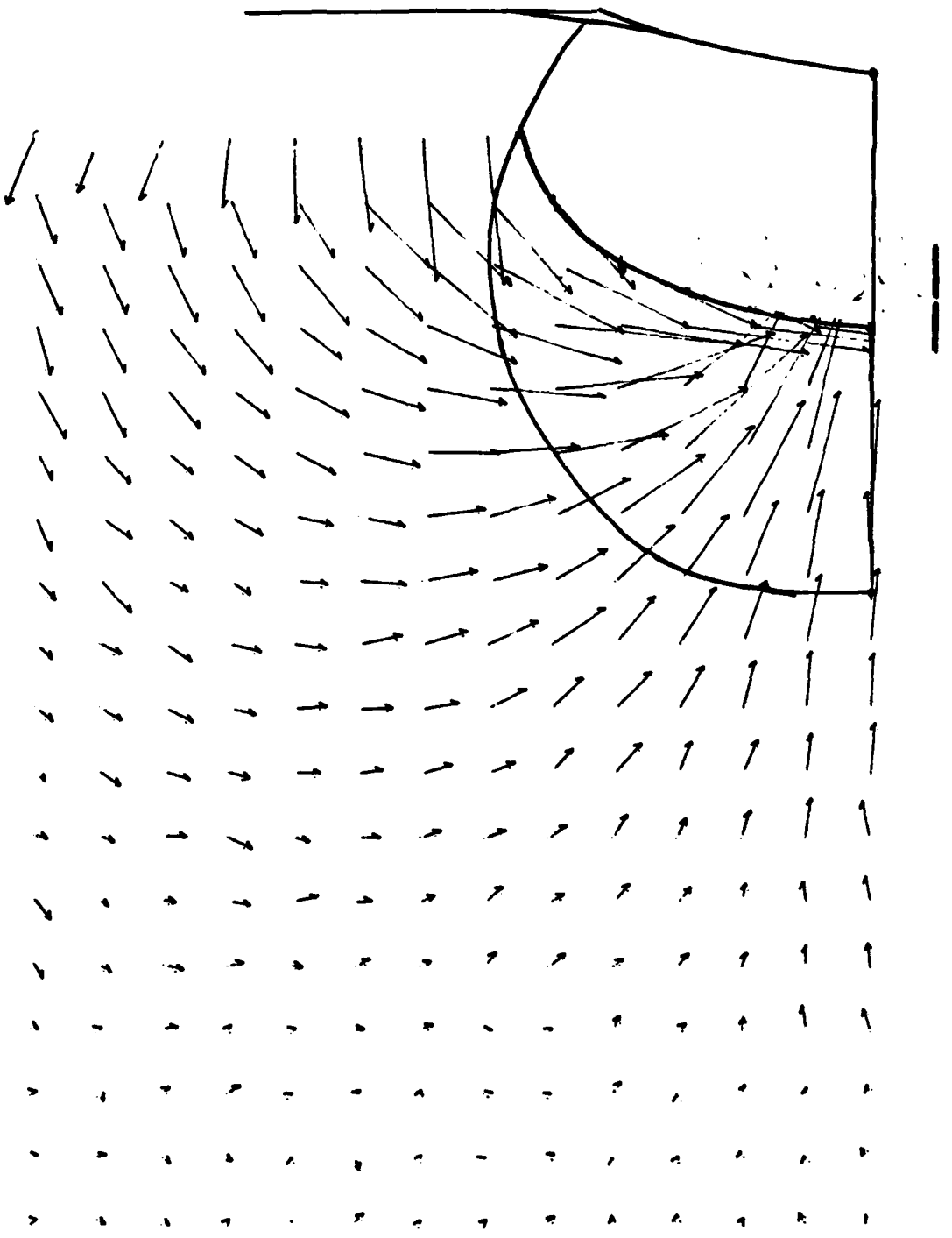

FIG. 25 - FLOW FIELD MAP OF FUSELAGE STATION 4 ALONG BOATTAIL OF C-130

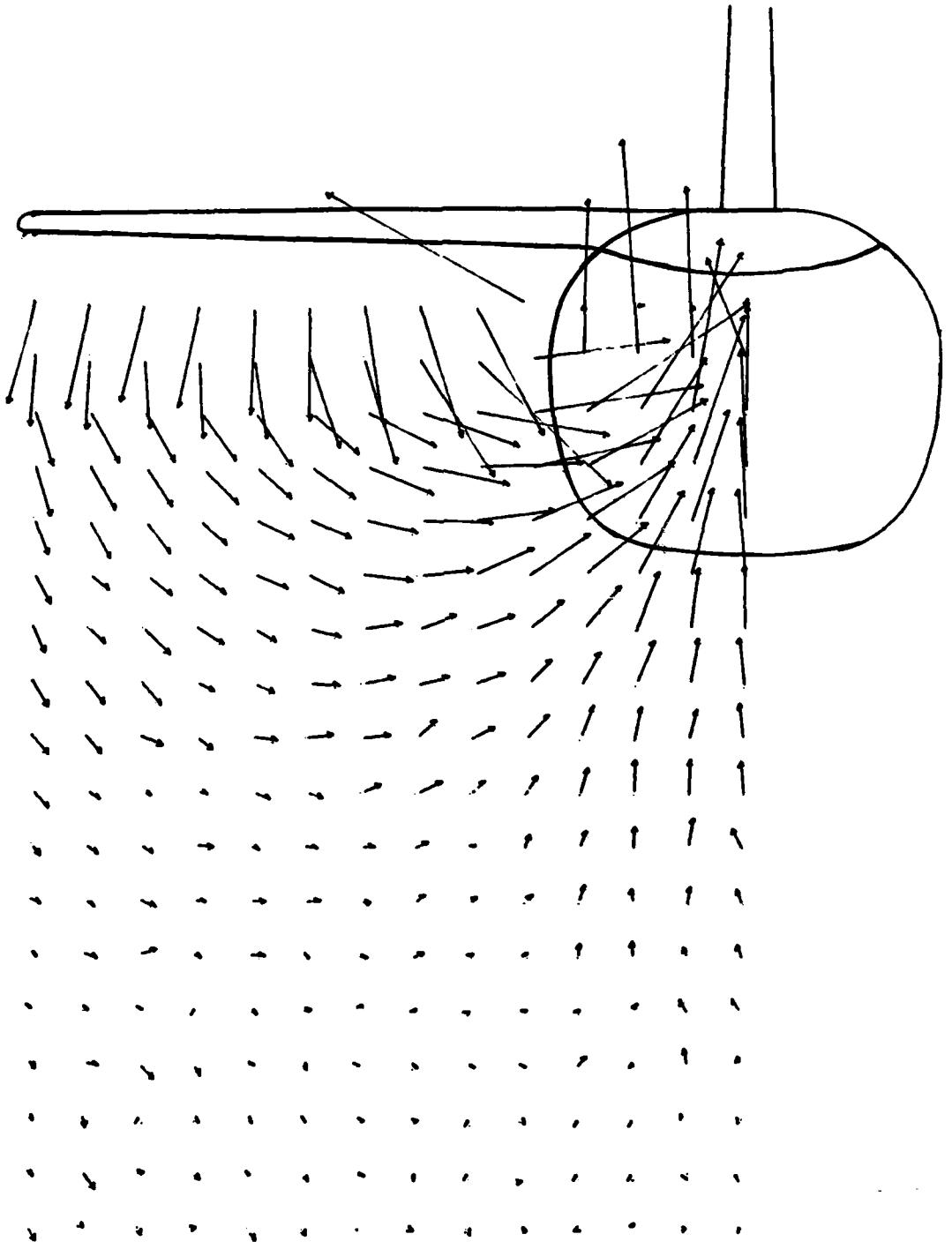

FIG. 26A - FLOW FIELD MAP OF FUSELAGE STATION 5 ALONG BOATTAIL OF C-130

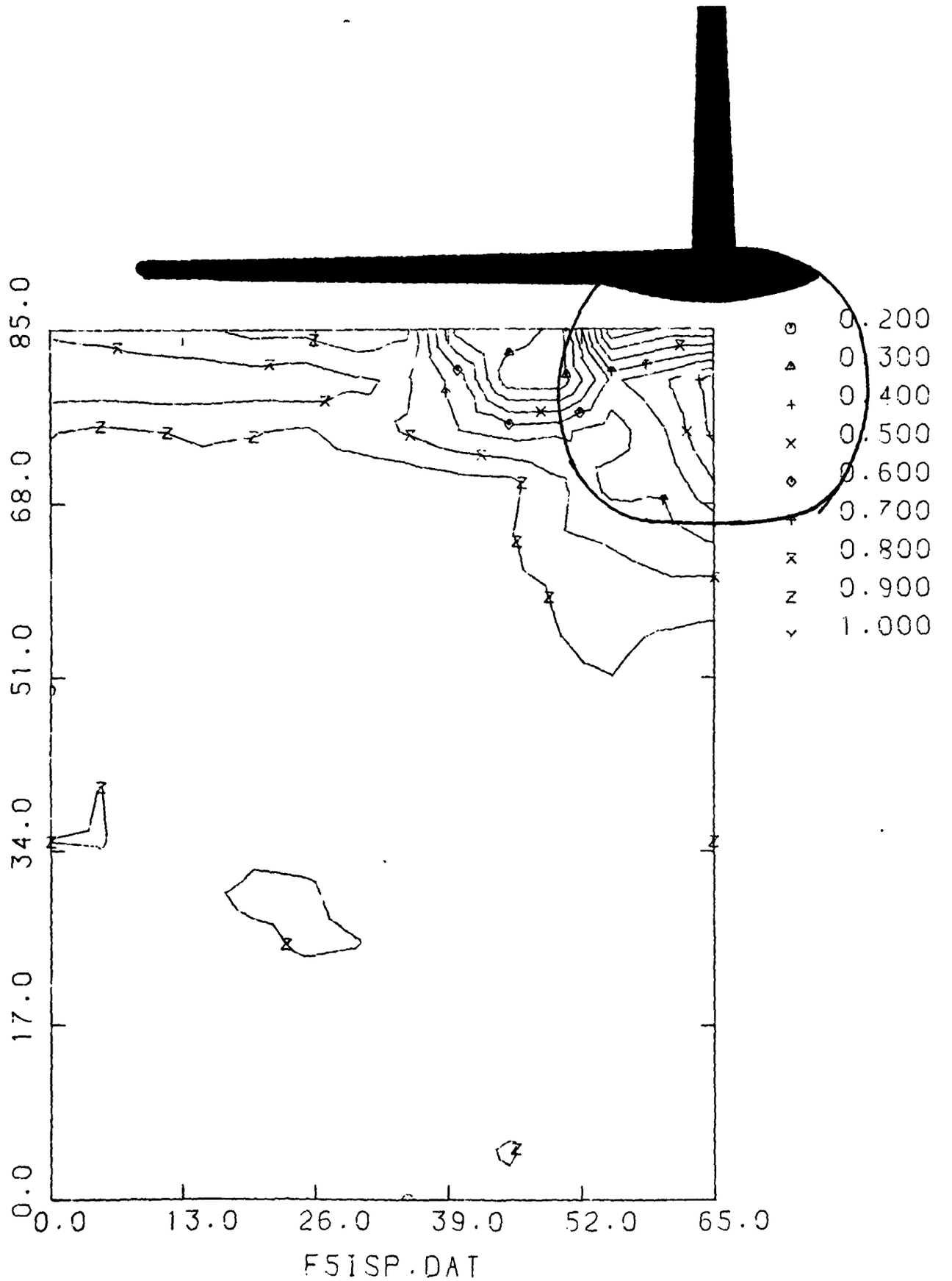

FIB. 26B - ISOLINES OF TOTAL PRESSURE/DYNAMIC PRESSURE ON FUSELAGE STATION 5

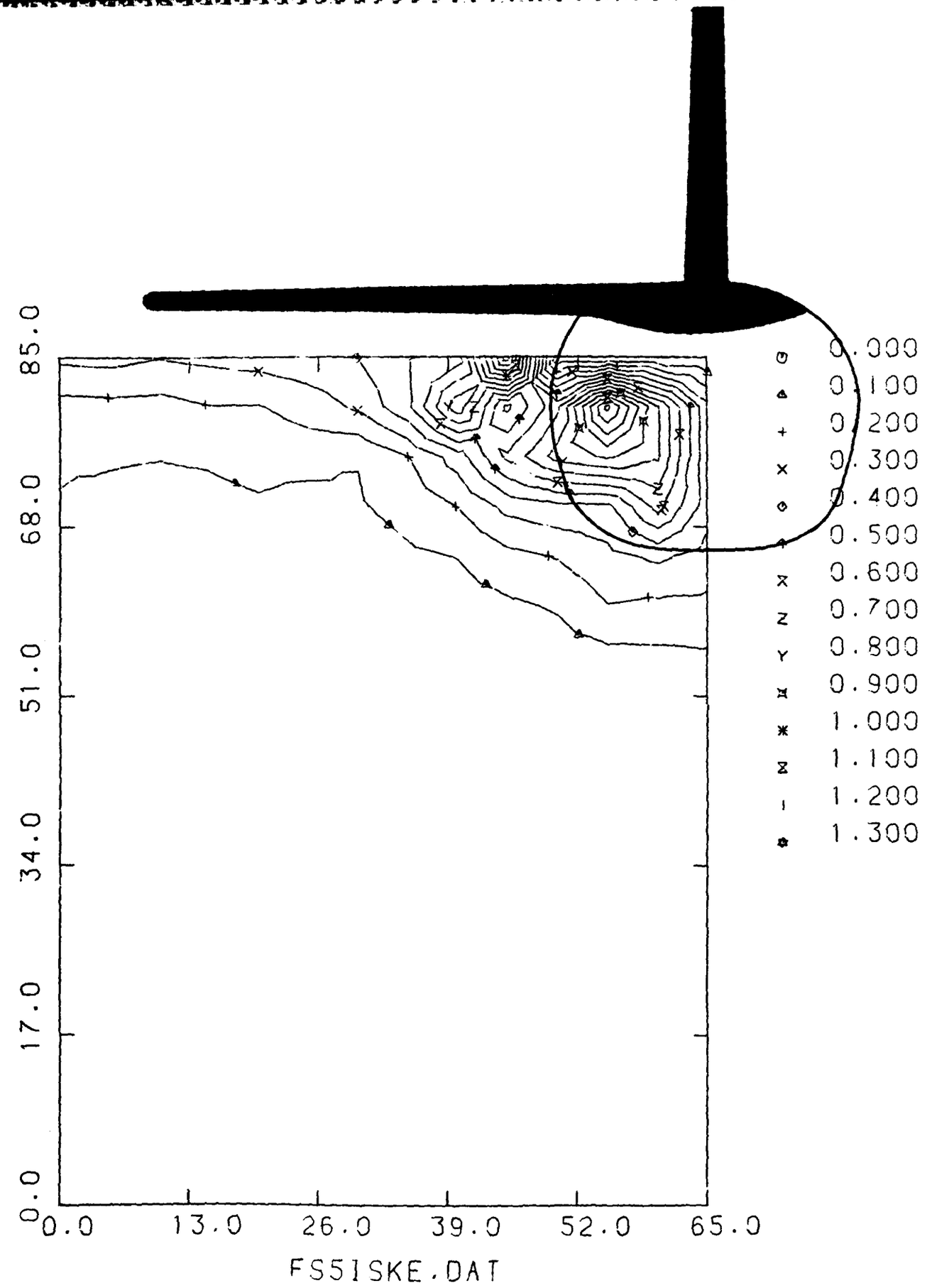

FIG. 26C - ISOLINES OF CROSS FLOW KINETIC ENERGY AT FUSELAGE STATION 5

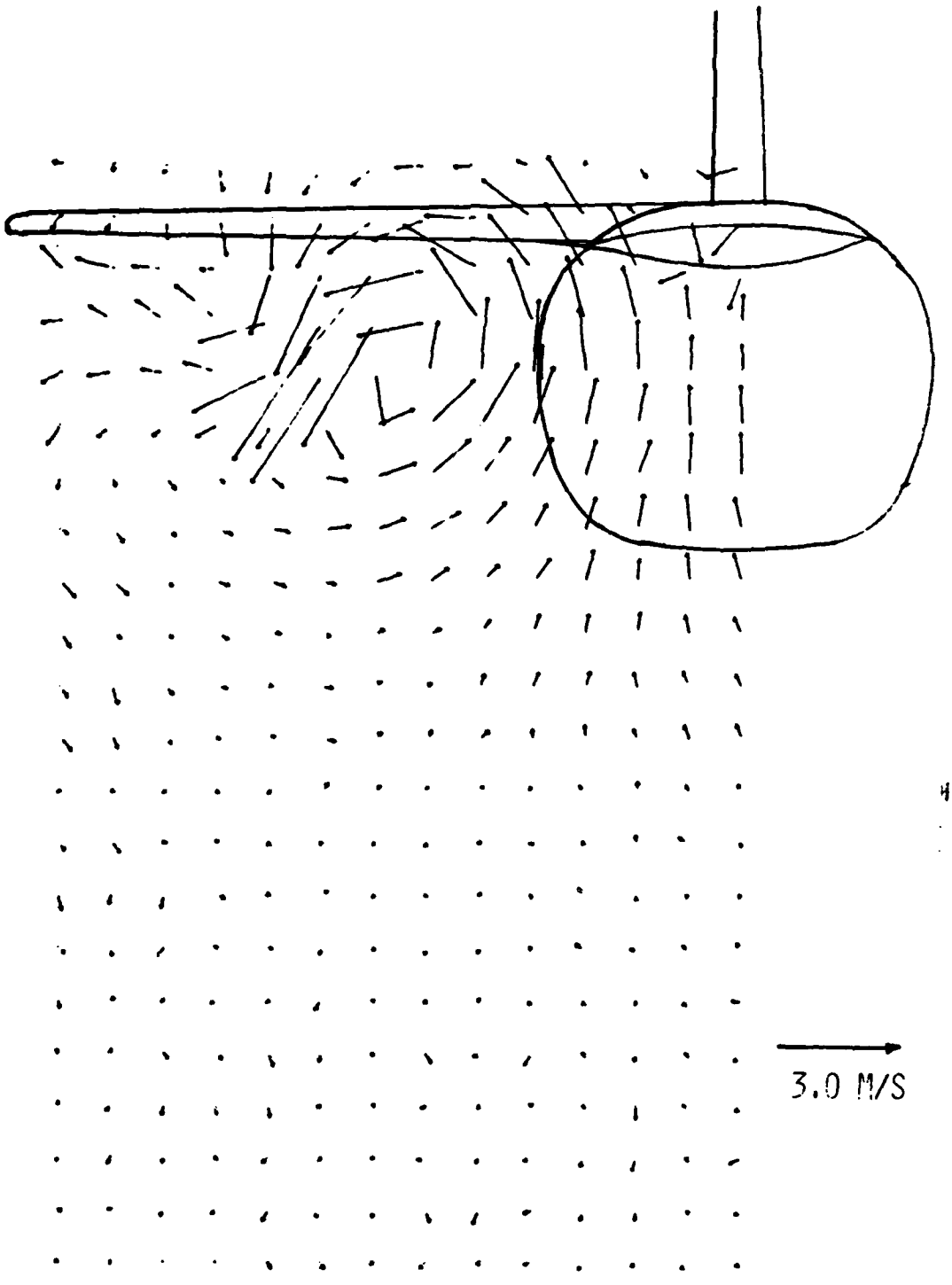

FIG. 27A - FLOW FIELD MAP OF FUSELAGE STATION 6
(DOWNSTREAM OF C-130)

FIG. 27B - ISOLINES OF TOTAL PRESSURE/DYNAMIC PRESSURE ON FUS. STA. 6

- CHARACTERISTIC ISOLINES OF PRESSURE LOSS DUE TO WAKE INDUCED BY AIRCRAFT BOATTAIL.
- MEASUREMENTS TAKEN AT 1 FUSELAGE DIAMETER DOWNSTREAM OF FUSELAGE

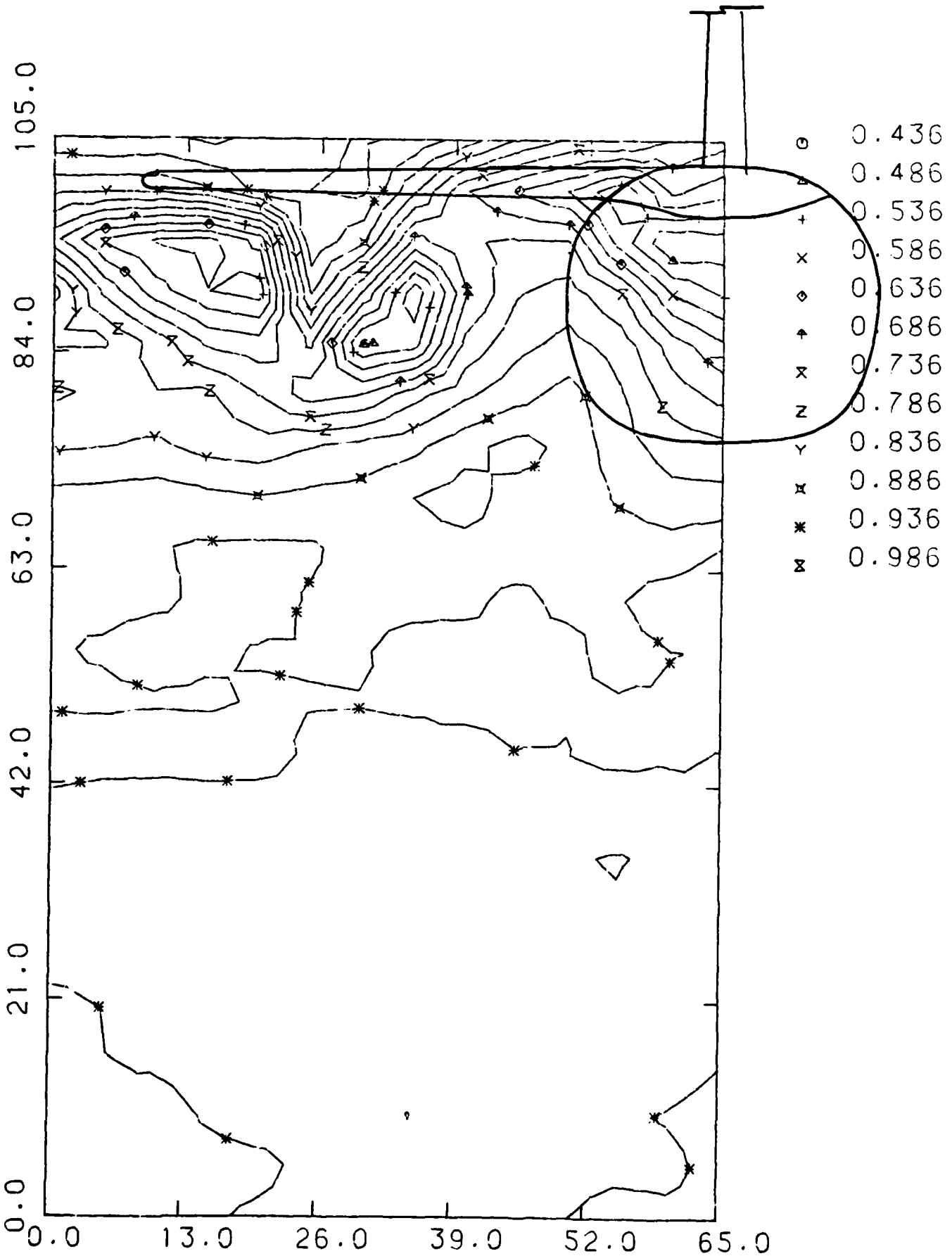

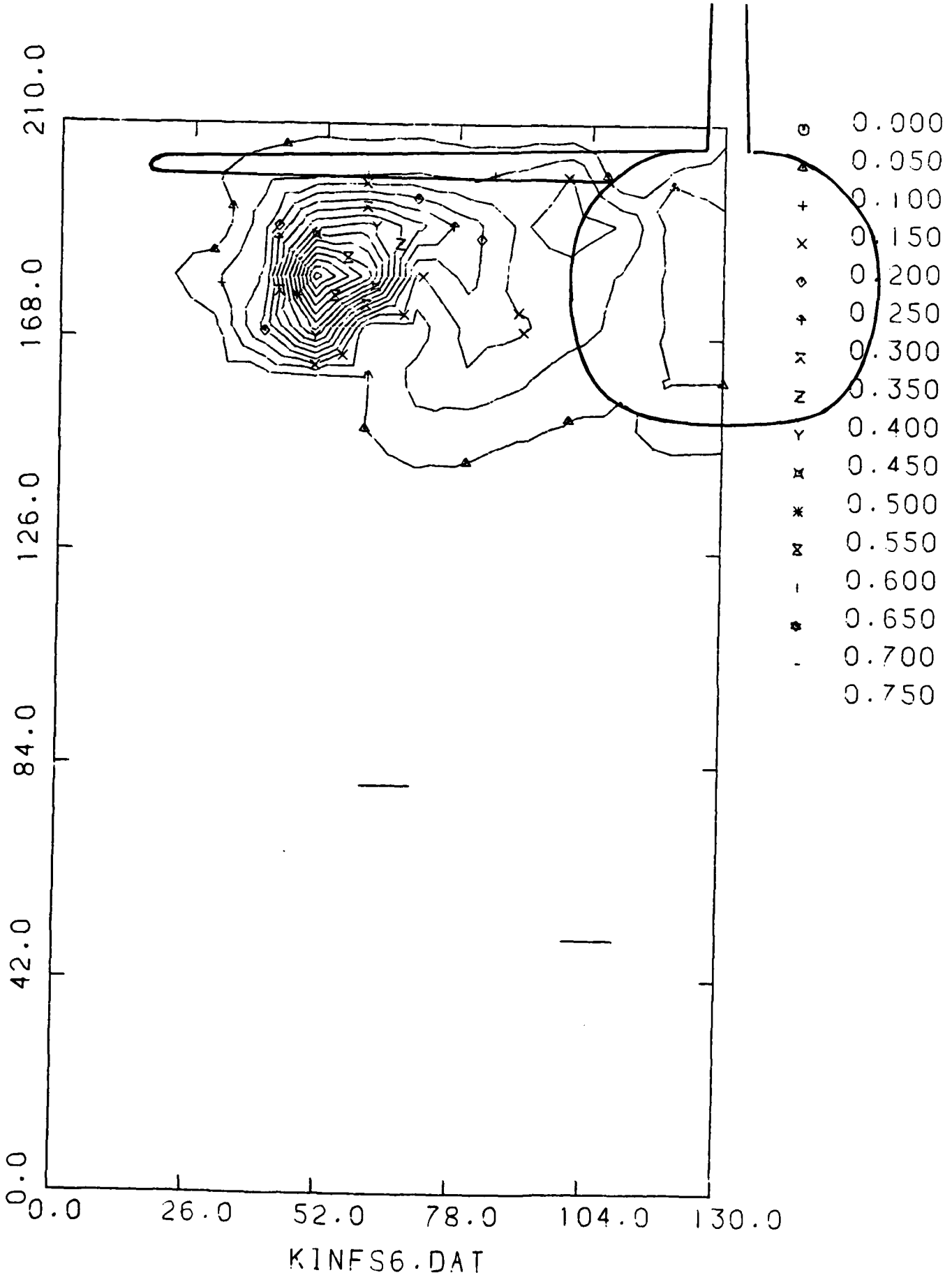

FIG. 27C - ISOLINES OF CROSS FLOW KINETIC ENERGY AT FUSELAGE STATION 6

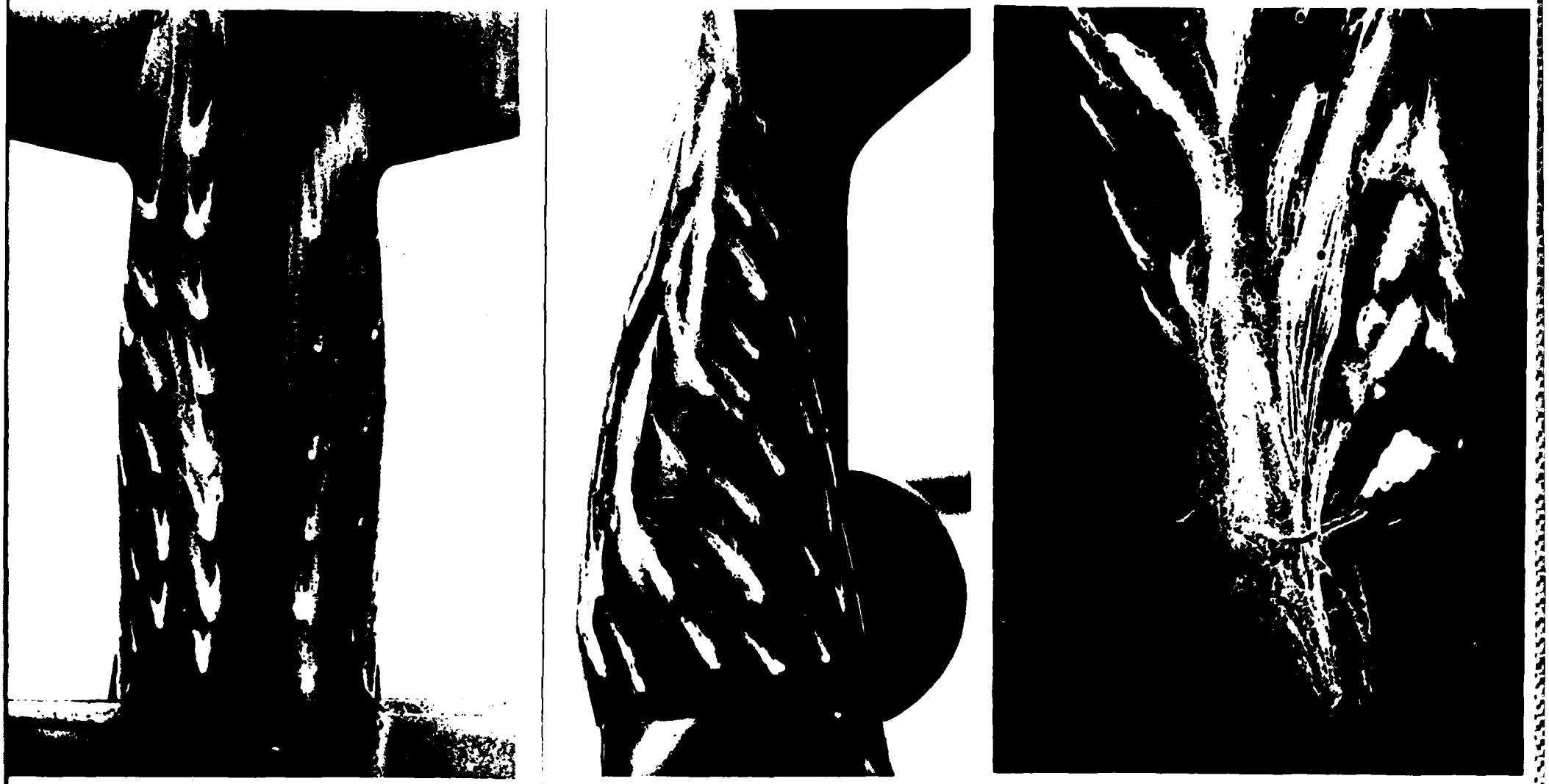

A B C

FIGS. 28A.B.C - LIMITING STREAMLINES VISUALIZATION ON C-130 (TOP, SIDE AND BOTTOM VIEWS)

FIG. 29 - TOP AND SIDE VIEW DRAWING OF DELTA WING USED FOR EXPERIMENTS

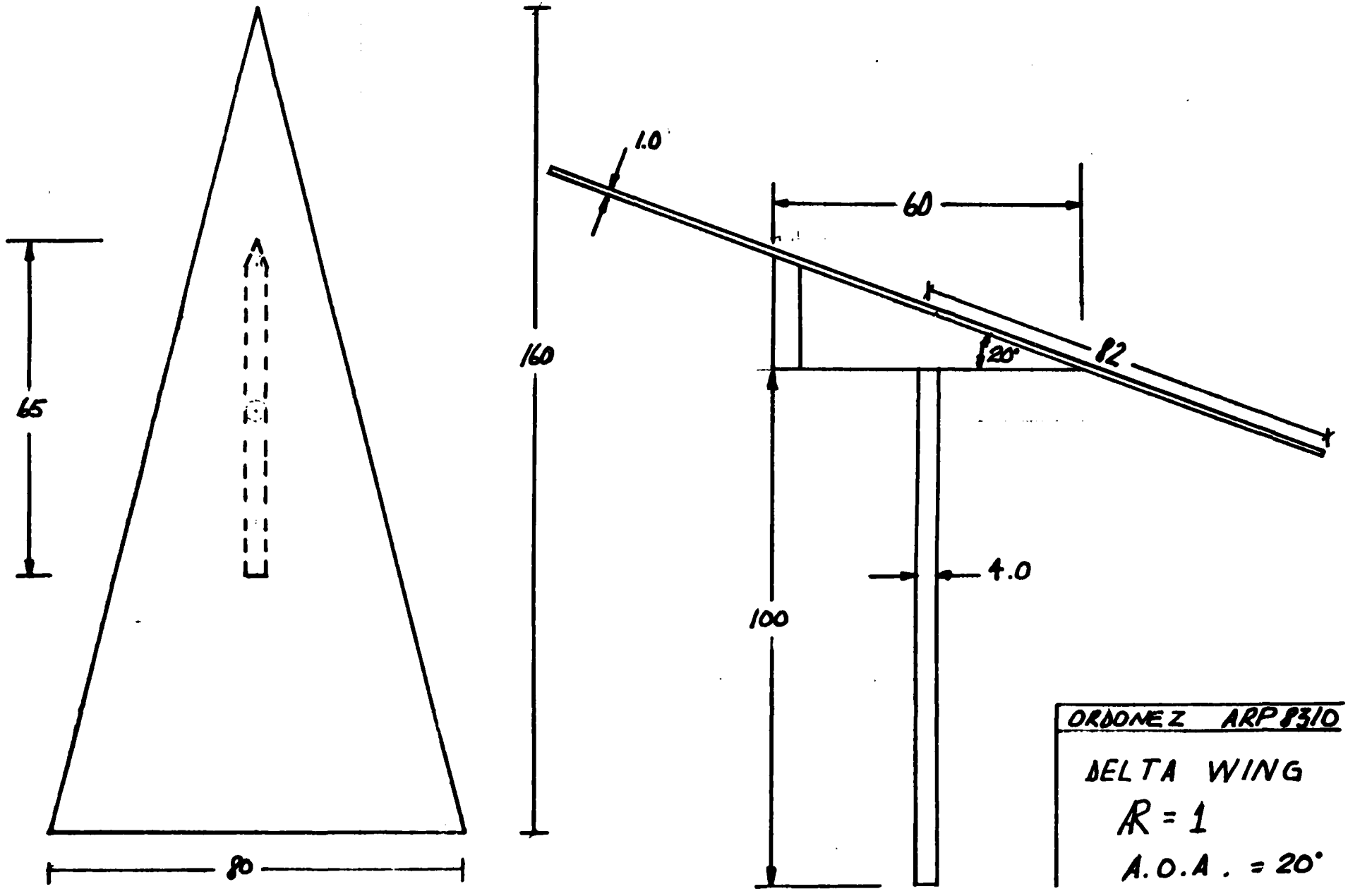

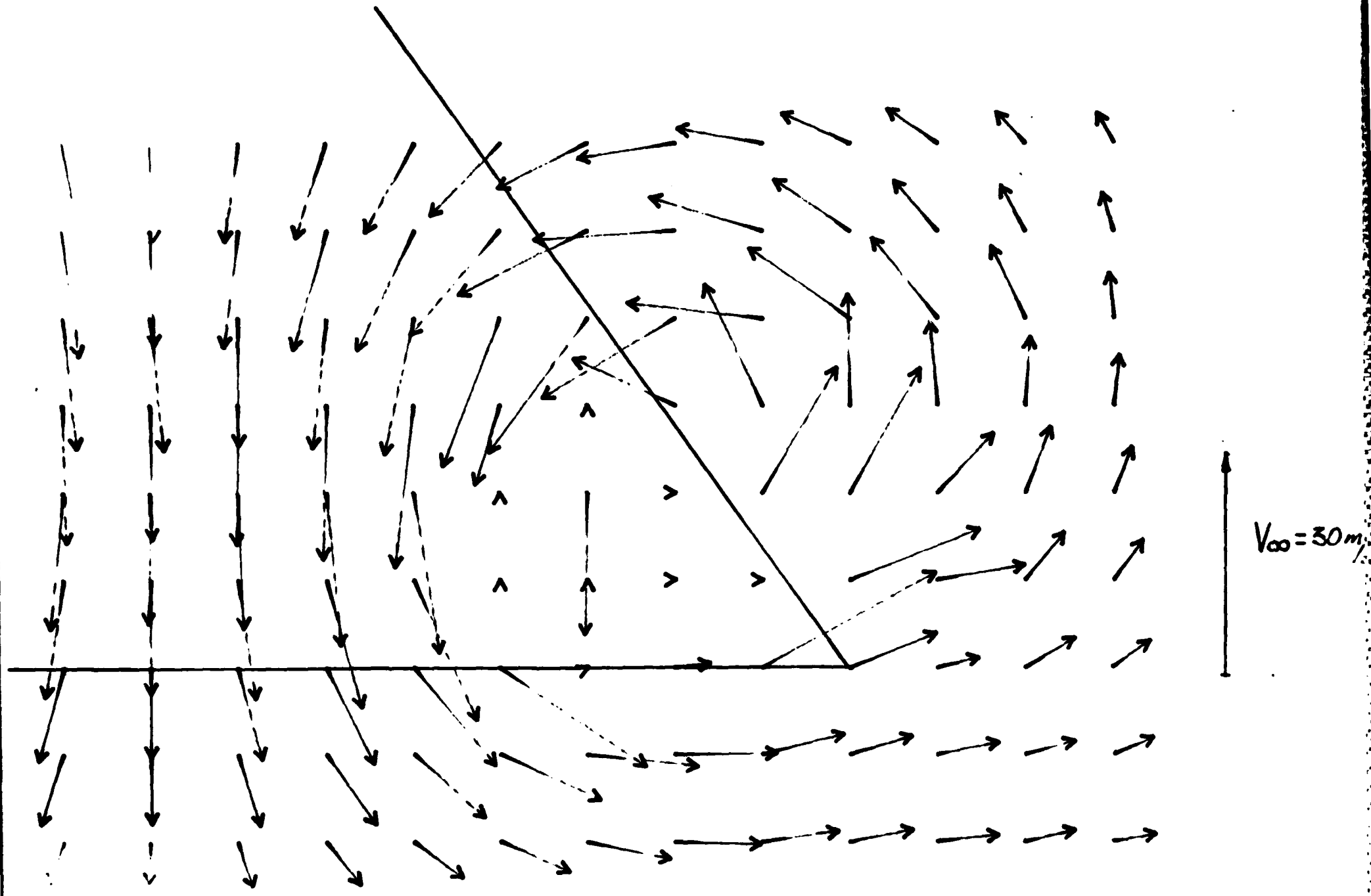

FIG. 30A - FLOW FIELD AT $\varepsilon = 0.625$ DOWNSTREAM OF DELTA WING

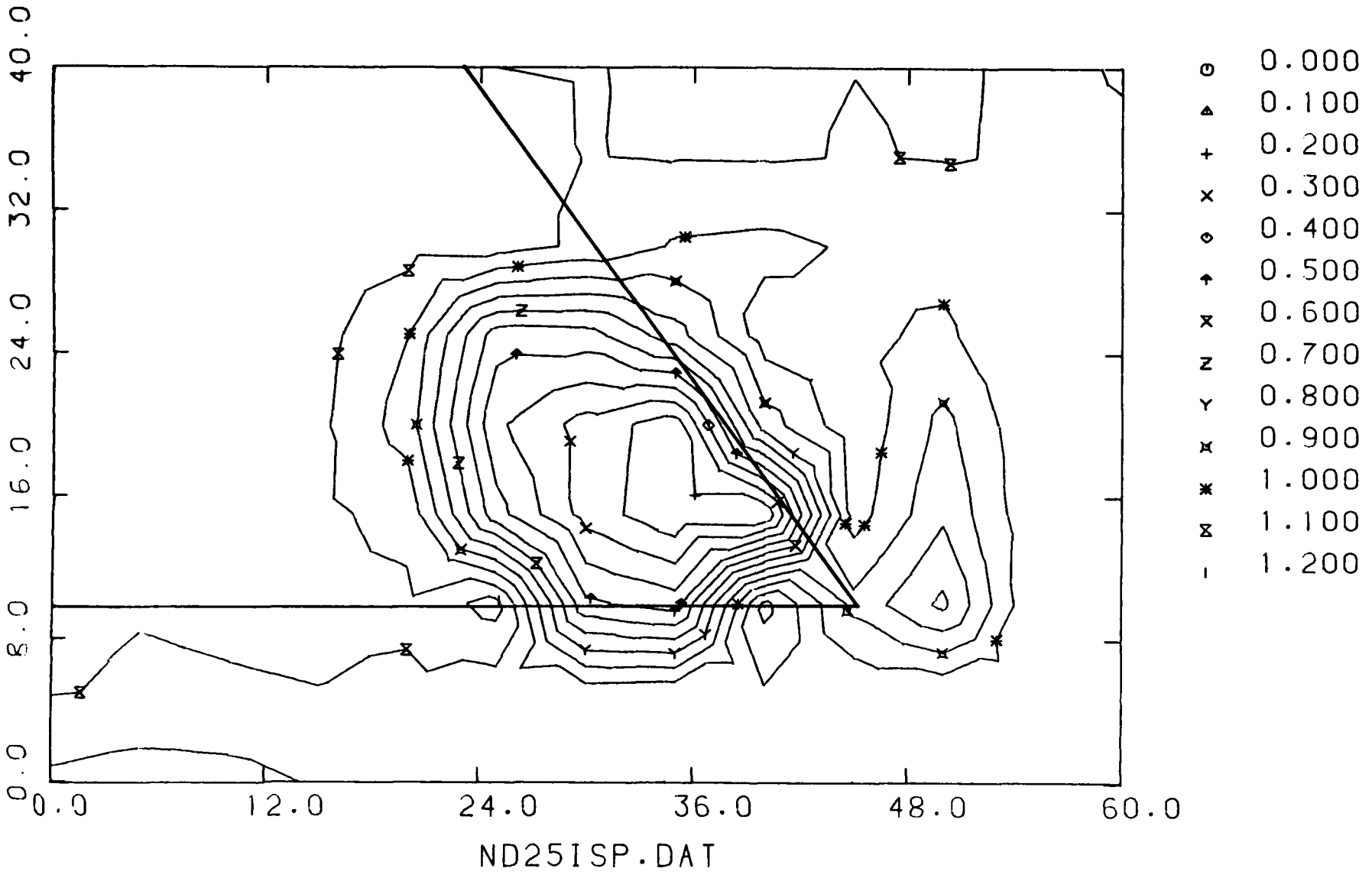

FIG. 30B - ISOLINES OF TOTAL PRESSURE/DYNAMIC PRESSURE AT ε = 0.625 DOWNSTREAM OF DELTA WING

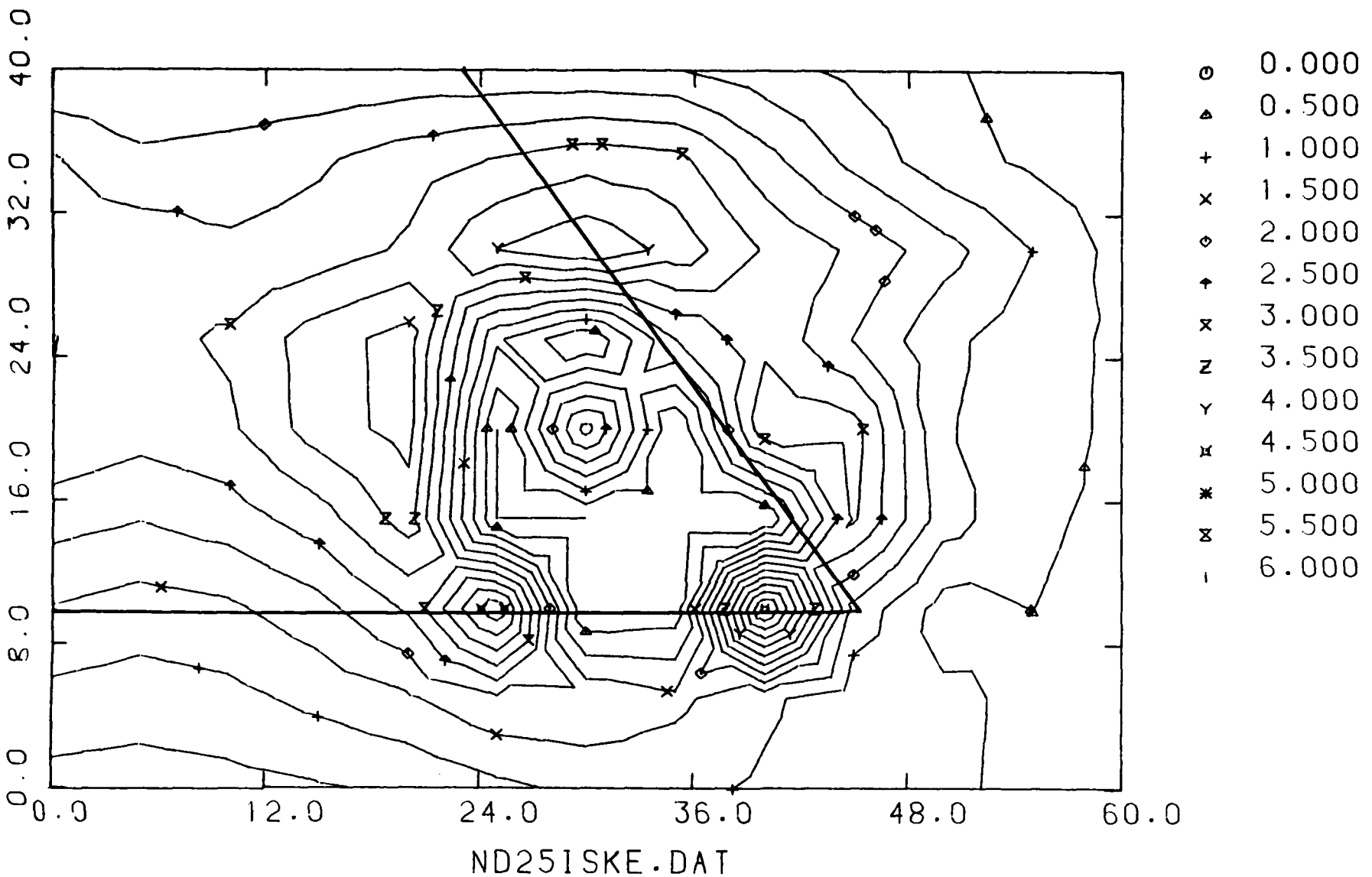

FIG. 30C - ISOLINES OF DIMENSIONLESS CROSS FLOW KINETIC ENERGY AT $\xi = 0.625$ DOWNSTREAM OF DELTA WING

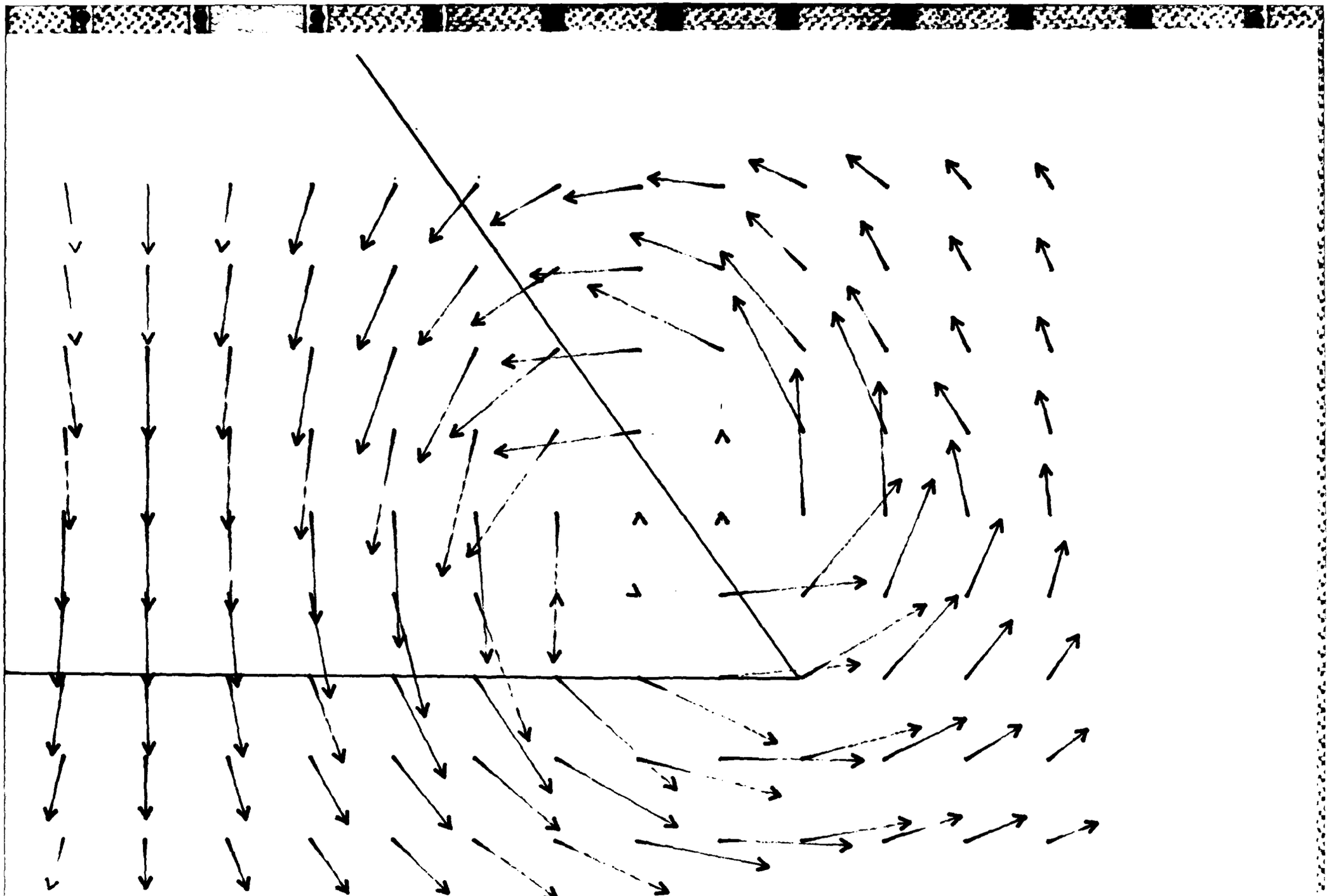

FIG. 31A - FLOW FIELD AT ε = 1.875 DOWNSTREAM OF DELTA WING

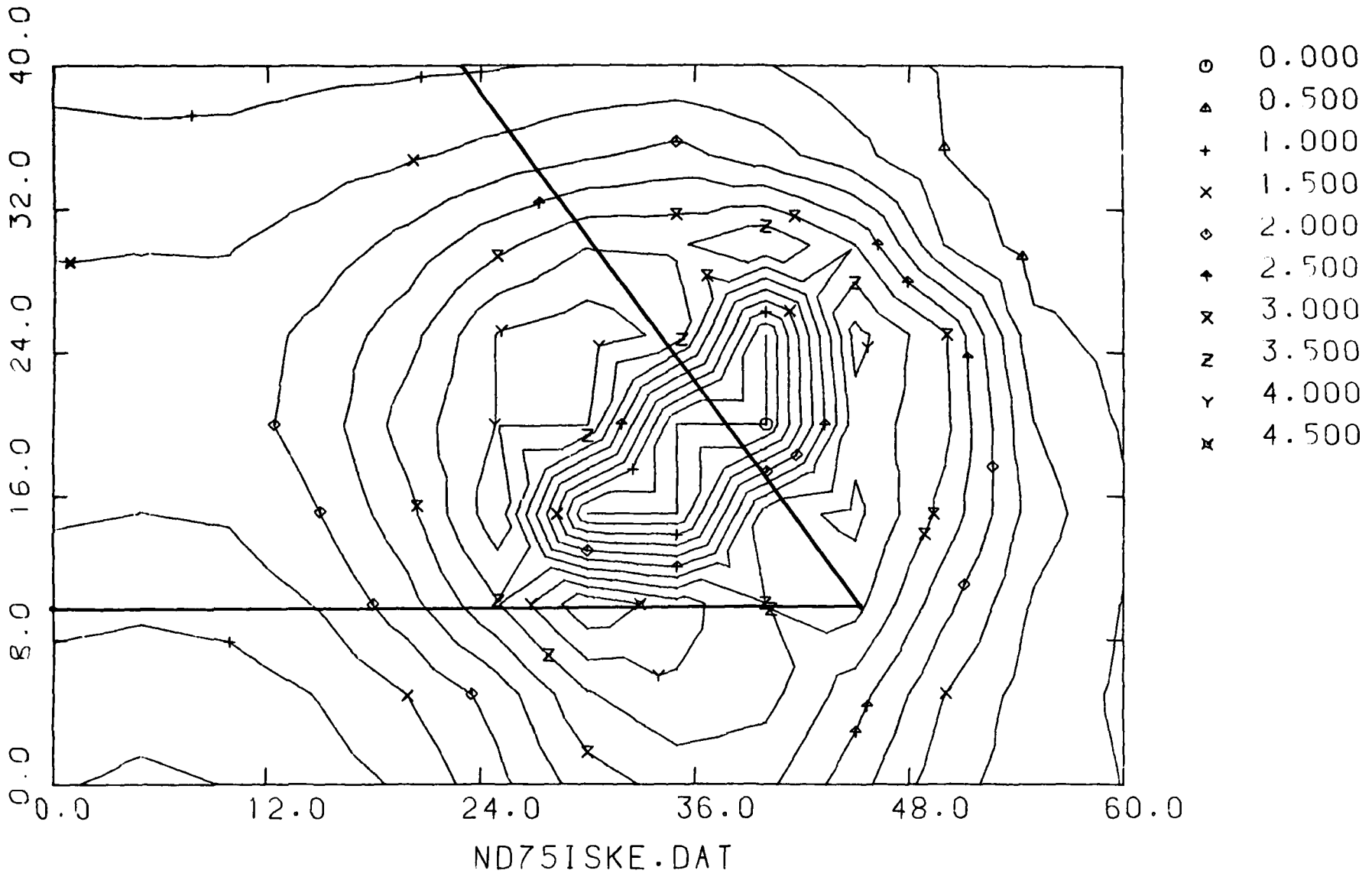

FIG. 31B - ISOLINES OF DIMENSIONLESS CROSS FLOW KINETIC ENERGY AT ξ = 1.875 DOWNSTREAM OF DELTA WING

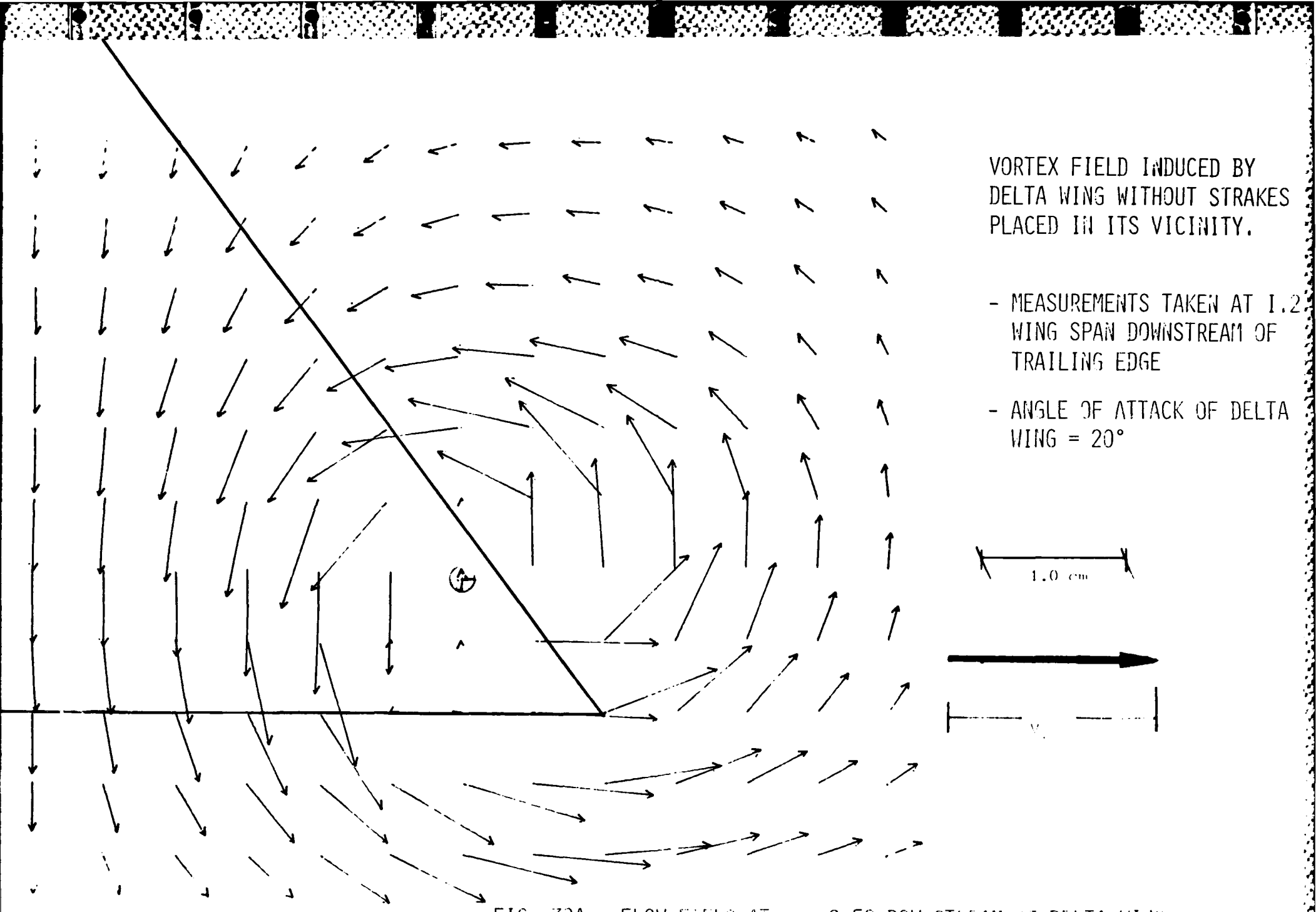

FIG. 32A - FLOW FIELD AT x = 2.50 DOWNSTREAM OF DELTA WING

ISOLINES OF $\frac{\text{TOT.LOC.PRESSURE}}{\text{DYNAMIC PRESSURE}}$ FOR A VORTEX AT I.2 WING SPAN DOWNSTREAM OF TRAILING EDGE. (ε = 2.5)

FIG. 32B

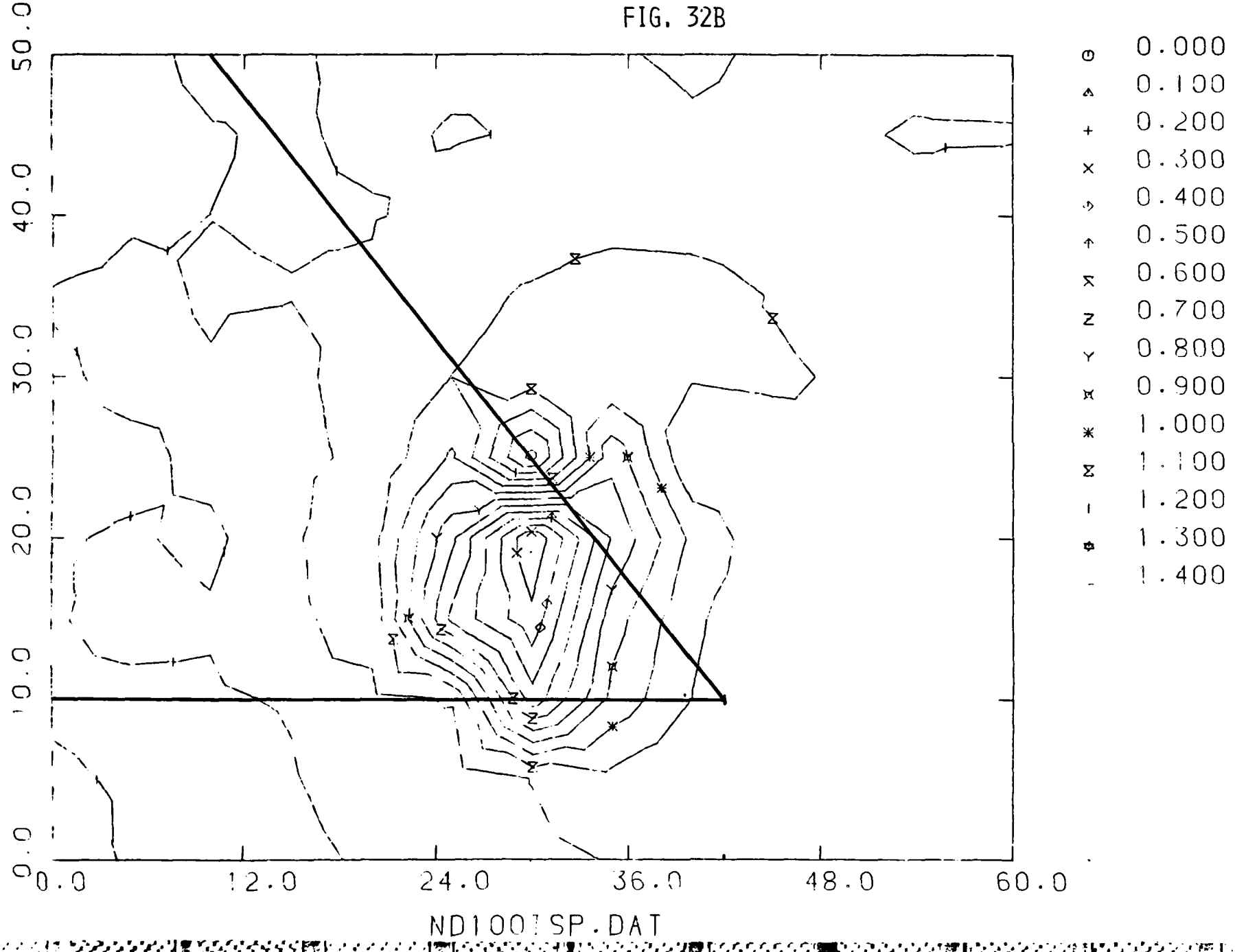

FIG. 32C - ISOLINES OF DCFKE AT ξ = 2.5 DOWNSTREAM OF DELTA WING

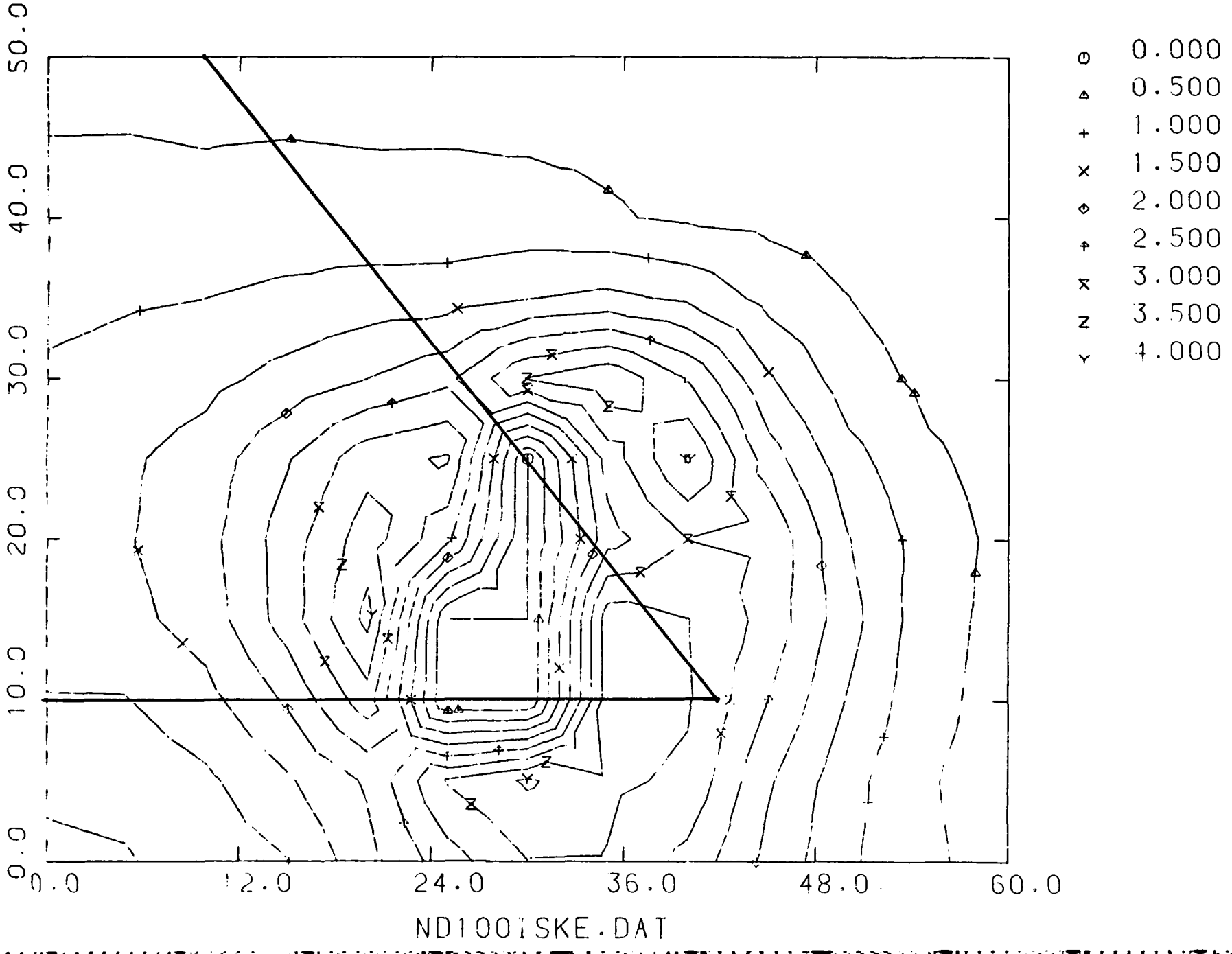

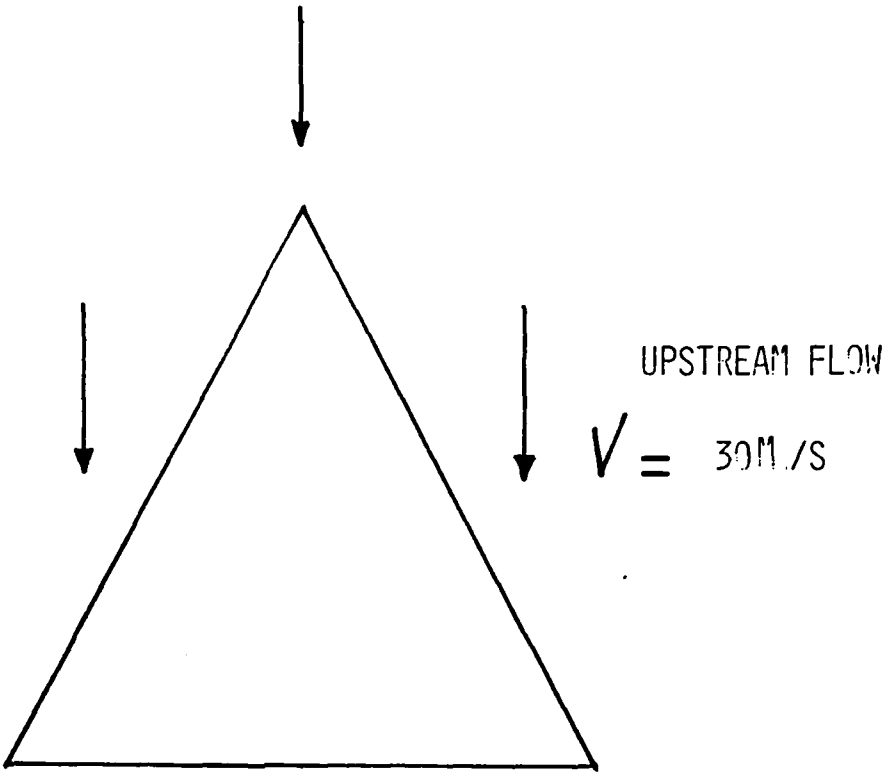

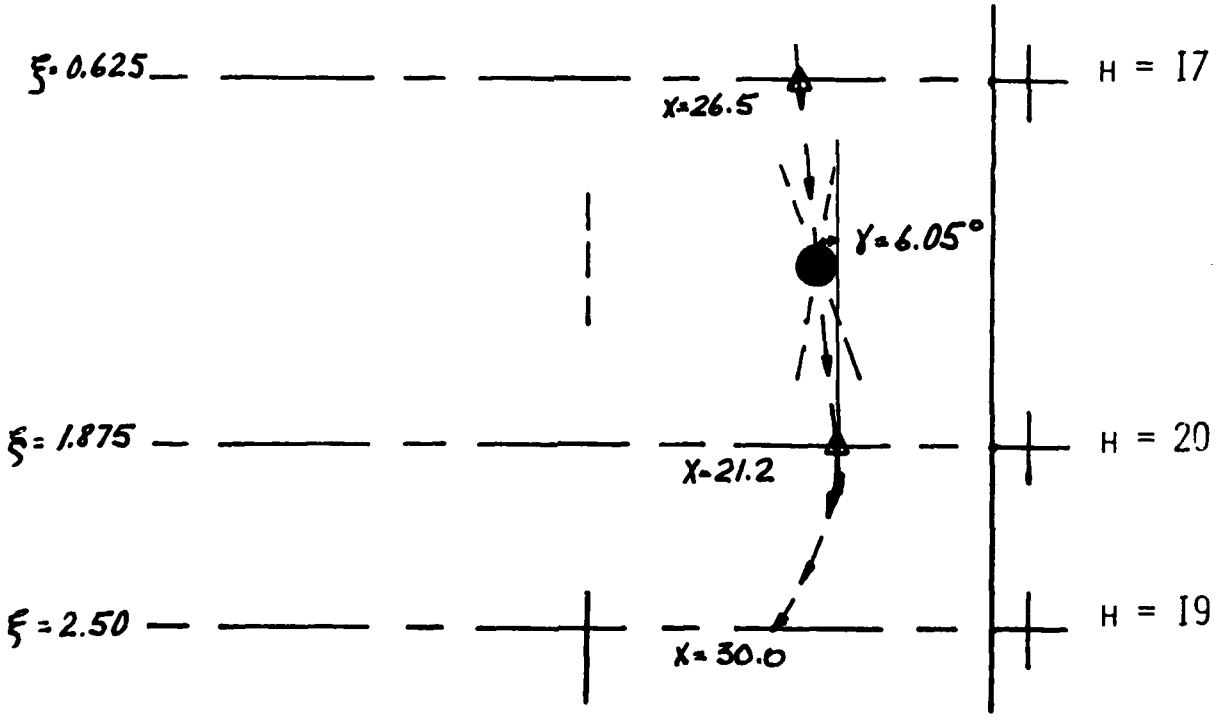

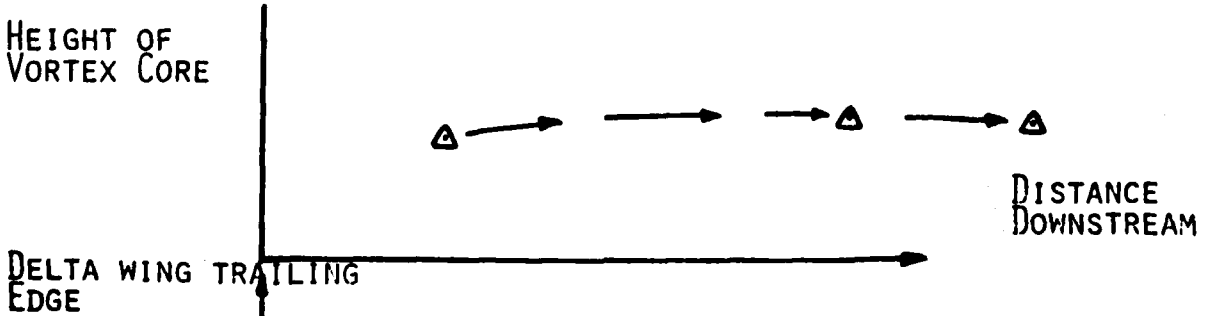

FIG. 23 VORTEX CORE PATH SCHEMATIC

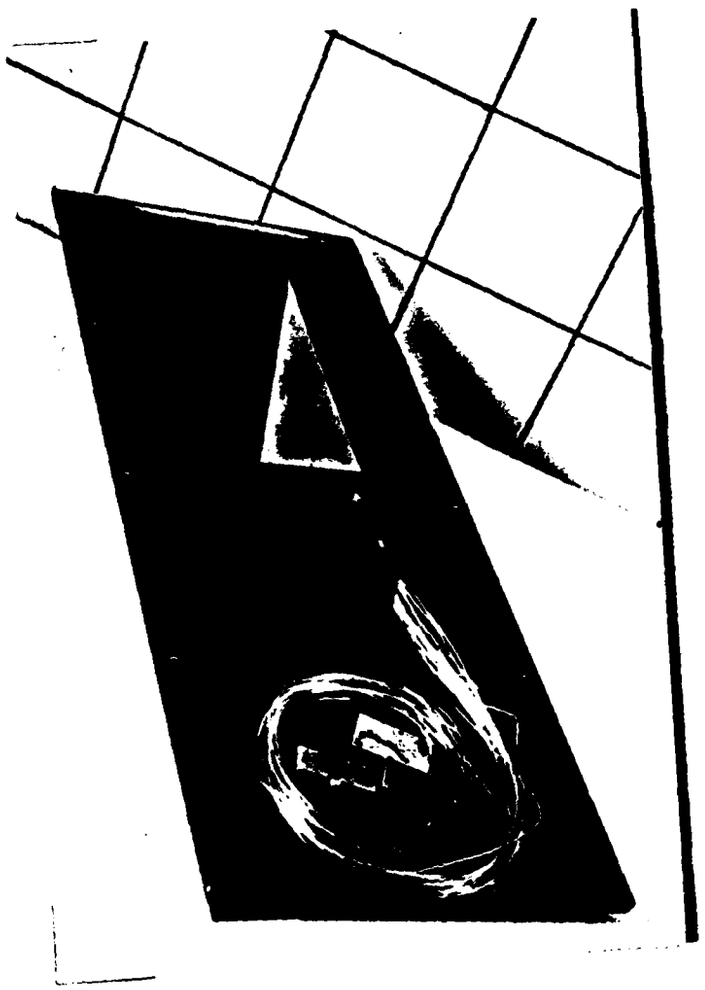

FIG. 34 - DELTA WING AND STRAKES EXPERIMENTAL SET UP IN L-2A

THIN STRAKES

(DIMENSIONS IN MM.)

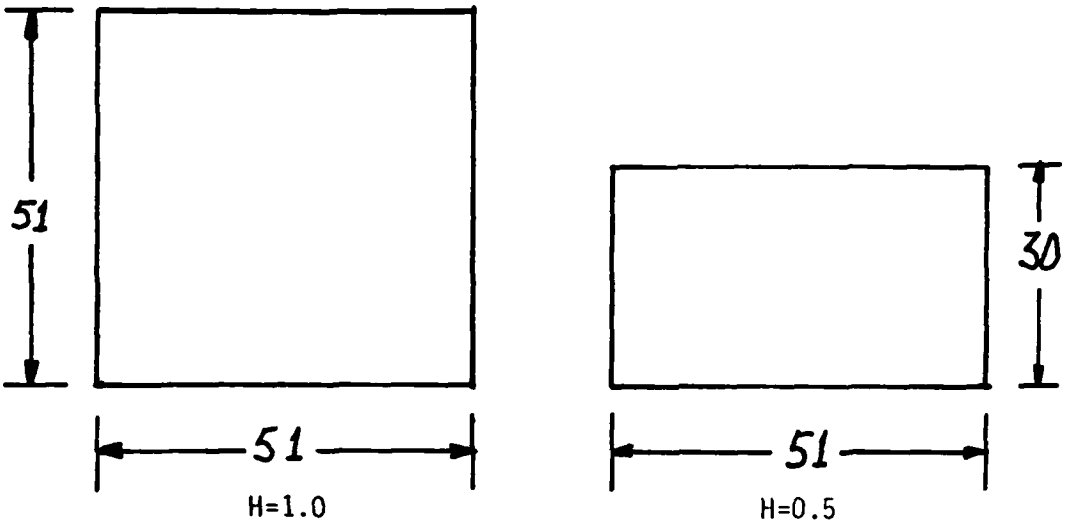

STRAKES THICKNESS

= 0.80 mm.

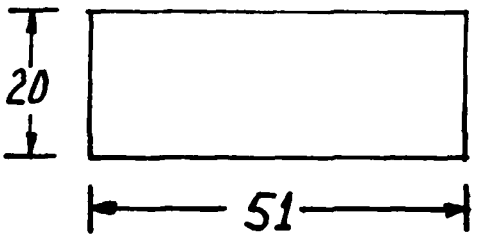

H=0.

THICK STRAKE

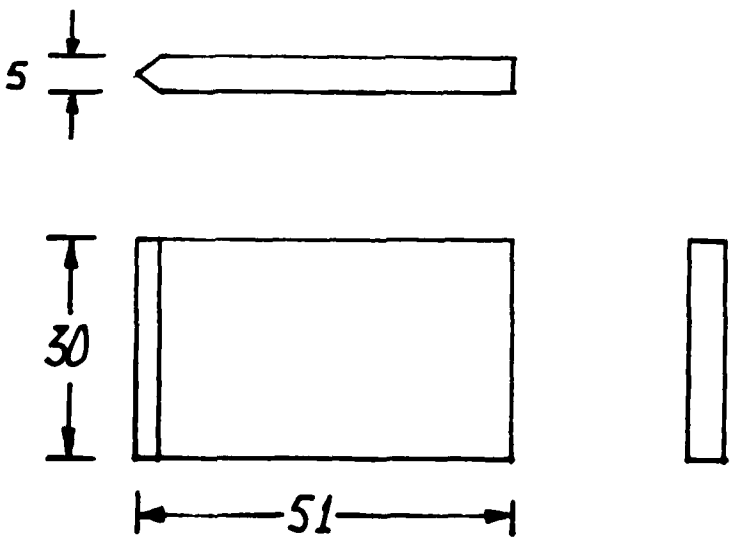

FIG. 35 - STRAKES CONFIGURATIONS (H = 0, 0.5, 1.0)

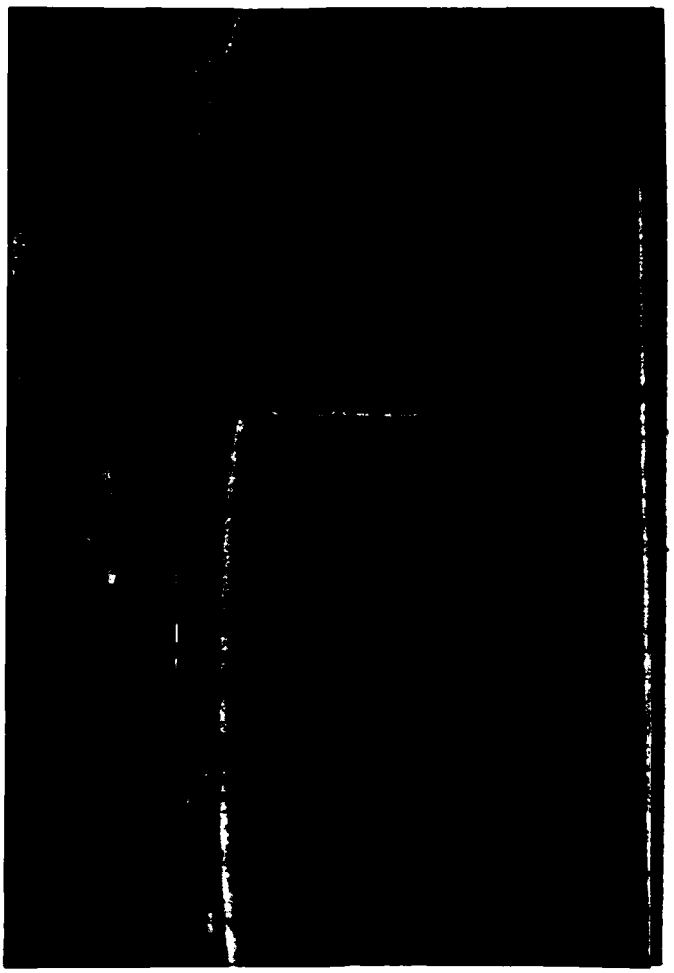

FIG. 36 - WATER TUNNEL DELTA WING - STRAKE SET UP

FIG. 37 - PARAMETRIC DEFINITION

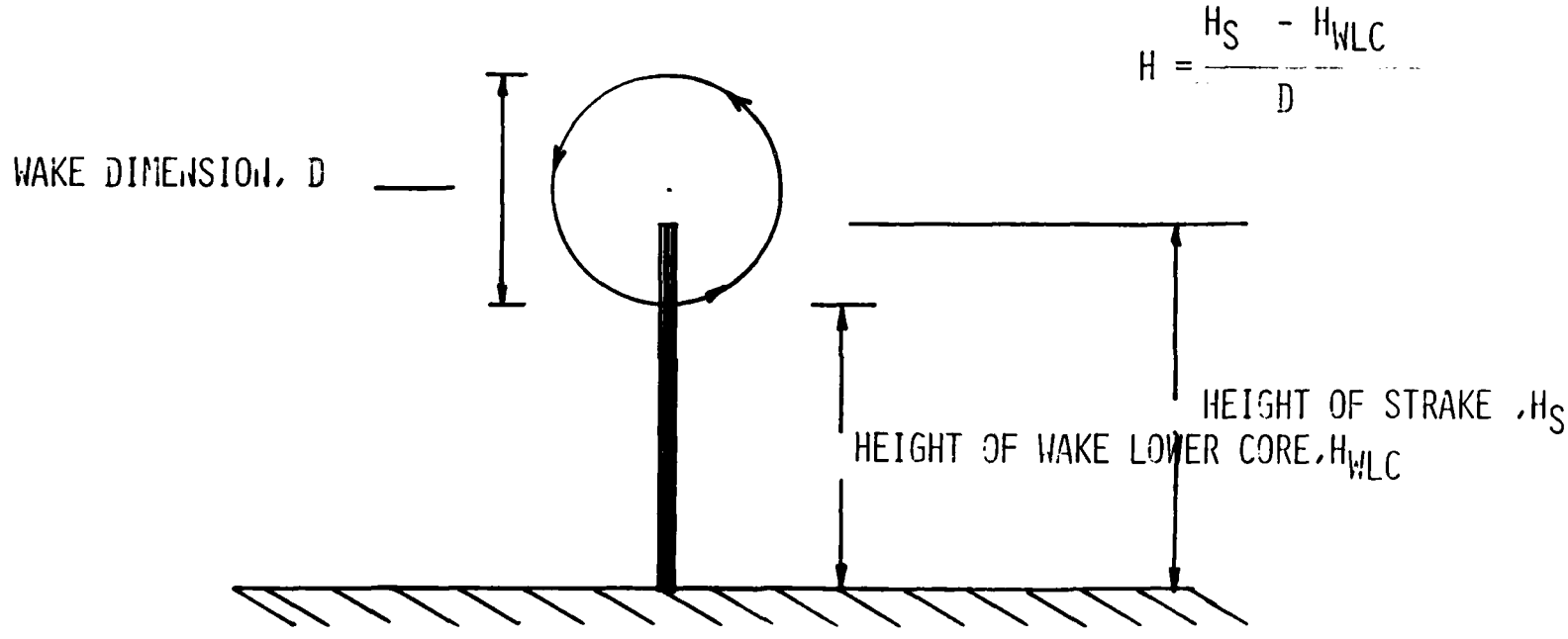

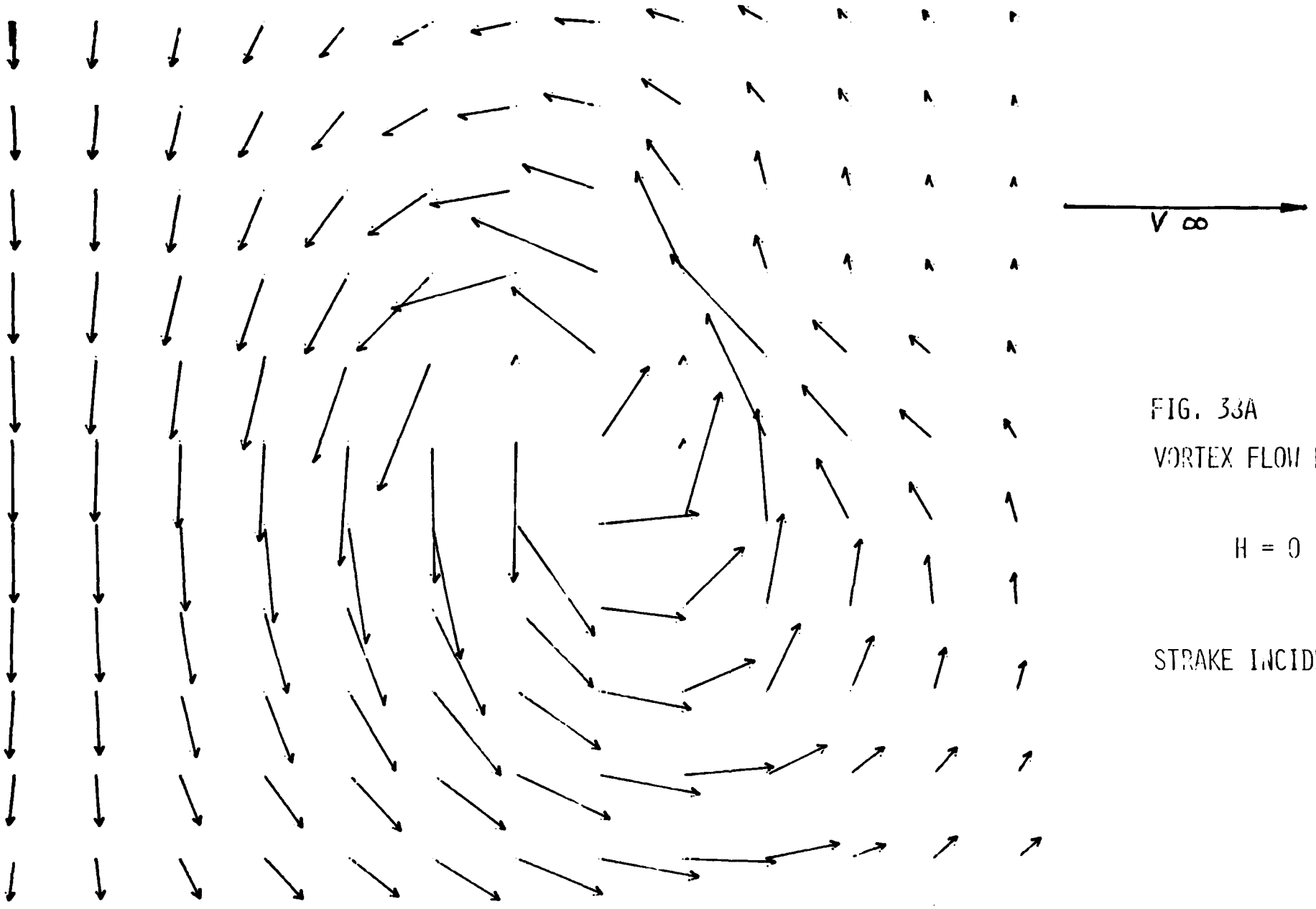

FIG. 33A

VORTEX FLOW FIELD FOR

H = 0

STRAKE INCIDENCE = -10°

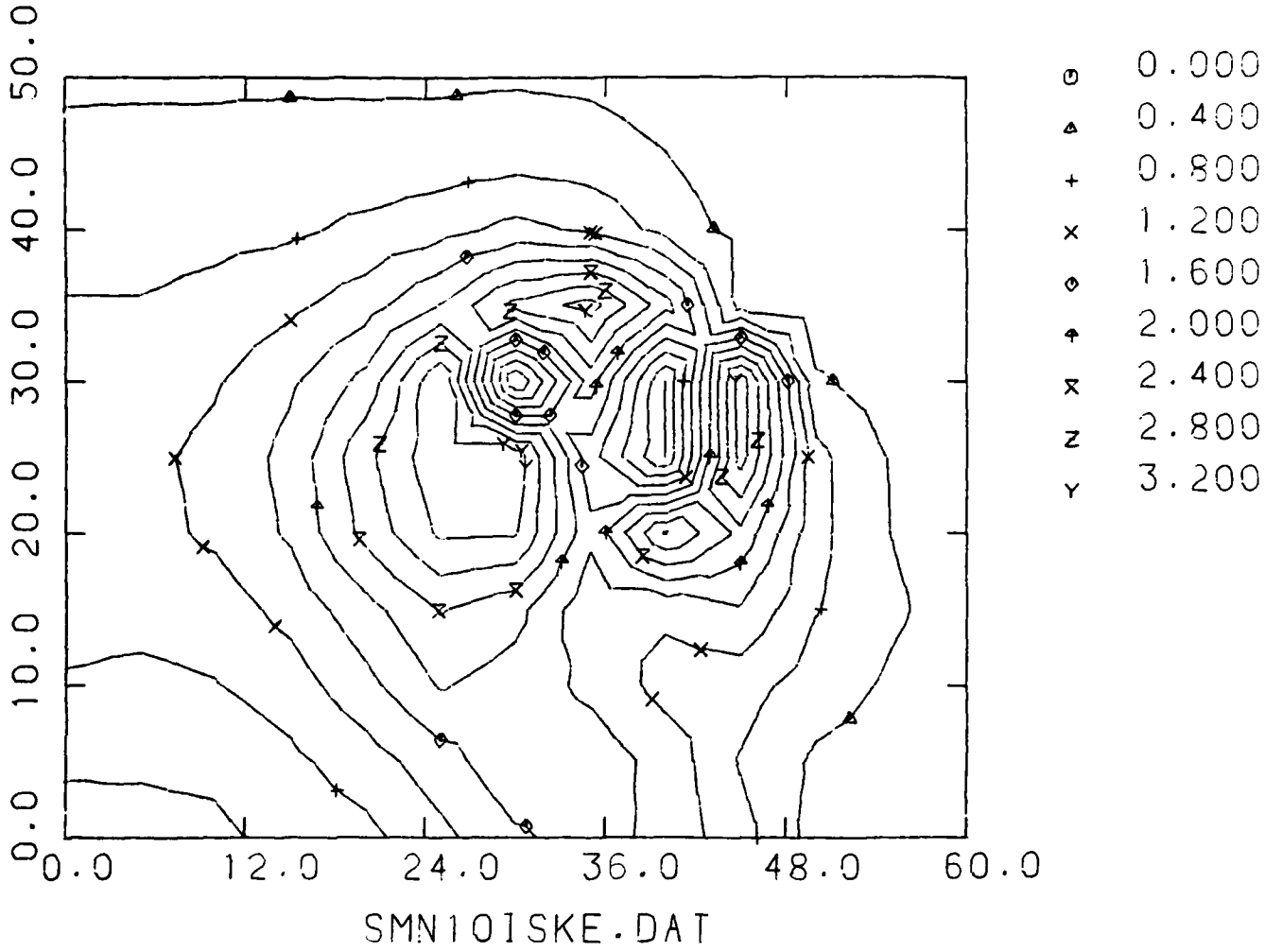

FIG. 38B – ISOLINES OF DIMENSIONLESS CROSS FLOW KINETIC ENERGY (DCFKE) DOWNSTREAM OF H = 0, α_R = -10 THIN STRAKE

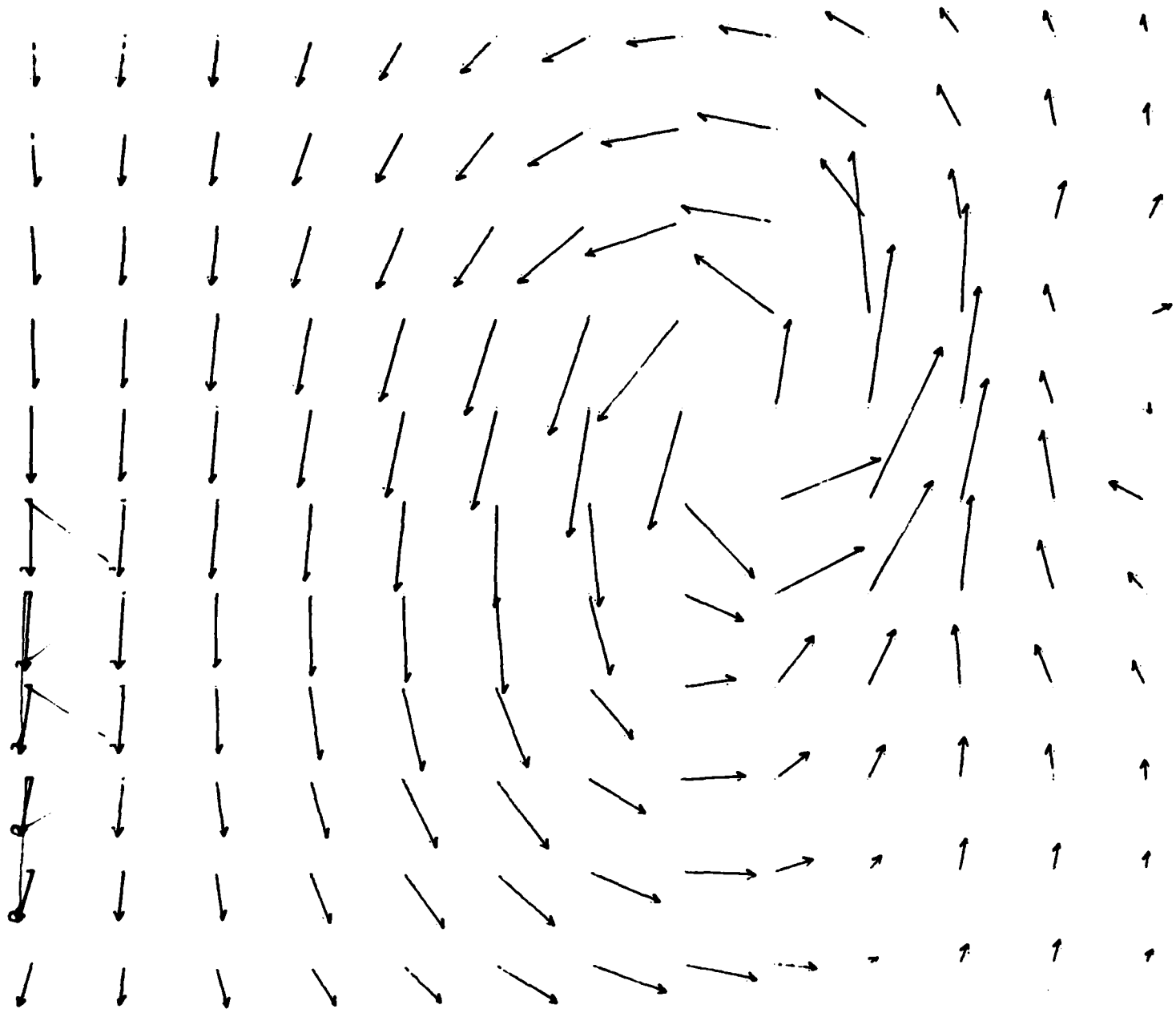

FIG. 39A

FLOW FIELD DOWNSTREAM OF h = 0, THIN STRAKE AT α_R = 0

FIG. 39B

ISOLINES OF TOTAL LOCAL PRESSURE / DYNAMIC PRESSURE FOR

$H = 0.$

$\alpha_R = 0.$ THIN STRAKE

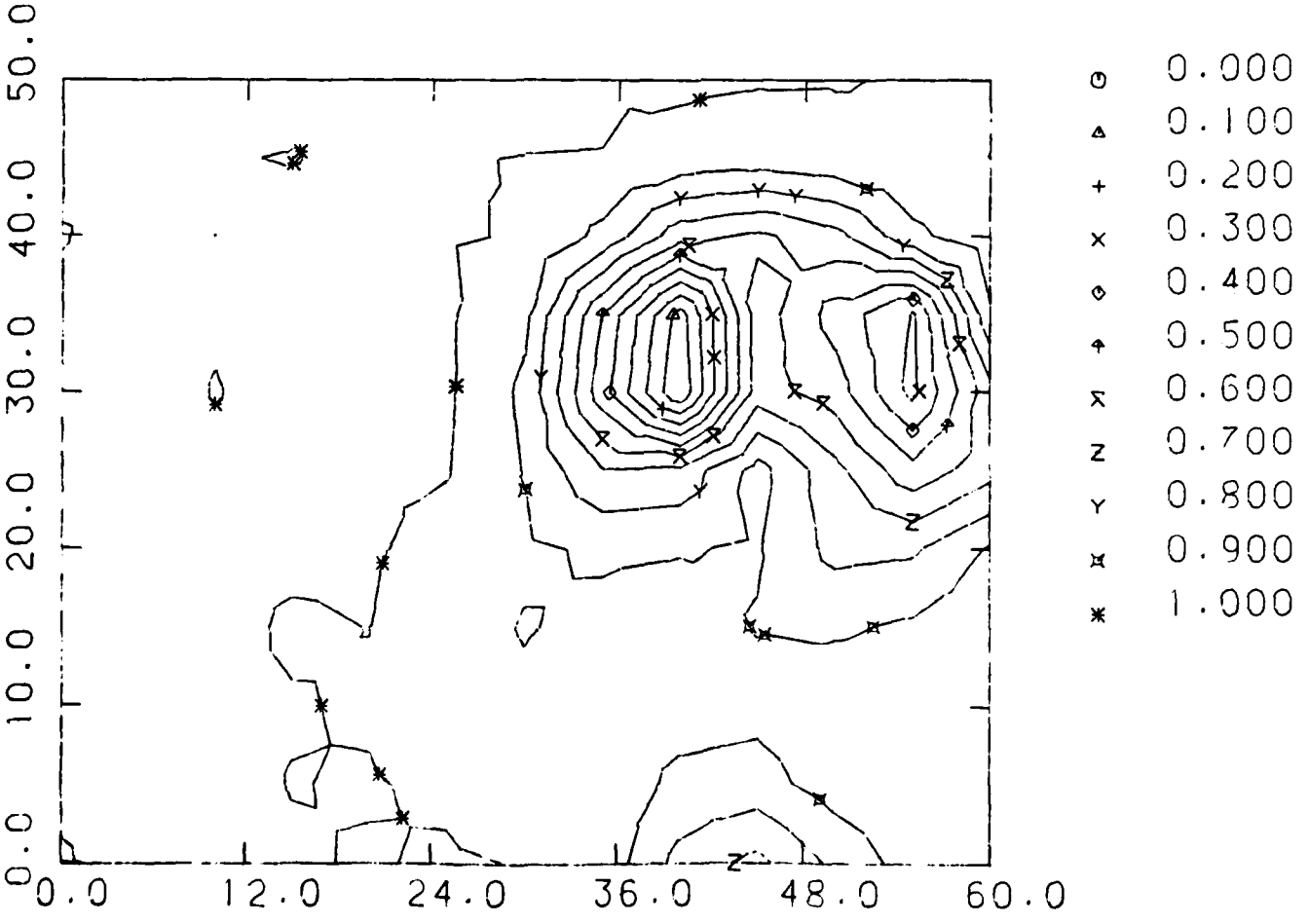

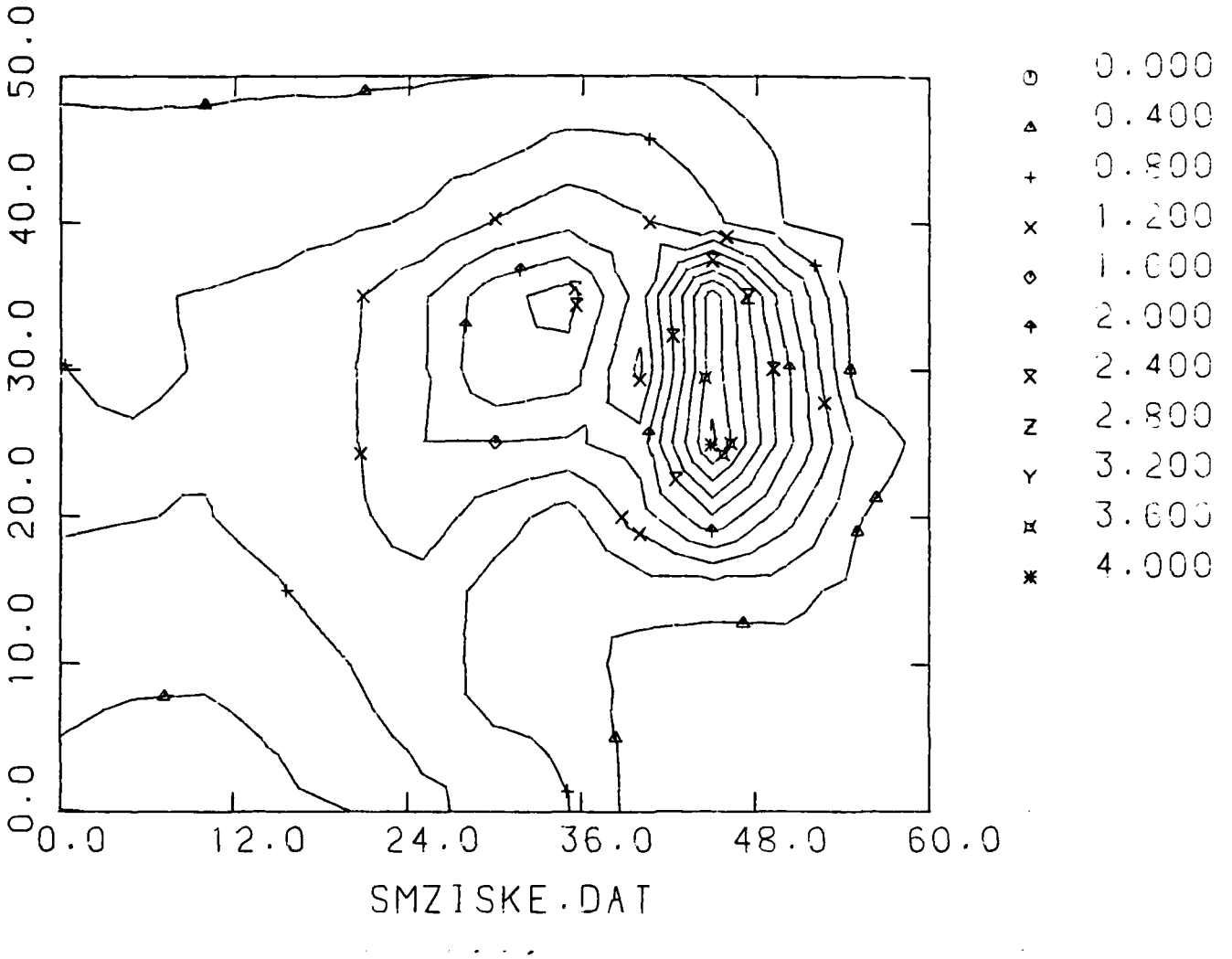

FIG. 39C - ISOLINES OF DCFKE DOWNSTREAM OF H = 0, α_R = 0 THIN STRAKE

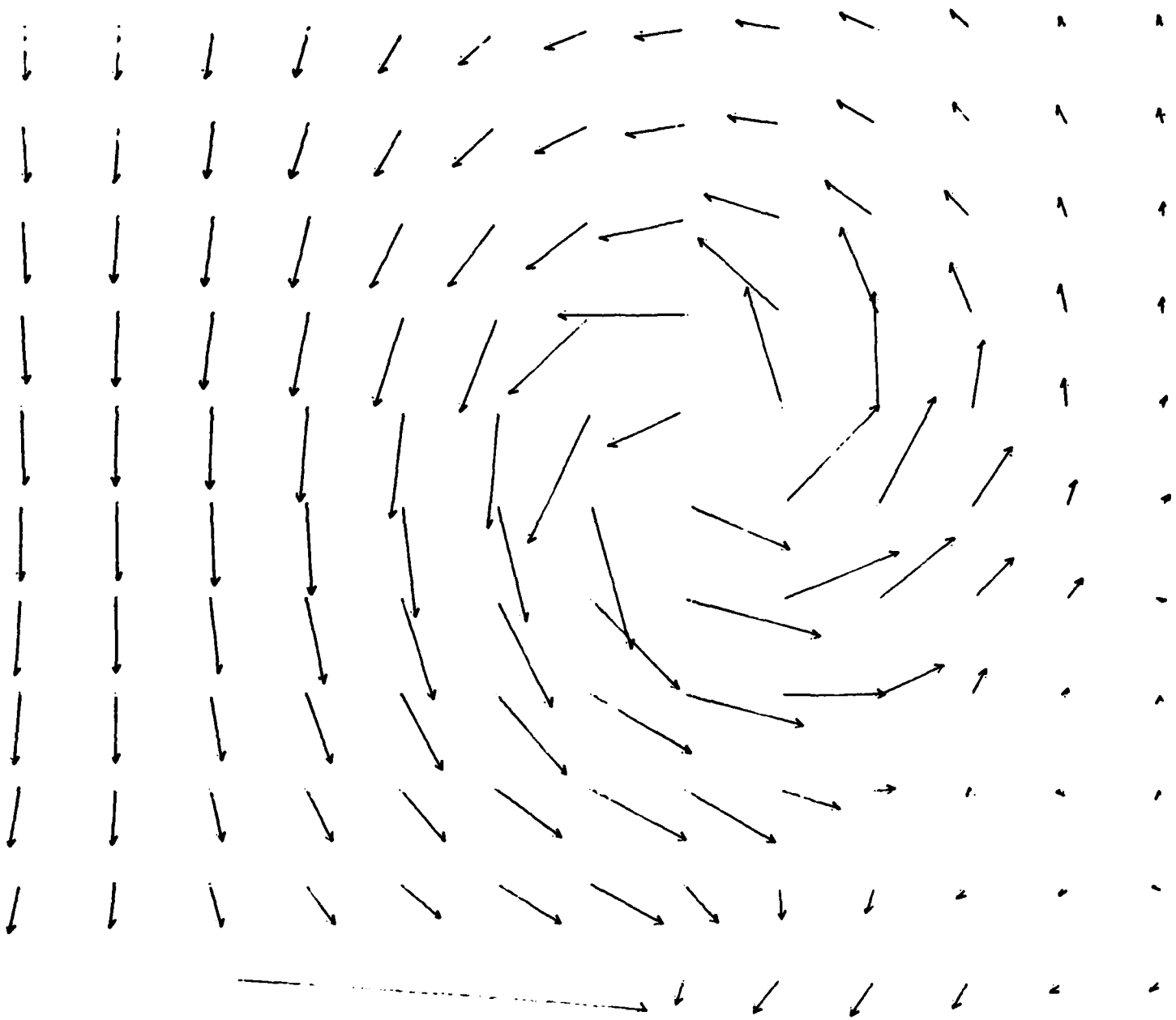

FIG. 40A

RESULTANT FLOW FIELD
DOWNSTREAM OF STRAKE OF
RATIO = 0
AT POSITIVE INCIDENCE
W.R.T. INCOMING VORTEX
α_R = 15 THIN STRAKE

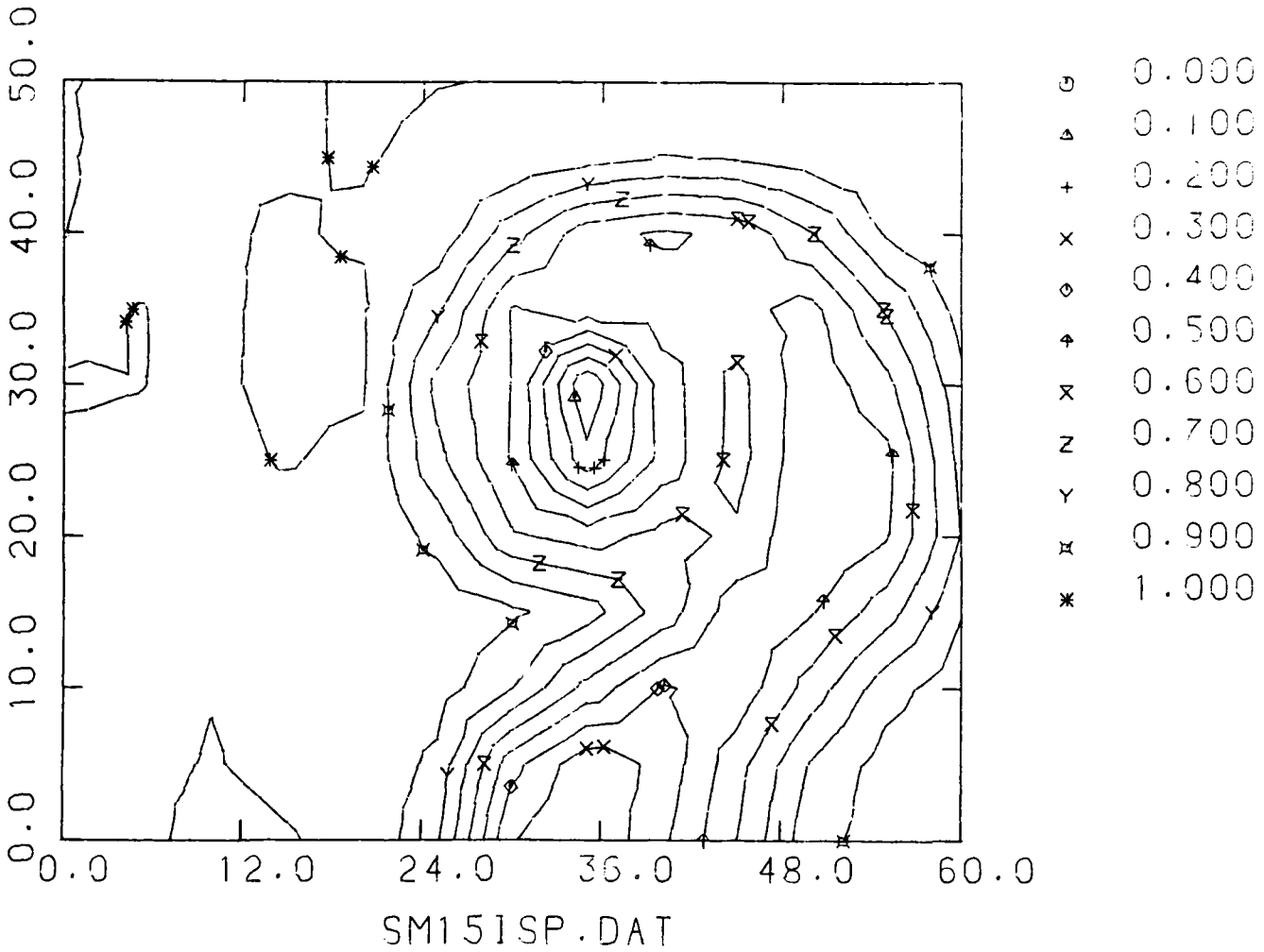

FIG. 40B - ISOLINES OF P_R DOWNSTREAM OF H = 0, α_R = 15 THIN STRAKE

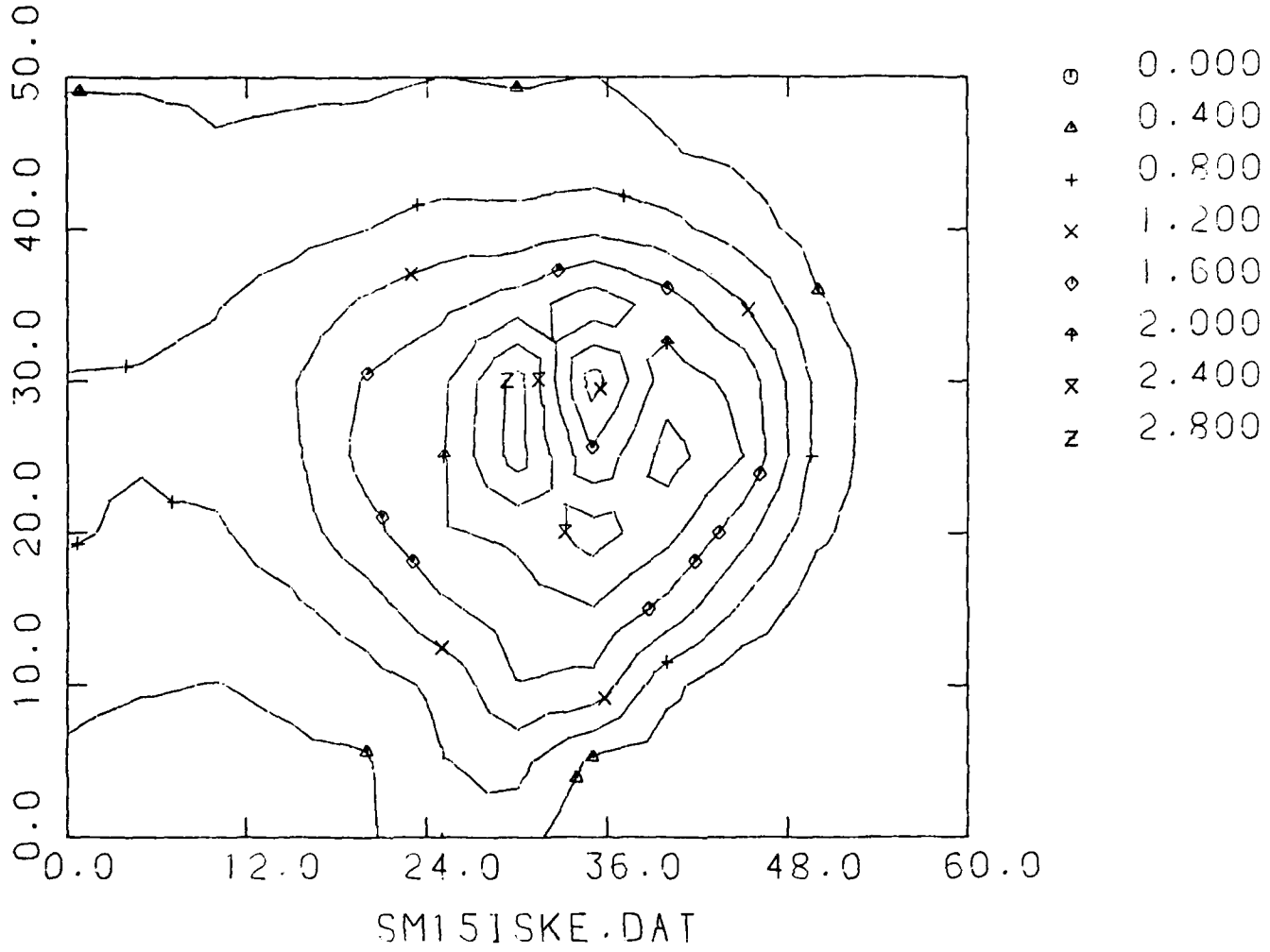

FIG. 40C - ISOLINES OF DCFKE DOWNSTREAM OF H = 0, α_R = 15 THIN STRAKE

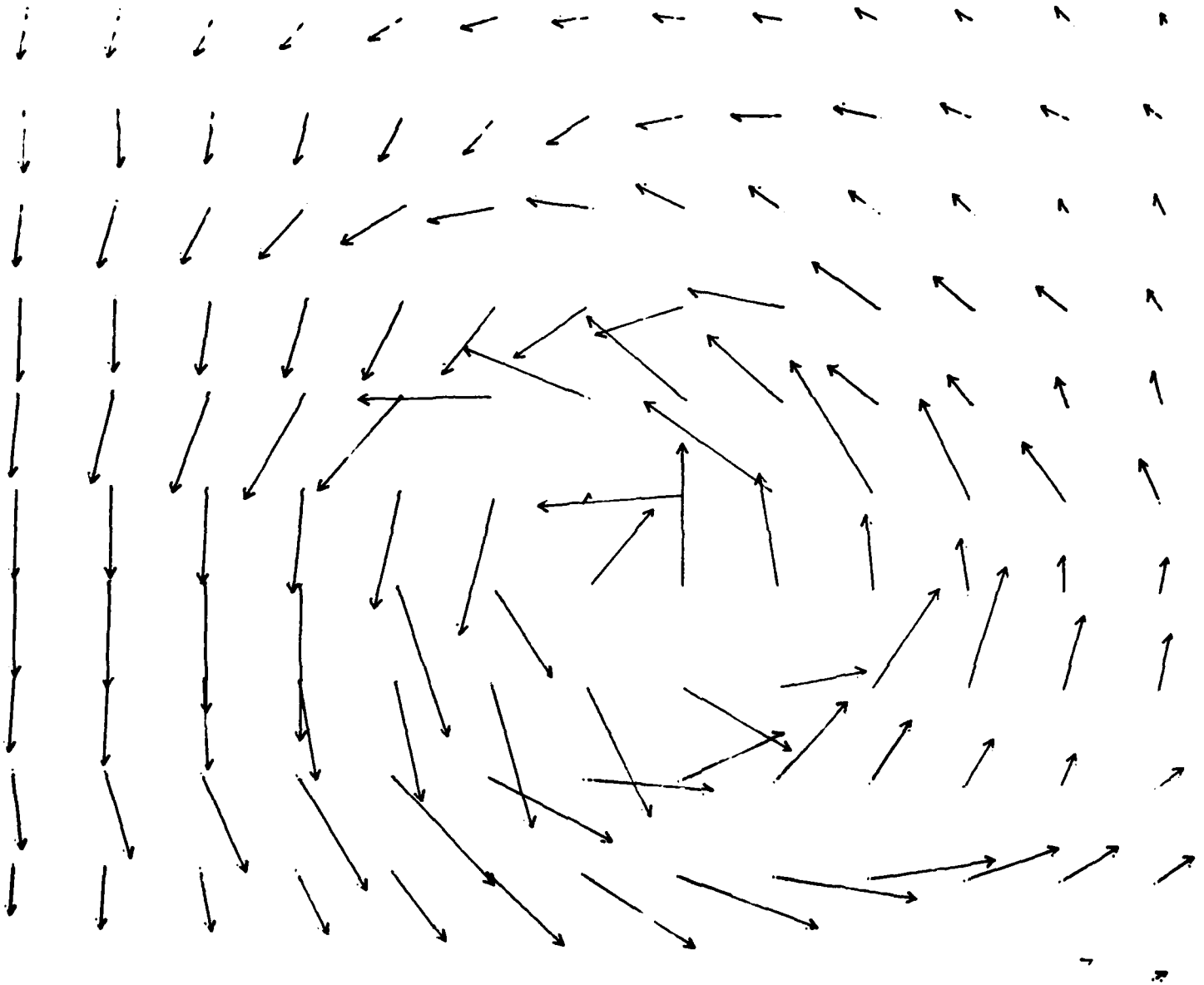

FIG. 41A

RESULTANT VORTEX WHEN STRAKE OF RATIO

α_R = -15, H = 0.5 IS PLACE

AT A NEGATIVE INCIDENCE

(THIN STRAKE)

FIG. 41B

TOTAL PRESSURE / DYNAMIC PRESSURE RATIO FOR A FLOW FIELD DOWNSTREAM OF A STRAKE OF RATIO H = 0.50 AT NEGATIVE ANGLE OF ATTACK. (α_R = - 15)
(THIN STRAKE)

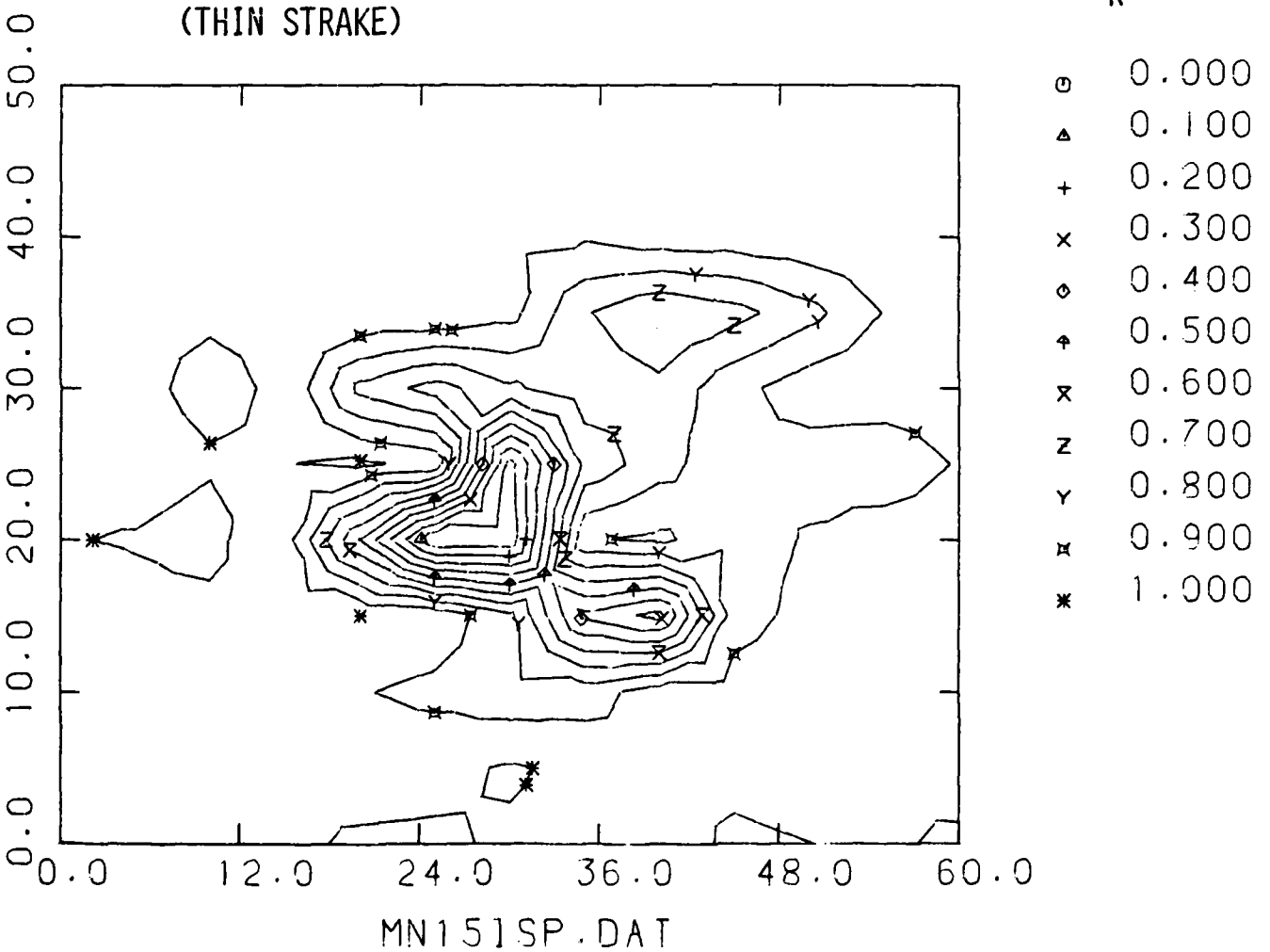

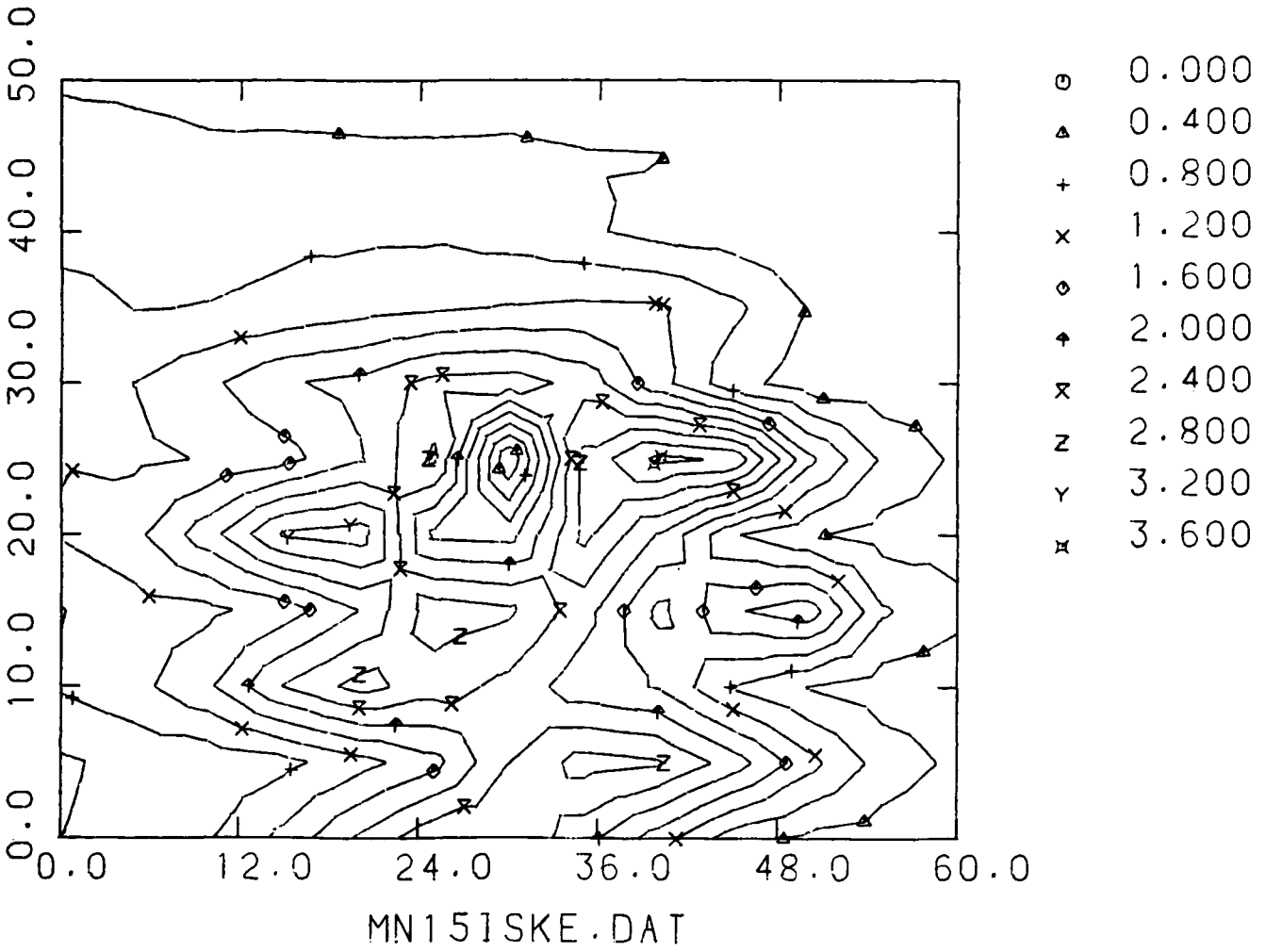

FIG. 41C - ISOLINES OF DCFKE DOWNSTREAM OF H = 0.5, $\alpha_R = -15$
THIN STRAKE

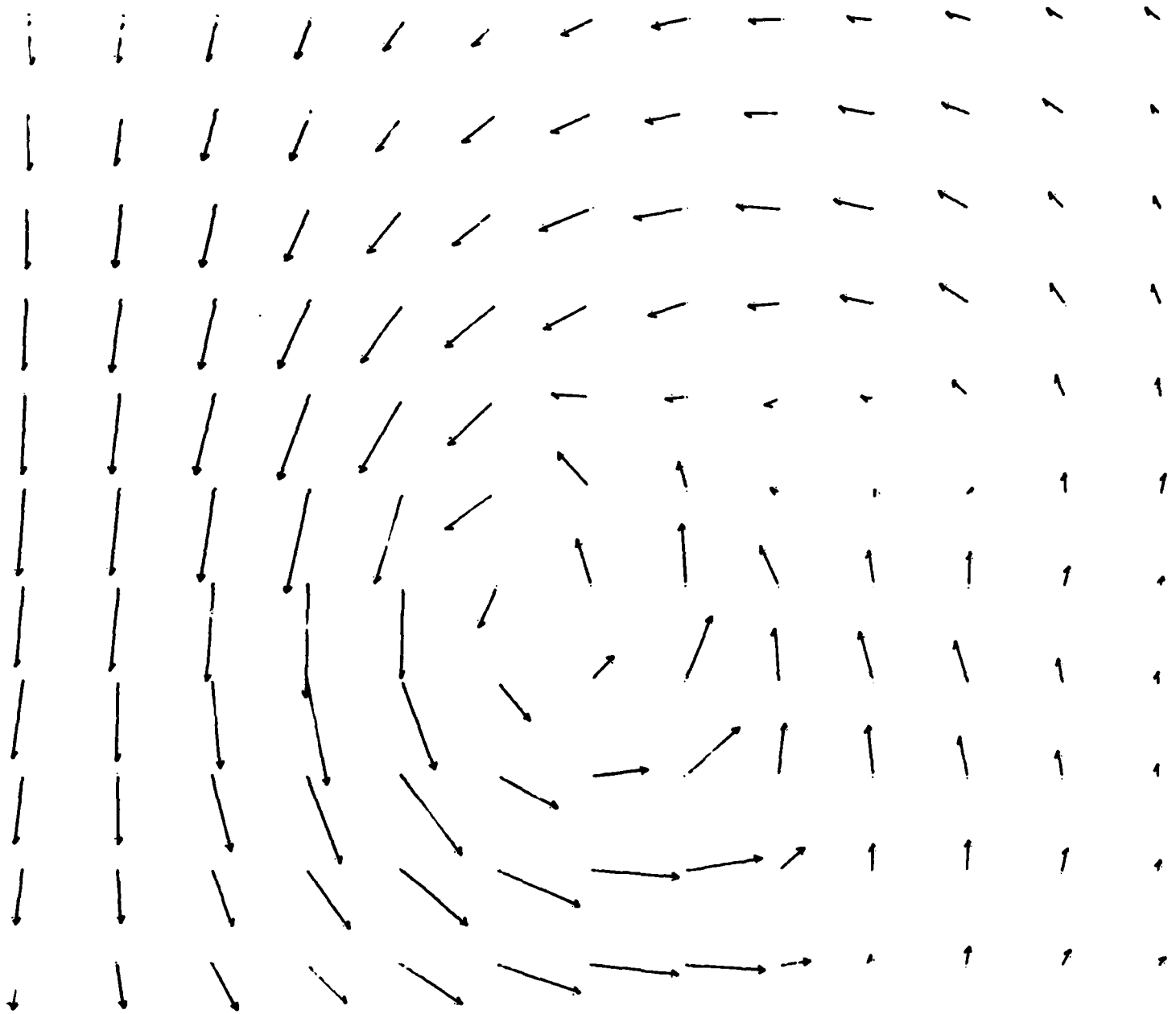

FIG. 42A

" STREAMLINING" EFFECT PRODUCED BY PLACING A STRAKE OF RATIO

H = 0.5

IN VORTICAL FLOW AT 0 INCIDENCE

FIG. 42B

ISOLINES OF $\frac{\text{TOTAL LOCAL PRESSURE}}{\text{DYNAMIC PRESSURE}}$ WHEN STRAKE OF H = 0.5

AT ZERO INCIDENCE ALONG THE VORTEX PATH

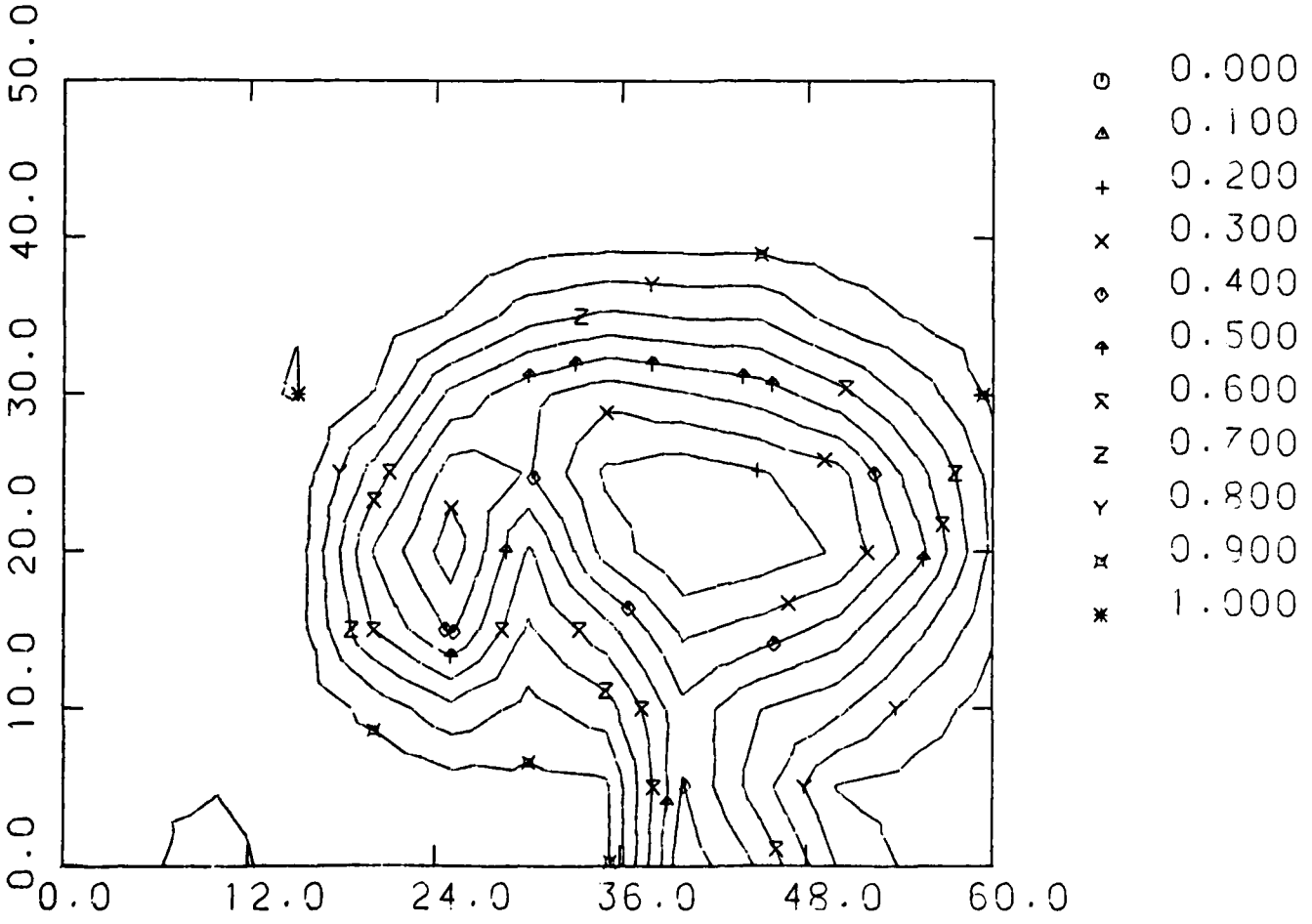

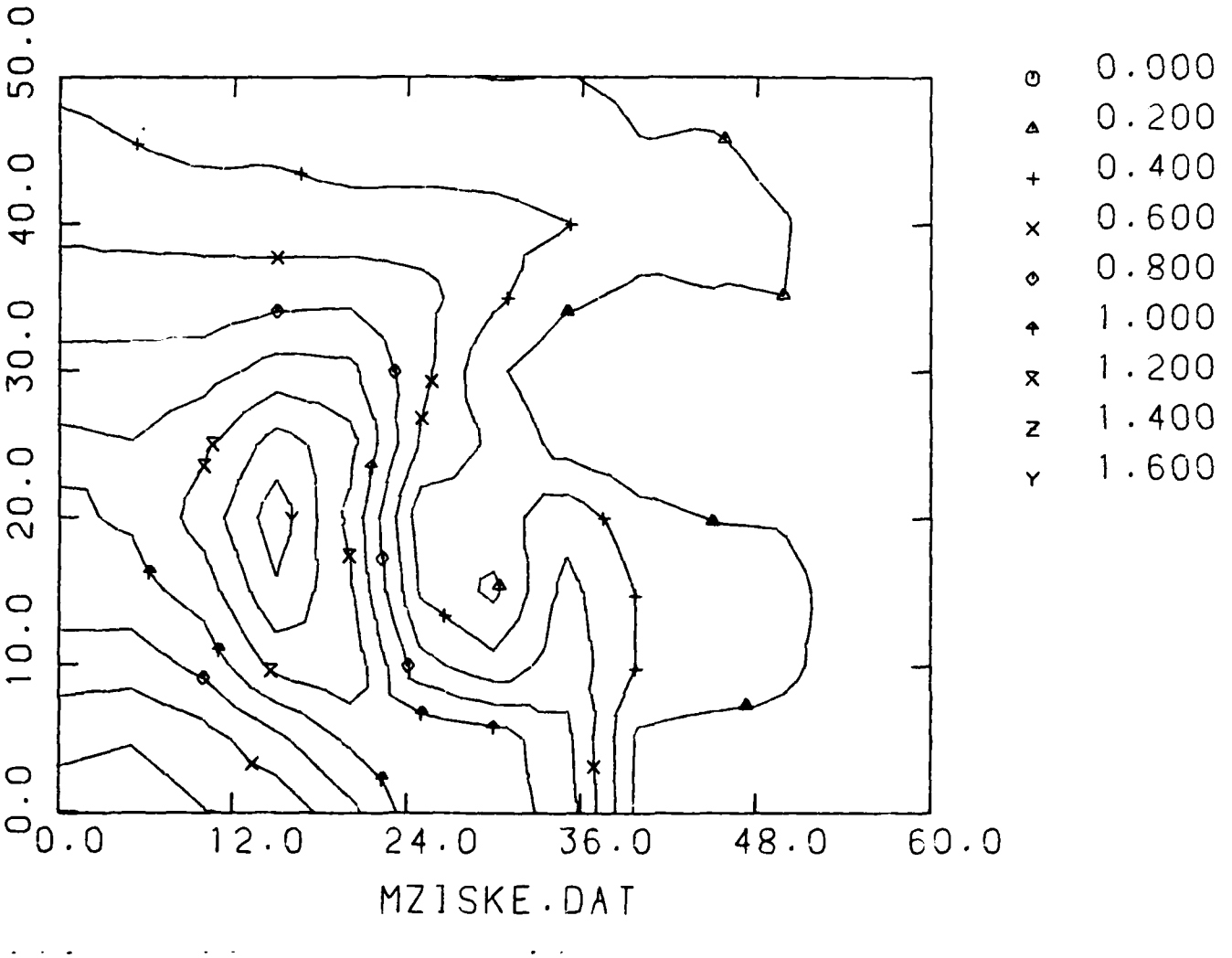

FIG. 42C - ISOLINES OF DCFKE DOWNSTREAM OF H = 0.5, α_R = 0 THIN STRAKE

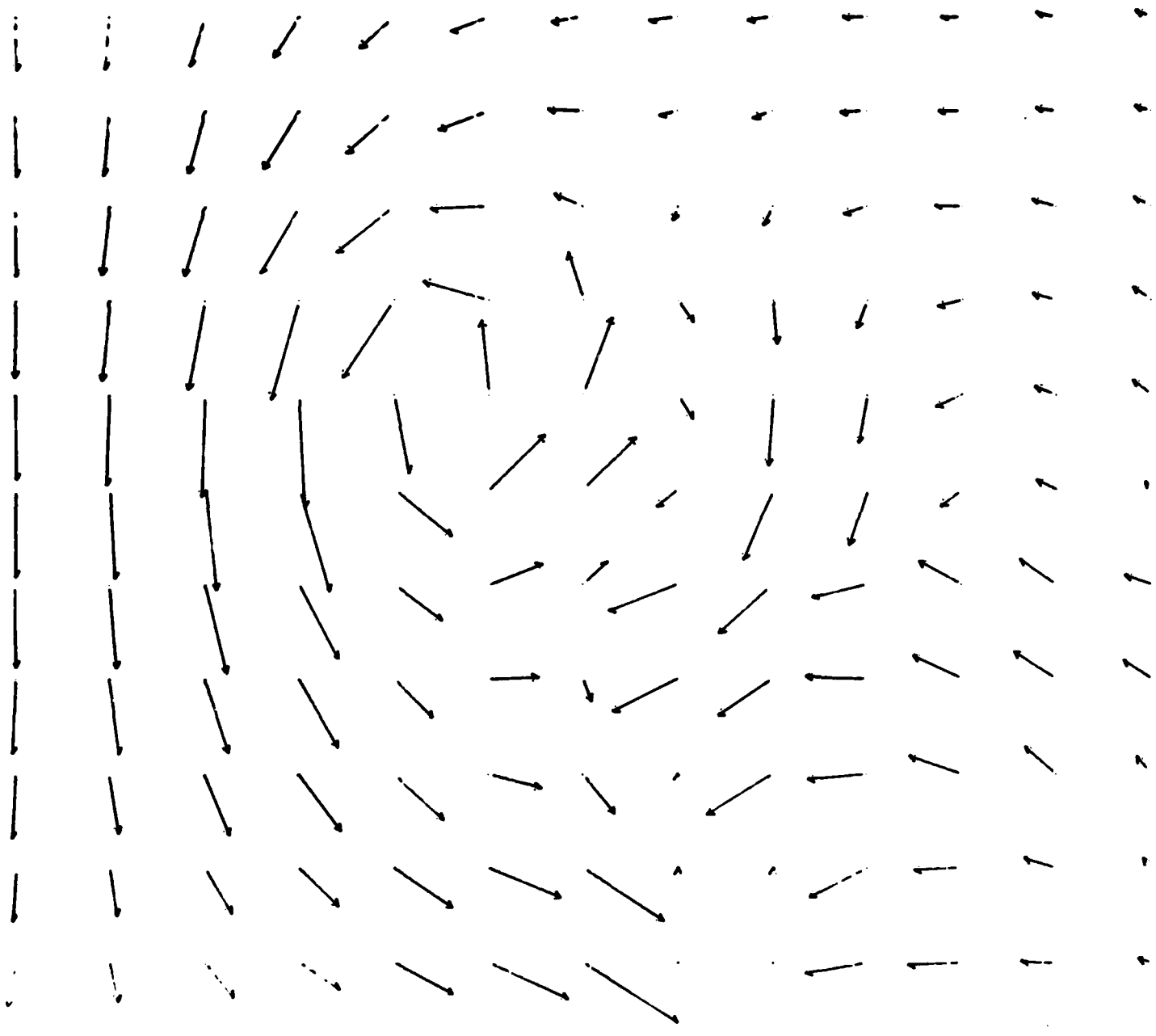

FIG. 43A

" DOUBLE VORTEX" OF OPPOSITE MAGNITUDE EFFECT CREATED BY LOCATING STRAKE OF

H = 0.5 RATIO AT

POSITIVE INCIDENCE. α_R = 15

NET RESULT IS A DECREASE IN CROSS FLOW KINETIC ENERGY

FIG. 43B

BIFURCATION OF VORTICAL FLOW WHEN A STRAKE OF RATIO $\eta = 0.5$

IS PLACED ALONG THE VORTEX CORE PATH AT $\alpha_R = 15°$

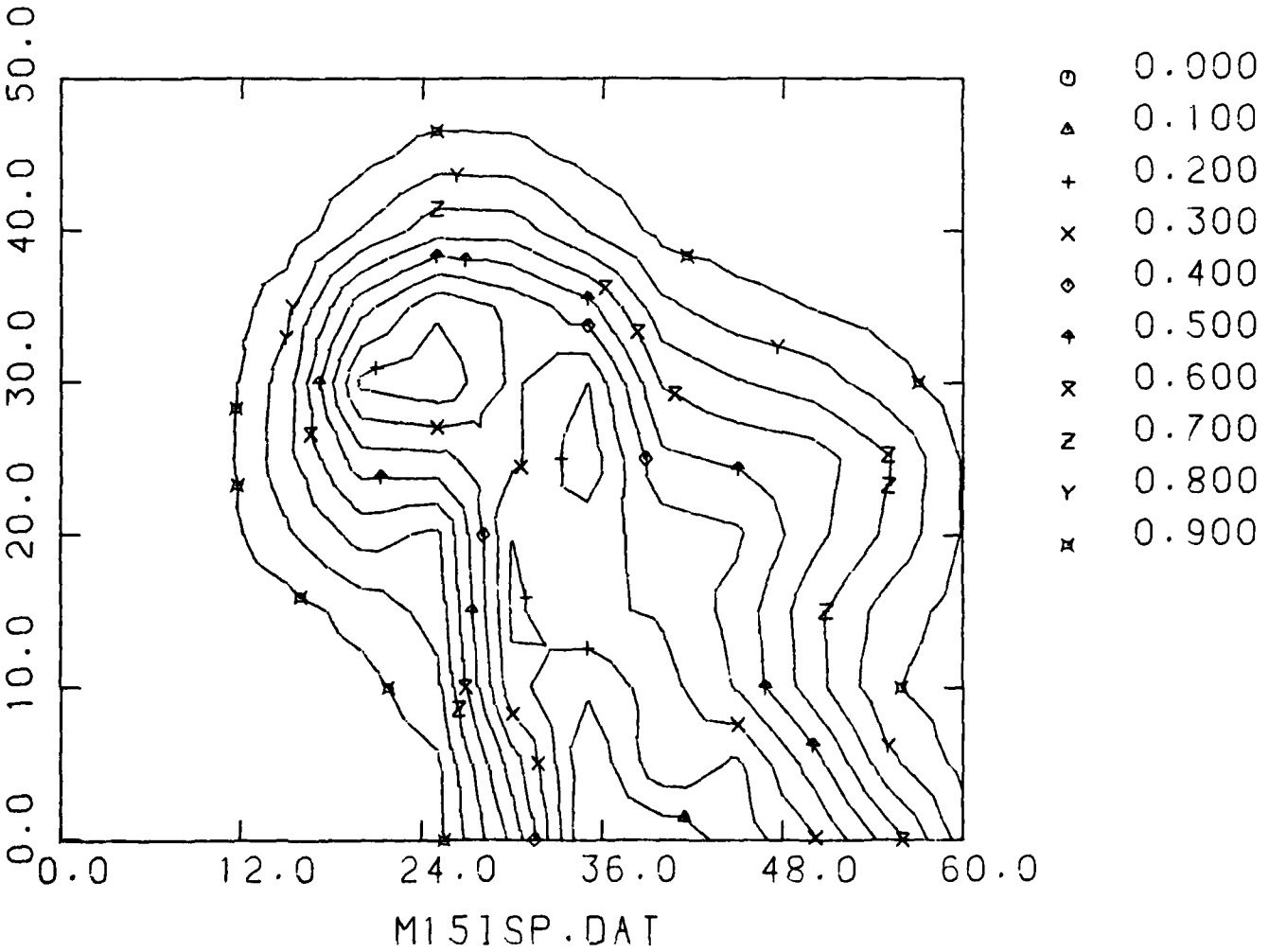

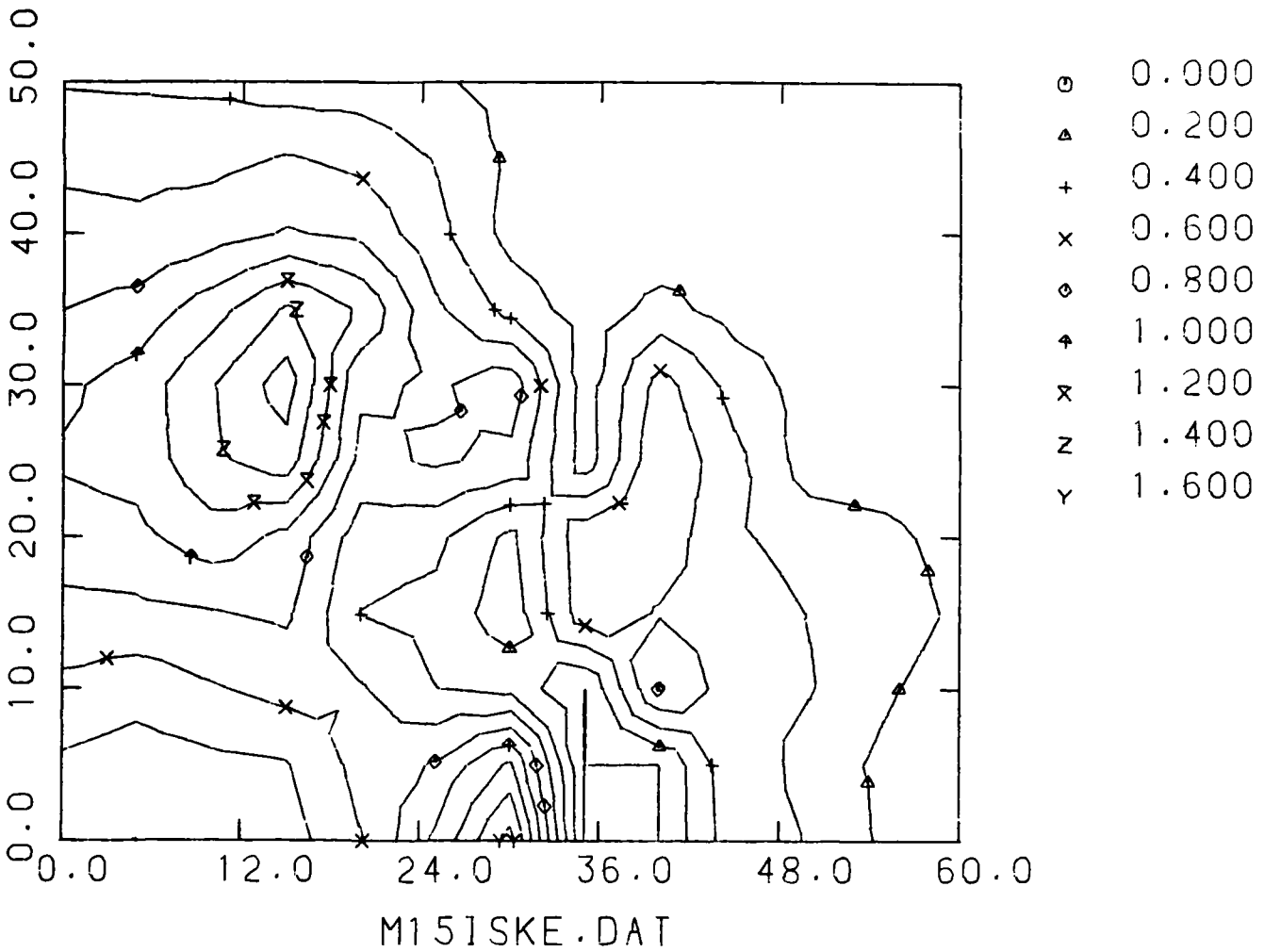

FIG. 43C - ISOLINES OF DCFKE DOWNSTREAM OF H = 0.5, α_R = 15 THIN STRAKE

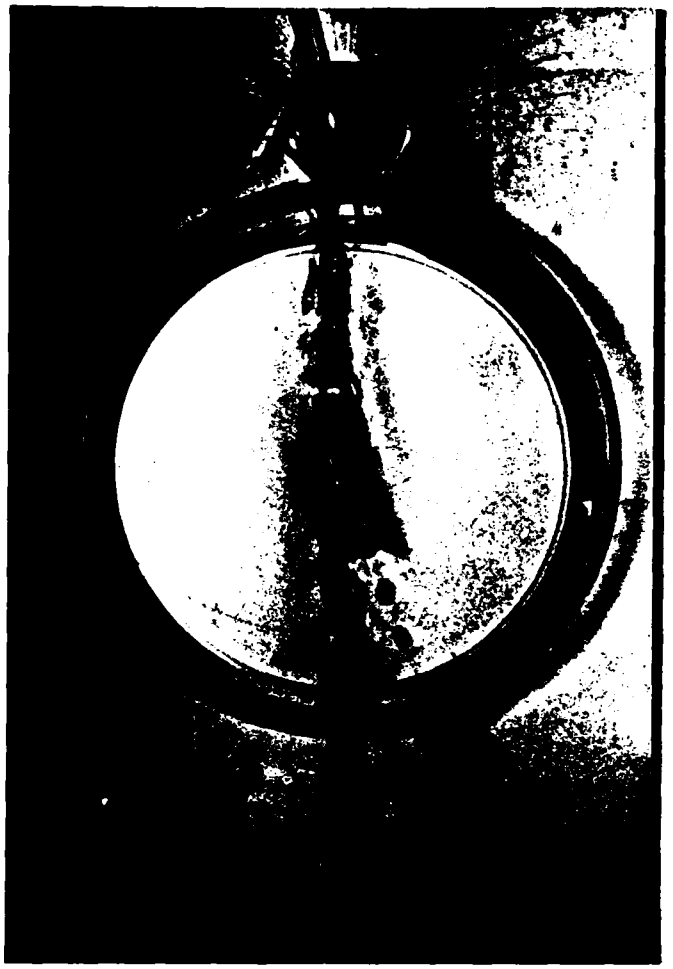

(A) $\alpha_R = -15$

(B) $\alpha_R = 0$

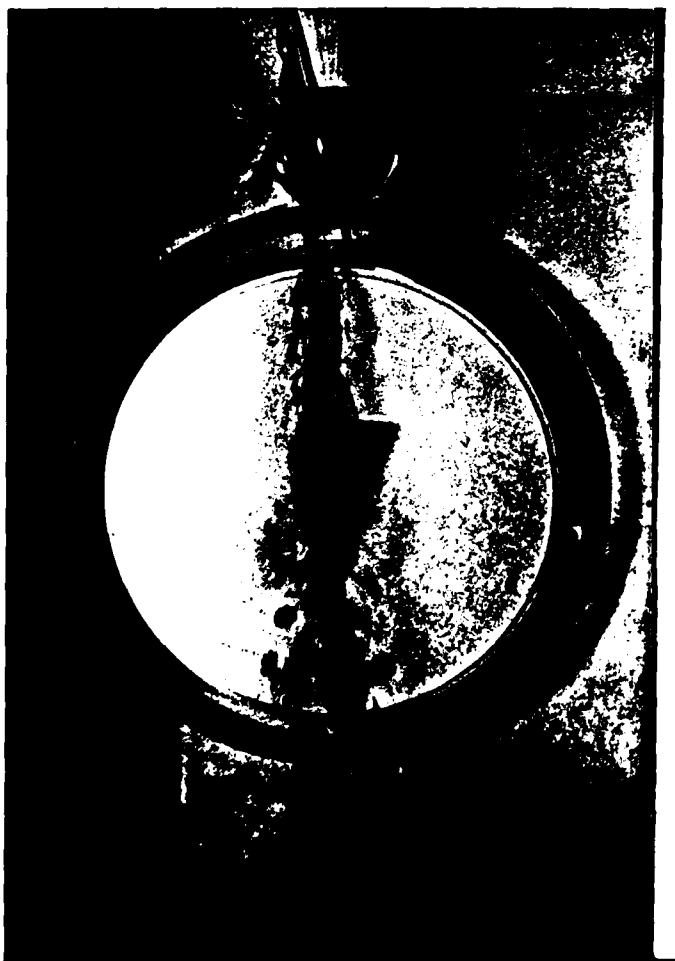

(C) $\alpha_R = 15$

FIG. 44 - WATER TUNNEL VISUALIZATION FOR H = 0.5 THIN STRAKE DOWNSTREAM OF DELTA WING

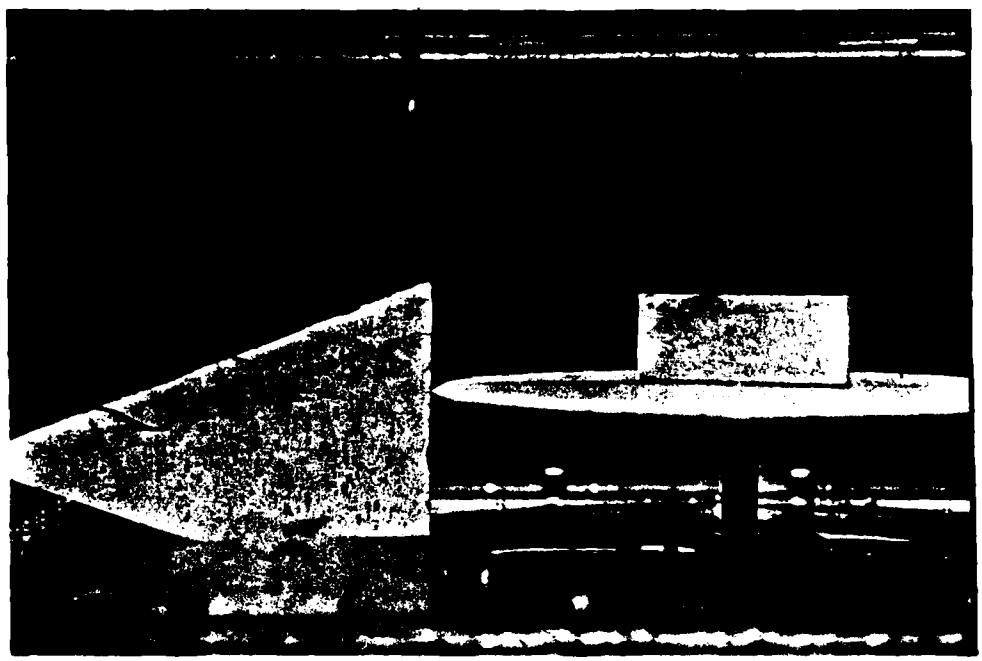

FIG. 44D - WATER TUNNEL VISUALIZATION (SIDE VIEW)
FOR H = 0.5, α_R = 15° THIN STRAKE

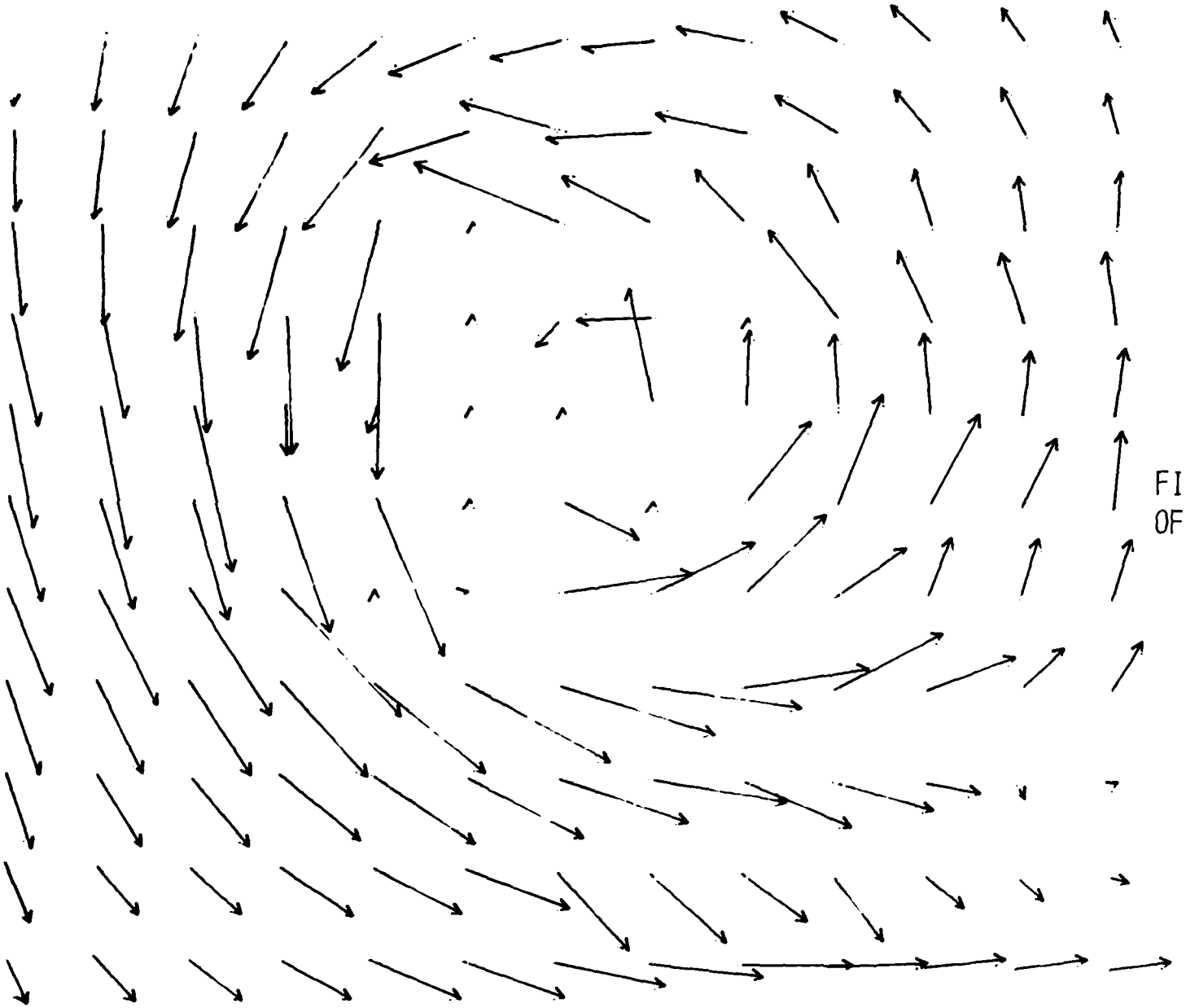

FIG. 45A - FLOW FIELD DOWNSTREAM OF H = 1.0, α_R = -15 THIN STRAKE

FIG. 45B

ISOLINES OF $\frac{\text{TOTAL LOCAL PRESSURE}}{\text{DYNAMIC PRESSURE}}$ DOWNSTREAM OF A STRAKE OF

RATIO $\frac{\text{H WAKE}}{\text{H STRAKE}} = 1.0$

STRAKE ANGLE OF ATTACK = - 15°

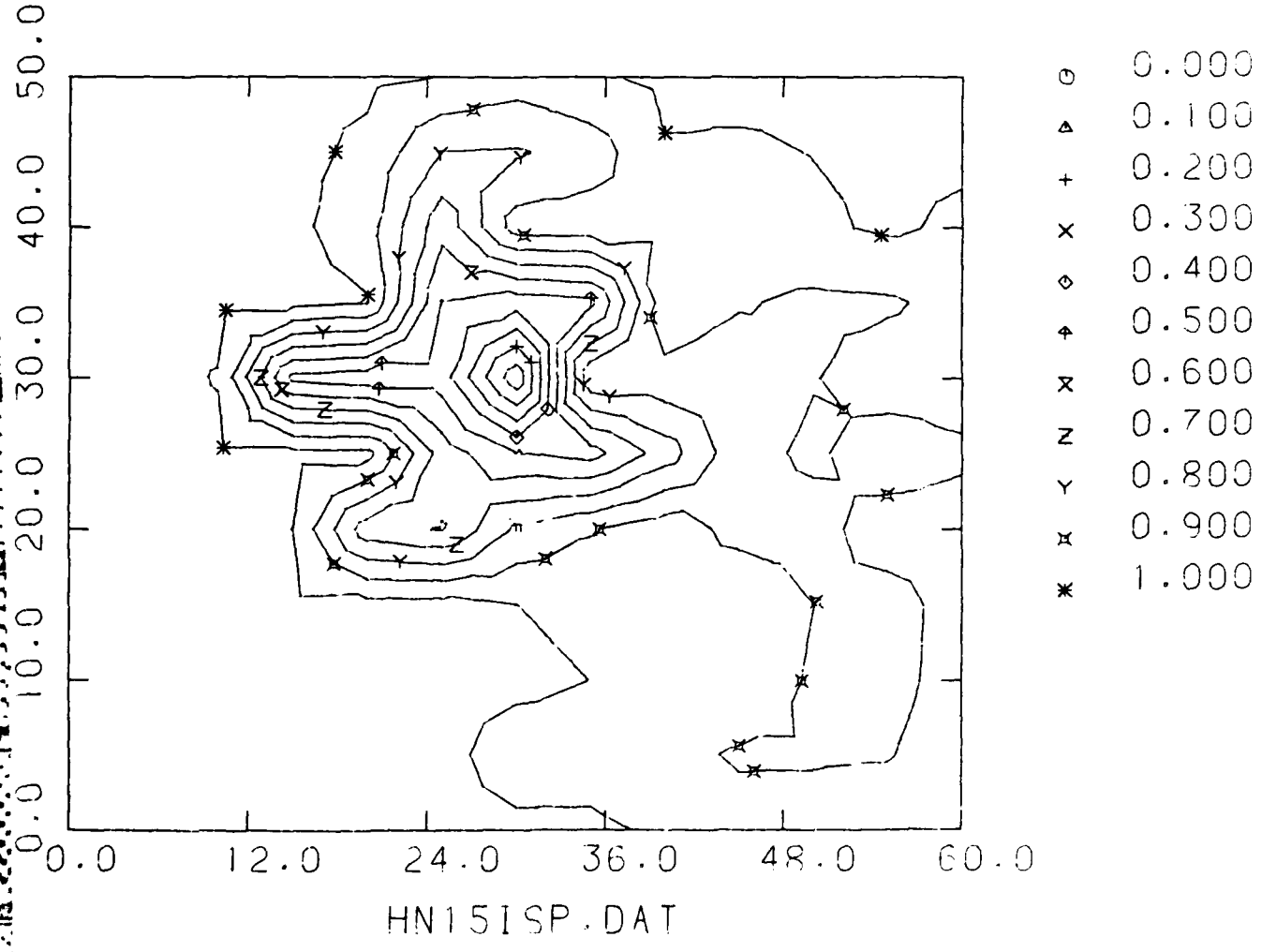

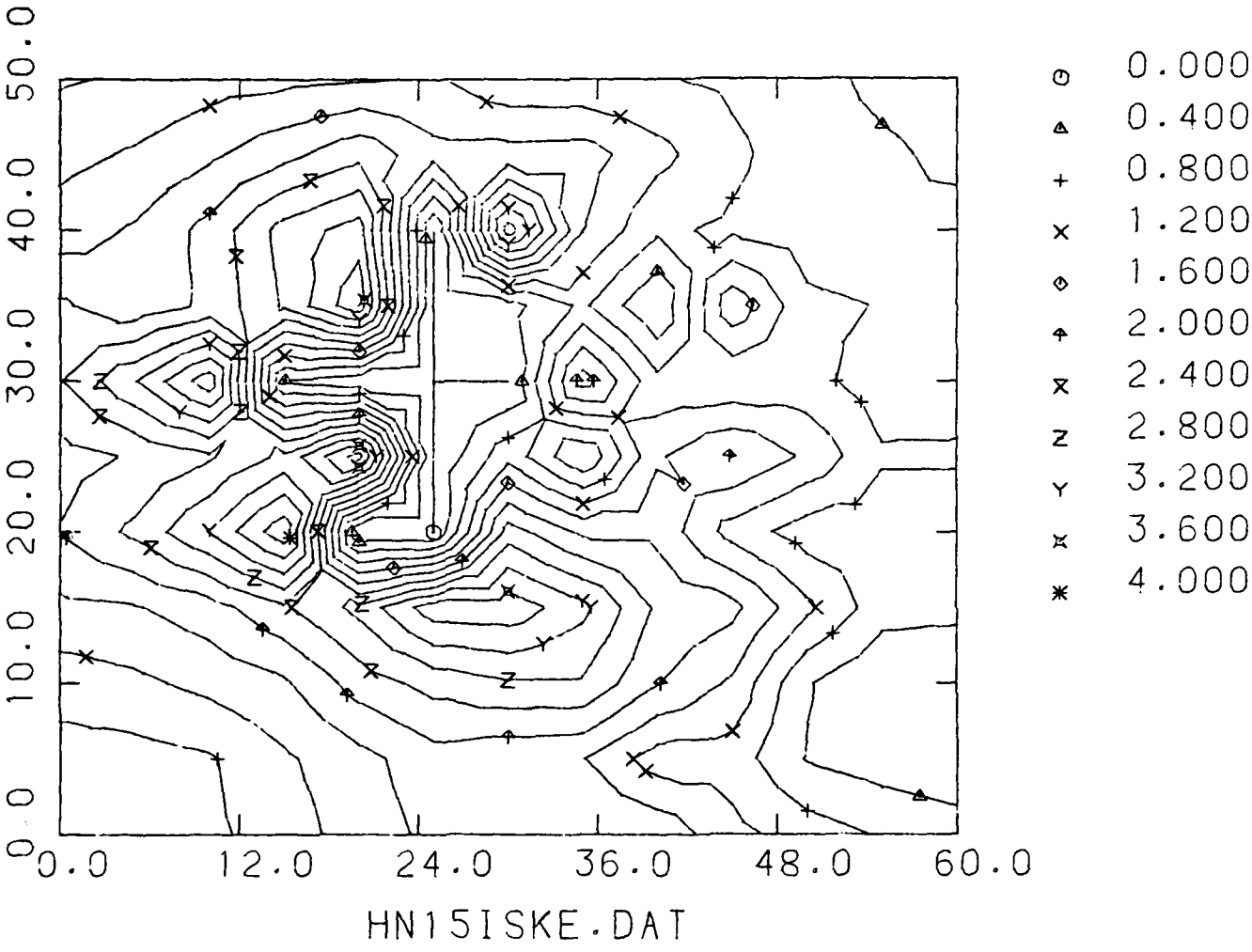

FIG. 45C - ISOLINES OF DCFKE DOWNSTREAM OF H = 1.0, α_R = -15 THIN STRAKE

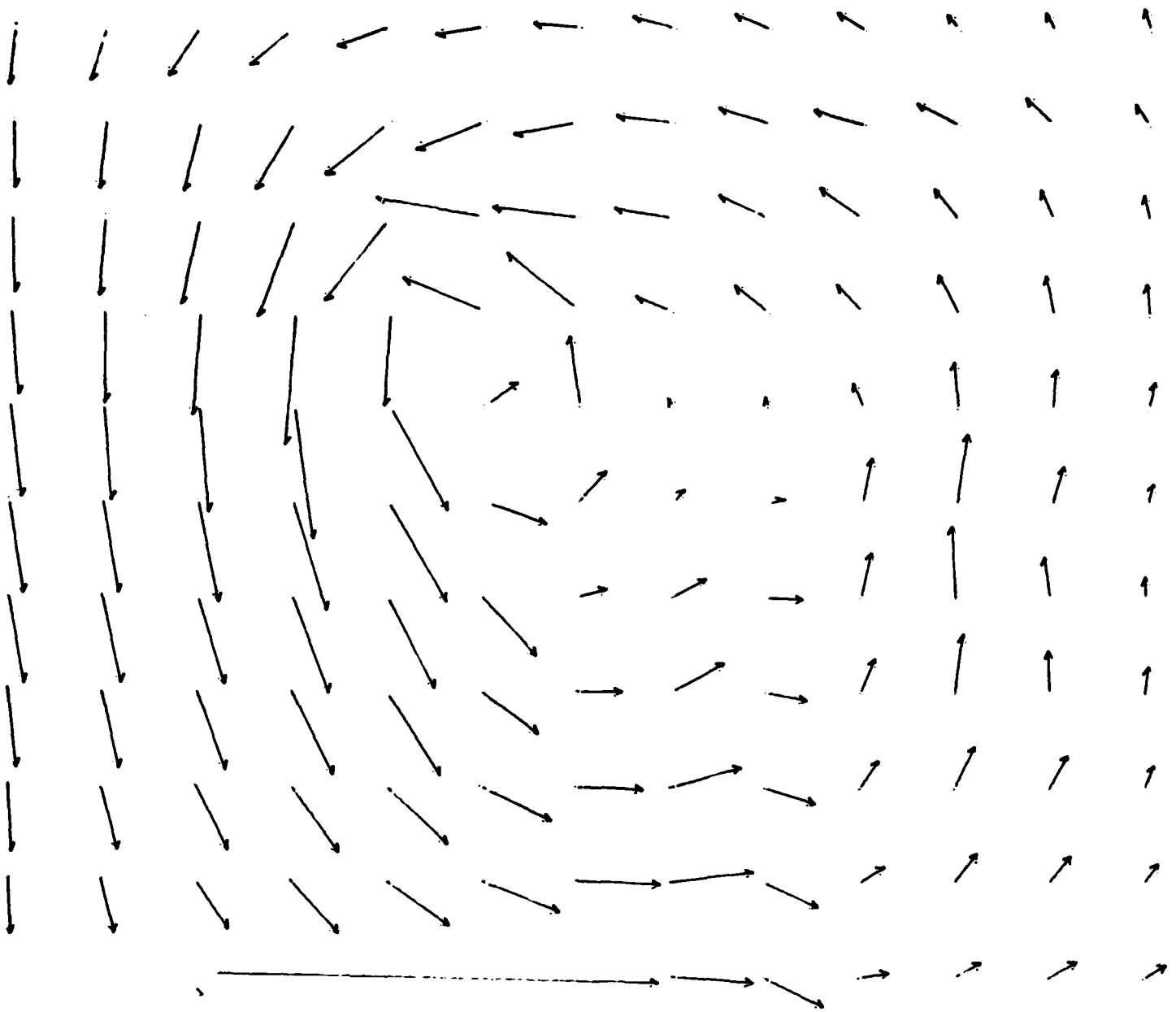

FIG. 46A– FLOW FIELD DOWNSTREAM OF $h = 1.0$, $\alpha_R = 0$ THIN STRAKE

FIG. 46B

BIFURCATION OF VORTICAL FLOW WHEN A STRAKE OF RATIO $H = I.0$

IS PLACED ALONG THE VORTEX CORE. ($\alpha_R = 0$)

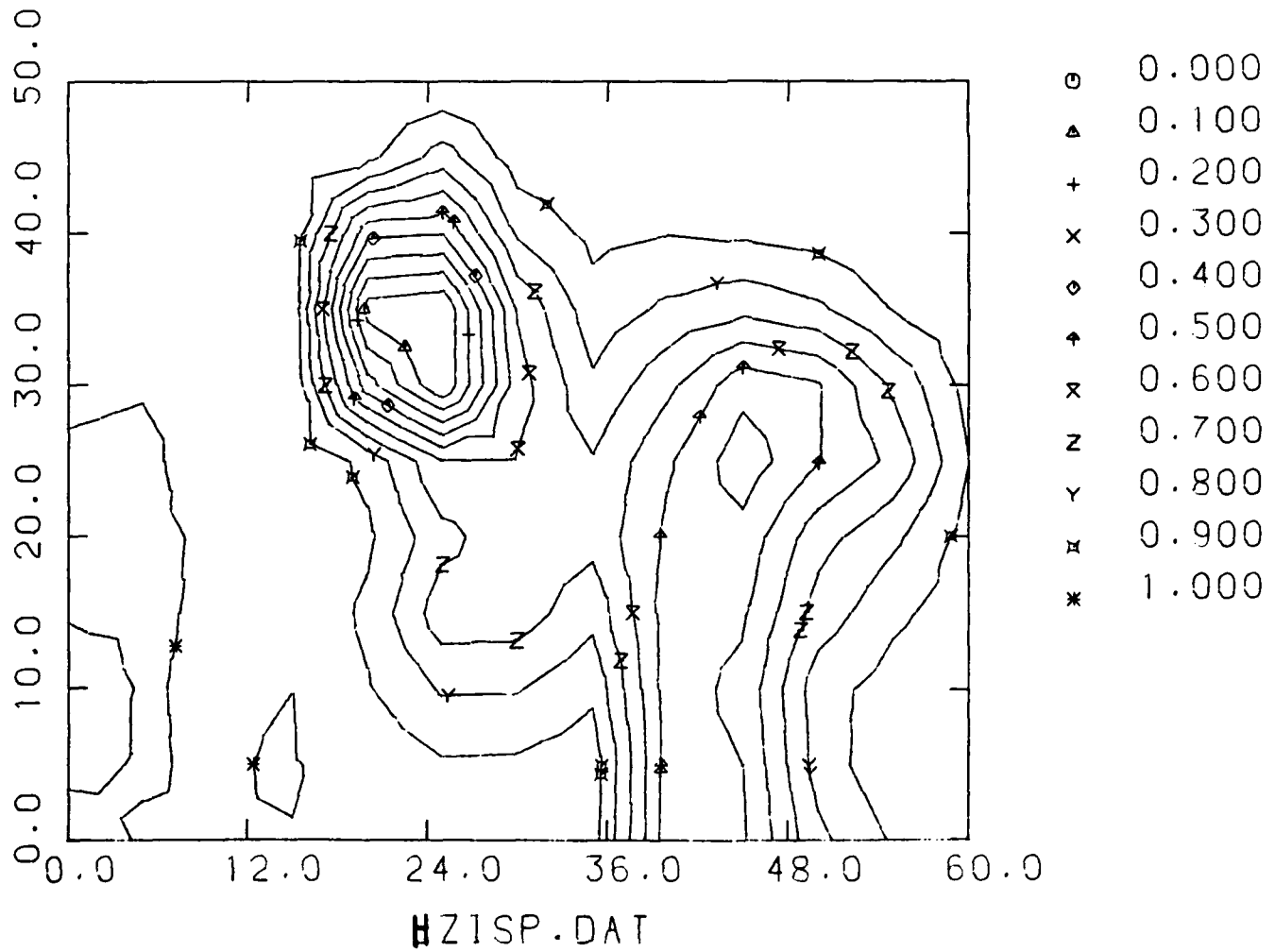

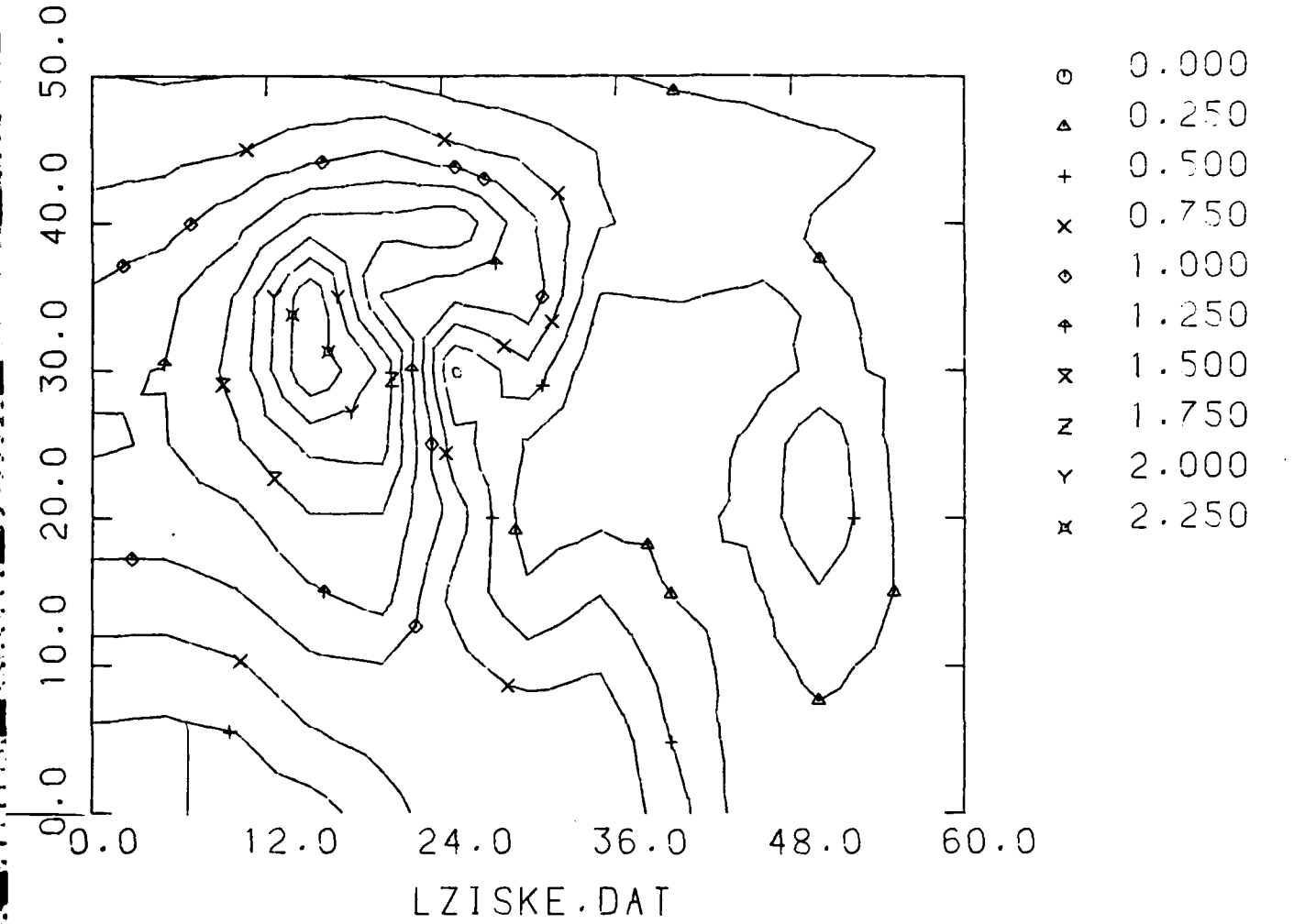

FIG. 46C - ISOLINES OF DCFKE DOWNSTREAM OF H = 1.0, α_R = 0 THIN STRAKE

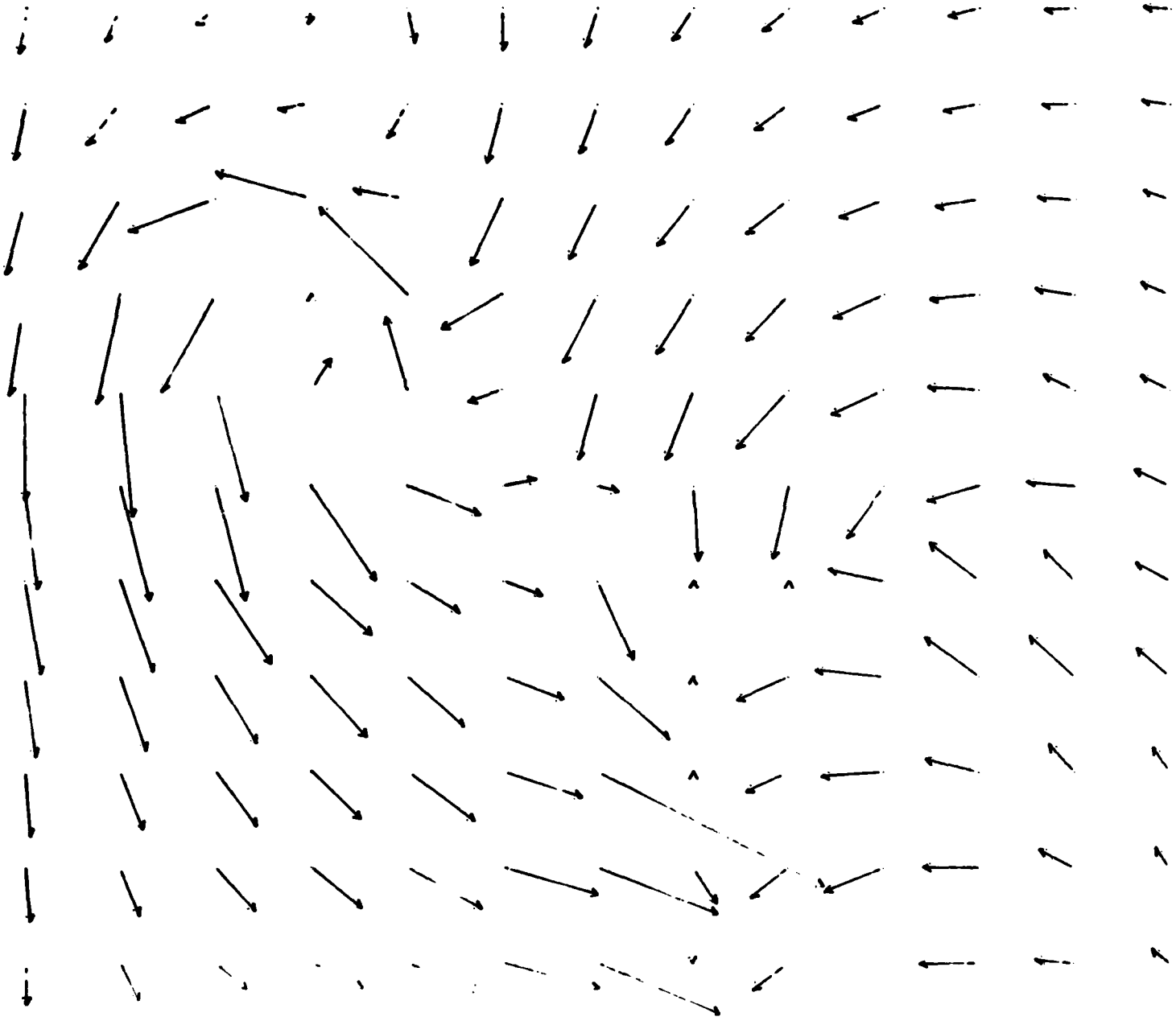

FIG. 47A

FLOW FIELD DOWNSTREAM OF STRAKE OF RATIO

H = I.0

AT POSITIVE INCIDENCE
α_R = 15 THIN STRAKE

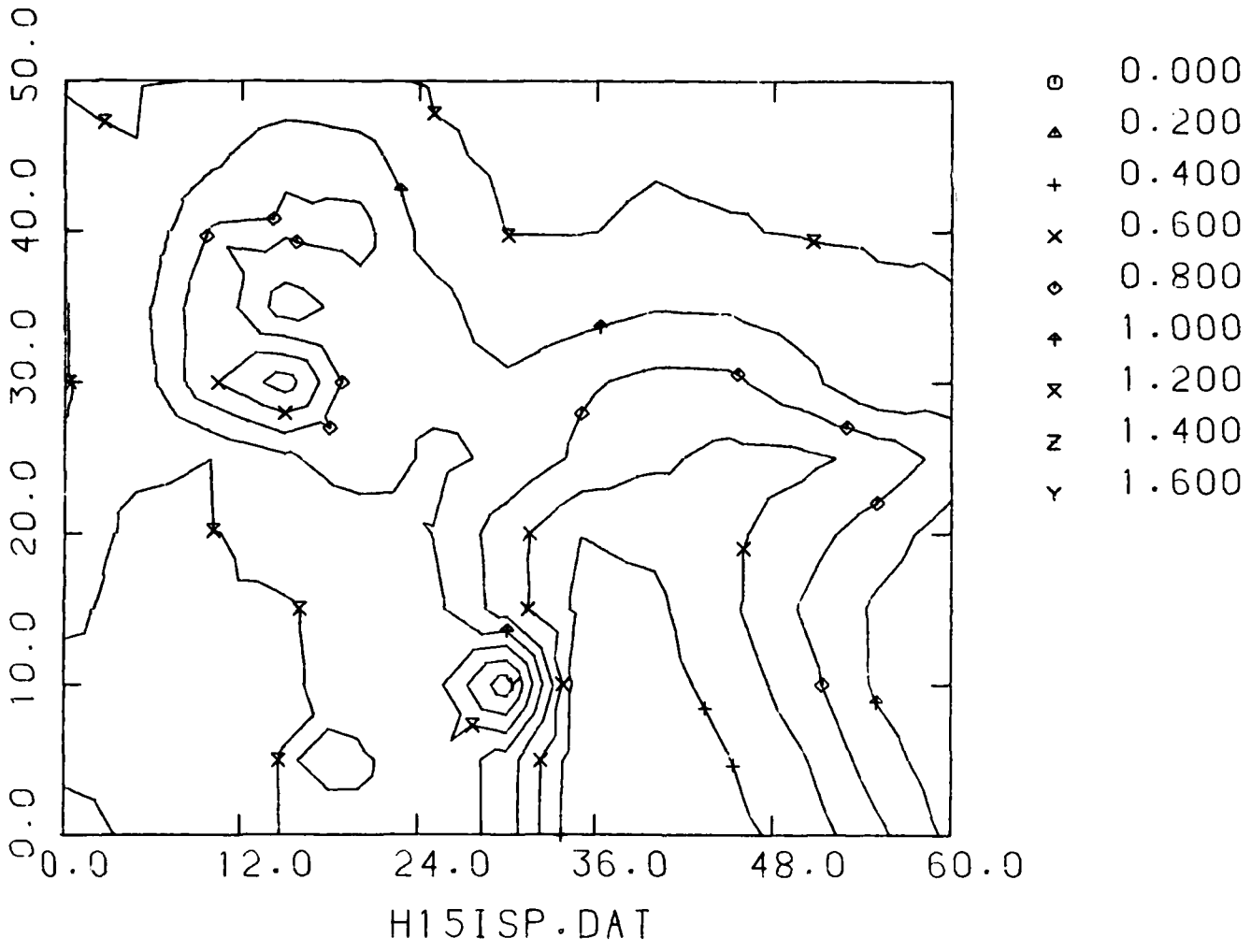

FIG. 47B - ISOLINES OF P_R DOWNSTREAM OF H = 1.0, α_R = 15 THIN STRAKE

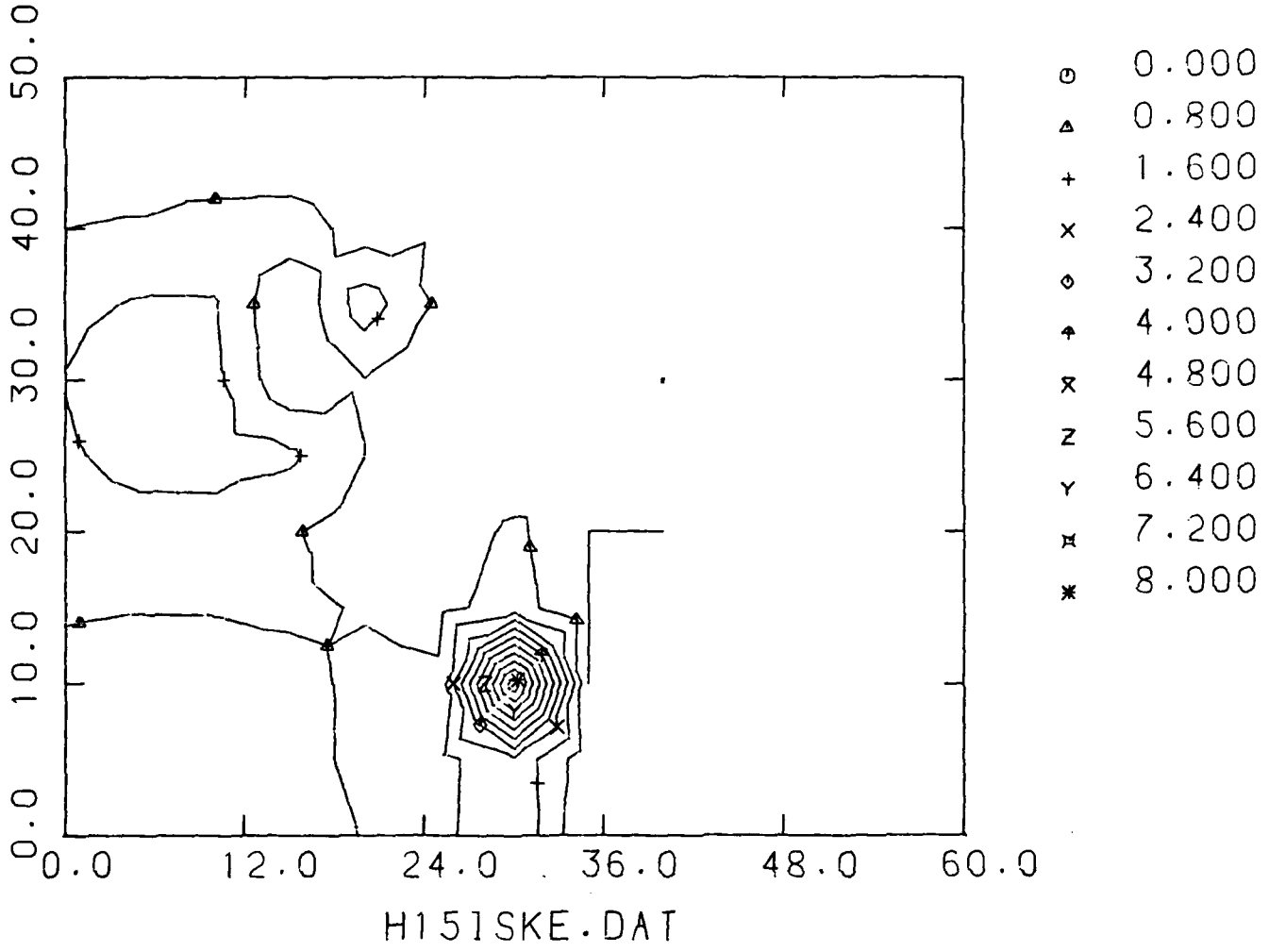

FIG. 47C - ISOLINES OF DCFKE DOWNSTREAM OF H = 1.0, α_R = 15 THIN STRAKE

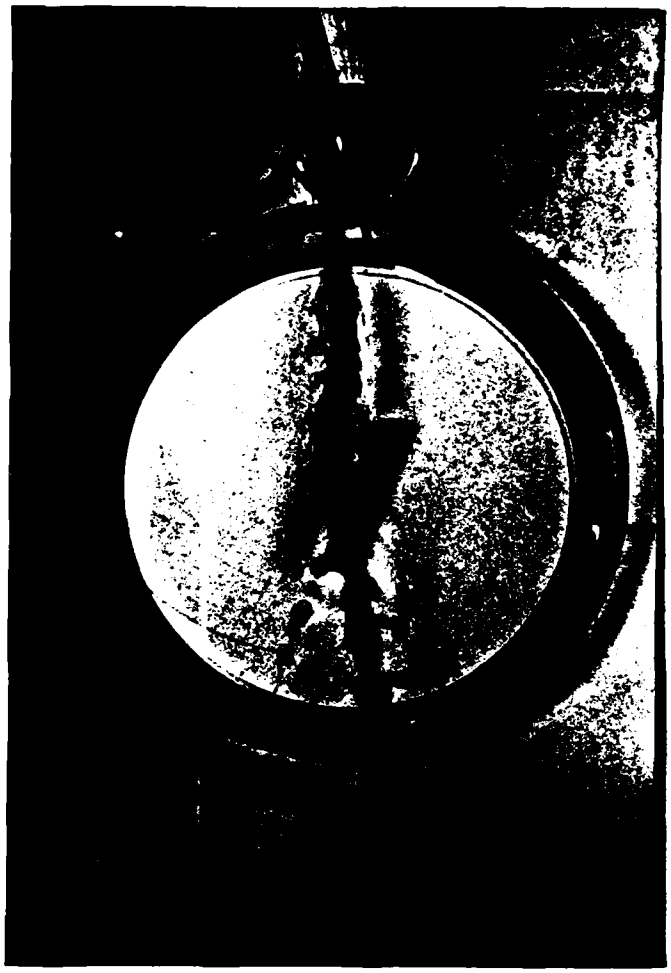

H = 0

H = 0.5

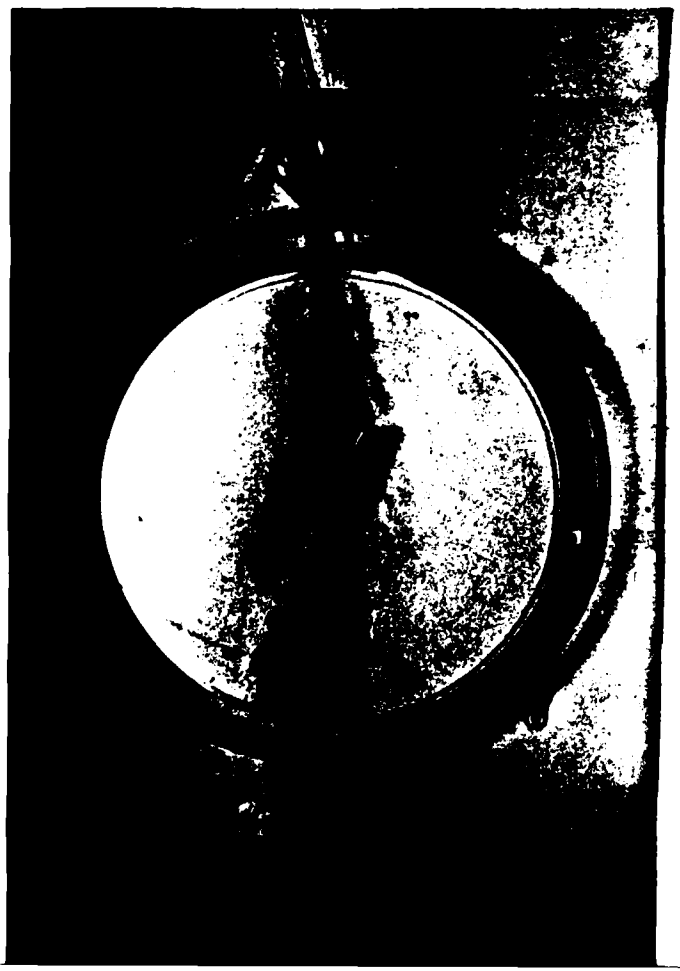

H = 1.0

FIG. 48 - WATER VISUALIZATION FOR THIN STRAKE AT α_R = 15 DOWNSTREAM OF DELTA WING

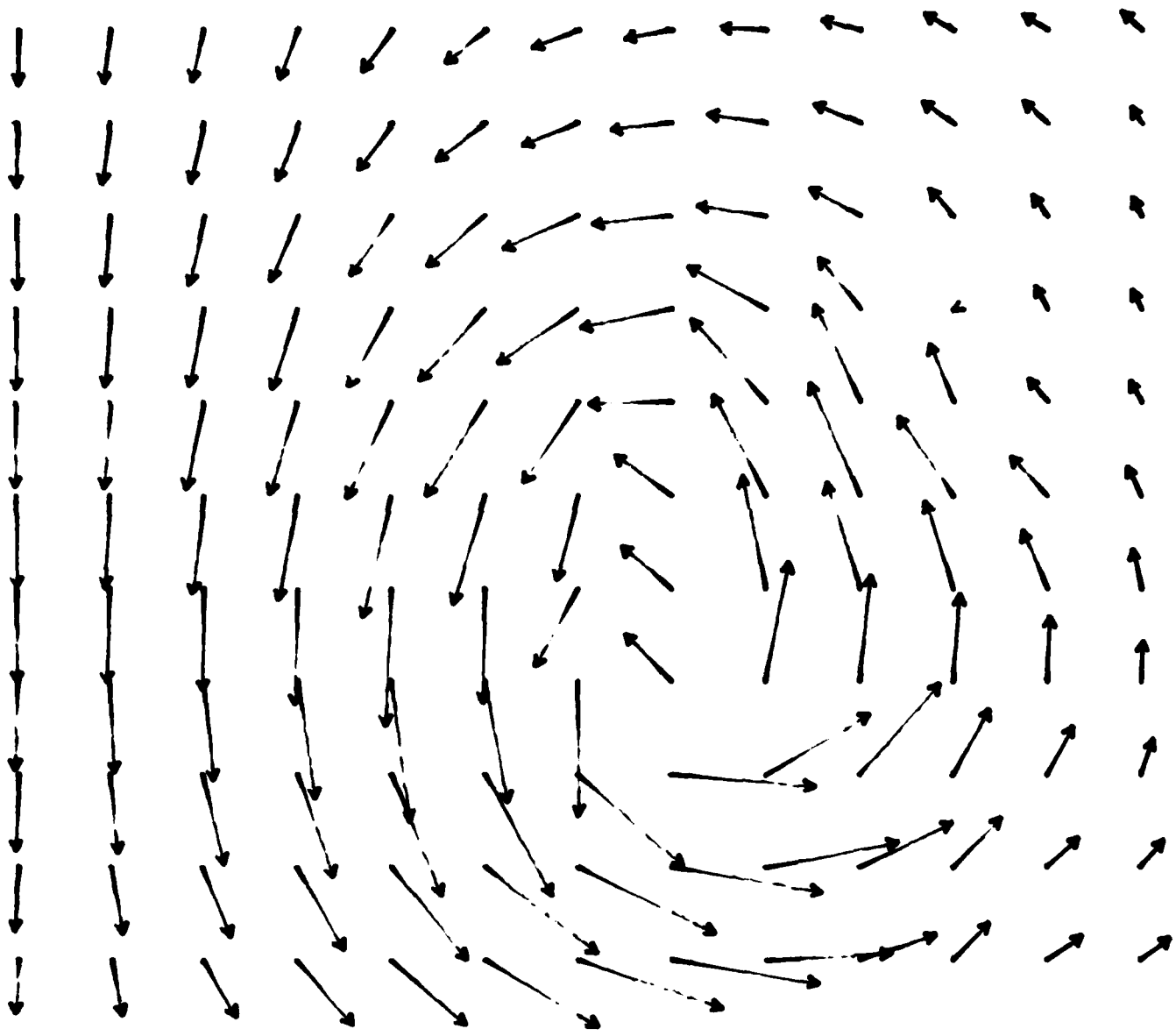

FIG. 49A - FLOW FIELD DOWNSTREAM OF H = 0.5, α_R = -15 THICK STRAKE

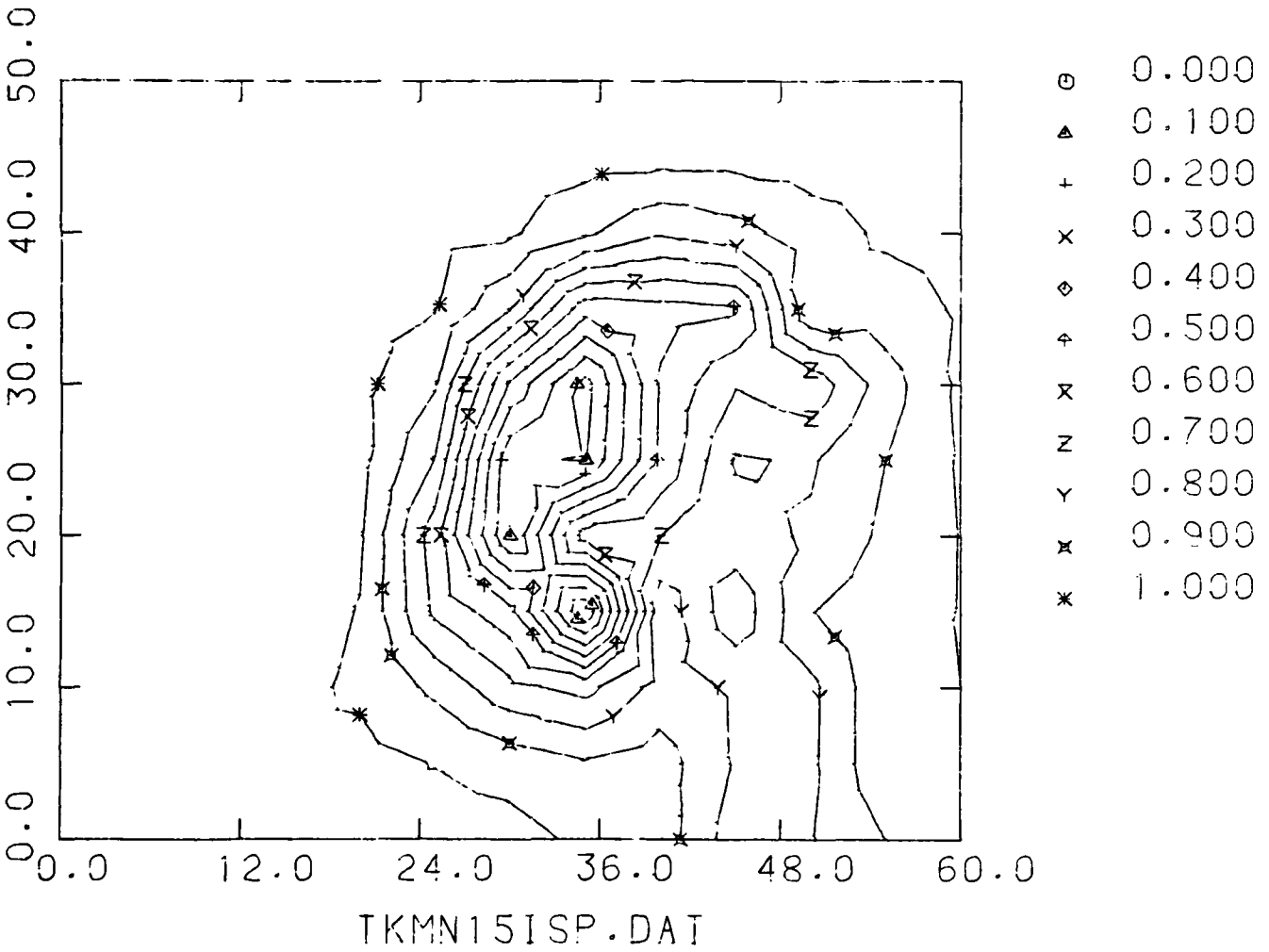

FIG. 49B – ISOLINES OF P_R DOWNSTREAM OF H = 0.5, α_R = -15 THICK STRAKE

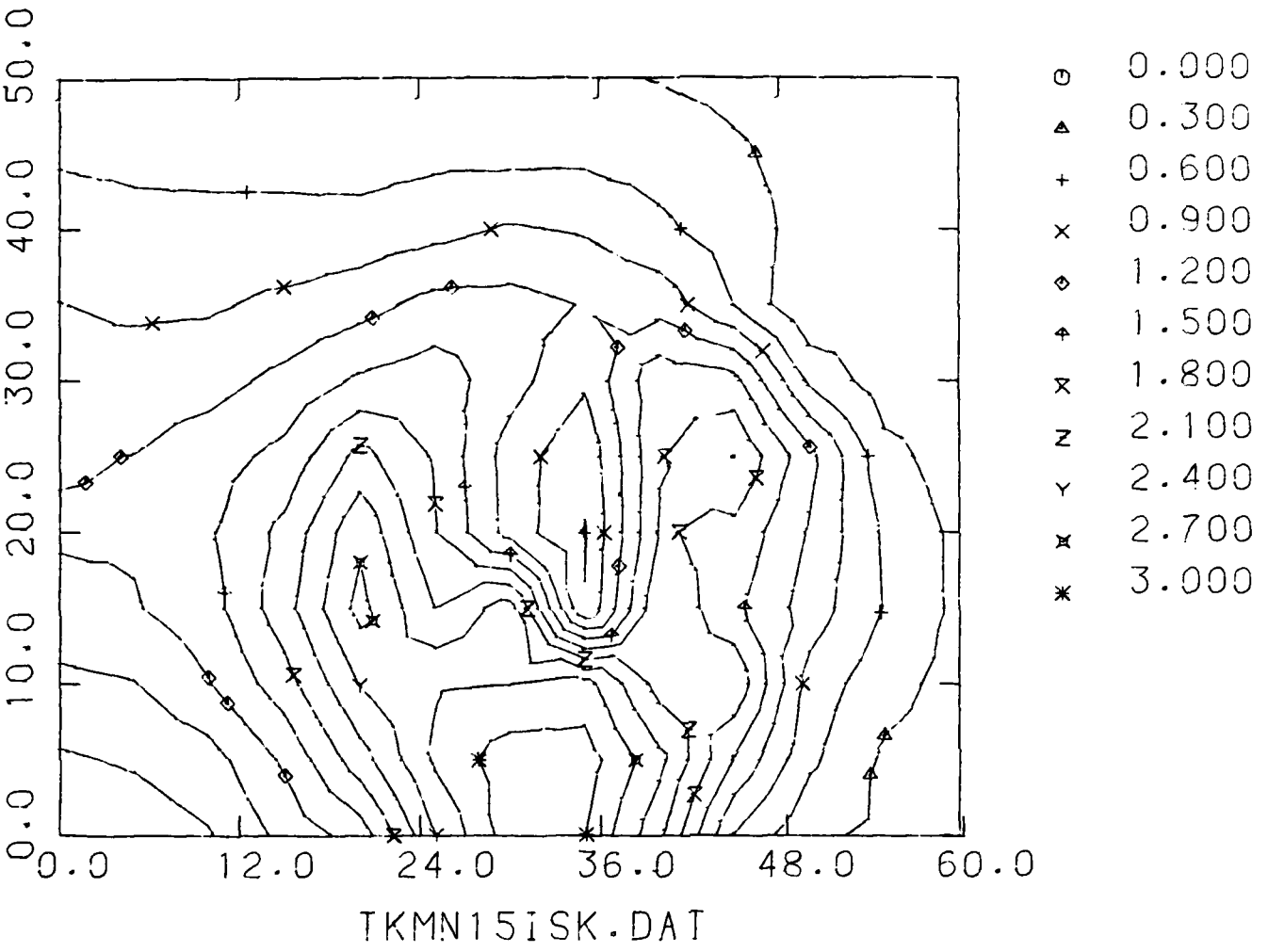

FIG. 49C – ISOLINES OF DCFKE DOWNSTREAM OF H = 0.5, α_R = -15 THICK STRAKE

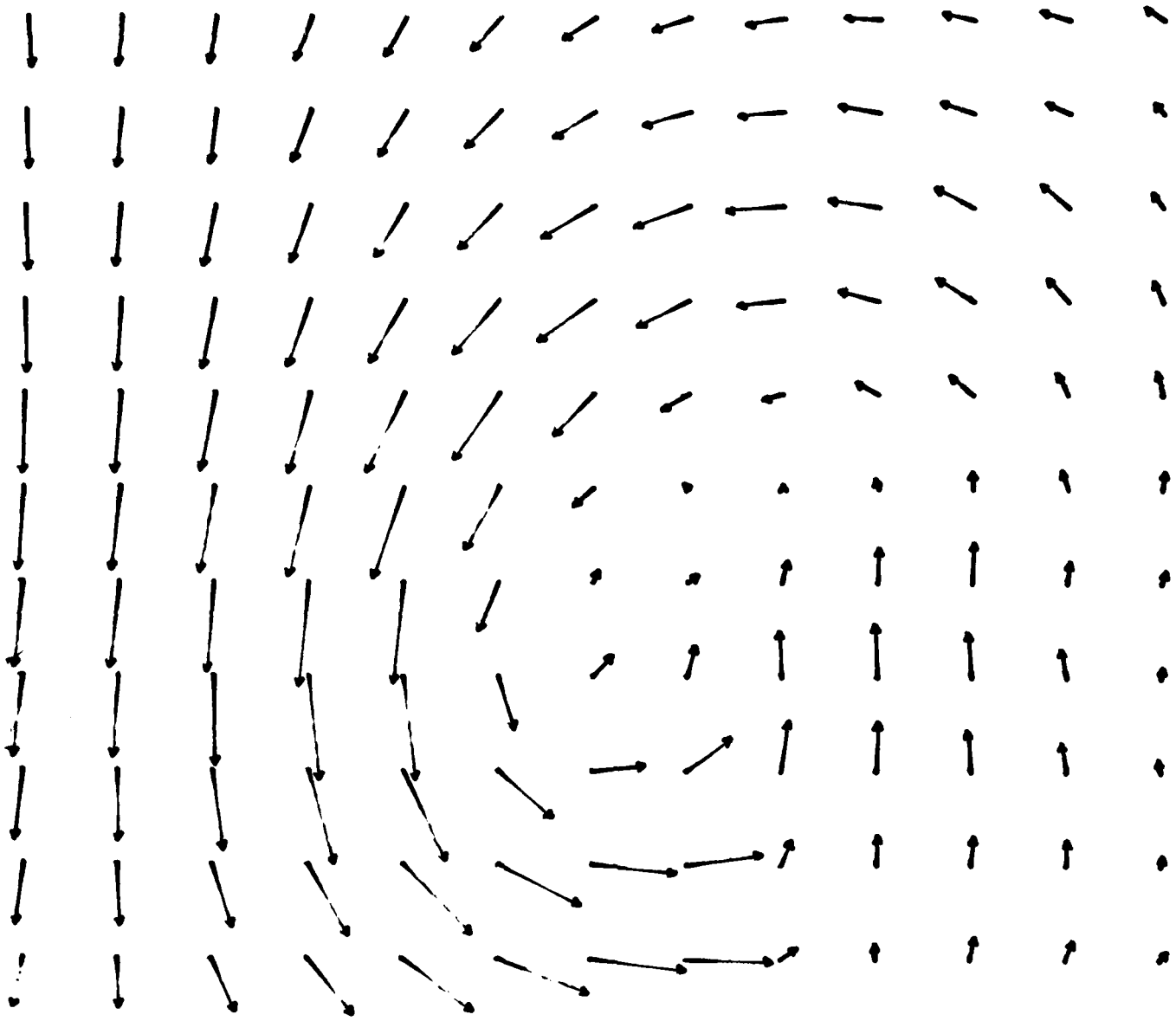

FIG. 50A - FLOW FIELD DOWNSTREAM OF H = 0.5, α_R = 0 THICK STRAKE

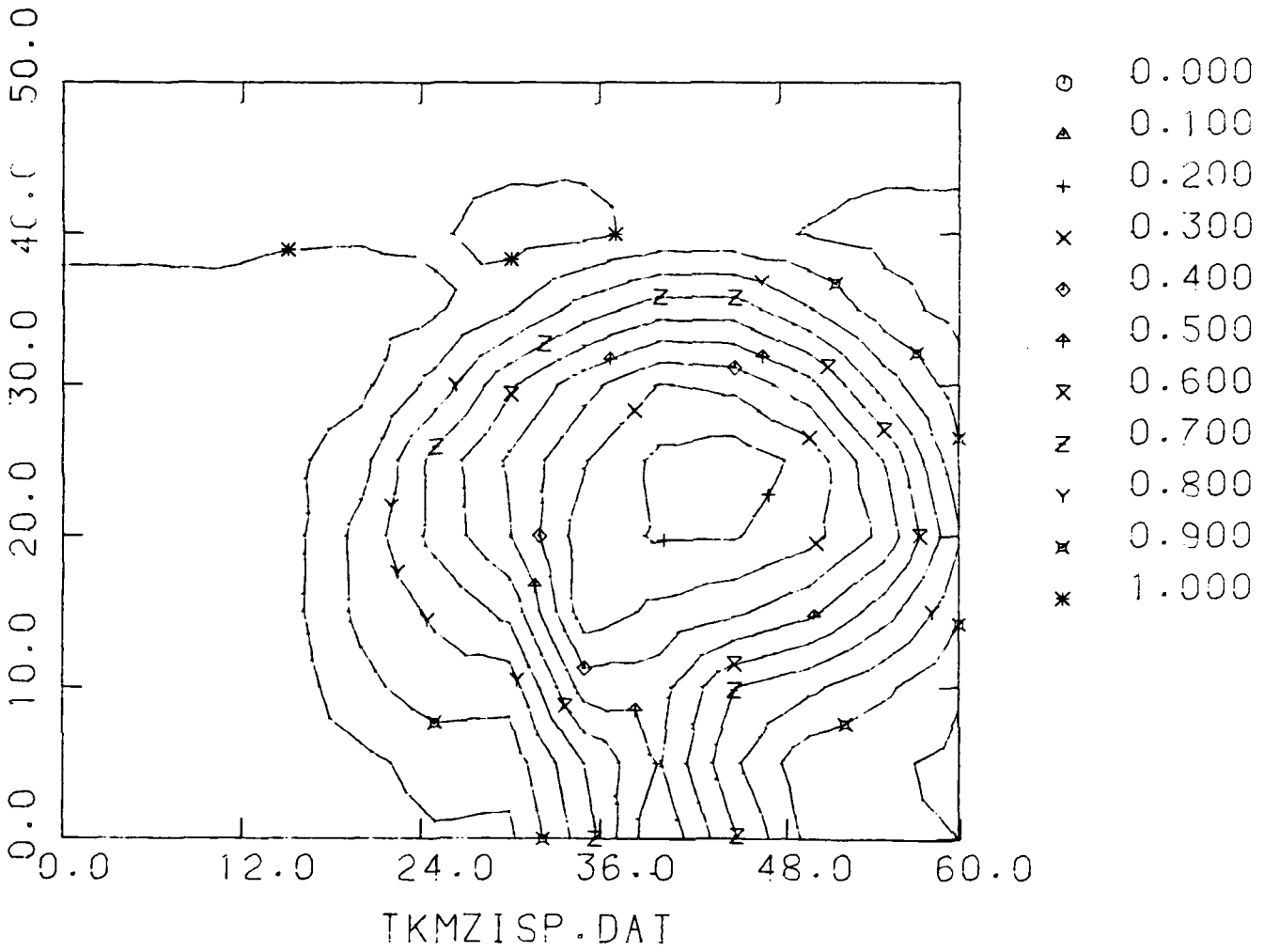

FIG. 50B - ISOLINES OF P_R DOWNSTREAM OF H = 0.5, α_R = 0 THICK STRAKE

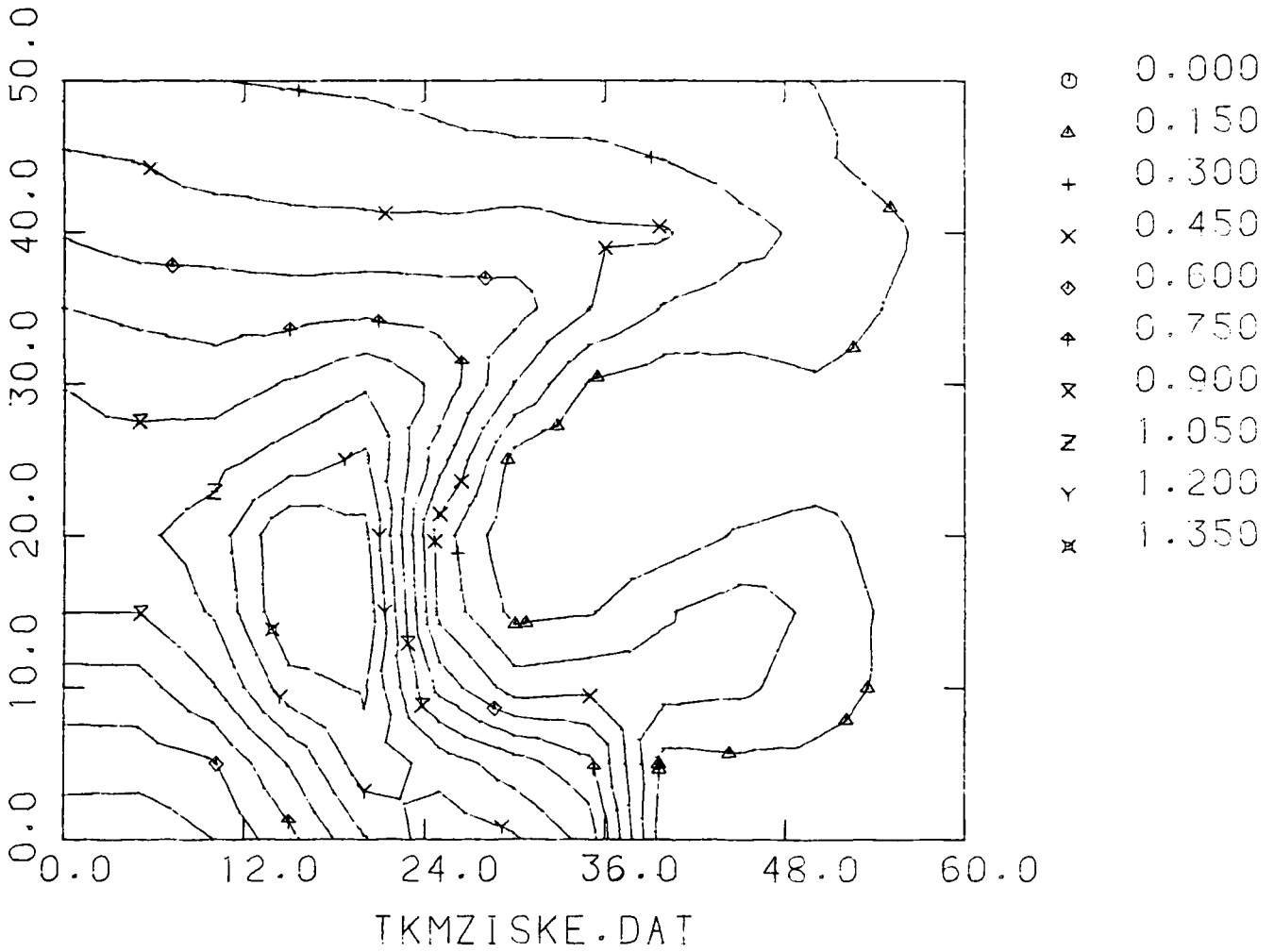

FIG. 50C - ISOLINES OF DCFKE DOWNSTREAM OF H = 0.5, α_R = 0 THICK STRAKE

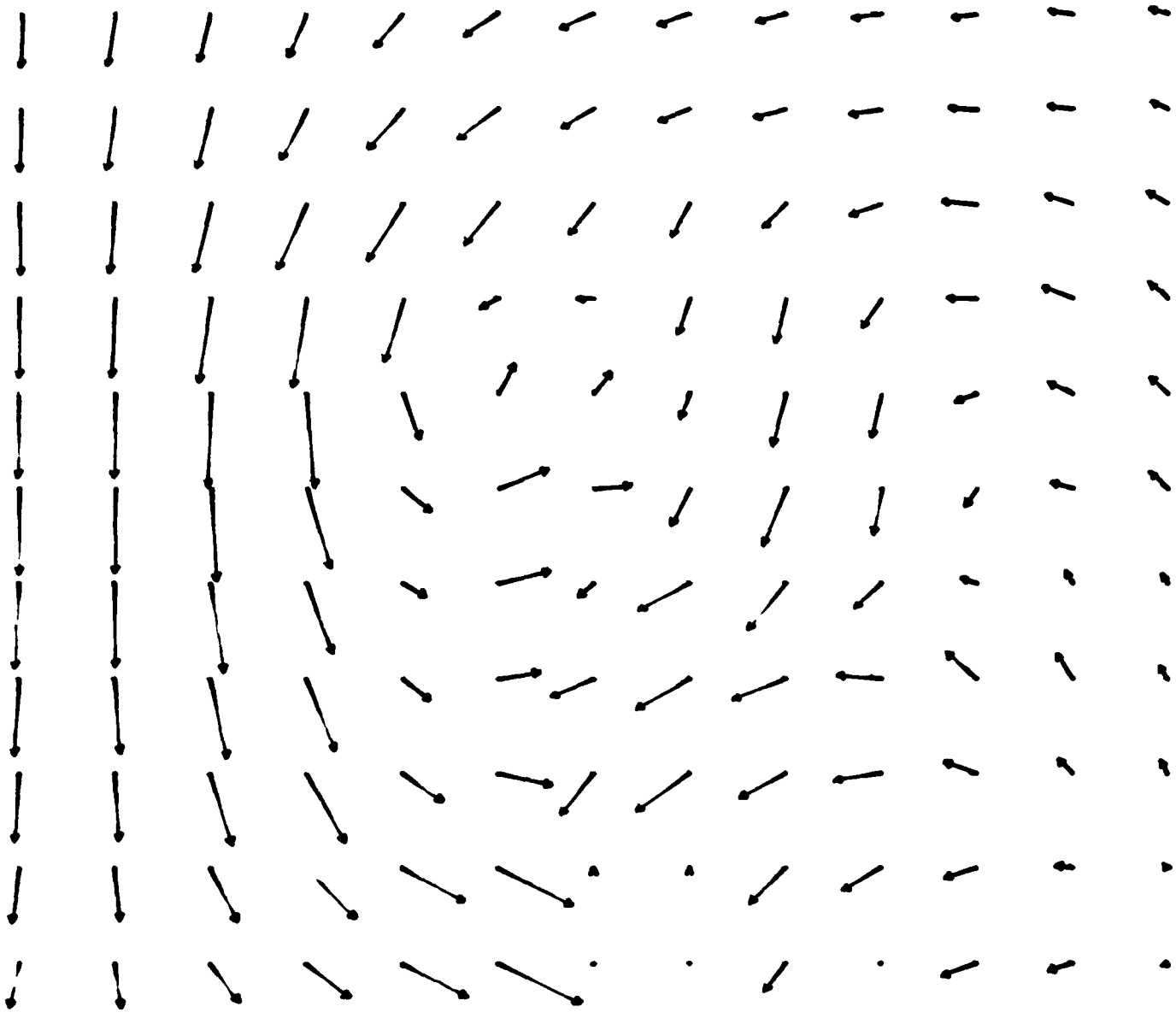

FIG. 51A - FLOW FIELD DOWNSTREAM OF H = 0.5, α_R = 15 THICK STRAKE

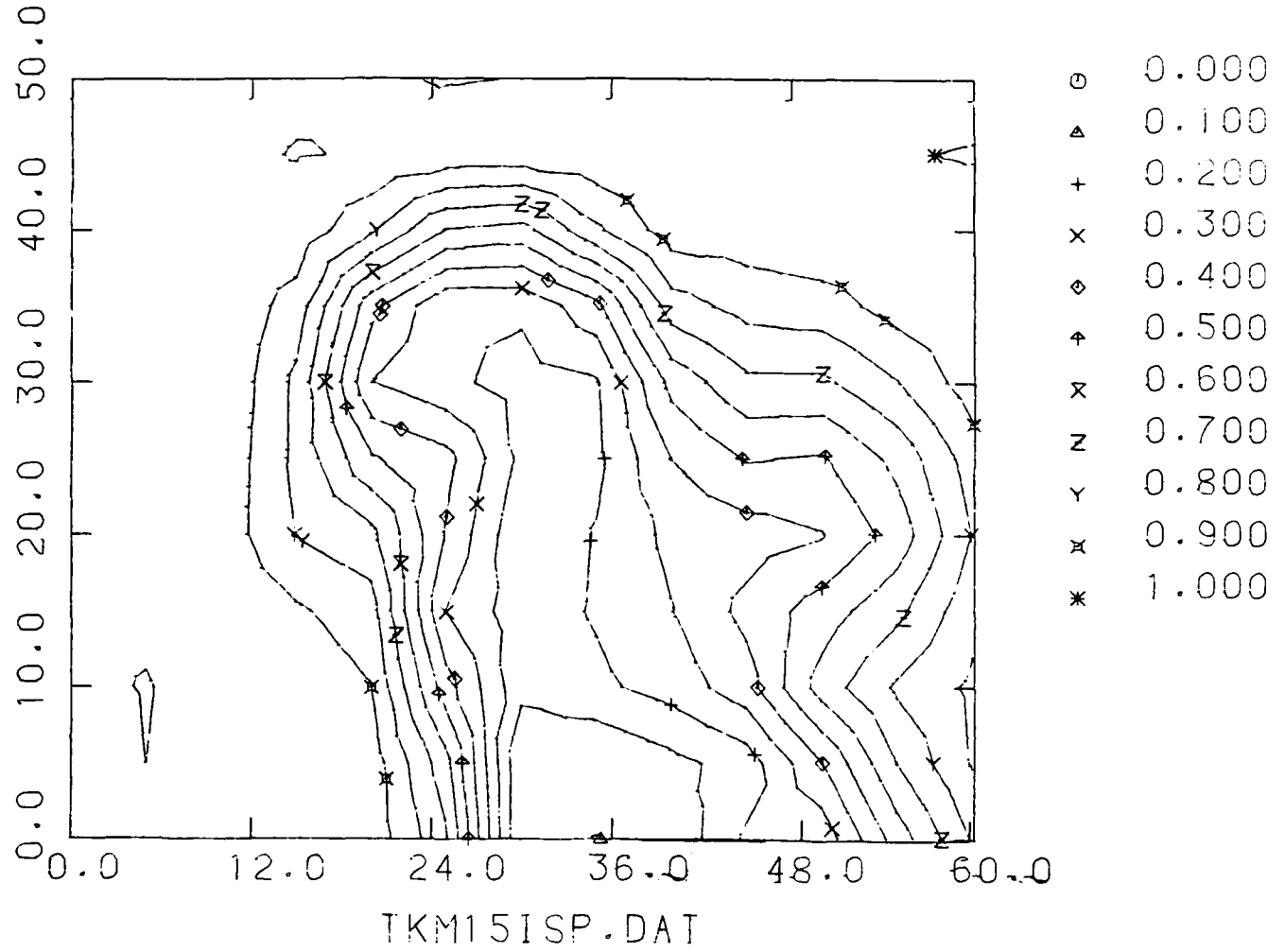

FIG. 51B - ISOLINES OF P_R DOWNSTREAM OF H = 0.5, α_R = 15 THICK STRAKE

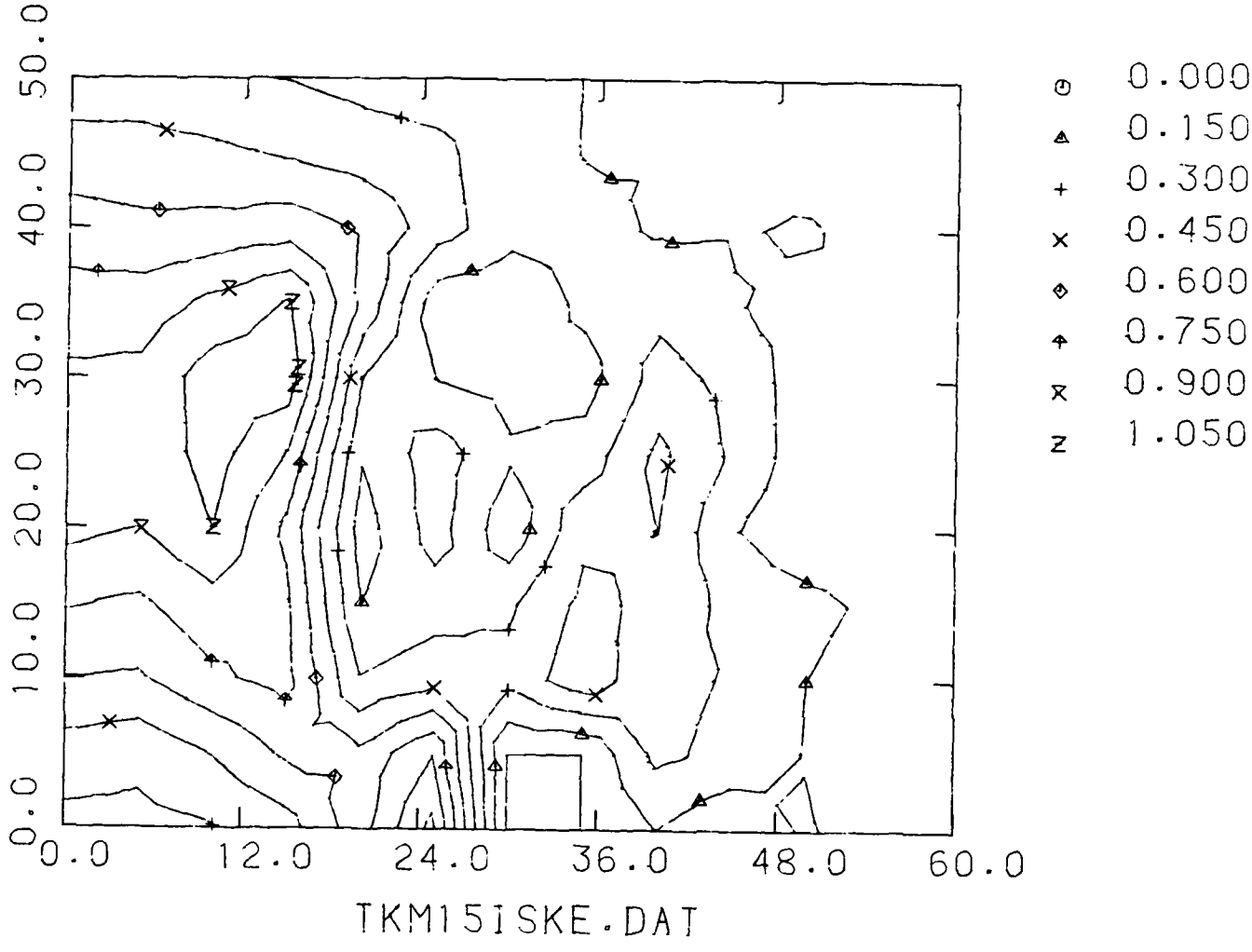

FIG. 51C – ISOLINES OF DCFKE DOWNSTREAM OF H = 0.5, α_R = 15 THICK STRAKE

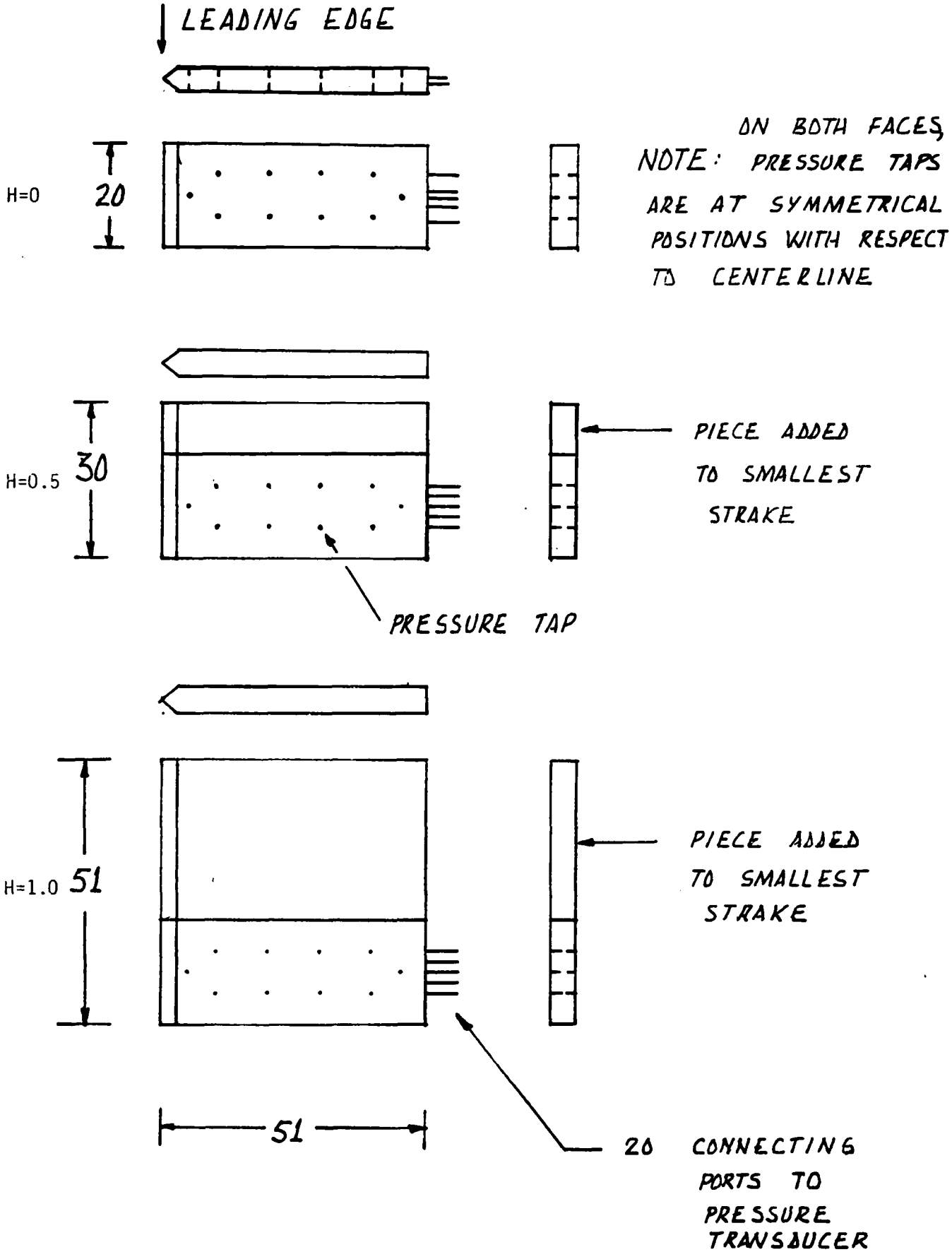

FIG.52A - STRAKES WITH PRESSURE TAPS TESTED

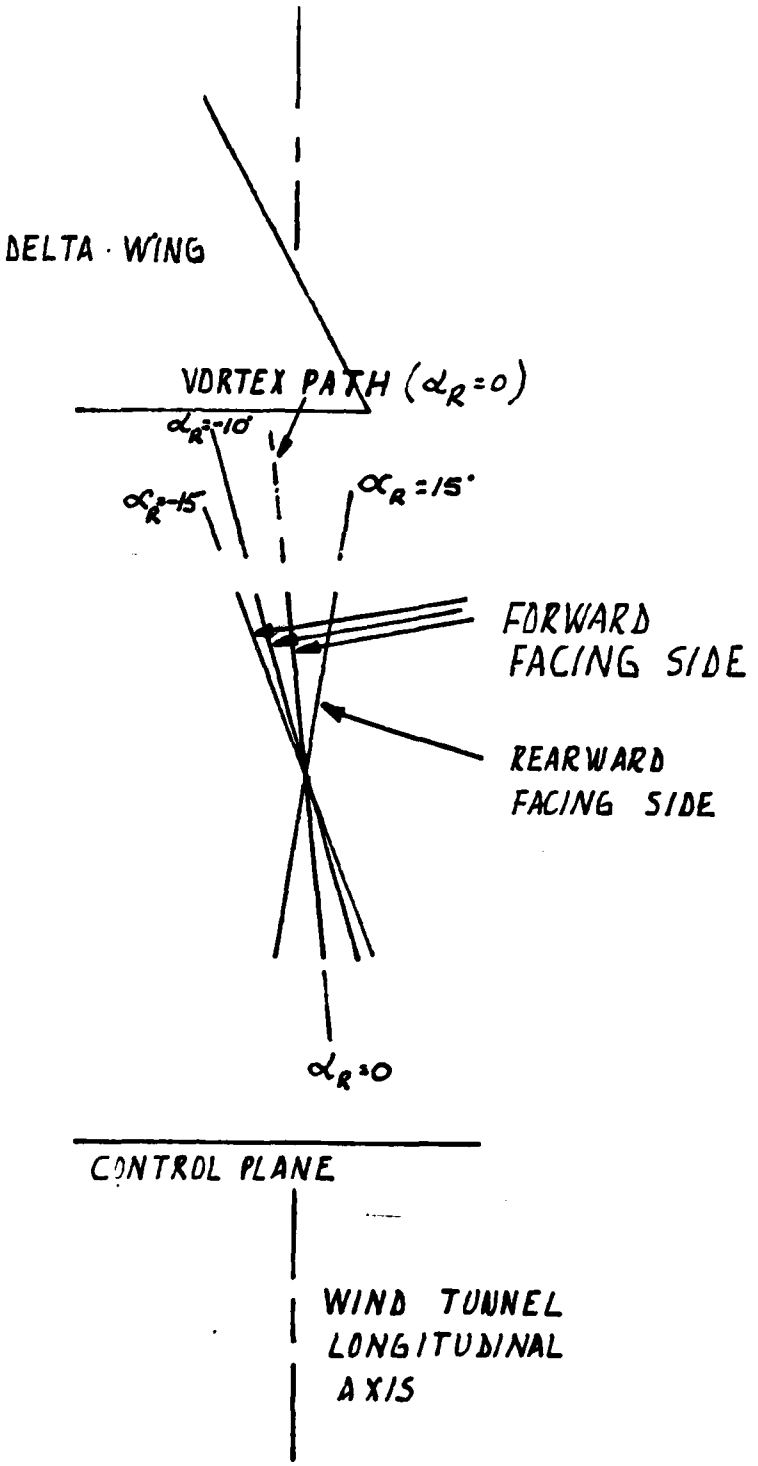

FIG. 52B - VORTEX PATH AND STRAKE WALLS ORIENTATION AT THE α_R TESTED

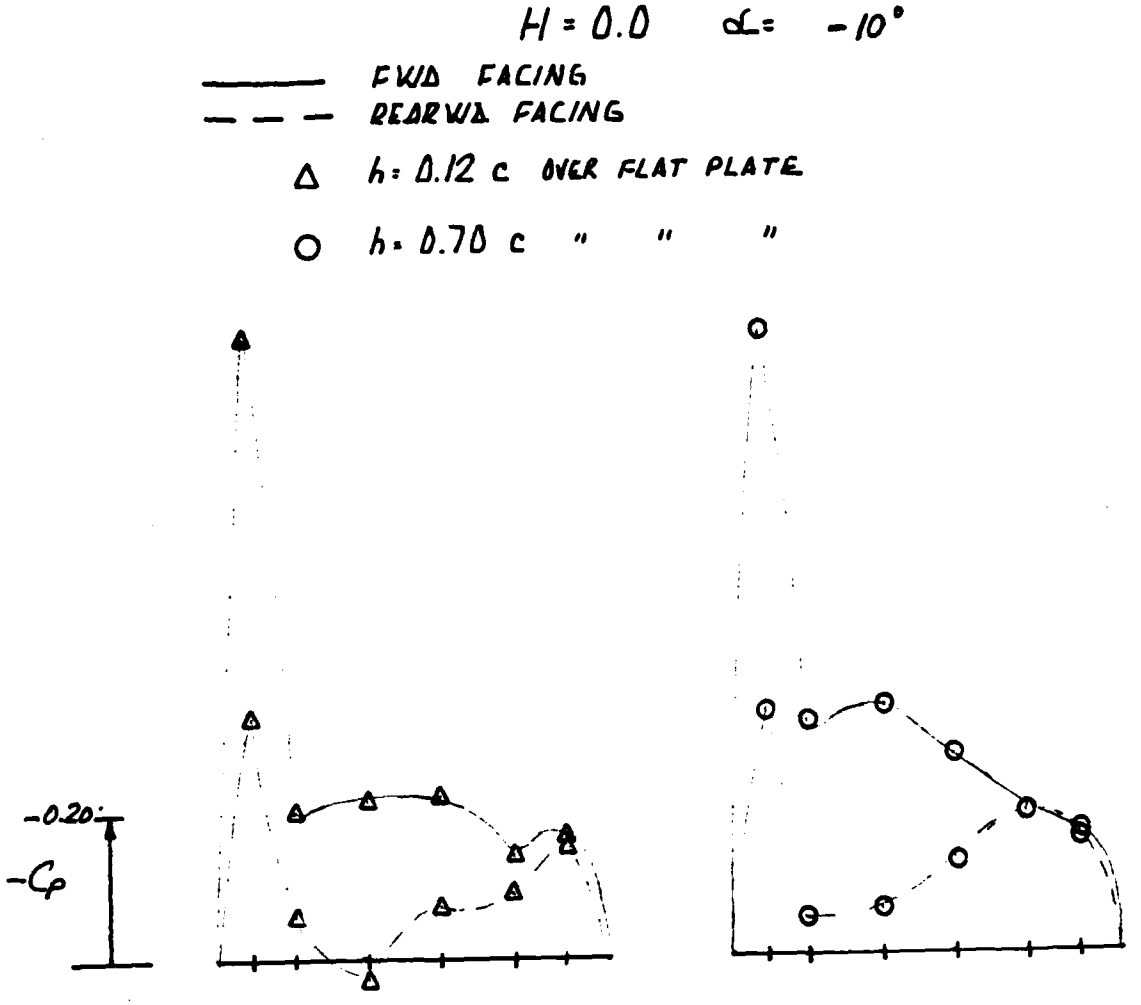

FIG. 53A - PRESSURE DISTRIBUTION ON STRAKE TESTED

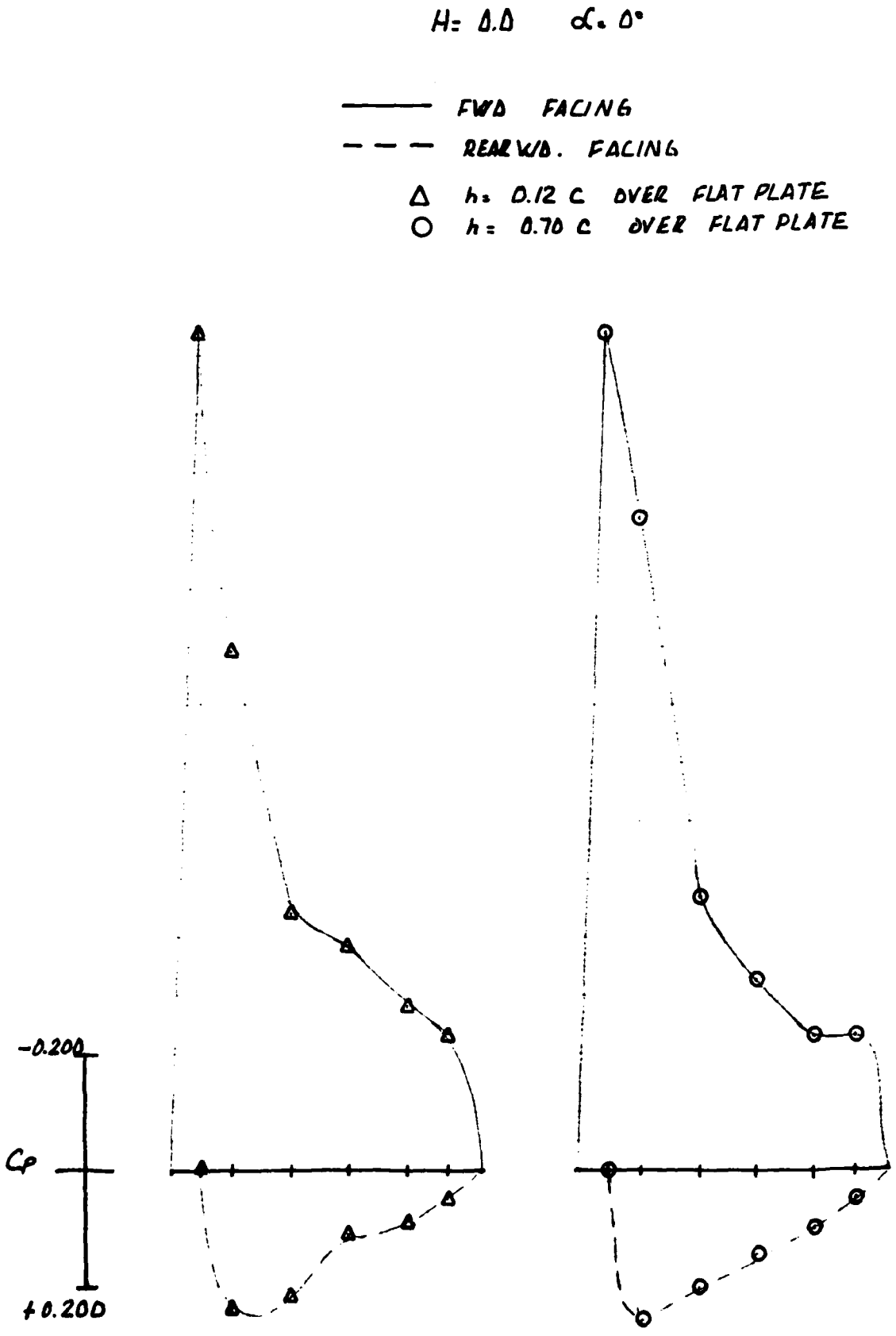

FIG. 53B - PRESSURE DISTRIBUTION ON STRAKE TESTED

H= 0.0 α= 15°

——— FWD. FACING

– – – – REARWD. FACING

△ h= 0.12 c OVER FLAT PLATE

○ h= 0.70 C OVER FLAT PLATE

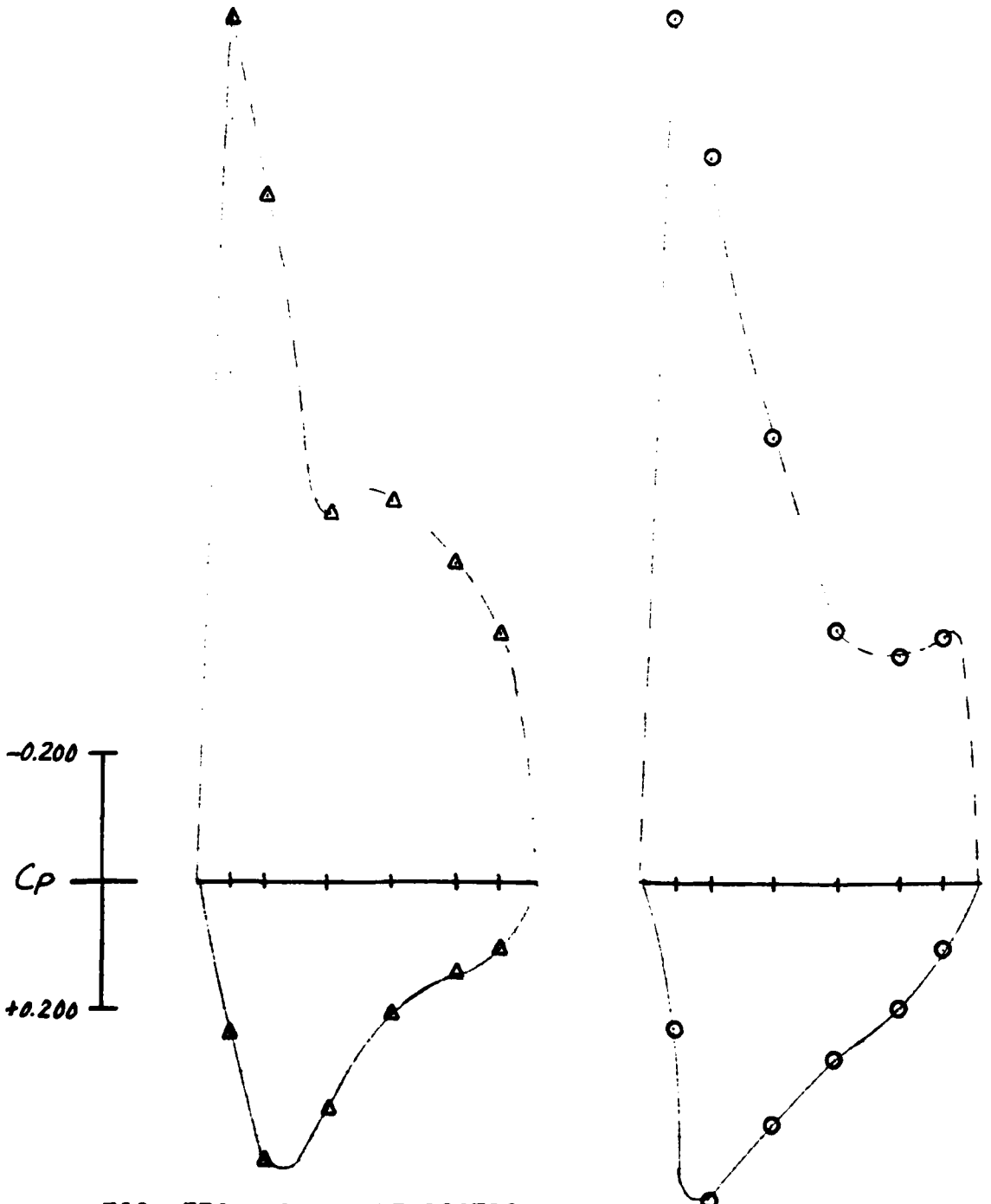

FIG. 53C - PRESSURE DISTRIBUTION ON STRAKE TESTED

$H = 0.5 \quad \alpha = -15°$

——— FWD. FACING

– – – – REARWD. FACING

△ $h = 0.12c$ OVER FLAT PLATE

○ $h = 0.70c$ OVER FLAT PLATE

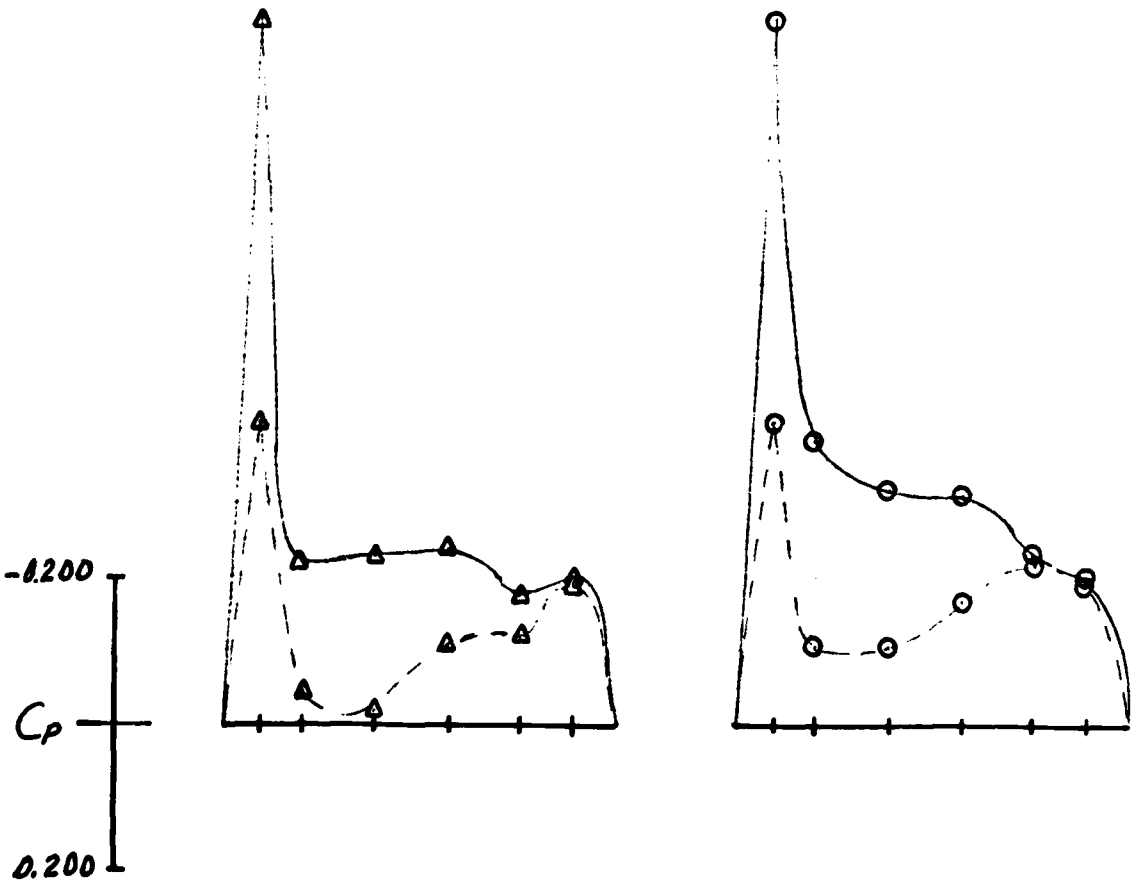

FIG. 54A - PRESSURE DISTRIBUTION

$H = 0.5 \qquad \alpha = 0°$

——— FWD. FACING

– – – – REARWD. FACING

△ $h = 0.12\ c$ OVER FLAT PLATE

○ $h = 0.70\ c$ OVER FLAT PLATE

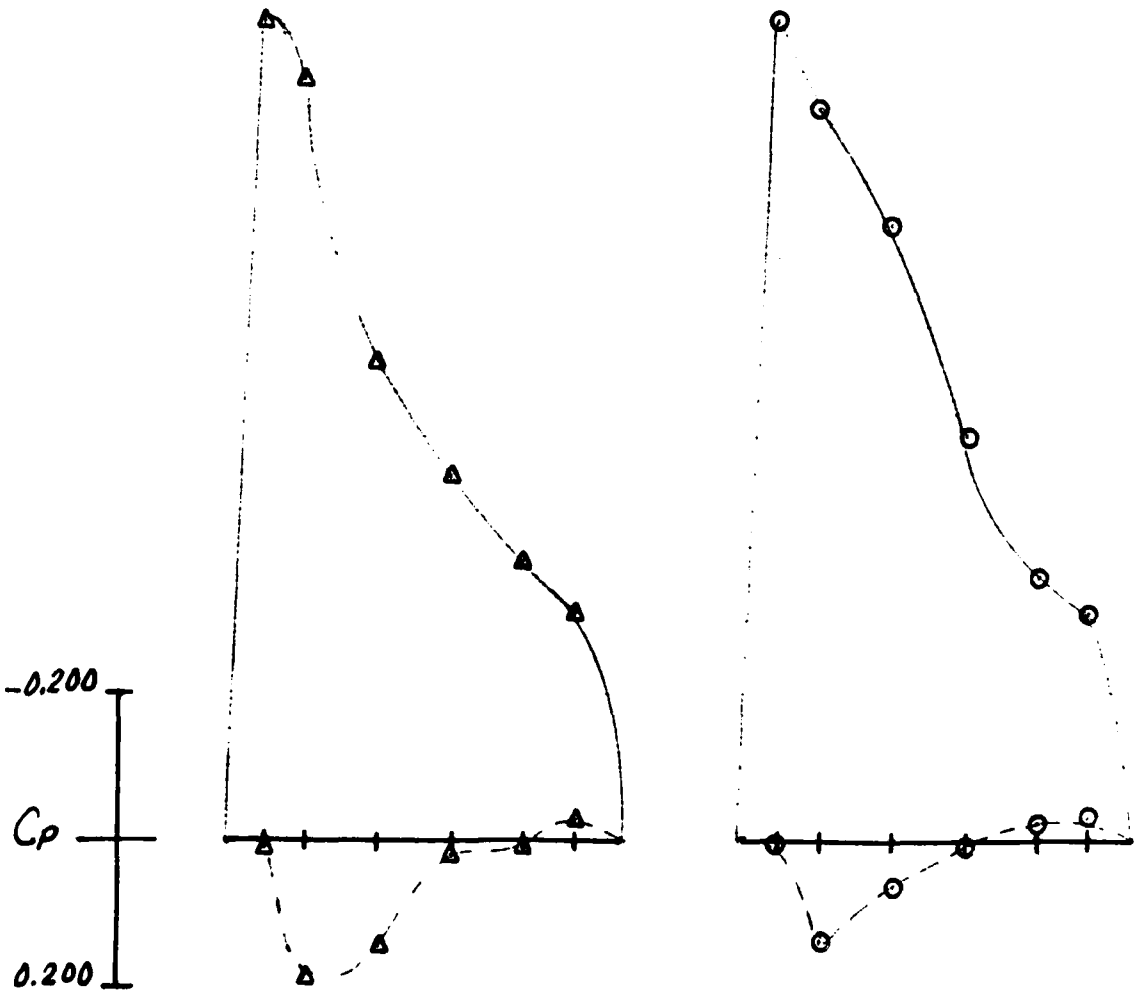

FIG. 54B - PRESSURE DISTRIBUTION

$H = 0.5 \quad \alpha = 15°$

——— FWD FACING

– – – – REARWD. FACING

△ $h = 0.12\,c$ OVER FLAT PLATE

○ $h = 0.70\,C$ OVER FLAT PLATE

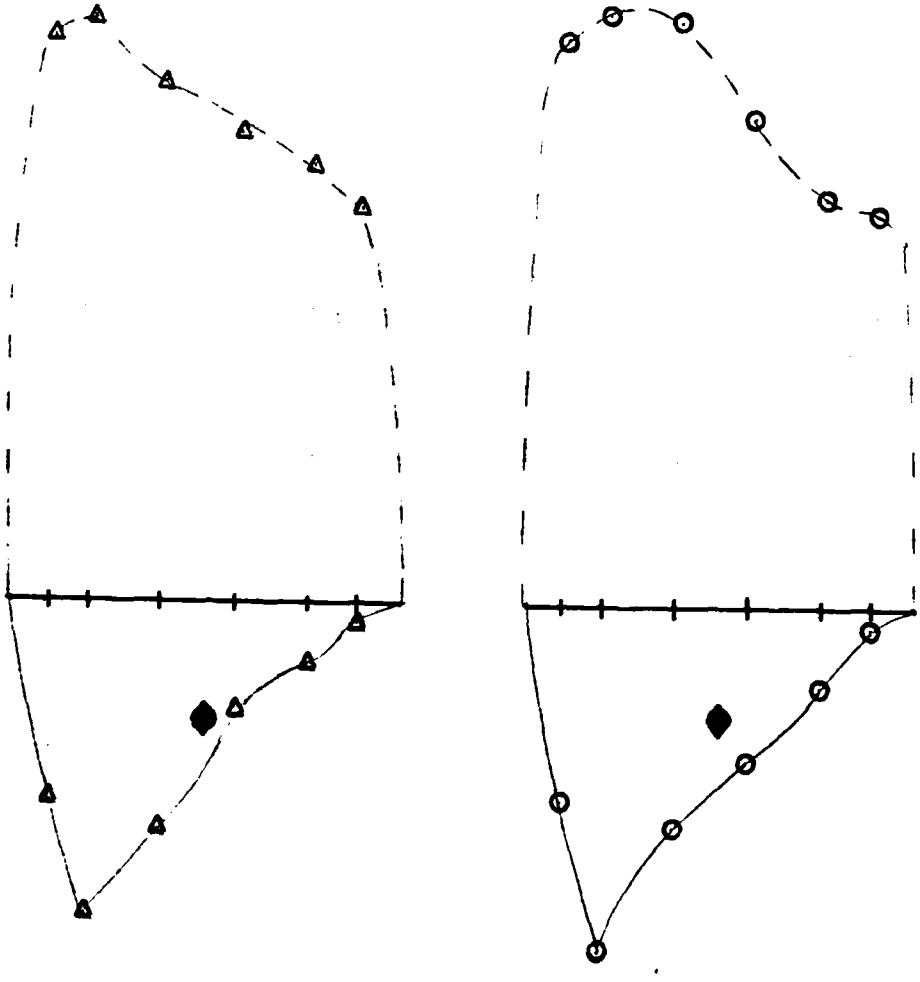

NOTE : BLACK DIAMOND DATA POINT DENOTES PRESSURE MEASURED BY THIN STRAKE PLACED ON AIRCRAFT AFTERBODY AT $H = 0.5$ $\alpha = 15°$ PLACED AT FUSEAGE STATION 3 - SEE FIG. 56 A

FIG. 54C - PRESSURE DISTRIBUTION

$H = 1.0$ $\alpha = -15°$

——— FWD. FACING

— — — REARWD. FACING

△ $h = 0.12c$ OVER FLAT PLATE

○ $h = 0.70c$ " " "

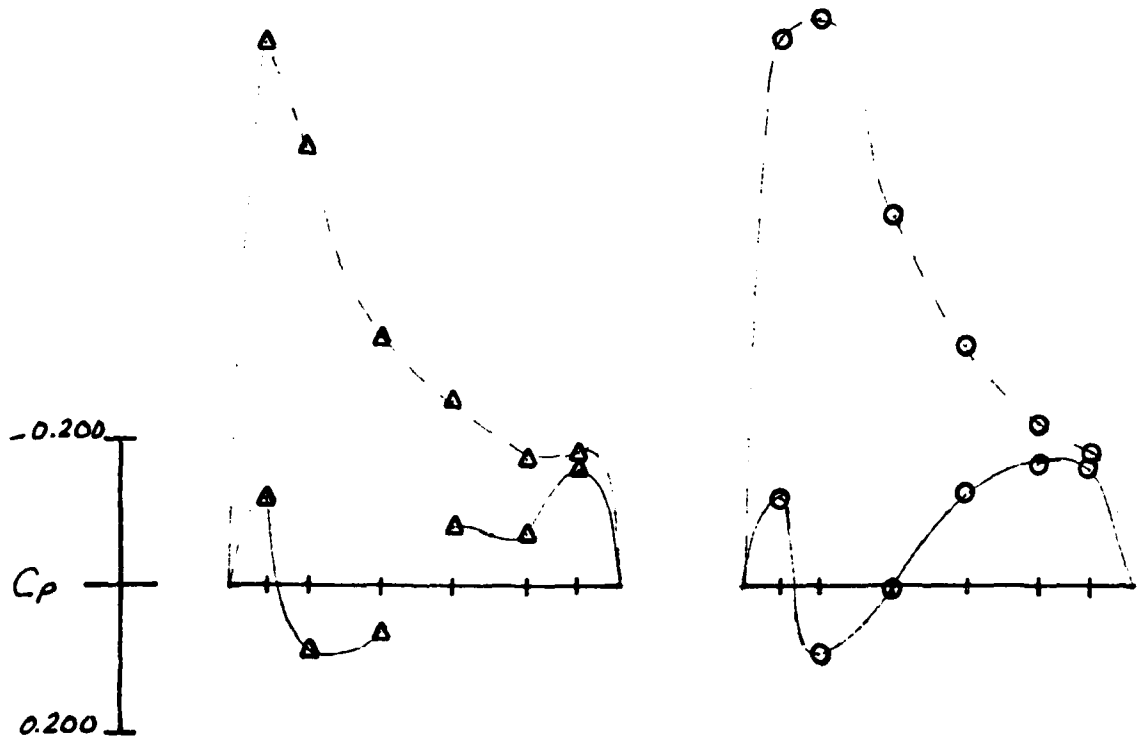

FIG. 55A - PRESSURE DISTRIBUTION

$H = 1.0 \quad \alpha = 0°$

——— FWD. FACING

– – – – REARWD. FACING

△ h: 0.12 c OVER FLAT PLATE

○ h: 0.70 c OVER FLAT PLATE

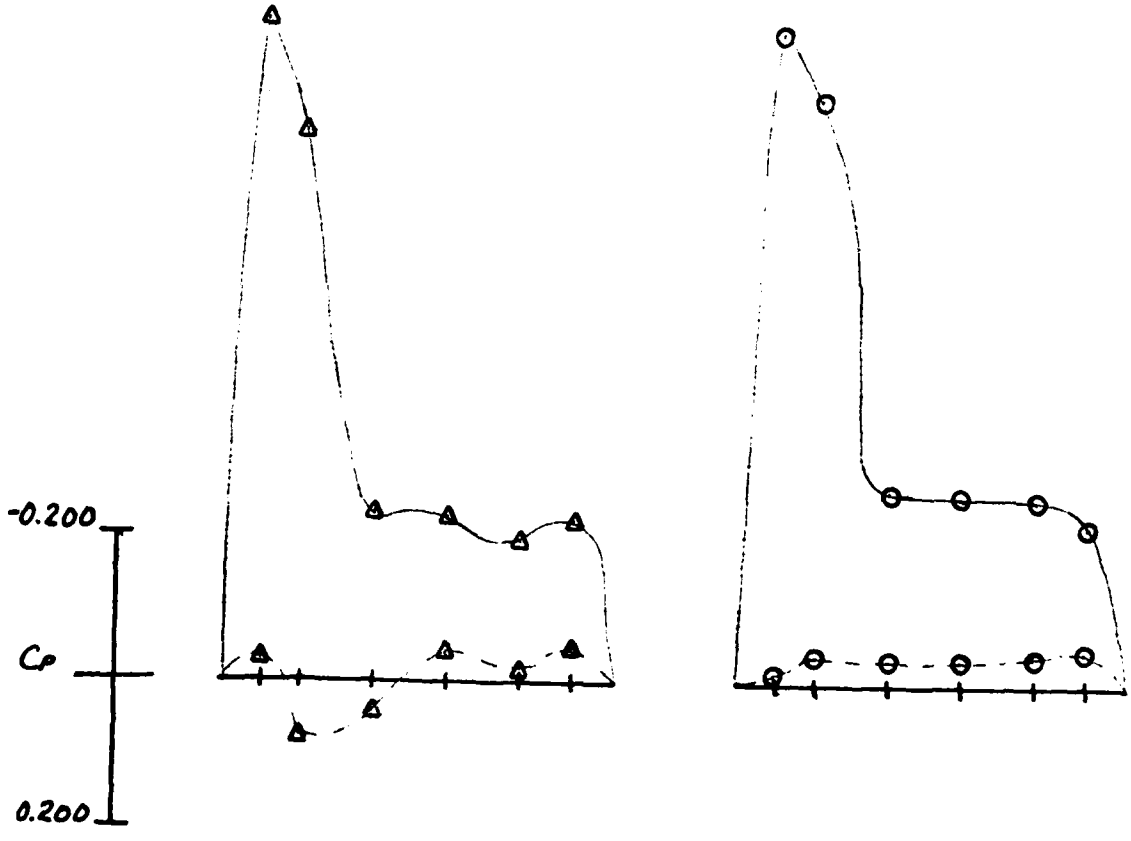

FIG. 55B - PRESSURE DISTRIBUTION

$H = 1.0 \quad \alpha = 15°$

——— FWD FACING

— — — REARWD. FACING

△ $h = 0.12c$ OVER FLAT PLATE

○ $h = 0.70c$ OVER FLAT PLATE

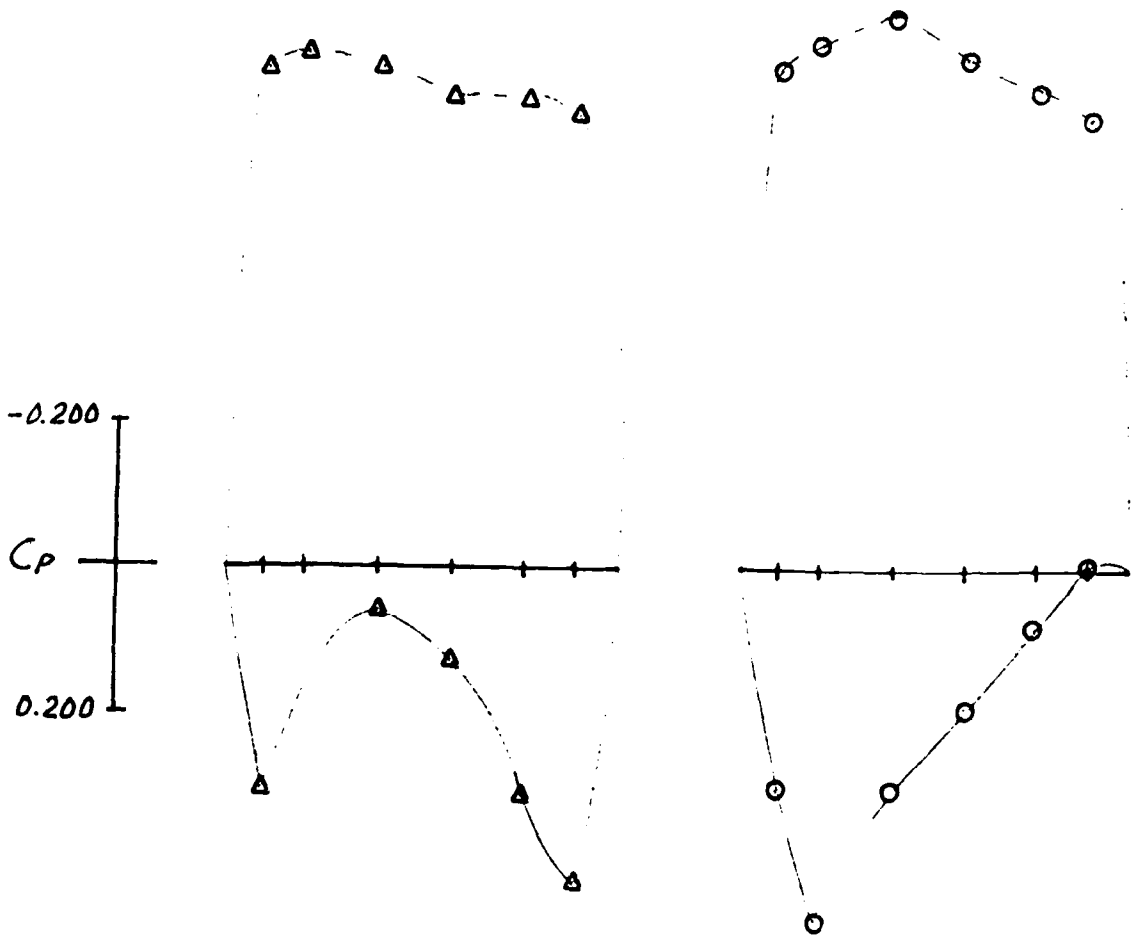

FIG. 55C - PRESSURE DISTRIBUTION

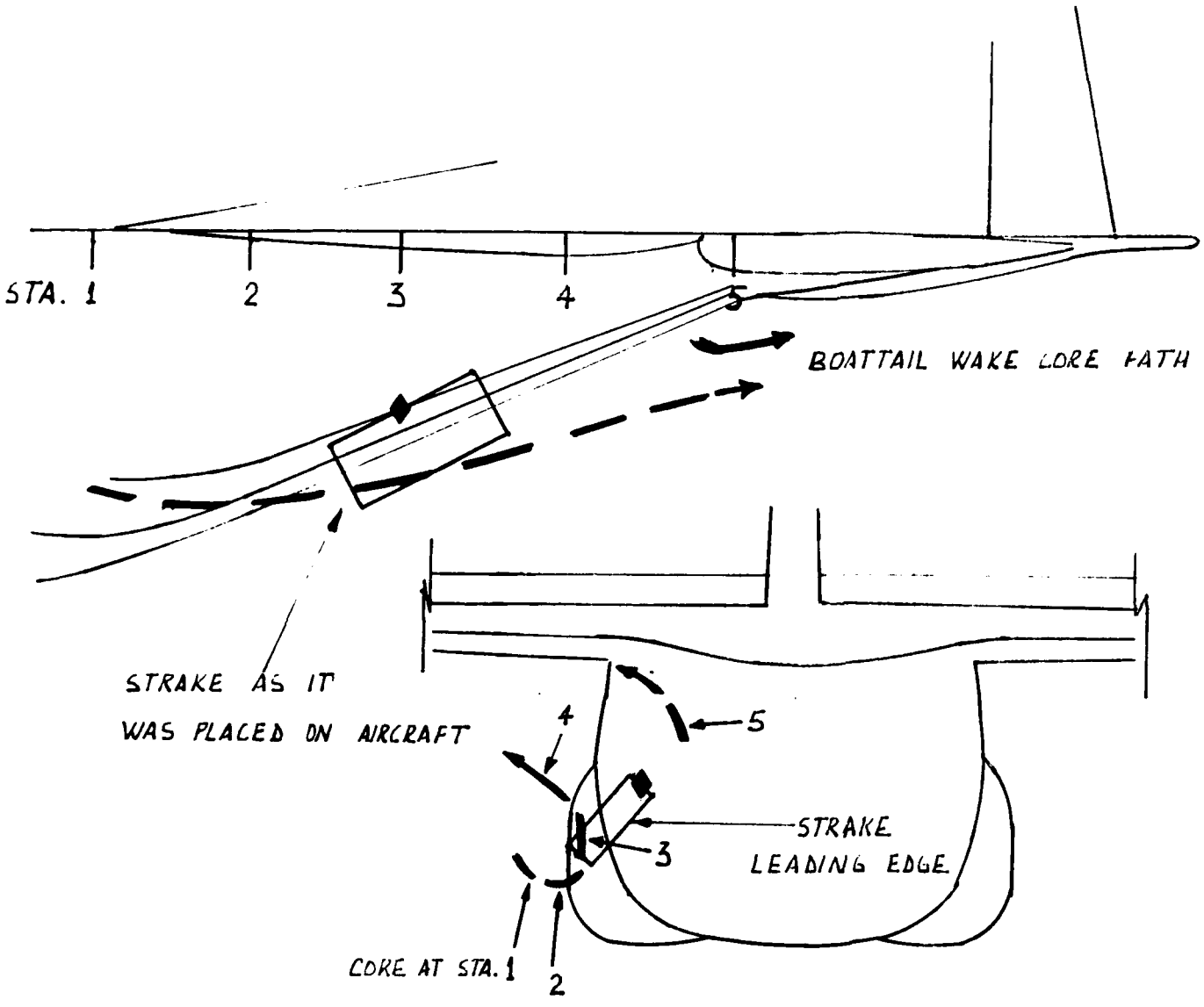

FIG. 56A - SCHEMATIC OF BOATTAIL INDUCED WAKE PATH

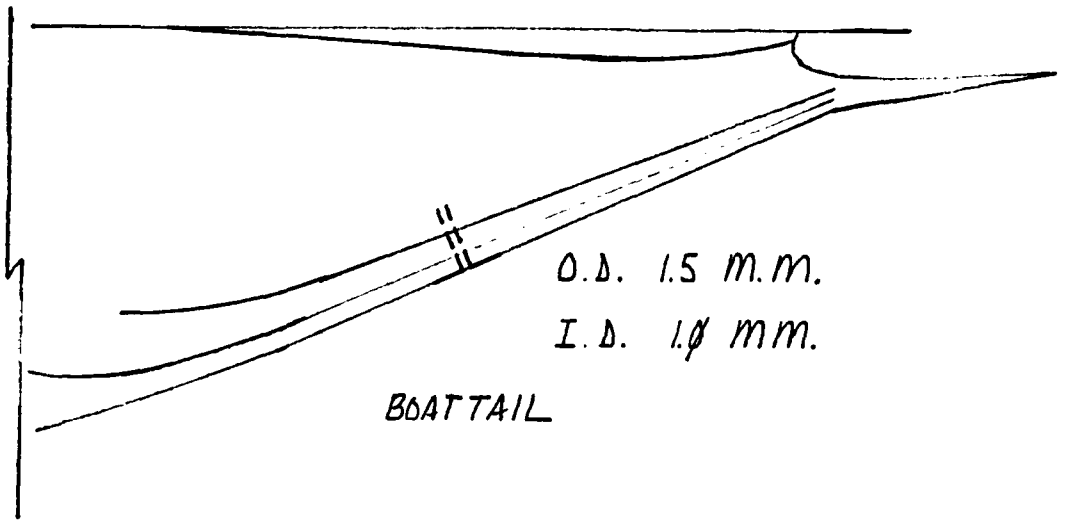

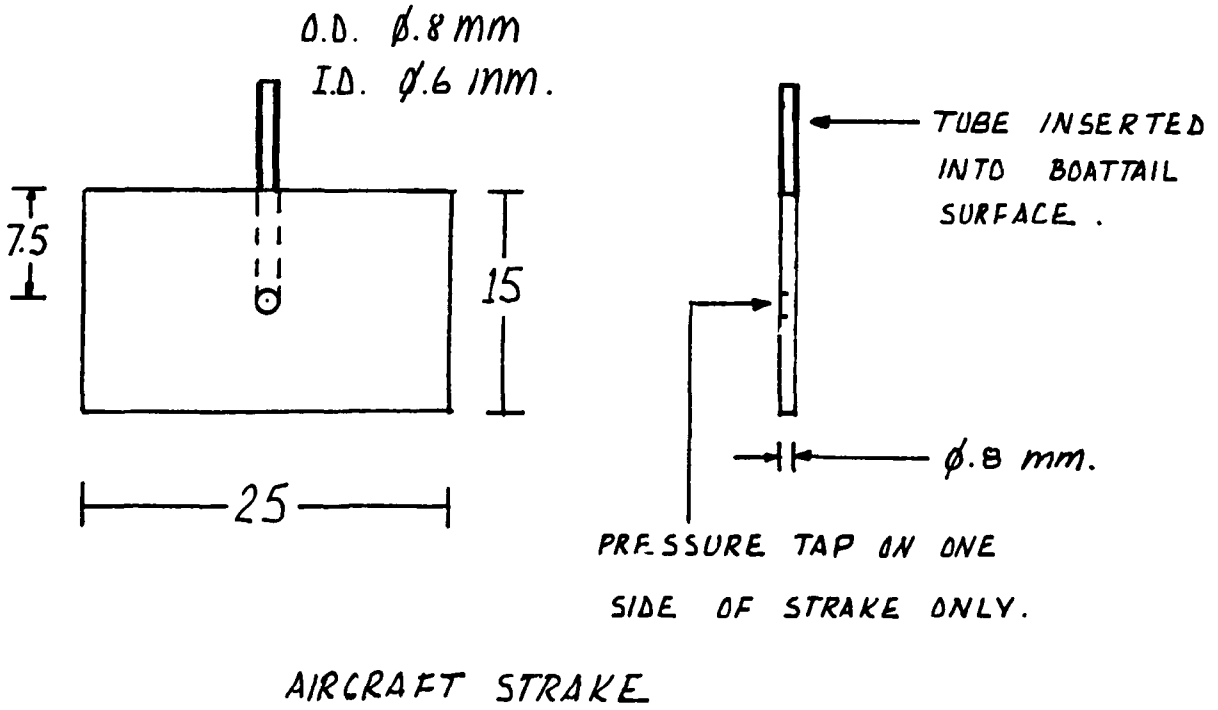

FIG. 56B - STRAKE CONFIGURATION TESTED ON C-130 BOATTAIL

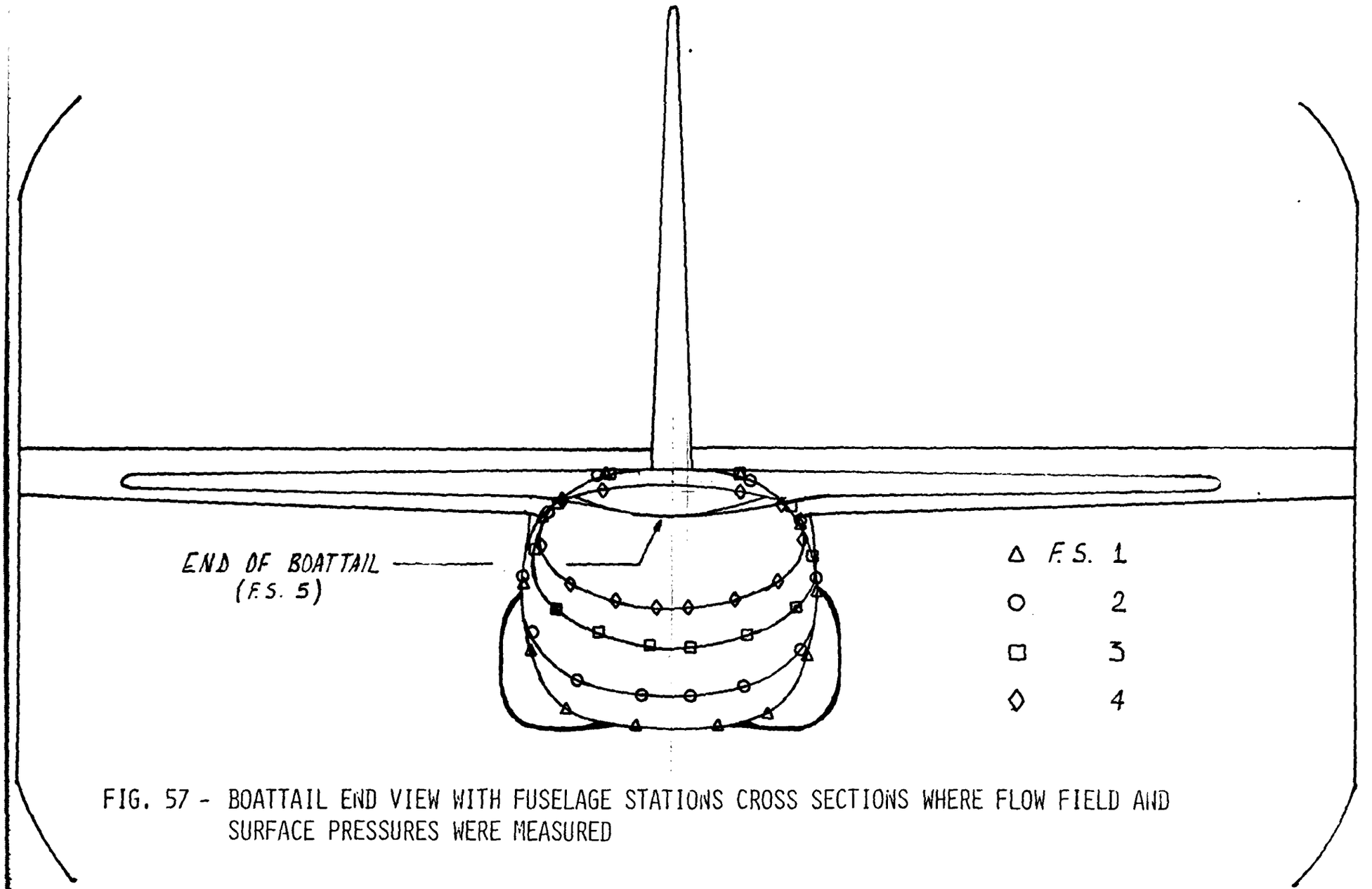

FIG. 57 - BOATTAIL END VIEW WITH FUSELAGE STATIONS CROSS SECTIONS WHERE FLOW FIELD AND SURFACE PRESSURES WERE MEASURED

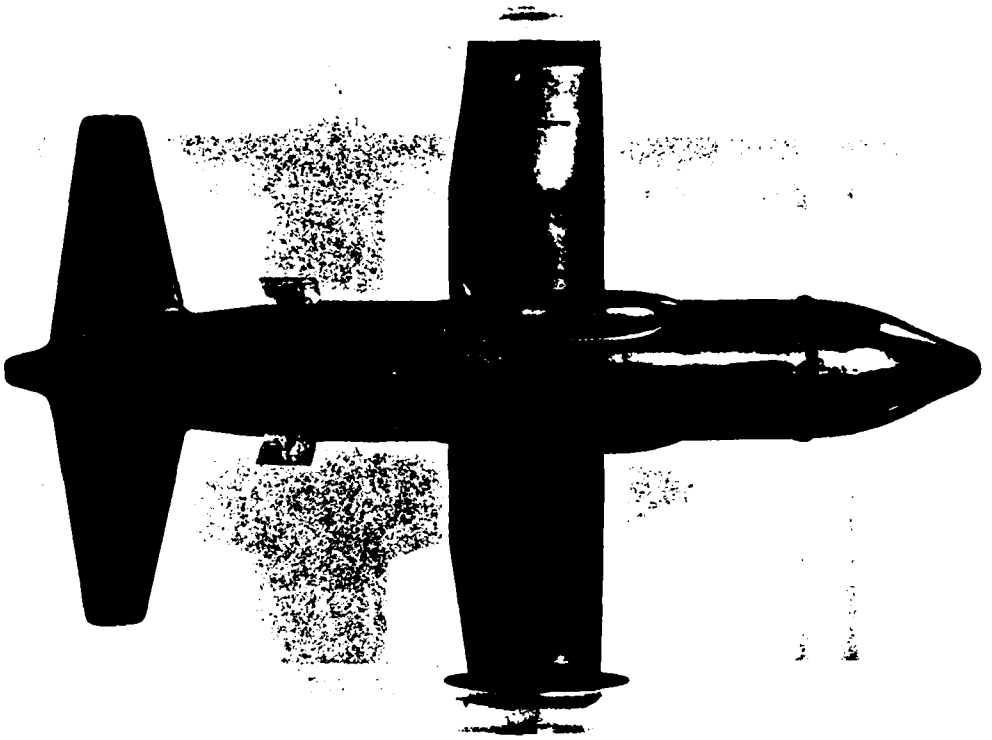

A

B

FIG. 58A,B - VIEWS OF C-130 AIRCRAFT WITH STRAKES PLACED ON IT

A B C

FIG. 59 - LIMITING STREAMLINES VISUALIZATION ON C-130 WITH STRAKES

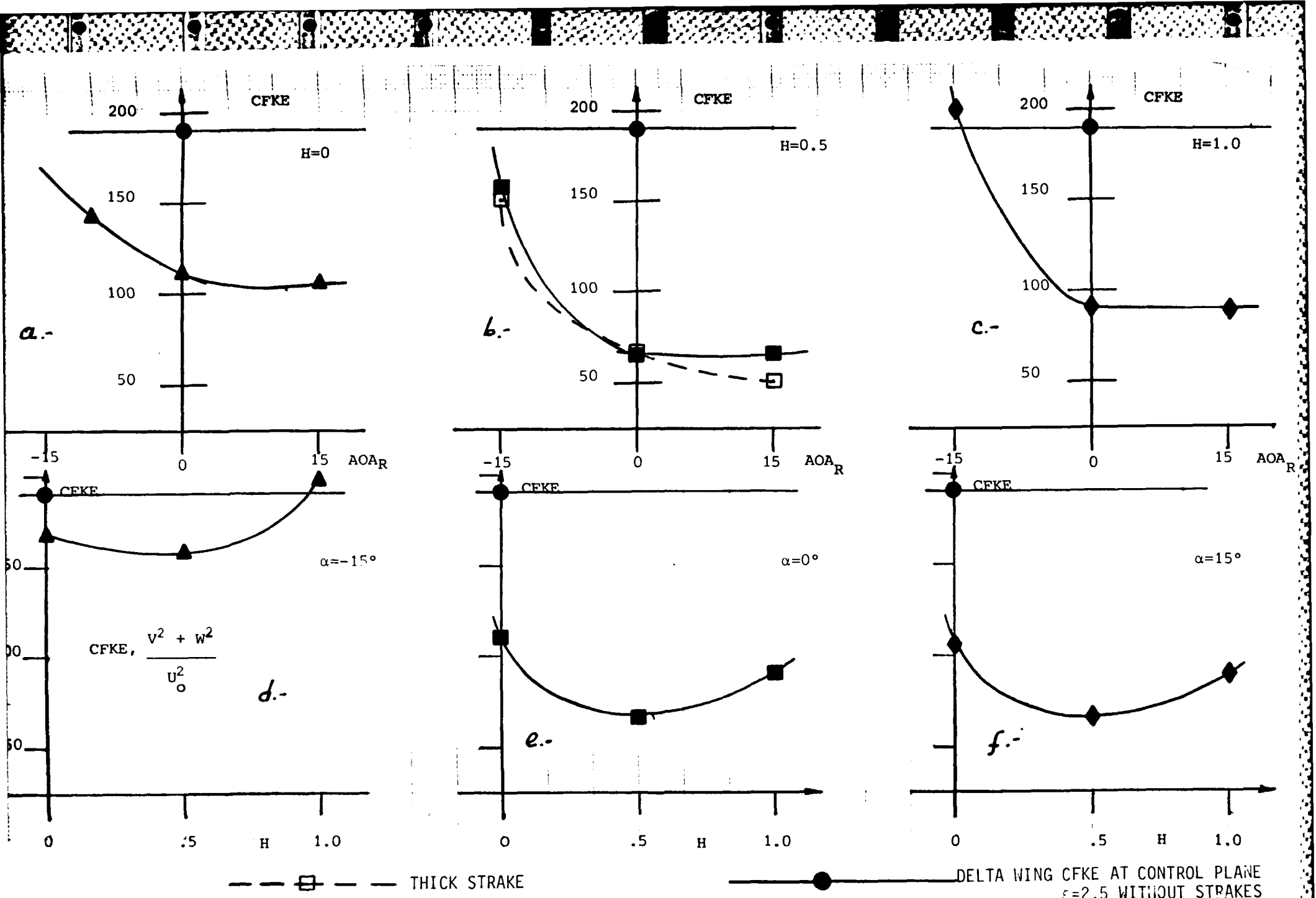

FIG. 60 - PLOTS OF DCFKE INTEGRATED DOWNSTREAM OF STRAKES OF DIFFERENT H, α_R

FIG. 61

PRESSURE DISTRIBUTION ON C-130 BOATTAIL WITH AND WITHOUT STRAKES